ENRICHMENT AND IDENTIFICATION OF AMMONIA TOLERANT MICROORGANISMS IN DIFFERENT ANAEROBIC WASTE TREATMENT SYSTEMS

by

Sunirat Rattana

A dissertation submitted to the

Graduate School-New Brunswick

Rutgers, The State University of New Jersey

In partial fulfillment of the requirements

For the degree of

Doctor of Philosophy

Graduate Program in Environmental Sciences

Written under the direction of

Professor Donna E. Fennell

And approved by

_____

_____

_____

_____

New Brunswick, New Jersey

January, 2016

ABSTRACT OF THE DISSERTATION

Enrichment and identification of ammonia tolerant microorganisms
in different anaerobic waste treatment systems

by Sunirat Rattana

Dissertation Director:

Donna E. Fennell

During anaerobic digestion (AD) of high-nitrogen wastes, organically bound nitrogen is released as ammonia. If ammonia concentrations are too high, ammonia toxicity may occur and contribute to reactor failure. To avoid ammonia toxicity, operators often blend low and high nitrogen wastes to achieve lower ammonia concentrations. However, if better AD performance and process stability can be achieved when ammonia is high, then feedstock blending would be unnecessary and the ammonia released could be harvested at high concentrations as a fertilizer or energy source. The goal of the research described in this dissertation was to enrich and identify ammonia tolerant microorganisms from different anaerobic waste treatment systems including: landfill leachate obtained from a bioreactor landfill in New Jersey and a traditional landfill in Thailand; an anaerobic digester treating swine waste; and a municipal wastewater treatment plant sludge digester. Total ammonia nitrogen (TAN) concentrations of up to 12.5 g TAN/L were imposed on reactors inoculated from the different treatment systems and were fed glutamate as a model nitrogen-containing substrate.

A longer start-up phase, decreased methane production, and accumulation of volatile fatty acids (VFAs) generally occurred at high TAN concentrations. Microbial community shifts were evident and were related to different TAN concentrations, fluctuations in VFA concentrations, and methane production. The Thailand reactors appeared to have the greatest intrinsic ammonia resistance. Compared to the other inocula, little reactor instability was observed in Thailand leachate enrichments, even at the highest TAN concentrations. In constrast, the municipal anaerobic digester sludge had no instrinsic capacity to adapt to ammonia stress. Divalent cation effects (Ca^{2+} and Mg^{2+}) to counteract ammonia toxicity were also investigated in the swine waste digestate reactors. The presence of counter ions was related to enhanced tolerance by certain microbial strains to ammonia.

Microbial community analysis of 16S rRNA genes using denaturing gradient gel electrophoresis (DGGE) and 454 pyrosequencing, revealed that phylotypes related to *Tepidanaerobacter acetatoxydans*, an anaerobic, syntrophic acetate-oxidizing bacterium, in the phylum Firmicutes was dominant in reactors inoculated with landfill leachate (both Thailand and New Jersey) and swine waste digestate (including Ca^{2+}-amended reactors). In contrast, phylotypes matching *Thermanaerovibrio acidaminovoran*, a moderately thermophilic, syntrophic, glutamate-degrading bacterium, was detected at low TAN concentrations, mainly in reactors inoculated with wastewater sludge digestate.

Archaeal community analysis revealed that phylotypes matching *Methanosarcina spp.* in the phylum Euryarchaeota were dominant in reactors inoculated with Thailand landfill leachate, swine waste digestate (target 0.5 to 5 g TAN/L) and swine waste digestate with divalent cation addition—all of which exhibited relatively stable operation.

The presence of *Methanosarcina* spp. at higher TAN concentrations thus suggested that its presence may impart reactor resistance at high TAN concentrations. In contrast, reactors from New Jersey landfill leachate, second generation reactors from swine waste digestate (target 5 to 12.5 g TAN/L), and reactors from the municipal wastewater treatment plant sludge digester had phylotypes matching *Methanoculleus* spp. as the dominant methanogens. These reactors generally excibited greater reactor instability as indicated by VFA accumulation and decreased methane production.

Overall, this study provides important information about ammonia tolerant microorganisms from different anaerobic waste treatment systems. Different systems had very different capacities for adapting to ammonia stress. Knowledge of inoculum sources containing ammonia-tolerant microbial communities could aid in developing bioaugmentation strategies for more rapid adaptation of AD systems treating high nitrogen wastes.

ACKNOWLEDGEMENTS

First, I would like to thank my advisor, Dr. Donna E. Fennell, for allowing me the opportunity to pursue my Ph.D. study at Rutgers. I am grateful for her kind support and assistance over five and a half years. I am thankful for her advice on research direction, valuable insights, and encouragement. I would like to thank my committee members- Dr. Lily Young and Dr. Peter Strom of Rutgers University and Dr. Tom Richard of Penn State University for their willingness to serve as committee members. I am thankful for their time and support.

I am grateful for the sources of funding throughout my study: the Royal Thai Government, the New Jersey Water Resources Research Institute (NJWRRI), and Teaching Assistance Fellowship from the Department of Environmental Sciences, Rutgers University.

I would like to thank Dr. Valdis Krumins, who provided guidance, shared research experience, and offered support through the entire experimental period. I would also like to thank Dr. Weimin Sun for his assistance, especially in depositing nucleotide sequences in the databases.

Many thanks to the people who supported me for getting samples and technical support —Dr. Max M. Häggblom; Dr. Serpil Guran and Mr. David Specca from New Jersey Agricultural Station (EcoComplex); Ms. Laurie Van Genderen from Burlington County, New Jersey; Mr. Francis Bonaccorso from the Joint Meeting of Essex and Union Counties (JMEUC) wastewater treatment plant, Elizabeth, New Jersey; Mr. Richard Crone from Pinehurst Acres Farm, Danville, Pennsylvania; and Officers at Lamchabang Municipality, Chonburi, Thailand. I must also acknowledge the help of the people in the

Department of Environmental Sciences for their technical and administrative assistance, especially Ms. Maria Rivera.

I would like to thank my dear colleagues from Dr. Fennell's lab and neighbouring labs for their friendships and encouragement, especially Ms. Amanda Luther, Mr. Huajun Zhen, Mrs. Mpho Batlhophi, and Mr. Haider Almnehlawi.

Last but not least, I would like to express my deepest love to my parents Mr. Suwan and Mrs. Pannee, my brothers Mr. Narongsak and Mr. Siripong Rattana, and my partner, Mr. Ira Morenberg who was always there for me.

TABLE OF CONTENTS

LIST OF TABLES

LIST OF ILLUSTRATIONS

Chapter 1 Introduction

1. 1 Rationale and Potential for Anaerobic Digestion

Global energy demand was predicted to be increasing by one-third from 2011 to 2035 with the projected share of fossil fuels meeting that dedmand falling from 82% at the present time to only 76% by 2035 (IEA 2013). In 2011, U.S. energy consumption was about 98 quadrillion BTUs (quads) with over 40 quads used to generate electric power. Of this, approximately 70% came from fossil fuels (USDOE 2013). Since most energy produced is from fossil fuels, developing alternative renewable energy is a worldwide challenge. Currently, 29 states and the District of Columbia have enforced the Renewable Portfolio Standard (RPS) or similar laws to determine their own levels of renewable energy generation and technologies for shaping the U.S. energy system, following annual projections of energy supply, demand, and prices. Among those renewable energy sources, solar, wind, hydro, geothermal, and biogas production from landfills and anaerobic digestion of biomass are qualified options to achieve the renewable energy target (USEIA 2014).

Anaerobic digestion (AD) is a carbon-neutral technology that produces biogas consisting of mainly methane (CH_4), and carbon dioxide (CO_2), with traces of other gases. Biogas has been utilized as a direct combustion source for centuries. Now usages of biogas are moving toward new applications such as biogas-fueled fuel cells to generate power and heat for onsite needs and power for export back to the grid, and hydrogen production for fuel cell powered electric vehicles (Figure 1.1)

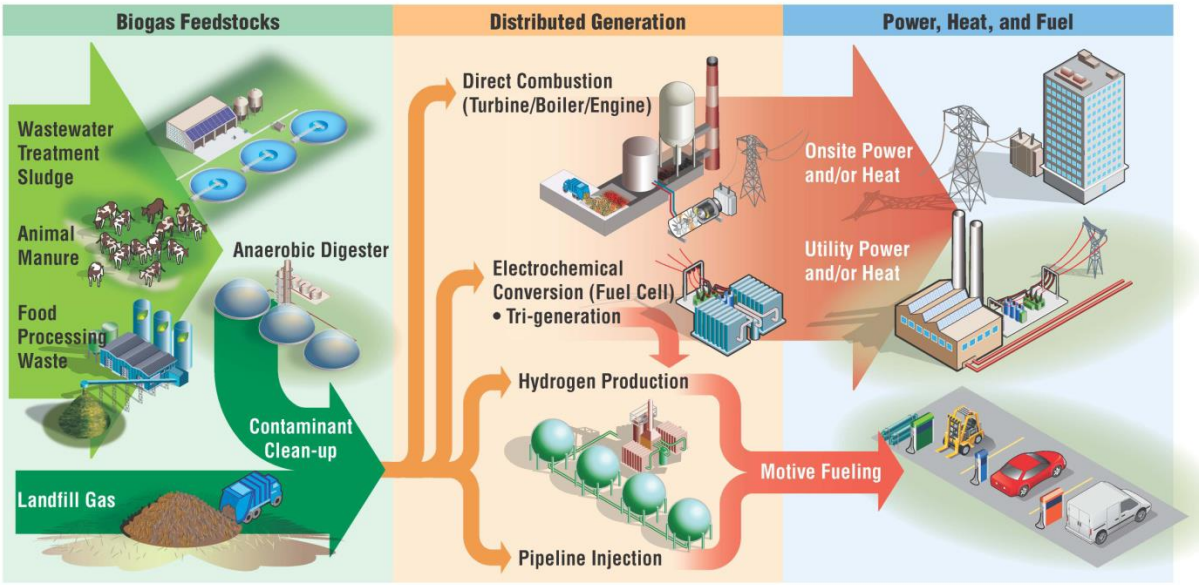

Figure 1.1 Biomass to electricity, heat, and hydrogen pathways (USDOE 2013)

Biogas could become an important source of renewable energy and is currently also a focus of attention regarding climate change, as outlined in *Climate Action Plan-Strategy to Reduce Methane Emissions*, released in March 2014 (USDA, USEPA, USDOE 2014). It is known that methane, one of the major greenhouse gases, has a global warming potential about 21 times greater than carbon dioxide over a 100-year period (USEPA 2014). As a result, the *Biogas Opportunities Roadmap* was proposed to promote the use of biogas systems in the United States through voluntary actions from the agricultural sector (USDA, USEPA, USDOE, 2014). Solutions to enhance biogas potential according to the roadmap are as follows:

- Promote Biogas Utilization through Existing Agency Programs
- Foster Investment in Biogas Systems
- Strengthen Markets for Biogas Systems and System Products

- Improve Communication and Coordination

To enhance the utilization of biogas systems following the first solution, several actions involving related agencies will be implemented. These include:

- *Technical and Financial Assistance* by USDA's Natural Resources Conservation Service (NRCS)
- *Partnerships* by EPA through the AgSTAR program, the Landfill Methane Outreach Program, the Combined Heat and Power Partnership, and the Sustainable Materials Management program
- *Transportation Fuel* by DOE to include biogas option in the Vehicle Technology Office's Fuel and Lubricant Technologies Program
- *Renewable Energy* by DOE to analyze the impact of biogas on electricity generation and fuel production including integration of biogas with wind and solar for distributed renewable energy
- *Research and New Technology* by USDA's Agricultural Research Service and National Institute of Food and Agriculture to improve research in ***anaerobic digestion*** for nutrient recovery, particularly nitrogen and phosphorus, including investigating agronomic and economic viability of using captured nutrients as fertilizers, soil amendments, and biochar production from biosolids

The *Biogas Opportunities Roadmap* pointed out that the agricultural sector, especially livestock manure, could be a major biogas source. From a total of 2,116 digesters currently being operated in the U.S., about 59% (1,241 digesters) are at

WWTPs, 30% (636 digesters) are at landfill-based energy projects, and 11% (239 digesters) are on farms (Figure 1.2) (USDA, USEPA, USDOE 2014). The number of biogas systems could reach a total of 13,008 digesters if all potential projects were fully realized. Sixty four percent of the biogas systems would potentially use livestock manure. Thus proper management of anaerobic digestion from the agriculture sector should be a significant goal.

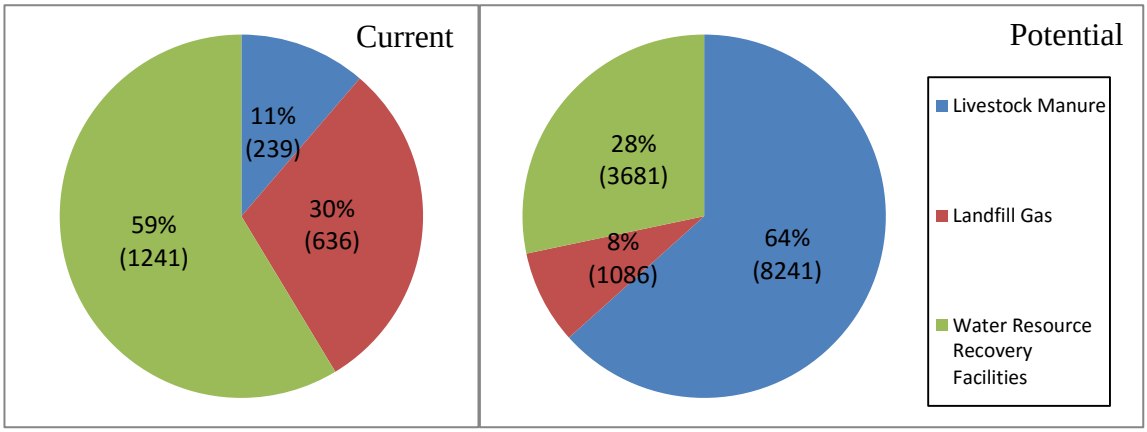

Figure 1.2 Current operational and potential biogas systems in the United States (USDA, USEPA, USDOE 2014)

Number in ( ) represents the number of anaerobic digesters

1.2 Anaerobic Digestion Overview

Anaerobic processes for treatment of wastewaters and sludges are well over 100 years old (Rittmann and McCarty 2001). This technology converts organic wastes into methane gas, a source of energy, and provides many potential benefits. Another major advantage of anaerobic treatment is lower yield of biological solids, which results in less sludge for disposal since only a small portion of the waste is converted to cells (McCarty

1964) when compared to aerobic treatment that needs to add oxygen or nitrate as electron acceptors (Rittmann and McCarty 2001). Organic matter and carbon dioxide act as electron acceptors in anaerobic digestion, and no oxygen or other electron acceptors have to be added. However, during anaerobic digestion, organically bound nitrogen and phosphorus are released as soluble forms. Therefore these soluble nutrients in anaerobically digested waste streams must be captured to avoid release into water bodies. Furthermore, because there is no degradation pathway (Berge et al. 2006) for reduced nitrogen in anaerobic systems, nitrogen released as ammonia tends to accumulate and may cause reactor instability and failure. A free ammonia concentration of 1.1 g N/L or more was found to cause inhibition in anaerobic treatment of swine manure at pH 8.0 (Hansen et al. 1999). Total ammonia nitrogen (TAN) concentration causing 100% inhibition of thermophilic anaerobic digestion occurred in the range of 8-13 g N/L (Sung and Liu 2003). It is vital to control ammonia concentration while operating anaerobic reactors because ammonia inhibition is a factor causing increases in volatile fatty acids (VFAs), a parameter that indicates process instability (Angelidaki and Ahring 1993, Nakakubo et al. 2008, Schnurer and Nordberg 2008).

Although high ammonia concentration contributes to the reactor failure, ammonia can also potentially be harvested for fertilizer or energy recovery. Enabling operation of anaerobic reactors under high ammonia concentrations could allow more efficient direct capture and re-use of ammonia as a fuel or fertilizer. Concentrating the ammonia for capture is preferable to its widespread release in dilute treated effluent. Babson et al. (2013) performed an energy balance of an anaerobic digestion system that incorporates ammonia separation and recovery with ammonia conversion to hydrogen (Anaerobic

Digestion-Bioammonia to Hydrogen (ADBH). The study showed that at a C: N ratio of 17 or less the energy output from the ADBH system was greater than AD generating methane alone. Ammonia, in addition to methane, could be an alternative fuel source for hydrogen production. Therefore, optimization of AD reactors treating high-N wastes could allow ammonia to be captured for energy recovery more efficiently.

The challenge is how to operate stable anaerobic treatment of high-N waste while capturing ammonia as an energy source. One possibility is to optimize the blend of feedstocks (i.e., high-N blended with low-N wastes), and thus maintain low ammonia concentrations in the digesters. If ammonia does build up and cause inhibition and process instability, strategies for optimizing recovery of the AD process are available. The presence of counter ions in the reactor liquid also enhanced tolerance of certain microbial strains to ammonia. It was found that methane synthesis activity in K^+ depleted cells of *Methanospirillum hungatei*, an ammonia sensitive archaeal strain, was recovered by adding Ca^{2+} or Mg^{2+} to the culture (Sprott and Patel 1986).

In addition to divalent cation addition, bioaugmentation is another approach reported to overcome or prevent ammonia inhibition. Bioaugmentation is a technique that adds exogenous, beneficial microorganisms to an engineered process. One approach is to immobilize the beneficial microbial culture on granules to allow a highly concentrated biomass source (Stephenson and Stephenson 1992). In a simpler approach, Nielsen and Angelidaki (2008) concluded that dilution with fresh manure (perhaps providing additional active microbes) improved operation of an ammonia-inhibited anaerobic digester treating cattle manure. More methane was produced compared to dilution with digested manure and water, even though fluctuations in volatile fatty acids were

observed. A recent study by Fotidis et al. (2013) investigated bioaugmentation of anaerobic reactors with a specific ammonia tolerant syntrophic acetate-oxidizing (SAO) co-culture (i.e., *Clostridium ultunense* spp. nov. grown with a fast-growing hydrogenotrophic methanogen *Methanoculleus bourgensis* MS2^T). When subjected to high ammonia loadings (3-5 g NH_4^+-N/L) in fed-batch reactors, bioaugmentation reduced the lag period and the maximum growth rate (μ_{max}) was increased by more than 40%. On the other hand, bioaugmentation using *Clostridium ultunense* spp. nov. grown with a slower growing hydrogenotrophic methanogen, *Methanoculleus* spp. strain MAB1, to an upflow anaerobic sludge blanket (UASB) reactor was not successful. In a third recent study, bioaugmentation with an SAO culture added to reactors exposed to increasing ammonia up to 11 g NH_4^+-N/L, did not protect reactors against instability. Even in un-bioaugmented reactors under ammonia stress the microbial community eventually shifted from the initial primarily aceticlastic pathway to syntrophic acetate oxidation (SAO) (Westerholm et al. 2012). These studies all revealed the fact that adaptation of methanogenic microbial communities can occur in high ammonia reactors. In addition, operating parameters and especially types of methanogens present in the reactors appear to play one of the most important roles in protecting reactors from upset.

Although current research has at its disposal the use of highly sensitive molecular techniques to monitor microbial communities, the idea of identifying and manipulating the microbial community to improve stability of AD is not new. For example, decades ago, Velsen (1979) reported adaptation of methanogenic sludge to high ammonium nitrogen (5 g NH_4^+-N/L) in anaerobic reactors inoculated with digested piggery manure and sewage sludge. Thus,

the work performed for this dissertation builds on a long history of efforts to improve AD technology.

A driving hypothesis of this study is that anaerobic digesters can be operated at high ammonia concentrations once microbial communities have acclimated or ammonia tolerant organisms have had time to increase in population size. One important question is whether all communities can make that shift—are ammonia tolerant organisms found everywhere? Or, is bioaugmentation beneficial for some systems? Thus, it is important to gain a better understanding of the identities of microorganisms tolerant to high ammonia concentration and how widely distributed they are in anaerobic systems. This knowledge will allow engineering advances to be made in improving anaerobic treatment with the goal of allowing higher ammonia concentrations to exist in digesters that could then allow more efficient and economical recovery of ammonia for energy or fertilizer utilization.

1.3 Goal and Objectives

The overall goal of this study was to enrich and identify microbial communities (bacteria and archaea) tolerant to high ammonia concentrations from different engineered waste treatment systems. Knowledge of how microbial communities change in response to ammonia stress and determining whether established systems harbor ammonia-tolerant members will aid in operating stable anaerobic reactors treating high nitrogen content wastes. The specific objectives of the dissertation were:

(1) To characterize microbial communities (bacteria and archaea) that become dominant under different ammonia concentrations in anaerobic enrichments

established from various sources including two landfill leachates, a municipal wastewater treatment plant sludge digester, and a swine waste digester;

(2) To link microbial communities in ammonia-stressed anaerobic enrichments to operating parameters including methane production and volatile fatty acid production;

(3) To determine if divalent cation addition (Mg^{2+} and Ca^{2+}) can counteract toxicity of ammonia in anaerobic enrichments established from a swine waste digester.

1.4 Dissertation Overview

This dissertation consists of five chapters.

Chapter 1 - Introduction

Chapter 2 - Literature Review

Chapter 3 - Ammonia Tolerant Microorganisms in Two Landfill Leachates

Chapter 4 - Ammonia Tolerant Microorganisms from Swine Waste Digestate and Wastewater Sludge Digestate Inocula

Chapter 5 - Divalent Cation Effects to Counteract Ammonia Toxicity

Chapter 6 - Conclusions and Environmental Implications

Chapter 2 Literature Review

2.1 Anaerobic Digestion Process

Anaerobic digestion (AD) of waste consists of three basic steps (Figure 2.1) (Rittmann and McCarty 2001): (1) hydrolysis, (2) fermentation (acidogenesis), and (3) methanogenesis. *Hydrolysis* is the first process involving consortia of microorganisms that hydrolyze complex organic matter such as lipids, polysaccharides, and protein to simple organics such as fatty acids, monosaccharides, and amino acids. Then *fermentation* (acidogenesis) is a second step by which fermentative bacteria ferment simple organic substrates (monomers) to organic acids or short-chain volatile fatty acids (VFAs) (acetate, propionate, butyrate), H_2, and CO_2. The VFAs such as propionate and butyrate serve as both electron donors and acceptors and are further fermented to acetate, H_2, and CO_2 as the final products of fermentation processes. At this stage, acetogens sometimes called "homoacetogens" may also use CO_2 to oxidize H_2 and form only acetate (Ragsdale and Pierce 2008). Acetate can also be utilized by acetogens via syntrophic acetate oxidation (SAO) to form H_2 and CO_2. The last step in anaerobic digestion is *methanogenesis* carried out by methanogens to produce CH_4 and CO_2. There are two groups of methanogens: (1) aceticlastic methanogens, which metabolize the methyl group of acetate to methane and the carboxyl group of acetate to CO_2 and (2) hydrogenotrophic methanogens, which metabolize H_2 as an electron donor and CO_2 as an electron acceptor to form methane. The stoichiometry of anaerobic digestion reactions of organic matter (using $C_6H_{12}O_6$ as a model) may be summarized as follows (Angenent et al. 2004):

Hydrogen fermentation to acetic acid

$$C_6H_{12}O_6 + 2H_2O \rightleftarrows 4H_2 + 2CH_3COOH + 2CO_2 \quad \text{Eq. 2.1 (a)}$$

Hydrogen fermentation to butyric acid

$$C_6H_{12}O_6 \rightleftarrows 2H_2 + CH_3CH_2CH_2COOH + 2CO_2 \quad \text{Eq. 2.2 (a)}$$

Fermentation to ethanol

$$C_6H_{12}O_6 \rightleftarrows 2CH_3CH_2OH + 2CO_2 \quad \text{Eq. 2.3 (a)}$$

Propionic acid production with hydrogen

$$C_6H_{12}O_6 + 2H_2 \rightleftarrows 2CH_3CH_2COOH + 2H_2O \quad \text{Eq. 2.4 (a)}$$

Syntrophic propionic acid oxidation

$$CH_3CH_2COOH + 2H_2O \rightleftarrows CH_3COOH + 3H_2 + CO_2 \quad \text{Eq. 2.5 (b)}$$

Syntrophic butyric acid oxidation

$$CH_3CH_2CH_2COOH + 2H_2O \rightleftarrows 2CH_3COOH + 2H_2 \quad \text{Eq. 2.6 (b)}$$

Syntrophic acetic acid oxidation

$$CH_3COOH + 2H_2O \rightleftarrows 4H_2 + 2CO_2 \quad \text{Eq. 2.7 (c)}$$

Aceticlastic methanogenesis

$$CH_3COOH \rightleftarrows CH_4 + CO_2 \quad \text{Eq. 2.8 (d)}$$

Hydrogenotrophic methanogenesis

$$4H_2 + CO_2 \rightleftarrows CH_4 + 2H_2O \quad \text{Eq. 2.9 (e)}$$

The letter in parenthesis is the reaction shown in Figure 2.1.

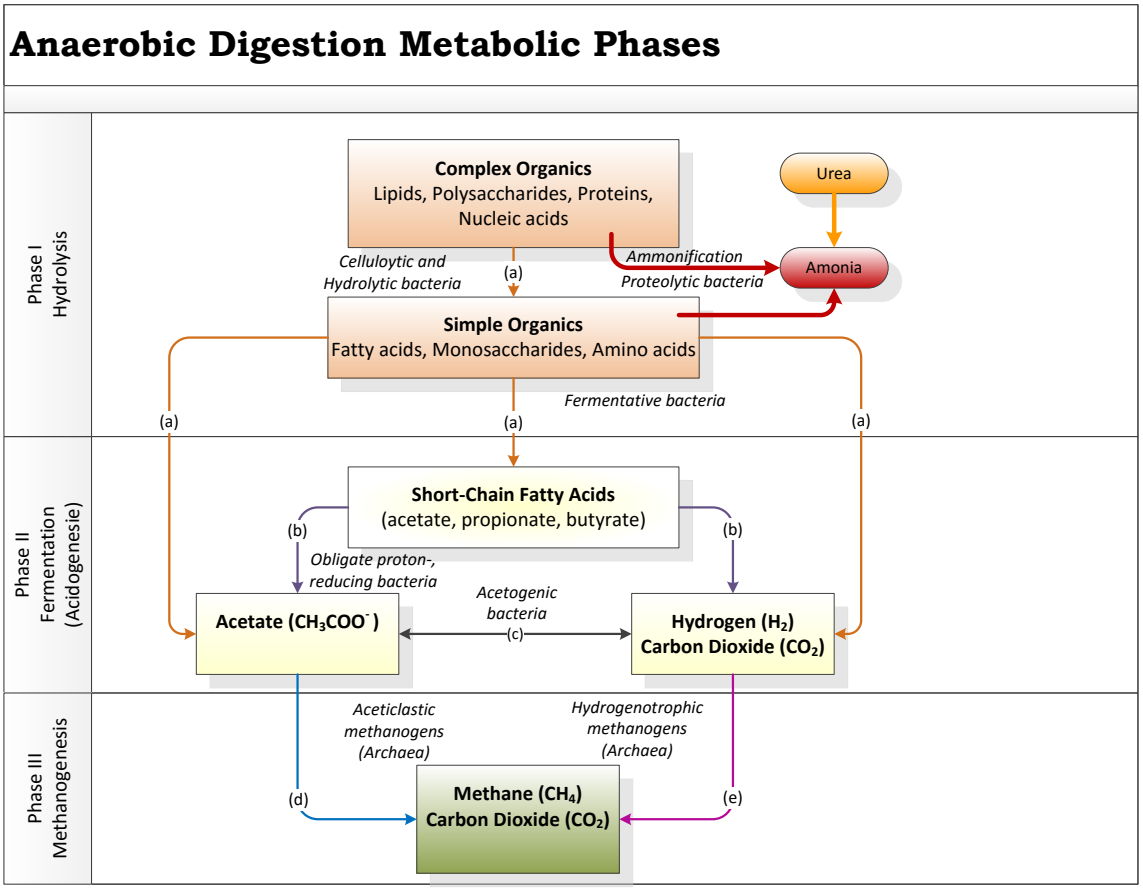

Figure 2.1 Anaerobic digestion metabolic phases

(modified from Klass 1984, Stams 1994, Rittmann and McCarty 2001)

Anaerobic digestion involves different groups of microorganisms. The thermodynamics and kinetics governing the various reactions are essential to the effectiveness of the operation of the mixed microbial community, and this is highly dependent on the original organic matter composition (Rittmann and McCarty 2001), especially the fiber content in the cell wall of the original organic matter (Bufflere et al. 2006). AD of agricultural wastes thus has hydrolysis as a rate-limiting step because of the recalcitrance of the lignin fraction of the waste under anaerobic conditons. Conversely,

AD of wastewaters and sludges tend to have methanogenesis as a rate-limiting step since the energy available to methanogens is less than that available to hydrolytic and fermentative organisms and since the methanogens tend to be slow growing. The kinetics of biogas production suggests that the degradation can be described by a simple first-order reaction (Weiland 2010). However, different groups of bacteria and methanogens may not proceed through the first-order reaction when fermenting complex wastes, as was observed in a study of digestion of apple and orange production residues (Bufflere et al. 2006). Since anaerobic operation is driven by the structure and activity of the different microorganisms, it is important to balance microbial populations to maintain AD performance.

The performance of anaerobic digesters can be evaluated by several indicators such as pH, the VFA concentrations, and methane production, which can be represented as the Biochemical Methane Potential (BMP) value. During the start-up period, the reactor should be maintained at certain pHs and VFA concentrations. The pH range should be between 6.5-8.5 with an optimum pH of 6.8-7.2 (Santosh et al. 2004, Weiland 2010). The VFA concentration is a key indicator of system performance and process instability (Ahring et al. 1995). These organic acids have been termed volatile acids because of their capabilities to be distilled from boiling water in their un-ionized form. Acetic, propionic, and butyric acids are the major VFAs during AD treatment (Barredo and Evison 1991) and are mainly presented in high concentrations as intermediates during start-up or overloading conditions (Rittmann and McCarty 2001). The concentration of VFAs, particularly acetic acid, should be below 2,000 mg/L for stable operation (Santosh et al. 2004).

The BMP value is an indicator of process performance. It is a measure of substrate biodegradability determined by monitoring cumulative methane production from an anaerobically incubated sample (Owen et al. 1979) and can be expressed as the amount of methane produced per gram of volatile solids (VS) (Bufflere et al. 2006, Lesteur et al. 2010). Owen et al. (1979) described anaerobic bioassay techniques for assessing methane potential and found that the digestibility of alkaline pretreated peat increased with increasing treatment temperature. In addition, the BMP value can be used to define the organic loading rate (OLR), and methane production kinetics. However, BMP is a relatively time consuming test (about 30 days). Therefore, a combination of pyrolysis-UV oxidation and near-infrared (NIR) spectrometry was recently introduced as a method to indicate methane potential of feedstocks (Lesteur et al. 2010). The pyrolysis-UV step accelerates the degradation process and NMR was used to characterize organic matter components. Together these processes were intended to increase the sensitivity, selectivity and speed of obtaining the BMP value.

Other factors controlling the performance of AD are temperature, C:N ratio, and hydraulic retention time (HRT) (Santosh et al. 2004). Temperature plays an important role in biogas production with commercial digestion facilities typically operated under mesophilic (35°C) or thermophilic (55°C) conditions. A C:N ratio of 20-30:1, with the largest percentage of the carbon being readily degradable, has been suggested for the most stable AD performance (Santosh et al. 2004). HRT is the average time spent by the input slurry inside the digester. A shorter HRT may risk washout of active biomass from the digester while a longer HRT (30-50 days) requires a larger volume of the digester, hence more capital cost (Santosh et al. 2004). An AD study of sewage sludge as a

feedstock indicated that digester failure under volumetric stress (decreasing HRT) is dissimilar to the failure under organic stress loading (increasing OLR) (Kidby and Nedwell 1991). Under volumetric overload by sewage sludge, H_2 did not accumulate when biogas and methane production initially decreased, rather H_2 accumulated after reactor failure had occurred. Thus, the use of H_2 as an early warning parameter may be of limited value in sewage sludge digesters. This study suggested, however, that monitoring of H_2 concentration may be exploited with reactors treating high organic wastes.

2.2 Ammonia Toxicity

Anaerobic processes are sensitive to pH and a variety of inhibitory substances (Tchobanoglous et al. 2003). High alkalinity is required to assure that pH is maintained near neutrality for better AD performance. The breakdown of protein and amino acids normally produce ammonia, which forms alkalinity. When ammonia combines with CO_2 and H_2O, the $NH_4(HCO_3)$ that is produced can act as a natural pH buffer. However, ammonification of high protein content wastes may cause toxicity to the system when excessive ammonia is produced (Figure 2.1). It has been suggested that the un-ionized form of ammonia (NH_3) more often causes inhibition because of its capability to penetrate through the cell membrane (Kadam and Boone 1996). The ionized form of NH_3 is ammonium ion (NH_4^+). Whether NH_3 or NH_4^+ is more inhibitory to the anaerobic process depends on the distribution of the two species.

$$NH_4^+ \rightleftarrows H^+ + NH_3 \qquad \text{Eq. 2.10}$$

The summation of NH_3 and NH_4^+ is represented by total ammonia nitrogen (TAN).

$$[\text{TAN}] = [\text{NH}_3] + [\text{NH}_4^+] \qquad \text{Eq. 2.11}$$

The relative concentration of NH_3 is a function of pH and dissociation constant (K_a).

$$[\text{NH}_3\text{-N}] = \frac{[TAN]}{1+\frac{[\text{H}^+]}{[\text{Ka}]}} \qquad \text{Eq. 2.12}$$

K_a of ammonia in water at 25°C = $10^{-9.26}$ and at 35°C = $10^{-8.95}$

At high pH and high temperature, TAN is made up of a relatively higher proportion of NH_3-N.

Examples of literature reports describing ammonia inhibition in anaerobic digesters are shown in Table 2.1

Table 2.1 Threshold values of ammonia inhibition in different systems

Parameters	Treatment	Threshold Value (g-N/L)	References
NH_3	Acetate, pH 7.9	0.15	(McCarty and McKinney (1961)
	Swine manure, pH 8.0, thermophilic	1.1	(Hansen et al. 1998)
	Cattle manure, pH 7.7, thermophilic	0.65	(Angelidaki and Ahring 1993)
	Beet-sugar wastewater, pH 7.5, mesophilic	0.08	(Koster and Lettinga 1984)
	Organic household waste, pH 7.6, mesophilic	0.22-0.28	(Gallert and Winter 1997)
NH_4^+	Beet-sugar wastewater, pH 7.5, mesophilic	1.7	(Koster and Lettinga 1984)
	Sewage sludge, pH 7.2-7.4, mesophilic	1.21-2.36	(Velsen 1979)
TAN	Cattle manure, pH 7.7, thermophilic	>4	(Angelidaki and Ahring 1993)
	Synthetic wastewater, pH 6.5-8.0, thermophilic	>4	(Sung and Liu 2003)
	Food waste, pH 7.5, mesophilic	>3.78	(Sheng et al. 2013)

Table 2.2 Reported and calculated threshold values of ammonia inhibition in mesophilic systems

pH	Treatment	Threshold Value (g-N/L)			References
		NH_3	NH_4^+	TAN	
7.3	Sewage sludge	0.04[b]	1.79[a]	1.8[b]	(Velsen 1979)
7.5	Beet-sugar wastewater	0.06[b]	1.7[a]	1.76[b]	(Koster and Lettinga 1984)
	Beet-sugar wastewater	0.08[a]	2.25b	2.3[b]	(Koster and Lettinga 1984)
	Food waste	>0.13[b]	3.62[b]	>3.78[a]	(Sheng et al. 2013)
7.6	Organic household waste	0.22-0.28[a]	4.92-6.27[b]	5.14-6.55[b]	(Gallert and Winter 1997)

[a] reported value

[b] calculated value

The difference in ammonia inhibition thresholds that have been reported can be attributed to the differences in feedstocks and inocula concentrations, temperature, pH, and acclimation conditions. For example when NH_3 concentration was high, reducing the operating temperature below 55°C resulted in an increase in biogas yield as methanogenic activity increased (Angelidaki and B.K.Ahring 1994, Garcia and Angenent 2009). Reactor process stability was also greater with lower VFA concentrations.

Ammonia inhibition or an overload on the system is often evidenced through an increase in organic acid concentrations. VFA accumulation in anaerobic reactors is generally the result of a process imbalance, and may not be the original cause of inhibition (Ahring et al. 1995). An increase in VFA concentration will lead to a decrease

in pH and inhibition of methanogenesis, and perhaps also of hydrolysis/acidogenesis (Fotidis et al. 2013). Sung and Liu (2003) found that as TAN concentrations increased to 5.77 g N/L, VFAs accumulated as high as 2,730 mg as acetic acid/L and caused a decrease in pH and alkalinity. Acetic acid is usually present at high concentration, while propionic acid and butyric acid, which are present at lower concentrations, are more inhibitory to methanogens (Weiland 2010). It was also reported that VFA inhibition is associated with their undissociated (protonated) forms. For example, inhibition of propionate utilization was attributed to toxicity of undissociated propionic acid (Fukusaki et al. 1990). Thus, in AD systems with a low pH value, the inhibiting effect of VFAs is potentially much greater than in digesters operating at higher pH values (Weiland 2010).

2.3 Strategies for Overcoming Ammonia Toxicity

Several strategies for overcoming ammonia toxicity in AD have been reported. Anaerobic co-digestion of different waste streams to control the C:N ratio at a level that results in uninhibitory ammonia concentrations has been reported, and is quite common. For example, blending of biodiesel waste glycerin with municipal wastewater sludge (Razaviarani and Buchanan 2015), solid slaughterhouse waste and manure with fruit and vegetable wastes (Alvarez and Liden 2008), swine waste and paper sludge (Parameswaran and Rittmann 2012), and food and landscape waste (Drennan and DiStefano 2014), have been investigated. In another control strategy (with respect to VFA concentrations), an ammonia-inhibited continuously stirred tank reactor (CSTR) treating cattle manure recovered after dilution of the biomass with reactor effluent (Nielson and Angelidaki 2008). In contrast, Nielson and Angelidaki (2008) concluded that dilution

with fresh manure (perhaps providing additional active methanogens) improved methane production in an ammonia-inhibited anaerobic digester treating cattle manure, even though fluctuations in volatile fatty acids were observed. It also has been reported that increasing the HRT increased the methane yield during swine manure digestion at 4.6 g TAN/L (Hansen et al. 1999). In addition to ammonia, sulfide produced during AD may also inhibit biogas production. Addition of activated carbon or $FeCl_2$ could counteract the inhibition via adsorption or subsequent precipitation as FeS (Hansen et al. 1999). These strategies may also benefit AD under ammonia stress. For example, Ortner et al. (2014) reported that $FeCl_2$ addition during anaerobic digestion of N-rich slaughterhouse waste resulted in decreasing VFAs from 10,000 mg/L to 700 mg/L, with increasing specific methane yields, within three weeks.

Elements such as potassium, calcium, and magnesium are important requirements for growth of microorganisms. The desired concentration in AD for calcium is generally 100-200 mg/L and for magnesium is 75-250 mg/L (McCarty 1964). Reactor failure from high ammonia concentration was also decreased by addition of divalent ions such as magnesium (Mg^{2+}) and calcium (Ca^{2+}), which appeared to be antagonistic to ammonia toxicity (McCarty and McKinney 1961). Divalent ion antagonism may be an important phenomenon in acetate fermentation. High rates of acetate utilization were obtained in the presence of low concentrations of calcium, magnesium, ammonium, and potassium ions in the seed sludge during acclimation (McCarty and McKinney 1961). Divalent ions could bridge between negatively charged groups on cell surfaces, thus resulting in microbial aggregation (Mahoney et al. 1987, Yu et al. 2001). Cation antagonism effects resulted in successful digestion of sewage sludge and swine manure at ammonia nitrogen

concentrations in excess of 1,500 mg/L (Velsen 1979). Addition of calcium was reported to decrease ammonia toxicity to methane synthesis in cell suspensions of *Methanothrix concilii*, an ammonia sensitive aceticlastic methanogen (Sprott and Patel 1986) (Figure 2.2). In addition, magnesium, an important ion present in many enzymes catalyzing ATP-dependent reactions, may stabilize proteins in the presence of denaturing concentrations of ammonia (Kadam and Boone 1996).

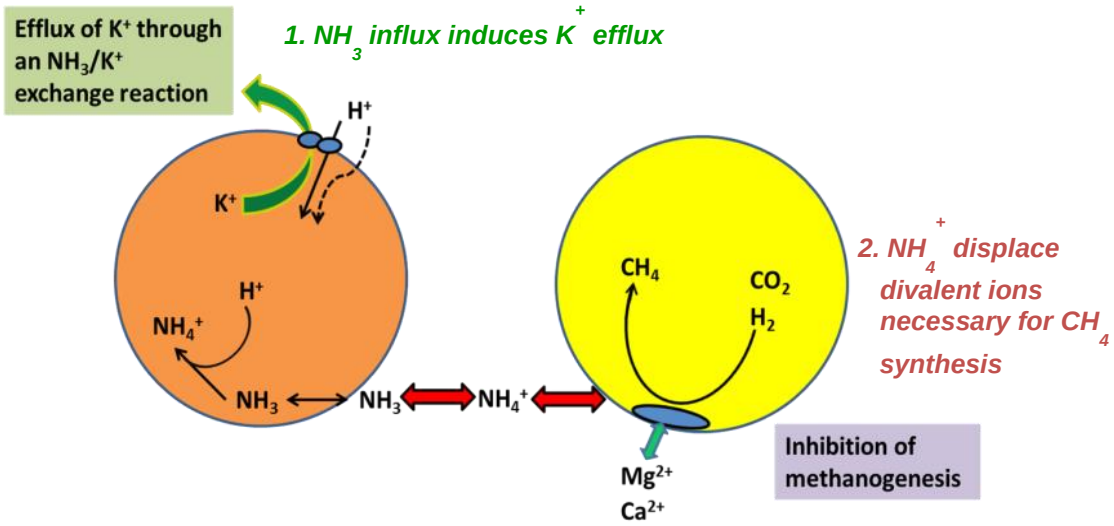

Figure 2.2 Models hypothesized to illustrate two separate interactions of ammonia with *Methanospirillum hungatei* cells (Sprott and Patel 1986)

2.4 Energy Conservation in AD

Different groups of microorganisms are known to be involved in the AD processes (Figure 2.1). The mixed communities include fermentative bacteria, obligate proton-reducing bacteria, acetogens, and methanogens. Since methanogenic conversion in AD provides only a small amount of energy, these microorganisms are forced into an efficient cooperation. Syntrophic relationships occur between methanogens and certain hydrogen-producing bacteria when methanogens utilize hydrogen produced by the bacteria, maintaining a low partial pressure of hydrogen ($H_2 < 10^{-4}$ atm) that provides for a thermodynamically favorable reaction (Tchobanoglous et al. 2003). As a result, the fermentation reactions proceed. This utilization of H_2 by methanogens is termed *interspecies hydrogen transfer* (McInerney and Bryant 1981). Several examples of this process are discussed below.

Methanogenesis from acetate to CH_4 and CO_2 can occur through two processes. The first process is aceticlastic methanogenesis where acetate is oxidized to CH_4 and CO_2. This reaction is an exergonic reaction ($\Delta G^{0'}$ = -31.0 kJ/mol acetate) and only for systems at moderate temperature and low salt contents (Worm et al. 2010). It was reported that only a few species are known to carry out this process, e.g., *Methanosarcina barkeri, Methanonococcus mazei*, and *Methanothrix soehngenii* (Tchobanoglous et al. 2003); and *Methanosaeta sp.* (Fotidis et al. 2013, Hattori 2008). The second process by which acetate may be converted to methane is composed of two reactions—syntrophic acetate oxidation (SAO) and hydrogenotrophic methanogenesis. The biochemistry of SAO is a reversal of the homoacetogenic acetate formation pathway (so-called Wood-

Ljungdahl pathway or CO-dehydrogenase pathway) (Ragsdale and Pierce 2008, Worm et al. 2010). In SAO, both methyl and carboxyl groups of acetate are oxidized to CO_2 and H_2 by syntrophic acetate-oxidizing bacteria (SAOB). The reaction is extremely unfavorable ($\Delta G^{0'}$ = +104.6 kJ/mol acetate) under standard conditions. However, this reaction can proceed when hydrogenotrophic methanogens consume the H_2 produced ($\Delta G^{0'}$ = -135.6 kJ/mol H_2). Thus, the overall reaction becomes exergonic with the same stoichiometry as acetoclastic methanogenesis ($\Delta G^{0'}$ = -31.0 kJ/mol acetate) (Hattori 2008). This is another example of interspecies hydrogen transfer where in this case the energy is shared by syntrophic acetate-oxidizing bacteria and hydrogenotrophic methanogens. The low amount of energy available explains why these syntrophs are slow growers and difficult to isolate (Hattori 2008). In addition, temperature and concentration of substrates and products, are additional factors affecting the energy available to the syntrophic acetate oxidizer and partner methanogens. The Gibbs free energy change ($\Delta G'$) for syntrophic acetate-oxidation becomes more favorable under lower H_2 partial pressures and higher temperatures, while that of the H_2-consuming methanogenesis becomes unfavorable under the same conditions (Hattori 2008).

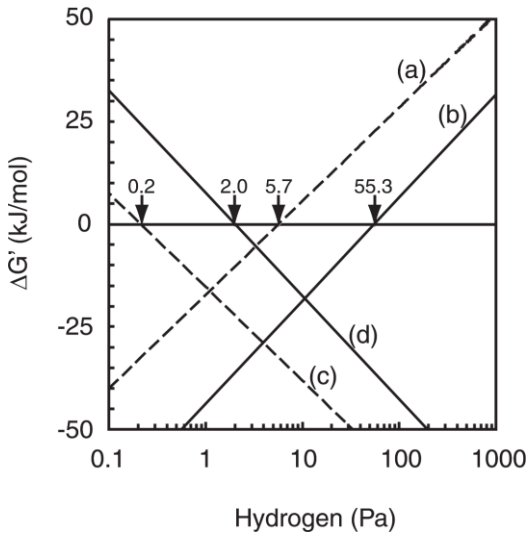

Figure 2.3 Effects of temperature and hydrogen partial pressure on the Gibbs free energy change (ΔG') for the oxidation of acetate to H_2/CO_2 or methanogenesis from H_2/CO_2. Acetate oxidation to H_2/CO_2 at (a) 25°C and (b) 55°C. Methanogenesis from H_2/CO_2 at (c) 25°C and (d) 55°C. Arrows represent the H_2 partial pressure (Pa) at which ΔG' for the reactions is zero (Hattori 2008)

Propionate is another key intermediate that is produced during AD. Oxidation of propionate must occur in coculture with hydrogen-utilizing methanogens. The propionate-degrading bacterium, *Syntrophobacter wolinii*, was reported to produce acetate, CO_2, and H_2 (or formate) from propionate in coculture with *Methanospirillum hungatei* (Boone and Bryant 1980). To make the energy yield from propionate oxidation favorable, the concentrations of H_2 and formate must be extremely low (10^{-6} to 10^{-4} atm or 0.1 to 10.1 Pa) (Fig. 2.2) and this can be achieved by creating precipitates to shorten the interbacterial distances or via presence of hydrogenotrophic methanogens (Bok et al. 2004).

2.5 Microbial Community Structure and Interactions under Ammonia Stress

Ammonia at high concentrations is considered toxic to methanogens (Calli et al. 2005, Fotidis et al. 2013, Prochazka et al. 2012). However, the toxic effect of ammonia may be diminished by acclimation or adaptation of the population (Gallert et al. 1998, Westerholm et al. 2011b). Sung and Liu (2003) studied the combined effects of TAN, pH, and acclimation on methanogenic activity. It was reported that acclimation influenced the degree of ammonia inhibition. Koster and Lettinga (1984) stated that acetotrophic methanogens are more sensitive to NH_4^+-N than hydrogenotrophic methanogens. Hydrogenotrophic methanogens dominate in most agricultural AD systems at high ammonia concentrations whereas acetotrophic methanogens can be observed only in low ammonia concentration AD systems (Weiland 2010). However, upon acclimation to acetate and ammonia (7 g NH_4^+-N/L), a shift in the bioconversion pathway for acetate resulted in the dominance of *Methanosarcina sp.*, which can also utilize H_2 and CO_2 (in addition to acetate) to produce methane (Fotidis et al. 2013). Microbial community dynamics during an ammonia induced (5.2 g TAN/L or 0.25 g NH_3-N/L) shift to SAO revealed that the bacterial community structure changed continuously throughout the time series with systematic changes in community evenness and functional content (Werner et al. 2014). In addition, bacteria from the Bacteroidetes and Firmicutes were the most diverse phyla and were also the most abundant (Werner et al. 2014).

Additional evidence of ammonia acclimation was observed through monitoring COD removal efficiency in reactors. Calli et al. (2005) found high COD removal

efficiencies (78-96%) in UASB reactors treating wastewater after seed sludges had been allowed to adapt to elevated concentrations of free ammonia up to 0.8 g N/L. However, propionate accumulated when free ammonia was greater than 0.2 g N/L, because propionate degrading acetogenic bacteria were apparently inhibited. This result is in accord with reports from Koster and Lettinga (1984) and Fukuzaki et al. (1990) who concluded that propionic acid can only be degraded at extremely low hydrogen concentrations (10^{-6} to 10^{-4} atm or 0.1 to 10.1 Pa). These low concentrations only exist when hydrogenotrophic methanogens are not inhibited by overloaded ammonia. Fukuzaki et al. (1990) noted that both hydrogenotrophic and acetoclastic methanogens might play a role in enhancing degradation of propionate to CH_4 and CO_2. In addition, Lier et al. (1993) also reported that propionate degradation deteriorated when the propionate-oxidizing acetogens and/or the hydrogenotrophic methanogens are inhibited. The influence of the microbial community structure on process stability and biogas yield, under different reactor conditions requires further efforts and detailed analysis to fully understand all the relationships (Fotidis et al. 2013, Weiland 2010).

2.6 Glutamate Degradation and Microbial Energetics

High-N wastes may consist, in part, of proteins. Anaerobic digestion of proteins, which consist of about 20 structurally different amino acids, requires distinct biochemical pathways (Worm et al. 2010). The combined oxidation and reduction of pairs of amino acids (Stickland reaction) is a well-known mechanism by which proteolytic *Clostridia* degrade amino acids (Worm et al. 2010). Deamination is the first step in the degradation of amino acids performed by anaerobic bacteria in three ways: 1) oxidative NAD(P)-

dependent deamination of alanine, valine, leucine, or isoleucine leads to fatty acids, ammonia, and H_2 products; 2) reductive deamination, in which reducing equivalents are used to convert an amino acid to its corresponding fatty acid, with concomitant production of ammonia; and 3) redox-neutral reaction resulting in the production of a keto acid (Worm et al. 2010).

In the work described in this dissertation, glutamate was used as a model nitrogen-containing substrate. Glutamate is an abundant amino acid in protein. Weng and Jerist (1976) investigated the biochemical mechanisms of L(+)-glutamic acid degradation in AD using ^{14}C labeled compounds and concluded that glutamic acid was degraded to CH_4 and CO_2 through mesaconic, pyruvic, lactic, propionic and acetic acids. Two moles of acetic acid were produced for each mole of glutamic acid metabolized and represented the major volatile acid intermediate. Several studies have reported that glutamate is fermented by a variety of anaerobic bacteria. Glutamate is fermented to acetate and butyrate by members of the class Clostridia known as hydrogen producers supplying hydrogen as a substrate to hydrogenotrophic methanogens (Kim et al. 2014, Madigan and Martinko 2006, Worm et al. 2010). *Thermanaerovibio acidaminovorans* also oxidizes glutamate to propionate in syntrophic association with hydrogen scavenger *Methanobacterium thermoautotrophicum* (Baena et al. 1999). In addition, glutamate is oxidized to acetate, CO_2, NH_4^+, traces of propionate and H_2 by *Caloramator coolhaasii* (Plugge et al. 2000); and to acetate, propionate, H_2, CO_2, and traces of succinate by *Gelria glutamica* (Plugge et al. 2002) in co-culture with *Methanobacterium thermoautotrophicum* Z-245^T. The free energy for the conversion of glutamate at 55°C is as follows (Plugge et al. 2002):

$Glutamate^- + 3H_2O \rightarrow 2acetate^- + HCO_3^- + H^+ + NH_4^+ + H_2$ Eq. 2.13

At 10^5 Pa H_2, $\Delta G' = -41.6$ kJ …… (a)

1 Pa H_2, $\Delta G' = -73.1$ kJ …… (b)

$Glutamate^- + 4H_2O \rightarrow propionate^- + 2HCO_3^- + NH_4^+ + 2H_2$ Eq. 2.14

At 10^5 Pa H_2, $\Delta G' = -16.0$ kJ …… (a)

1 Pa H_2, $\Delta G' = -79.0$ kJ …… (b)

From Eq. 2.11 (a), the reaction is shown to yield a low amount of energy (-16.0 kJ/mol glutamate) at 10^5 Pa H_2. In syntrophy with methanogens (Eq. 2.11 (b), the free energy available is higher (-79.0 kJ/mol glutamate), since the hydrogen formed is consumed via interspecies hydrogen transfer.

Theoretical methane production

A stoichiometric equation for microbial synthesis and growth when glutamate is used as an electron donor and CO_2 is used as an electron acceptor follows Equation 2.12. Ammonium is also used as a nitrogen source for synthesis in this reaction (Rittmann and McCarty 2001).

$$R = f_e R_a + f_s(R_c - R_d) \quad \text{Eq. 2.15}$$

where R is a complete reaction

f_e is the fraction of the election-donor substrate used for energy generation

f_s is the fraction of the election-donor substrate used for synthesis

R_a is the electron acceptor half-reaction

R_c is the cellular biosynthesis half-reaction

R_d is the electron-donor substrate half-reaction

Calculation of the theoretical methane production is as follows:

$R_a: \ \frac{1}{8}CO_2 + H^+ + e^- \rightarrow \frac{1}{8}CH_4 + \frac{1}{4}H_2O$ Eq. 2.16

$R_c: \ \frac{1}{5}CO_2 + \frac{1}{20}HCO_3^- + \frac{1}{20}NH_4^+ + H^+ + e^- \rightarrow \frac{1}{20}C_5H_7O_2N + \frac{9}{20}H_2O$ Eq. 2.17

$-R_d: \ \frac{1}{18}C_5H_9NO_4 + \frac{4}{9}H_2O \rightarrow \frac{1}{6}CO_2 + \frac{1}{9}HCO_3^- + \frac{1}{18}NH_4^+ + H^+ + e^-$ Eq. 2.18

Assuming f_s = 0.08, f_e = 1-0.08 = 0.92 (Rittmann and McCarty 2001)

Then, $R = 0.056C_5H_9NO_4 + 0.178H_2O \rightarrow 0.004C_5H_7O_2N + 0.115CH_4 + 0.052CO_2 + 0.052NH_4^+ + 0.107HCO_3^-$ Eq. 2.19

The theoretical methane production is thus $\frac{0.115\ mol\ CH_4}{0.056\ mol\ glutamate} = 2.053\ mol\ CH_4$ from 1 mol of glutamate.

Carbonaceous oxygen demand (COD')

The amount of energy released from oxidation-reduction reactions of microorganisms per electron equivalent of an electron donor varies from reaction to reaction (Rittmann and McCarty 2001). A parameter such as carbonaceous oxygen demand (COD') is related to the electron equivalents of an electron donor or substrate oxidized, in this case, glutamate.

Calculation of COD' is as follows:

Organic half-reaction of glutamate (Rittmann and McCarty 2001):

$$\frac{1}{6}CO_2 + \frac{1}{9}HCO_3^- + \frac{1}{18}NH_4^+ + H^+ + e^- \rightarrow \frac{1}{18}COOHCH_2CH_2CHNH_2COO^- + \frac{4}{9}H_2O$$

Eq. 2.20

From Eq. 2.17, there are 18 e^- *eq*/mol glutamate.

Molecular weight of glutamate ($C_5H_9NO_4$) = 147.13 g/mol

Thus, the equivalent weight is $\frac{147.13\ g/mol}{18e^{-}eq/mol} = 8.17\ g/e^{-}eq$

if 1 mmol of glutamate was added to the reactor with 100 mL working volume,

the concentration of glutamate in the reactor is $\frac{1\ mmol\ glu \times \frac{147.13\ g}{mol\ glu}}{100\ mL} = 1.4713\ g/L$

or the concentration of glutamate in the reactor is $\frac{1.4713\ g/L}{8.17\ g/e^{-}eq} = \frac{0.18\ e^{-}eq}{L}$

One equivalent of any electron donor is equivalent to an oxygen demand of 8 g as O_2

Thus, the COD' becomes $\frac{0.18\ e^{-}eq}{L} \times \frac{8\ g\ OD}{e^{-}eq} = 1.44\ g\ COD'/L$

2.7 Bioaugmentation to Overcome Ammonia Inhibition

Microbial community shifts from aceticlastic methanogenesis to hydrogenotrophic methanogenesis that occur with increased ammonia loading have been reported (Werner et al. 2014). In addition, increasing ammonia concentrations influenced only acetogenic population structure, not acetogenic abundance (Westerholm et al. 2011b). These studies among others show that ammonia inhibition produces instability in the microbial communities in digesters. AD must operate with stability and reproducability to be a competitive and viable commercial technology. New approaches are needed for investigating the impact of ammonia on microbial populations in digesters (Fotidis et al. 2013), but this also suggests that knowledge of specific, ammonia-tolerant populations that could be propagated in AD reactors would be useful. Bioaugmentation, sometimes called bacterial augmentation or biomass enhancement, is addition of specific microorganisms or enriched consortia to an engineered processes to enhance a desired

activity or outcome (Stephenson and Stephenson 1992, Westerholm et al. 2012). Bioaugmentation is widely used in the field of bioremediation. Bioaugmentation can improve source zone remediation of chlorinated ethene by reducing lag times and costs (Stroo et al. 2012). Groundwater remediation as a robust industry has also been driven by the development of in situ treatment technologies, including bioaugmentation (Leeson et al. 2013). Bioaugmentation has been attempted for wastewater treatment (for a review see Herrero and Stuckey (2015)). In addition, bioaugmentation has abeen investigated for anaerobic digestion. Bioaugmentation with enrichment cultures of ammonia- and humic acid- resistant bacteria *Bacillus cereus* and *Enterococcus casseliflavus* from landfill leachate, was successful as seen from improved chemical oxygen demand (COD) removal efficiency, free ammonia, and humic acid removal rate (Yu et al. 2014a). Bioaugmentation of SAO cultures to anaerobic reactors treating stillage and cattle manure was found to be a possible method for decreasing the adaptation period when operating at high ammonia of 11 g NH_4^+-N/L (Westerholm et al. 2012). In that study, higher abundance of *Clostridium ultunense* and *Tepidanaerobacter acetatoxydans* were observed in the bioaugmented systems, as expected. An SAO co-culture (*Clostridium ultunense* spp. nov. living in association with *Methanoculleus* spp. strain MAB1) was bioaugmented to a mesophilic upflow anaerobic sludge blanket (UASB) reactor subjected to high ammonia concentration (Fotidis et al. 2013). Since the SAO culture contained slow-growing microbes (Schnurer and Nordberg 2008), addition of a fast-growing hydrogenotrophic methanogen *Methanoculleus bourgensis* $MS2^T$ in co-culture with an SAO culture resulted in the success of bioaugmentation up to 5 g NH_4^+-N/L (Fotidis et al. 2013). A summary of bioaugmentation conditions from each study is shown in Table 2.3.

Table 2.3 Summary of bioaugmentation conditions from each study

Ammonia concentration	Culture used	Volume of biomass	Substrates	Length of operation (Days)	Reactor operation	Results	References
3.6 g NH_3-N/L	-Ammonia resistant bacteria *Bacillus cereus* -Humic acid resistant bacteria *Enterococcus casseliflavus*	2 mL (OD_{600}= 1.0) in 20 mL leachate	LB medium	9	Not specified, mesophilic	- 76-90% COD removal rate in 2 days - 50% NH3-N removal rate - 40% humic acid removal rate	Yu et al. (2014b)
1.5-11 g NH_4^+-N/L	-SAO cultures *Clostridium ultunense*, *Tepidanaerobacter acetatoxydans*, *Syntrophaceticus schinkii*, *Methanoculleus* spp. strain MAB1	10 mL/day in 5 L reactor	Whole stillage, Cattle manure	460	CSTR, mesophilic	- No influence on the dominant pathways for acetate degradation - Higher abundances of *C. ultunense* and *T. acetatoxydans* - No operation improvement during periods of increasing ammonia levels	Westerholm et al. (2012)

Ammonia concentration	Culture used	Volume of biomass	Substrates	Length of operation (Days)	Reactor operation	Results	References
5 g NH_4^+-N/L	-SAO cultures *Clostridium ultunense*, *Methanoculleus* spp. strain MAB1, *Methanoculleus bourgensis* $MS2^T$	11 mL/d (OD_{600} =0.3-0.4) in 220 mL reactor	Glucose	154	UASB, mesophilic	- Bioaugmentation of *C. ultunense* with *M.* spp. strain MAB1 was not possible due to the slow maximum growth rate of the methanogenic culture - Addition of *M. bourgensis* $MS2^T$ led to 42% higher growth rate	Fotidis et al. (2013)

Chapter 3 Ammonia Tolerant Microorganisms in Two Landfill Leachates

3.1 Abstract

Ammonia inhibition is a frequent cause of instability in anaerobic waste treatment. Ammonia inhibition has been little studied in landfill ssystems, which are often sources of high ammonia leachate and which we hypothesized could contain ammonia-tolerant microbial communities. Microbial communities tolerant to high ammonia concentrations were enriched from landfill leachate waste streams obtained from New Jersey, USA and Chonburi, Thailand. The material obtained from New Jersey contained landfill leachate from a bioreactor landfill along with liquid leachate from an associated sludge composting facility and domestic sewage produced by the complex. The leachate from Thailand was obtained directly from a traditional landfill. Semi-continuous batch reactors operated at 35°C with a hydraulic retention time of 140 days were inoculated with the leachate and were operated for 300 days with glutamate as a sole model high-nitrogen substrate. Target total ammonia nitrogen (TAN) concentrations of 5 to 12.5 gTAN/L were imposed on the reactors. Microbial community analysis by denaturing gradient gel electrophoresis and 454 pyrosequencing of amplified bacterial and archaeal 16S rRNA genes revealed that community makeup varied in relation to the source of the inoculum, the imposed TAN and to reactor instability evidenced by observed fluctuations in volatile fatty acids concentrations, and methane production. The microbial community enriched from Thailand leachate with an imposed TAN of 12.5 g/L exhibited little acclimation time and produced the same methane volumes as the non-

TAN stressed controls. Phylotypes related to *Tepidanaerobacter acetatoxydans,* an anaerobic, syntrophic acetate-oxidizing (SAO) bacterium in the phylum Firmicutes and *Methanosarcina* spp. (Euryarchaeota) were dominant members of this ammonia tolerant community. In contrast, the microbial community enriched from the New Jersey waste with an imposed TAN of 12.5 g/L exhibited instability and ultimately produced only half of the methane as the non-TAN stressed controls. Here we show that a landfill in Thailand houses ammonia-tolerant organisms that acclimated rapidly to a high N model feedstock and operated with high methane production under an imposed TAN of 12.5 g/L. The New Jersey waste (leachate mixed with composting liquids and domestic wastewater) did not exhibit similar robustness.

3.2 Introduction

In 2011, U.S. energy consumption was about 98 quadrillion BTUs (quads), with over 40 quads used to generate electric power. Of this energy usage, approximately 70% came from fossil fuels (USDOE 2013). Increasing alternative renewable energy sources is therefore a critical challenge. Biogas, a mixture of methane (CH_4) and carbon dioxide (CO_2), could become a more substantial source of renewable energy (Weiland 2010). Methane generated from decaying organic matter is also an important greenhouse gas that should be controlled to meet emissions targets as emphasized in guidance documents including: *Climate Action Plan- Strategy to Reduce Methane Emissions*, released in March 2014 (USDA, USEPA, USDOE 2014).

Anaerobic digestion (AD) is a mature technology for treatment of wastes including wastewater treatment plant sludges (WWTPs) (Foresti et al. 2006) and

industrial and agricultural wastes (Angenent et al. 2004). The same process is responsible for biogas production during landfill operation (Berge et al. 2005). From a total of 2,116 biogas systems currently being operated in the U.S., about 59% (1,241 digesters) are at WWTPs, 30% (636 landfill-based energy projects) are at landfills, and 11% (239 digesters) are on farms (USDA, USEPA, USDOE 2014). During AD, organic N is released as ammonia, which is not further transformed in the absence of oxygen or nitrite. While ammonia can be further treated via nitrification-denitrification or anammox to produce inert N2, such treatment requires an expensive energy input for aeration and possibly electron donor (Berge et al. 2005). Because of ammonia inhibition, operating anaerobic reactors with high N feedstocks has been widely reported to contribute to reactor failure (Berge et al. 2006). Several studies have reported ammonia inhibition thresholds in various waste treatment systems in terms of free ammonia (NH_3), ammonium-N (NH_4^+-N), and total ammonia nitrogen (TAN). Free ammonia was shown to inhibit reactors in the range of 0.08-1.1 g NH_3-N/L (Gallert et al. 1998, Hansen et al. 1998, McCarty and McKinney 1961). Other studies reported ammonia inhibition by the ammonium ion between 1.2-2.4 g NH_4^+-N/L (Koster and Lettinga 1984, Velsen 1979), and further, total ammonia nitrogen of >4 g TAN/L (Angelidaki and Ahring 1993, Sung and Liu 2003) was also reported to be inhibitory.

Despite the problems with ammonia toxicity, AD of high N wastes could be desirable. Ammonia produced during AD has been used as commercial fertilizer and digestate has been used as a soil amendment (Weiland 2010). Additionally, ammonia liberated during AD could be recovered and used as a bioenergy source. Babson et al. (2013) performed an energy balance of a theoretical AD system that incorporated

separation and recovery of biologically-released ammonia with subsequent reforming of ammonia to produce hydrogen. That study showed that at feedstock C: N ratios of 17 or lower the energy output from the system with AD and ammonia to hydrogen recovery was greater than AD generating methane alone. Therefore, optimization of AD reactors treating high-N wastes could allow large amounts of ammonia to be captured for energy recovery while relieving some of the pressure to find land sinks for N recycling.

Strategies for overcoming ammonia toxicity in AD have long been a topic of research. These strategies include: dilution of continuously stirred tank reactors (CSTR) digesting cattle manure (Nielson and Angelidaki 2008); addition of activated carbon, $FeCl_2$, or glauconite as an ion exchange medium for ammonia (Weber and Digiano 1996); and increasing the hydraulic retention times (HRT) (Hansen et al. 1999).

An extensive number of scientific articles that report ammonia inhibition during AD, however, few of these studies have specifically focused on identifying microbial community responses to ammonia. Velsen (1979) reported gradual microbial community acclimatization to high ammonia during anaerobic digestion of sewage sludge and swine manure. It has observed that proteolytic and amino-acid fermenting bacteria may have unique properties that allow them to tolerate an environment where abundant ammonia is produced during deamination (Gallert et al. 1998). In the aforementioned study thermophilic communities were significantly more tolerant to ammonia than mesophilic communities. Indeed, *Peptostreptococcus anaerobius*, isolated from the bovine rumen, was described as a "hyper-ammonia producing (HAP)" bacterium because of its high rates of ammonification of protein in the high ammonia gut environment (Russell et al. 1988).

Dynamic shifts in microbial community makeup in response to increasing ammonia concentration during AD was reported in several studies (Demirel and Scherer 2008, Koster and Lettinga 1984, Schnurer et al. 1994, Schnurer and Nordberg 2008, Westerholm et al. 2011b, Westerholm et al. 2011c). In particular, syntrophic acetate oxidation became a dominant process at an ammonium concentration of 7 g NH_4^+-N/L in a methanogenic mesophilic (37°C) triculture (Schnurer et al. 1994). *Tepidanaerobacter acetatoxydans* Re1 (NR_074537.1), an anaerobic, syntrophic acetate-oxidizing bacterium (SAOB), was isolated and its activity was observed when the ammonium concentration exceeded 3 g NH_4^+-N/L (Schnurer and Nordberg 2008). This ammonium concentration produced a shift from aceticlastic methanogenesis to syntrophic acetate oxidation (coupled to hydrogenotrophic methanogenesis), which became thermodynamically favorable under the prevailing conditions (Schnurer and Nordberg 2008). Hattori (2008) stated that SAOB can oxidize acetate to produce H_2/CO_2 only when H_2 is utilized by hydrogen-scavenging methanogens. This fact was later supported by the observation of *T. acetatoxydans* acetate-oxidizing ability during co-cultivation with a hydrogen-consuming methanogen *Methanoculleus sp.* in mesophilic methanogenic reactors operating at 6.4 g NH_4^+-N/L (Westerholm et al. 2011c). The quantification of SAO microbial communities in reactors with up to 7 g NH_4^+-N/L also indicated a significant increase in the abundance of syntrophic acetate oxidizers with a decrease in the abundance of aceticlastic methanogens from the families Methanosaetaceae and Methanosarcinaceae (Westerholm et al. 2011b). Thus it appears that certain microbial community members may be selected under higher ammonia conditions.

We therefore hypothesized that microbial communities that have developed over long periods of time in high ammonia anaerobic environments may be tolerant to ammonia. The goal of this study was to enrich and characterize ammonia tolerant methanogenic microbial communities from anaerobic environments that may be high in ammonia. In particular we characterized landfill leachate microbial communities *(bacteria, archaea)* tolerant to high ammonia concentrations. It has been reported that young conventional landfill leachate typically contains about 2.7 g TAN/L (Calli et al. 2003) or ammonium nitrogen of <0.001-3 g NH_4^+-N/L (Santos et al. 2013). Free ammonia was reported at 0.43-0.58 g NH_3-N/L from conventional and bioreactor landfills (Berge et al. 2005), and at 0.8 g NH_3-N/L from a 20-year-old municipal landfill (Yu et al. 2014a). Landfill leachates from New Jersey, USA, and Chonburi, Thailand, were used as inoculum to compare microbial communities acclimated to high ammonia. The enrichments were established at concentrations of up to 12.5 g TAN/L. Identification of ammonia tolerant microorganisms in leachate could aid in developing more stable anaerobic digestion for high nitrogen wastes. Further, AD communities with high tolerance to ammonia will allow engineering advances to be made in treatment and harvest of ammonia for beneficial reuse and/or to produce hydrogen as an alternative energy.

3.3 Materials and methods

3.3.1 Leachate inoculum

Landfill leachates from two sites: 1) anaerobic bioreactor landfill, Burlington County, New Jersey, USA; and 2) conventional municipal landfill, Lamchabang, Chonburi, Thailand, were used as inocula. The sample from New Jersey was a composite of landfill leachate, wastewater from an associated sludge composting facility and sanitary wastewater typically generated and co-mingled within the waste handling complex. Three 1-L samples were collected in sterile plastic containers, transported to Rutgers University on ice and stored at 4°C for one day prior to use in establishing reactors. The entire 3 L volume was concentrated to 250 mL upon arrival by centrifuging at 15000 *g* for 10 minutes using an Allegra^{TM} 25R Centrifuge (Beckman Coulter, Indianapolis, IN, USA) and discarding excess supernatant. The concentrated sample was then used to inoculate reactors the same day.

A total of 3 L of sample from Thailand was collected from an observation well, placed in sterile plastic containers, and centrifuged on site as described above. The concentrated sample was placed in a sterile 250 mL Nalgene bottle and shipped to New Jersey within one week. The sample was stored at 4°C for one day prior to use in establishing reactors. The characteristics of the landfill leachates are shown in Table 3.1. Note that in contrast to what would be expected, the Thailand leachate characteristics (provided by officials on site) indicated a higher biochemical oxygen demand (BOD) than chemical oxygen demand (COD) value. It is not known why the BOD value was greater than the COD value.

3.3.2 Reactor set-up and operation

The 160-mL serum bottles (VWR, Radnor, PA, USA) were sterilized by autoclaving, made anoxic by purging with 99.998% nitrogen gas, which flowed through a sterile 0.45 μm filter, and 10 mL concentrated leachate was added via a sterile glass pipette. The total liquid volume of each bottle was adjusted to 100 mL with sterile anaerobic minimal medium (Fennell and Gossett 1997). A hydraulic retention time (HRT) of 140 days was maintained by a fill and draw exchange of 10% of the enrichment volume (10 mL) every two weeks, to achieve semi-continuous operation. Glutamate (1 mmol) was added via a sterile syringe initially and thereafter every two weeks as the sole carbon and energy source from a sterile 500 mM sodium glutamate stock solution. Treatments were established in triplicate with a target TAN of 5, 7.5, 10, or 12.5 g TAN/L by adding appropriate volumes of sterile, anoxic 5 M NH_4Cl stock solution initially, and after each fill and draw to maintain a constant imposed concentration. Actual TAN concentrations in the reactors as measured analytically every two months are shown in Table 3.2 and were slightly different than expected. Active controls were fed glutamate and background controls received no carbon source. Controls had no NH_4Cl added other than that in the minimal media and N was analytically determined to be 0.1 g TAN/L in a Thailand control reactor and 0.8 g TAN/L in a New Jersey control reactor. Bottles were incubated at 35°C in the dark and manually shaken every few days.

3.3.3 Analytical methods

Biogas volume produced from the reactor was measured by water displacement. Methane content was determined from a 250 μL headspace sample using a Pressure-Lok®

Series A-2 syringe (VICI® Precision Sampling, Baton Rouge, CA, USA) with a flame sterilized sideport needle. The sample was injected into an Agilent 6890 N gas chromatograph (Agilent Technologies, Santa Clara, CA, USA) equipped with a GS-GasPro capillary column (30 m x 0.32 mm I.D.; J&W Scientific, Folsom, CA, USA) and a flame ionization detector. Helium was the carrier gas at a constant pressure of 131 kPa. The oven temperature was 150°C. The resulting chromatographic peak area was compared to a five point calibration curve prepared using mixtures of 0 to 99% methane created by mixing volumes of methane (99% purity; Matheson Tri- Gas, Inc., Montgomeryville, PA, USA) and air. Methane production volume was calculated from the methane content and biogas volume at 998 mbar and 23°C. The moles of methane produced were then corrected to STP (1 atm, 0°C).

The volatile fatty acids acetate, propionate, and butyrate were measured every other fill and draw exchange (every month) by high performance liquid chromatography (HPLC). Reactor effluent samples (0.75 mL) were centrifuged at 9390 *g* (Eppendorf Model No. 5424) for 3 minutes and the supernatant was filtered using Spin-X Centrifuge Tube Filters, Corning Nylon Membrane, pore size 0.45 µm (VWR). Filtered samples were analyzed on a Beckman Coulter® System Gold™ HPLC (Beckman-Coulter, Fullerton, CA, USA) using a Bio-Rad® Aminex HPX-87H organic acid analysis column (Bio-Rad Laboratories, Hercules, CA, USA). The column was held at 60°C. The mobile phase was 0.008 N H_2SO_4 at a flow rate of 0.6 mL/minute. UV detection was at a wavelength of 210 nm. Chromatographic peak areas were quantified by comparison to standard curves of acetic, propionic, and butyric acids (99-99.7% purity, Sigma-Aldrich

Co., St. Louis, MO, USA) over a concentration range from 250 to 1,000 mg/L. The detection limit for the system was approximately 8.4 mg acetate/L.

Total ammonia nitrogen (TAN) was measured every two months by ion chromatography (IC). To convert free ammonia to ammonium ion, the pH of aqueous samples was adjusted to < 2 using 10 N H_2SO_4. Next, samples were centrifuged at 9390 *g* (Eppendorf Model No. 5424) for 3 minutes, and the supernatant was filtered using Spin-X Centrifuge Tube Filters, Corning Nylon Membrane, pore size 0.45 µm (VWR). The filtrate was diluted 800 times with MilliQ water, and analyzed for TAN using a Dionex ICS-1000 ion chromatograph equipped with an IonPac™ CS12A RFTC™ 4x250 mm cation column, and a CSRS™ 300 4 mm cation suppressor (Dionex Corporation, Salt Lake City, UT, USA). The mobile phase was 20 mN methanosulfonic acid. TAN was calculated from a standard curve over a range of 0.125 to 2 mM and corrected for dilution.

The pH was measured in the same day TAN was measured using an Accumet® Basic AB15 (Fisher Scientific, Pittsburgh, PA, USA) pH meter with symphony Ag/AgCl pH electrode (VWR). Free ammonia was then calculated from the equilibrium equation (Eqn. 1) below (Angelidaki and Ahring 1993):

$$[NH_3 - N] = \frac{[TAN]}{\left[1 + \frac{[H^+]}{K_a}\right]} \qquad \text{Eqn. 1}$$

where K_a (the dissociation constant) = 1.12 x 10^{-9} at 35°C.

Methane, VFAs, and TAN data are reported as an average of triplicate reactors ± one standard deviation.

3.3.4 Microbial community analysis

Bacterial and archaeal communities were analyzed using polymerase chain reaction (PCR) coupled to denaturing gradient gel electrophoresis (DGGE). DNA extraction from 1-3 mL enrichment samples was performed using the PowerSoil™ DNA Isolation Kit (MoBio Laboratories, Carlsbad, CA, USA) according to the manufacturer's instructions. The PCR amplification of partial bacterial 16S rRNA genes was performed with forward (338-GC F) and reverse (519R) primers (Nakatsu 2000). The PCR protocol was as follows: initial denaturation at 94°C for 5 minutes; 33 cycles of denaturation at 94°C for 30 seconds, annealing at 55°C for 30 seconds, and elongation at 72°C for 30 seconds; followed by a final extension step of 7 minutes at 72°C (Chen 2010). The PCR amplification of partial archaeal 16S rRNA genes was performed with ARC787f-GC and ARC1059r (Hwang et al. 2008, Merlino et al. 2013). To amplify the target DNA, a touchdown PCR amplification of archaeal 16S rRNA genes was used with the following conditions: initial denaturation at 94°C for 10 minutes; 20 cycles of denaturation at 94°C for 1 minute, annealing for 1 minute at a temperature that decreased by 0.5°C every cycle from 65°C to the 'touchdown' at 55°C, and elongation at 72°C for 1 minute; and finally, 20 cycles of denaturation at 94°C for 1 minute, annealing at 55°C for 1 minute, and extension at 72°C for 1 minute. Thus, the PCR was performed in a total of 40 cycles. A final extension step was performed at 72°C for 3 minutes. The PCR products were analyzed by electrophoresis on a 1.5% agarose gel, stained in 0.1% ethidium bromide (EtBr) solution for 30 minutes and visualized using UV on a Molecular Imager Gel Doc XR system (Bio-Rad Laboratories).

For DGGE, the quantified DNA in PCR products was loaded onto 8% polyacrylamide gels containing a gradient of 30-60% and 40-60% denaturant (100% denaturant contained 7M urea and 40% formamide) for bacteria and archaea, respectively. Electrophoresis was run at 60°C in 1xTAE buffer with operating conditions for bacteria: 4 h at 150V; and for archaea, 17 h at 90V. Gels were stained with SYBR® Gold nucleic acid stain (Invitrogen) for 30 minutes and documented with a Molecular Imager Gel Doc XR system (Bio-Rad Laboratories). Dominant bands were excised and DNA was eluted. The DNA fragment was then re-amplified using the DGGE primer set without GC clamp, and re-run on 1.5% agarose gel. The PCR products were purified with USB® ExoSAP-IT®, and sequenced (Genewiz, South Plainfield, NJ, USA). The sequences were compared with sequences deposited in the National Center for Biotechnology Information (NCBI) database using the BLAST program. All sequencing results were additionally confirmed by the RDP Native Bayesian rRNA Classifier Version 2.6, Sep 2013 (http://rdp.cme.msu.edu/classifier/hierarchy.jsp). A resulting gel image was analyzed for relative band intensities in each lane and calculated as percentage of band intensities using the ImageJ 1.48v quantification software (National Institutes of Health, USA), according to the manufacturer's protocol (http://imagej.nih.gov/ij). For each phylotype detected, the band intensities are reported as an average of triplicates ± one standard deviation.

The 454 pyrosequencing was performed for samples from the Thailand and New Jersey enrichments obtained from the highest TAN concentrations. The V2, V3, and V4 regions of the bacterial and archaeal 16S rRNA gene were targeted using the primers 515F and 909R (Wang et al. 2009). Barcoded amplicon sequencing processes were

performed by MR DNA (Shallowater, TX, USA) under the trademark (bTEFAP®). The bTEFAP® process was modified to utilize 16S rRNA gene bacterial primers (515F and 909R) (Wang et al. 2009). A single-step 30 cycle PCR using HotStarTaq Plus Master Mix Kit (Qiagen, Valencia, CA, USA) was used under the following conditions: 94°C for 3 minutes, followed by 28 cycles of 94°C for 30 seconds; 53°C for 40 seconds and 72°C for 1 minute; after which a final elongation step at 72°C for 5 minutes was performed. Following PCR, all amplicon products from different samples were mixed in equal concentrations and purified using Agencourt Ampure beads (Agencourt Bioscience Corporation, Beverly, MA, USA). Samples were sequenced utilizing a Roche 454 FLX titanium instrument and reagents following the manufacturer's guidelines.

The nucleotide sequences reported in this chapter were deposited in the NCBI nucleotide sequence databases under accession numbers SRS892986 and KR064311-KR064345.

3.4 Results

Anaerobic reactors inoculated with New Jersey and Thailand leachate were operated for 300 days under target TAN concentrations of 5 to 12.5 g TAN/L using glutamate as the sole carbon and energy source. Enrichments resulting from New Jersey and Thailand leachates showed different patterns of methane production, volatile fatty acids concentration trends, and microbial community members.

3.4.1 Methane production

The results revealed that increasing TAN resulted in inhibition of methane production (Fig. 3.1). Methane production in Thailand leachate reactors at 5 and 7.5 g TAN/L was initially the same as the active control (containing background TAN). A long start-up phase was observed in the 10 and 12.5 g TAN/L reactors; however, methane production increased dramatically after day 47 and remained stable by day 100, at a production rate slightly less than the active control. Methane production in the 12.5 g TAN/L reactors, the highest ammonia concentration, was the lowest of all, and only achieved about 80 % of that of the active control (Fig. 3.1A). Conversely, New Jersey leachate enrichments exhibited different methane production trends. All reactors with added TAN had a long start-up phase ranging from 50 to 98 days. After this period, only the 5 g TAN/L reactor produced as much methane as the active control while other reactors showed lesser methane production, especially the 12.5 g TAN/L reactor, which produced only 21% of that of the active control (Fig.3.1B). The high standard deviations observed for the New Jersey methane production values are likely a result of instability caused by ammonia stress conditions. Table 3.2 shows pH, total ammonia nitrogen concentration (TAN), calculated free ammonia (NH_3-N) and methane (CH_4) production in the Thailand and New Jersey leachate inoculated reactors. The data show that reactors inoculated with Thailand leachate constantly produced methane in a range of 40 to 60 mL or 1.4 to 2 mmol per two weeks, compared to the theoretically expected methane production of 2 mmol per two weeks at STP (see Eqn. 2.16). On the contrary, only 10 to 50 mL or 0.3 to 1.9 mmol of methane per two weeks was produced in reactors inoculated with New Jersey leachate. It was found that at the highest TAN concentration, methane production from New

Jersey leachate was 85% lower than the theoretical methane production and was approximately 77% less methane than Thailand leachate inoculated reactors.

3.4.2 Volatile fatty acids

Volatile fatty acid concentration is a key indicator of anaerobic digestion system performance. Acetate and propionate concentrations in the Thailand leachate reactors are shown in Fig. 3.2. Acetate was utilized immediately after reactor set up in the 5 and 7.5 g TAN /L reactors. In the high ammonia reactors (10 and 12.5 g TAN /L), acetate accumulated up to 1,000 to 2,000 mg/L before decreasing after day 48. By day 218, there were low acetate concentrations (<20 mg/L) in most reactors (Fig. 3.2A). Propionate concentrations in Thailand leachate inoculated reactors are shown in Fig. 3.2B. There was no propionate accumulation in the 5 g TAN /L reactors and some propionate accumulated in the 7.5 and 10 g TAN /L reactors initially, but was depleted by days 77 and 104, respectively. In the 12.5 g TAN /L reactors, propionate accumulated up to 1,630 (+/- 447) mg/L before decreasing after day 140 (Fig. 3.2B). Acetate and propionate concentrations in reactors inoculated with New Jersey leachate are shown in Fig. 3.2C and 3.2D. Ammonia stress conditions resulted in large standard deviations since the replicated did not behave similarly. Acetate concentrations in New Jersey inoculated reactors were generally higher than those for the Thailand leachate reactors. The 12.5 g TAN /L reactors tended to accumulate acetate as high as 4,200 (+/- 2,058) mg/L while the 5 and 7.5 g TAN /L reactors accumulated acetate initially with depletion occurring after 150 days (Fig. 3.2C). Propionate in the low and high TAN reactors obviously showed different trends. Propionate in the 5 and 7.5 g TAN /L reactors increased up to 900 to 3,500 mg/L before it gradually decreased to less than 50 to 500 mg/L after 190 days. Conversely, propionate in reactors with 10 and 12.5 g TAN /L increased and remained in a range of 3,000 to 4,000 mg/L

throughout the experimental period (Fig. 3.2D). The negative effect of VFAs on methane production at 12.5 g TAN/L is apparent in Fig. 3.3. After 225 days of operation, both acetate and propionate in Thailand leachate reactors decreased to less than 5 mmol/L (500 mg/L) whereas New Jersey leachate reactors showed increasing trends of both VFAs (40 to 70 mmol/L). Methane production in Thailand leachate reactors reached 1.6 mmol/two weeks whereas only <0.5 mmol/two weeks of methane was produced in the New Jersey leachate reactors. The results indicated that ammonia stress led to acetate and propionate accumulation and lower methane production in New Jersey leachate inoculated reactors compared to Thailand leachate inoculated reactors. Butyrate concentrations remained less than 20 mg/L in all reactors (data not shown). In addition, reactor pH slightly decreased with increasing TAN and VFA concentrations, however, pH was still near neutral for all reactors.

3.4.3 Microbial community

3.4.3.1 Denaturing gradient gel electrophoresis (DGGE)

Microbial communities differed with TAN concentration and leachate source. The bacterial communities exhibited a high diversity of bacterial phylotypes with similar number of bands in both systems (Fig. 3.4). Only the dominant bands were cut, sequenced, and compared with sequences deposited in the NCBI database. These were classified into phyla Firmicutes, Synergistetes, Thermotogae, Chloroflexi, and Bacteroidetes. A phylotype matching *Tepidanaerobacter acetatoxydans* (100% similarity) dominated in reactors at all TAN concentrations for Thailand and at the higher TAN concentrations for New Jersey leachate inoculated reactors (Fig. 3.4 and Table 3.4).

Band intensity analysis indicated that this phylotype matching *T. acetatoxydans* represented 50% of the total band intensity (OTU2) in Thailand reactors at 7.5 g TAN/L (Fig. 3.5) and 44% of the total band intensity (OTU3) in New Jersey enrichments at 10 g TAN/L (Fig. 3.6). In Thailand leachate reactors, a phyloype matching *Garciella nitratireducens* (100% similarity) (OUT1) dominated at 12.5 g TAN/L and phylotypes matching *Aminobacterium* spp. (87% similarity) (OTU3) dominated at 7.5 g TAN/L (Fig. 3.5). In New Jersey leachate reactors, a phylotype matching *T. acetatoxydans* was detected with a high band intensity at 10 and 12.5 g TAN/L (OTU3) and at 5 and 7.5 g TAN/L (OTU4) (Fig. 3.6). In addition, a phylotype matching *Thermanaerovibrio acidaminovorans* (88-92% similarity) was also detected in both Thailand and New Jersey leachate reactors.

The archaeal DGGE profiles for the enrichments from Thailand leachate inoculated reactors on day 134 and day 218 (Fig. 3.7) indicated fewer bands than observed for bacterial phylotypes. Only the dominant bands were cut, sequenced, and compared with sequences deposited in the NCBI database. Archaea were classified to the phylum Euryarchaeota with the closest match to *Methanosarcina* spp. at the early stage (Day 134), and *Methanosarcina* spp. and *Methanoculleus bourgensis* at the later stage of operation (Day 218) (Table 3.5). Band intensity analysis indicated that at the early stage (Day 134) phylotypes matching *Methanosarcina* spp. (OTU4) dominated in the 10 g TAN/L reactors with 70% band intensity (Fig. 3.8). At other TAN concentrations, phylotypes matching *Methanosarcina* spp. were also detected with lower band intensity (OTU1, OTU2, and OTU5). Phylotypes matching *Methanocalculus* spp. and *Methanomicrobium* spp. (91% similarity) were also detected (OTU3). A phylotype

matching *Methanosarcina concilii* (99% similarity) was only detected in the active and background controls (Fig. 3.8). At the later stage, phylotypes matching *Methanosarcina* spp. (OTU1, OTU3 and OTU4) dominated in 7.5 and 10 g TAN/L reactors and phylotypes matching *Methanoculleus* spp. (OTU2) dominated in 12.5 g TAN/L reactors (Fig. 3.9). A phylotype matching *Methanosaeta concilii* (97 – 99% similarity) (OTU5) also dominated in the low ammonia control reactors inoculated from Thailand leachate (Fig. 3.9 and Table 3.5).

Archaeal DGGE profiles for the New Jersey leachate inoculated reactors for day 154 and day 292 (Fig. 3.10) indicate that, in contrast to Thailand leachate inoculated reactors, phylotypes closely related to *Methanoculleus* spp. were dominant at all ammonia concentrations. Analysis of the microbial community at both the early stage (Day 154) and the later stage (Day 292) indicated the highest band intensity was for phylotypes matching *Methanoculleus* spp. at 10 g TAN/L (OTU3) (Fig. 3.11 and 3.12). In addition, the control and background reactors phylotypes matching *Methanosarcina* spp. and *Methanosaeta concilli* were detected (Fig. 3.11, 3.12 and Table 3.6).

3.4.3.2 Pyrosequencing

Bacterial and archaeal microbial composition at different taxonomic levels and the proportion of major phylotypes in both systems are summarized in Table 3.3 (genus level) and Fig. 3.13 (order level). Similar to findings from DGGE analysis, more phylotypes were detected among the bacteria than the archaea. Bacterial phylotypes were mainly distributed in the phyla Firmicutes, Bacteroidetes, Synergistetes, and Cloacimonetes. The most dominant bacterial phylum detected in the Thailand leachate reactors was Firmicutes (58%), followed by Bacteroidetes (17%), Spirochaetes (15%),

and Synergistetes (8%). Firmicutes was also the most dominant phylum in New Jersey leachate reactors (93%). Within the phylum Firmicutes, the most abundant class was Clostridia in both systems. Interestingly, Thailand leachate reactors seemed to have a more diverse bacterial community than New Jersey leachate reactors, which contained Thermoanaerobacterales as the only major order (Fig. 3.13A). *Tepidanaerobacter* spp. dominated with 19% and 60% genus abundance of the total bacterial community in Thailand and New Jersey leachate inoculated reactors, respectively (Table 3.3).

The archaeal community in Thailand leachate reactors was dominated by the orders Methanosarcinales, Methanomicrobiales, Methanobacteriales, and Thermoplasmatales (Fig. 3.13B). The abundance of the Methanosarcinales was much higher than for other orders. More than 58% of genus abundance of the total archaeal community was assigned to *Methanosarcina* spp. In contrast, the only archaea detected in New Jersey leachate inoculated reactors were *Methanoculleus* spp. in the order Methanomicrobiales (Table 3.3).

3.5 Discussion

This study indicates that the microbial communities enriched in Thailand leachate inoculated reactors were more resistant to higher TAN concentrations than those from New Jersey leachate. Even though ammonia inhibition did apparently result in a longer start-up phase with increasing TAN, methane production eventually reached the same level as in the control in the Thailand reactors. Other studies reported that ammonia concentration of more than 4 g TAN/L caused 100% inhibition of thermophilic cattle manure and wastewater anaerobic digestion (Angelidaki and Ahring 1993, Sung and Liu 2003). The results obtained in this study clearly illustrate that microbial communities in

the Thailand leachate were active and that they acclimatized to high TAN over time. One reason might be that leachate from the 30-year-old Thailand conventional landfill contained microbial communities that assisted the acclimatization process. In contrast, microbial communities in New Jersey leachate were unable to acclimate to high TAN during the 300 day time frame as indicated by decreasing methane production with increasing TAN. In the New Jersey inoculated rectors, methane production was approximately 77% less than that of Thailand inoculated reactors at the highest TAN concentration. Therefore, it can be concluded that TAN concentration inhibited methane production, in New Jersey leachate inoculated reactors. The results also indicated that the pH of the reactors slightly decreased with increasing TAN as a result of VFA accumulation. Thus, the calculated free ammonia also slightly decreased, indicating that the inhibition may be linked to ammonium as well as ammonia (Table 3.2). This finding is in agreement with Nakakubo et al. (2008) who proposed that TAN was a more significant factor than free ammonia in affecting the methanogenic activity of a well-acclimatized bacterial system.

Our results also indicate that the concentrations of VFA increased with increasing ammonia concentrations as reported previously (Angelidaki and Ahring 1993, Nakakubo et al. 2008, Schnurer and Nordberg 2008). The fact that acetate and propionate were depleted by Thailand microbial communities also confirmed that these reactors acclimated to ammonia stress better than New Jersey microbial communities. In the Thailand reactors amended with the highest TAN, only 263 (+/- 200) mg acetate/L was observed at the end of the experimental period and breakdown/turnover of propionate eventually occurred after an initial inhibition period of 140 days. This suggests adaptation of the communities to high ammonium nitrogen as reported previously (Velsen 1979). Fukuzaki et al. (1990) reported that

mesophilic propionate-acclimatized sludge could convert propionate to methane and carbon dioxide without accumulating acetate and hydrogen a fact that could result in low acetate accumulation in our study. In contrast, the New Jersey reactors at target 10-12 g TAN/L exhibited substantial VFA accumulation. In AD with overloaded conditions, cessation of propionate degradation has been attributed to an inhibitory effect on the propionate-oxidizing bacteria (either through toxicity or thermodynamic limitation) and/or on the hydrogen-consuming methanogens (Lier et al. 1993). In addition, high concentrations of propionate indicated low activity of propionate oxidizing bacteria (Prochazka et al. 2012). A propionate concentration of 12 mmol/L was reported to result in a decrease in the total bacterial concentration by ten fold (Wang et al. 2009) and propionate above 80 mmol/L inhibited methanogenesis as methanogen count decreased by at least two orders of magnitude (Barredo and Evison 1991). The highest propionate concentration observed in the New Jersey leachate reactors was 4,270 mg/L (58 mmol/L), which thus was assumed to decrease bacterial and methanogenic activities. Related studies also reported that acetate-utilizing methanogens were sensitive to high ammonium, which would result in cessation of VFA conversion to methane (Nakakubo et al. 2008). These might be the reasons why New Jersey high TAN reactors accumulated acetate and propionate when acetate-utilizing methanogens and propionate-oxidizing bacteria were exposed to high TAN levels.

Microbial community analysis revealed community shifts related to TAN concentration, volatile fatty acids, and methane production. More bacterial phylotypes than archaeal phylotypes were identified by both DGGE and 454 pyrosequencing. Thailand leachate inoculated reactors contained more bacterial phylotypes than New Jersey leachate inoculated reactors. Dominant species and community shifts were also

detected as previously reported in high ammonia conditions (Calli et al. 2005, Westerholm et al. 2011b). Pyrosequencing results generally confirmed the DGGE findings. The bacterial community shifted toward the Firmicutes phylum with Clostridia as the most abundant class in both systems. This result supported the findings from Kim et al. (2014) who found that Clostridia increased after 132 days of operation in the methanogenic and stabilizing reactors of a two-stage AD treating food waste leachate containing a high concentration of VFAs (12,400 ± 2,200 mg/L) (TAN concentration was not monitored). Many members of the class Clostridia obtain energy by fermenting amino acids and are known as acid and hydrogen producers supplying hydrogen as a substrate to hydrogenotrophic methanogens (Madigan and Martinko 2006).

Phylotypes closely matched to *Tepidanaerobacter* spp. (a member of the class Clostridia) were the most dominant bacteria in Thailand and in New Jersey reactors under all conditions. *Tepidanaerobacter acetatoxydans* is an anaerobic, syntrophic acetate-oxidizing bacterium that carries out the syntrophic acetate oxidation pathway and was observed to be dominant in anaerobic communities when the ammonium concentration was greater than 3 g NH_4^+-N/L (Schnurer and Nordberg 2008), 6.4 g NH_4^+-N/L (Westerholm et al. 2011c), and in a mesophilic (37°C) triculture at 7 g NH_4^+-N/L (Schnurer et al. 1994). Our study confirmed that a phylotype related to *T. acetatoxydans* (100% similarity) may also be enriched at TAN concentrations up to 11.4 g TAN/L, the highest concentration we observed.

In addition, *Garciella nitratireducens* (100% similarity), *Gelria* spp., and *Thermanaerovibrio acidaminovorans* were found in both Thailand and New Jersey systems. *G. nitratireducens* is an anaerobic, thermophilic, nitrate- and thiosulfate-

reducing bacterium that ferments organic acids and glucose into lactate, acetate, butyrate, H_2, and CO_2 (Miranda-Tello et al. 2003). In addition, it reduces thiosulfate to hydrogen sulfide and nitrate to ammonium. Sulfur metabolism, particularly sulfide release and transformation, represents an important biochemical process in anaerobic digesters (Vaccari et al. 2006). *Gelria glutamica* (Plugge et al. 2002) and *T. acidaminovorans* (Baena et al. 1999, Plugge and Stams 2001) are moderately thermophilic, syntrophic, glutamate-degrading bacteria that were studied during growth in co-culture with the hydrogenotrophic methanogen *Methanobacterium thermoautotrophicum* Z245. Finding glutamate-fermenting bacteria and SAOB at high TAN concentrations suggests that reactors inoculated with Thailand and New Jersey leachate produced methane from hydrogen via the SAO pathway following fermentation of glutamate.

Archaeal community analysis revealed that Thailand leachate inoculated reactors contained a greater number of archaeal phylotypes than New Jersey leachate inoculated reactors. In Thailand reactors, Methanosarcinales was the major order, followed by Methanomicrobiales, whereas Methanomicrobiales was the only major order found in New Jersey reactors (Fig. 3.13). Phylotypes similar to *Methanosarcina* spp. (of the order Methanosarcinales) were dominant in Thailand reactors at both the early stage (Day 134) and the later stage (Day 218) of operation, whereas *Methanoculleus* spp. dominated in New Jersey reactors at both stages (Day 154 and 292).

Even though *Methanosarcina* spp. living on acetate were found to be more sensitive than hydrogenotrophic methanogens to increasing ammonia concentrations (Sprott and Patel 1986), they were also shown to acclimate to high ammonia as shown by a sigmoidal growth rate pattern (Angelidaki and Ahring 1993). *Methanosarcina* spp.

were reported to be tolerant to ammonium levels up to 7 g NH_4^+-N/L in an additional study (Vrieze et al. 2012). *Methanosarcina* spp. alter their metabolic pathways in response to the surrounding conditions (Hao et al. 2011) and members belonging to the order Methanosarcinales were reported to act as hydrogenotrophic methanogens in conjunction with the SAO pathway (Westerholm et al. 2012). Our study showed that phylotypes related to *Methanosarcina* spp. were abundant (58.4% of the band intensity of total archaea community) in Thailand high TAN reactors (11.4 g TAN/L).

Methanosarcina spp. have been shown to thrive in the form of multicellular units at free ammonia concentrations of up to 750 mg NH_3-N/L (Calli et al. 2005). *M. mazei* and *M. acetivorans* were dominant species among those sequenced. These organisms convert acetate, methanol, and methylamines to methane, carbon dioxide, and ammonia (in case of methylamines) (Deppenmeier et al. 2002, Sowers et al. 1984). In addition, *M. mazei* coexisted with fermentative bacteria that produce acetate and contained transposases and proteins involved in stress response, and potassium ion uptake systems that related to ammonia toxicity (Deppenmeier et al. 2002). Sossa et al. (2004) concluded that a biofilm enriched with methylaminotrophic methanogenic archaea, represented mainly by family Methanosarcinanaceae, may be ammonia tolerant since ammonia is produced in the conversion of methylamine to methane. The results from the aforementioned studies, along with our findings support the idea that *Methanosarcina* spp. may be the ammonia resistant archaea in our system, especially at the highest TAN concentration. Under these conditions where SAOB are present at high abundance the *Methanosarcina* are likely operating as hydrogenotrophs.

New Jersey archaeal community analysis showed that phylotypes highly similar to *Methanoculleus* spp. dominated in all reactors. *Methanoculleus bourgensis* was the most closely related species among them. *M. bourgensis* is a hydrogenotrophic methanogen found to be well adapted in biogas communities encountering high salt and ammonia (Maus et al. 2012) and was reported to produce methane through the hydrogenotrophic pathway (Barret et al. 2013). In addition, *Methanoculleus* spp. were important partners during SAO under mesophilic conditions (Westerholm et al. 2012). The existence of *Methanoculleus* spp. therefore confirmed previous results of hydrogenotrophic methanogens in high TAN systems. Even though hydrogenotrophic methanogens were reported to be less sensitive than aceticlastic methanogens (Barret et al. 2013, Hao et al. 2011, Sprott and Patel 1986), New Jersey leachate microbial communities did not adapt and acclimate to high ammonia concentration as well as those from Thailand. One reason might be that New Jersey leachate was composed of low bacterial and archaeal community abundance, the absence of *Methanosarcina* spp., which were believed to create robustness and reactor stability at high TAN concentrations, could be an indication that these organisms were not present in high abundance in the original leachate. In addition, New Jersey leachate was blended with other (non-anaerobic process) wastes from the landfill complex.

Phylotypes closely related to *Methanosaeta concilii*, the most ammonia-sensitive methanogen (Steinhaus et al. 2007), was detected at high abundance in both Thailand and New Jersey active control and background reactors (with low TAN). It was previously shown that *Methanosaeta* spp. were abundant in anaerobic reactors treating young landfill leachate with low acetate levels (Calli et al. 2003). These organisms exclusively

utilized acetate (Hattori 2008), favored low acetate concentrations (Zhu et al. 2012) and had optimum growth conditions in the range of 0.25-1.1g NH_4^+-N/L (Steinhaus et al. 2007), which would be representative of only the lowest TAN concentrations in our experimental systems.

Overall, this study provides new information about ammonia tolerant microorganisms in two different landfill leachate systems at high TAN concentrations of up to 12.5 g TAN/L (averages of 11.4 to 11.8 g TAN/L, actual), concentrations that are higher than those reported for other studies. The presence of phylotypes related to *Tepidanaerobacter acetatoxydans* and *Methanosarcina* spp. in these high ammonia systems which exhibited high methane production (with respect to the maximum theoretically possible) and little VFA accumulation suggests a beneficial microbial systems for stable operation of AD treatment of high N wastes. These microorganisms could be used as bio-indicators of ammonia resistance in addition to physical and chemical parameters that are routinely measured to assess reactor stability. In addition, bioaugmentation with these microbes could possibly be applied to digesters facing N overload to enhance microbial activity and decrease the acclimation periodneeded under ammonia stress conditions. Moreover, operation of landfills containing high ammonia concentrations without re-circulating of leachate could be possible.

Identification of ammonia tolerant microorganisms as were found in the enrichments from Thailand landfill leachate could advance anaerobic treatment of high N wastes by decreasing the need to blend substrates and to allow harvest of ammonia at high concentrations for beneficial reuse such as cracking to produce hydrogen as an additional energy product.

Table 3.1 Characteristics of landfill leachate inoculum

Parameters	**Thailand**[a]	**New Jersey**[b]
pH	7.4-8.4	7.8-7.9
BOD (mg/L)	28,000	600
COD (mg/L)	16,000	2,400
Ammonia Nitrogen (mgN/L)	NA	820
TKN (mgN/L)	2,200	NA
Oil and Grease (mg/L)	NA	28
TSS (mg/L)	NA	120

[a] Conventional landfill leachate, data calculated from Dec. 2009-Jul. 2010
[b] Bioreactor landfill leachate plus wastewater from treatment facility, data calculated from Jan.-Jun. 2013
NA – data not available

Table 3.2 Total ammonia nitrogen concentration (TAN), calculated free ammonia (NH_3-N) and methane (CH_4) production in Thailand and New Jersey leachate inoculated reactors

	Thailand Leachate Reactors[a]				New Jersey Leachate Reactors[b]			
Target TAN (g N/L)	pH	Actual TAN (g N/L)	Calculated NH_3-N (g N/L)	CH_4 Production (mL/ two weeks)	pH	Actual TAN (g N/L)	Calculated NH_3-N (g N/L)	CH_4 Production (mL/ two weeks)
5	7.65 (0.08)	6.23 (0.16)	0.30 (0.04)	51.41 (2.68)	7.54 (0.15)	5.53 (0.48)	0.21 (0.10)	46.81 (0.79)
7.5	7.49 (0.05)	8.15 (0.23)	0.27 (0.03)	55.70 (3.68)	7.66 (0.04)	8.36 (0.07)	0.40 (0.03)	27.91 (0.32)
10	7.39 (0.02)	9.66 (0.13)	0.26 (0.01)	53.79 (2.24)	7.36 (0.09)	10.10 (0.18)	0.25 (0.06)	17.87 (4.65)
12.5	7.29 (0.12)	11.40 (0.30)	0.24 (0.06)	42.30 (8.58)	7.13 (0.05)	11.85 (0.23)	0.18 (0.02)	9.86 (1.36)
Active Control	7.37 (0.29)	0.07 (0)	0	52.62 (1.58)	7.82 (0.08)	0.76 (0.09)	0.05 (0)	47.74 (2.38)
Background Control	7.59 (0)	0	0	0.39 (0)	7.82 (0)	0	0	0.06 (0)

[a] data from day 218

[b] data from day 296

averages of three reactors and numbers in parentheses are standard deviations

Table 3.3 Summary of the major bacterial and archaeal phylotypes of the microbial community [a] data from day 218 ; [b] data from day 292

Phylum	Class	Order	Family	Genus	Genus % of total community	
					Thailand Leachate [a]	New Jersey Leachate [b]
Bacteria						
Firmicutes	Clostridia	Thermoanaerobacterales	Thermoanaerobacteraceae	*Tepidanaerobacter*	19.02	60.02
				Gelria	4.50	15.33
		Clostridiales	Clostridiaceae	*Garciella*	17.84	13.05
				Clostridium	3.64	0.67
			Ruminococcaceae	*Fastidiosipila*	1.25	0.03
			Peptococcaceae	*Cryptanaerobacter*	1.87	0
			Caldicoprobacteraceae	*Caldicoprobacter*	5.80	1.56
	Bacilli	Bacillales	Bacillaceae	*Bacillus*	2.37	0
Bacteroidetes	Bacteroidia	Bacteroidales	Porphyromonadaceae	*Proteiniphilum*	1.50	0.37
				Petrimonas	1.53	2.90
	Flavobacteriia	Flavobacteriales	Flavobacteriaceae	*Maritimimonas*	11.86	0
Synergistetes	Synergistia	Synergistales	Synergistaceae	*Thermovirga*	4.09	0.83
				Aminobacterium	4.29	1.72
Cloacimonetes		candidatus_cloacamonas			15.20	0
Other (Proteobacteria, Op9 (candidate division) , Chloroflexi, Thermotogae, Lentisphaerae, Spirochaetes)					5.24	3.54
Archaea						
Euryarchaeota	Methanobacteria	Methanobacteriales	Methanobacteriaceae	*Methanobacterium*	4.12	0
	Thermoplasmata	Thermoplasmatales	Thermoplasmataceae	*Thermoplasma*	3.46	0
	Methanomicrobia	Methanosarcinales	Methanosarcinaceae	*Methanosarcina*	58.40	0
			Methanosaetaceae	*Methanosaeta*	0.70	0
		Methanomicrobiales	Methanomicrobiaceae	*Methanomicrobiaceae*	0.25	0
				Methanoculleus	33.07	100

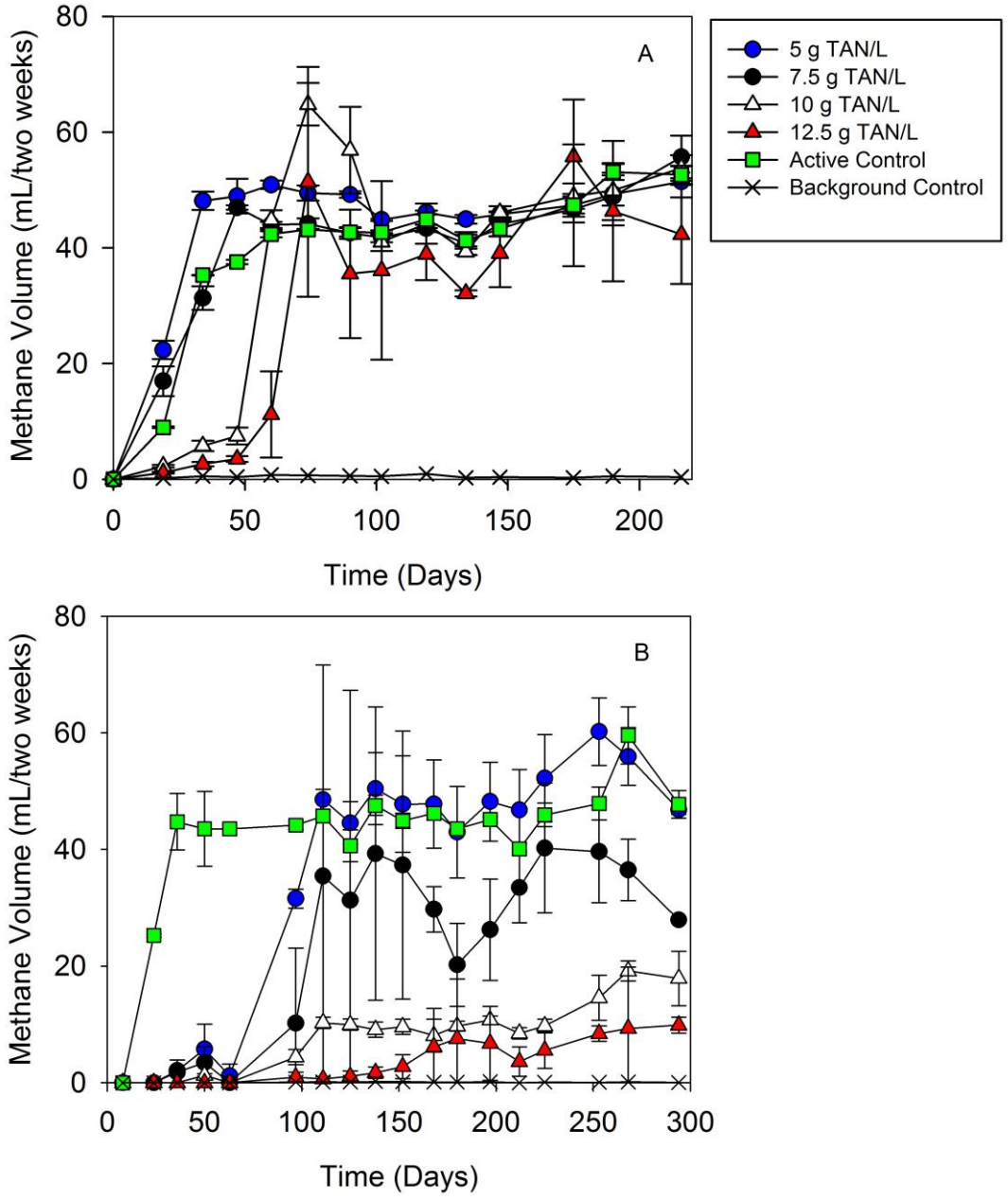

Fig. 3.1 Methane production from reactor inoculated with Thailand leachate (A) and New Jersey leachate (B). Symbols are averages of triplicates and error bars are ± one standard deviation.

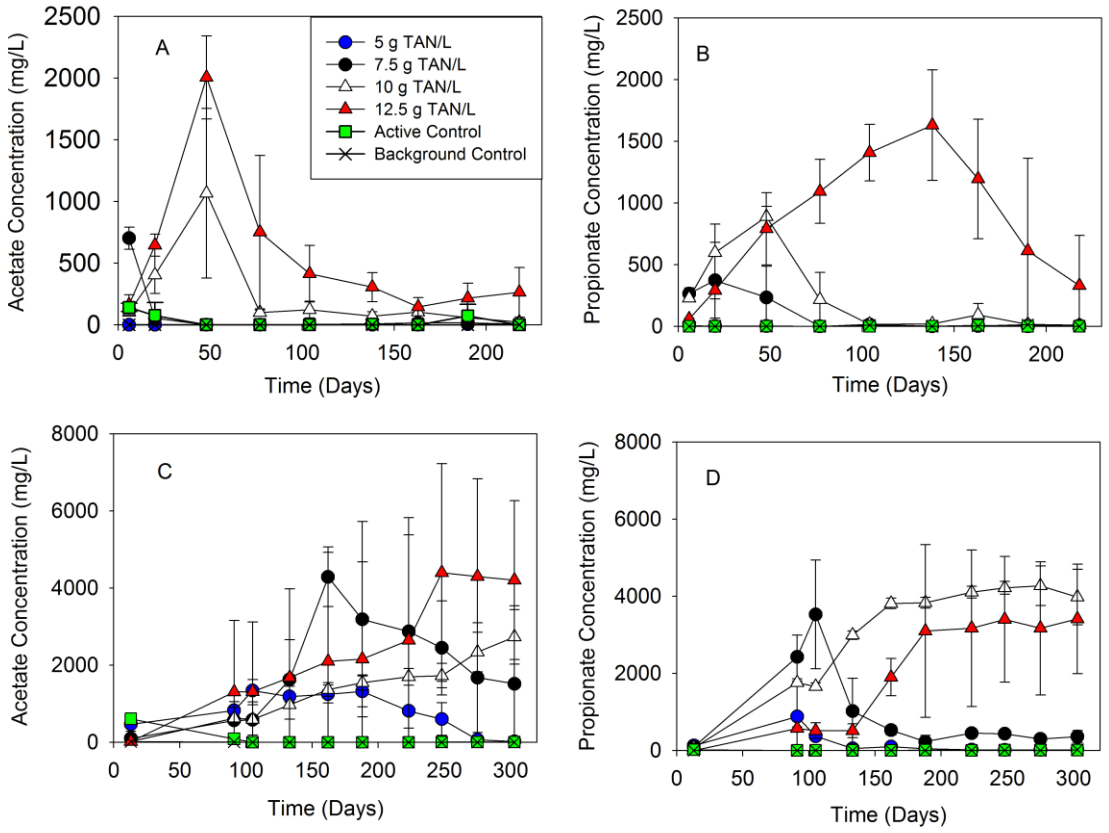

Fig. 3.2 Acetate and propionate concentration from reactors inoculated with Thailand leachate (A, B) and New Jersey leachate (C, D). Symbols are averages of triplicates and error bars are ± one standard deviation.

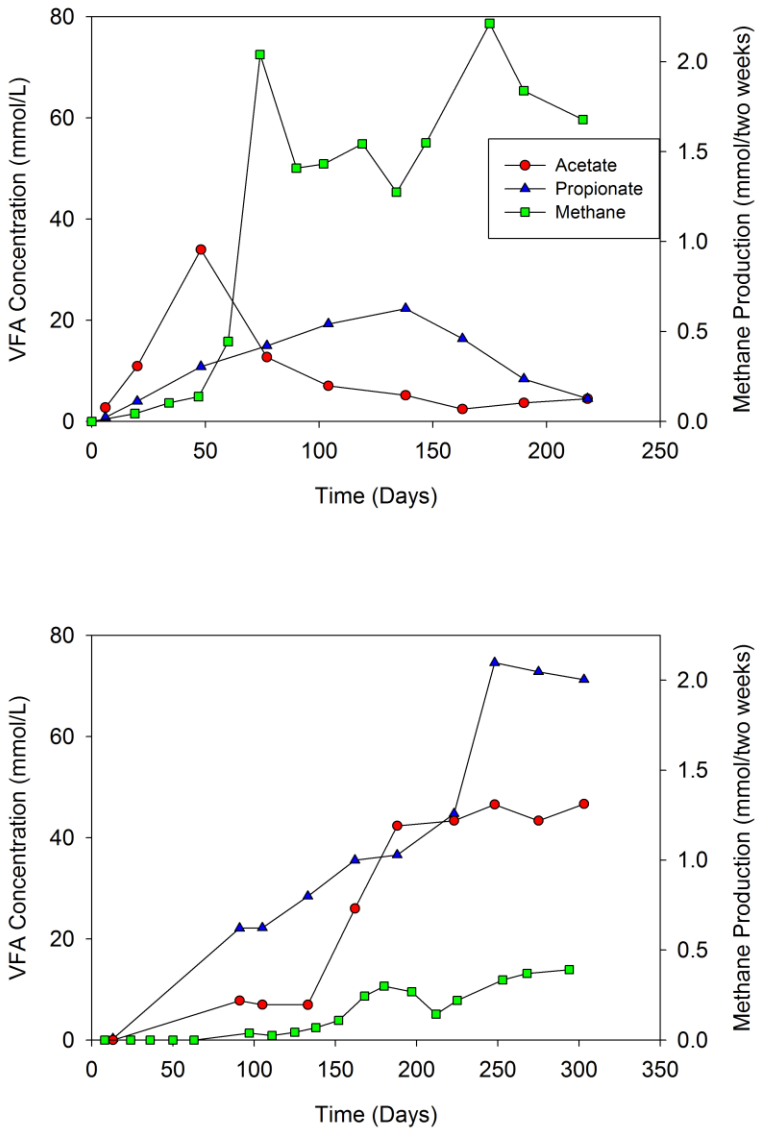

Fig. 3.3 Changes in acetate and propionate concentrations in Thailand (A) and New Jersey (B) leachate reactors at target 12.5 g TAN/L. Symbols are averages of triplicates.

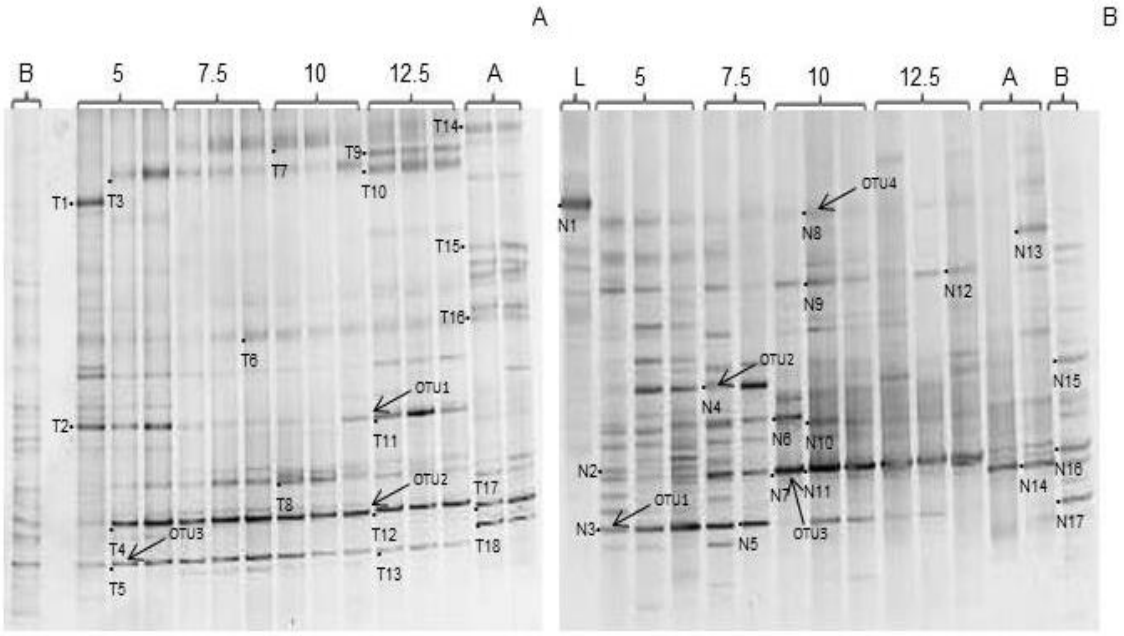

Fig. 3.4 Bacterial DGGE profiles of the 16S rRNA gene PCR products amplified from DNA extracted from reactors inoculated with Thailand leachate, Day 218 (A), and New Jersey leachate, Day 292 (B). Lanes are labelled with target TAN concentrations (g TAN/L); lane A, B, and L indicate the DGGE profile of active control, background, and leachate from New Jersey, respectively. Dots and numbers indicate the bands sequenced.

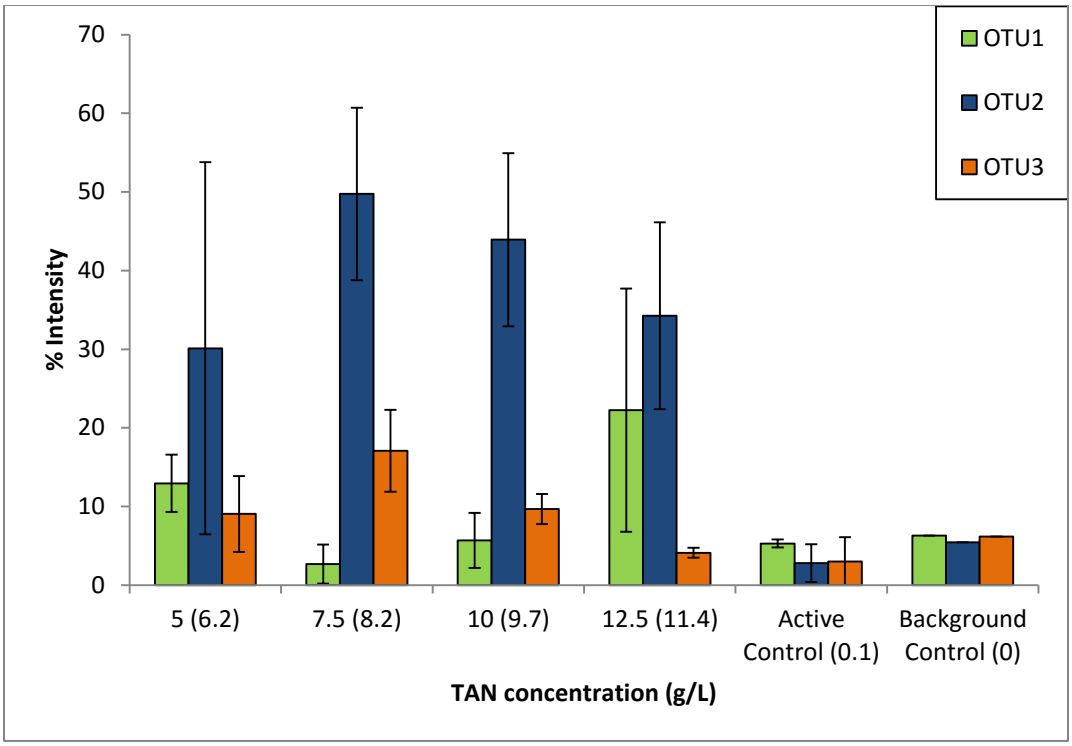

Fig. 3.5 The bacterial DGGE band intensity from reactors inoculated with Thailand leachate, Day 218, at target 5-12.5 g TAN/L. The numbers in parentheses represent actual TAN concentrations. Bars are averages and error bars are one standard deviation of the % of the total band intensity from triplicate DGGE lanes. The matches to specific phylotypes are: OTU1- *Garciella nitratireducens*; OTU2- *Tepidanaerobacter acetatoxydans*; and OTU3- *Aminobacterium sp.*

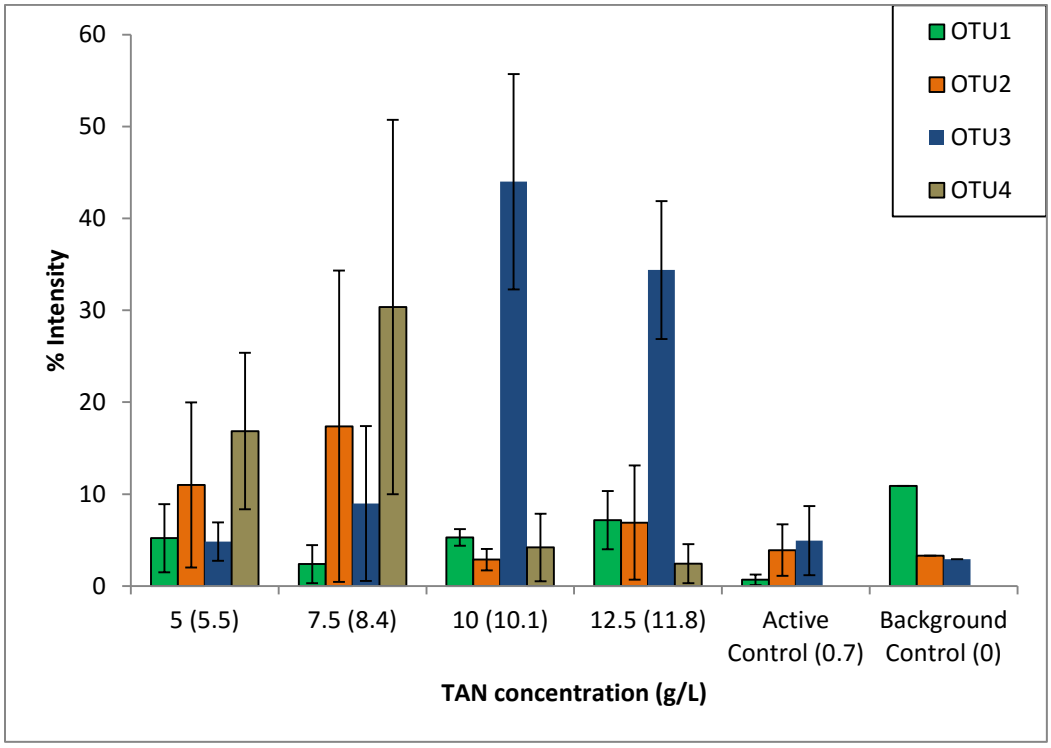

Fig. 3.6 The bacterial DGGE band intensity from reactors inoculated with New Jersey leachate, Day 292, at target 5-12.5 g TAN/L. The numbers in parentheses represent actual TAN concentrations. Bars are averages and error bars are one standard deviation of the % of the total band intensity from triplicate DGGE lanes. The matches to specific phylotypes are: OTU1- *Thermanaerovibrio sp.*; OTU2- *Thermanaerovibrio* spp; OTU3- *Tepidanaerobacter acetatoxydans*; and OTU4- *Tepidanaerobacter* spp.

Table 3.4 Bacterial DGGE 16S rRNA gene band identifications from Thailand and New Jersey leachate inoculated reactors

DGGE band	Closest match	Identity (%)	Phyla	Closest match Accession no.
Thailand				
T1	*Clostridium* spp.	84	Firmicutes	NR_102768.1
T2	*Sporanaerobacter acetigenes*	98	Firmicutes	NR_025151.1
T3	*Tepidanaerobacter* spp.	83	Firmicutes	NR_074537.1
T4	*Tepidanaerobacter* spp.	92	Firmicutes	NR_040966.1
T5	*Aminobacterium sp.*	87	Synergistetes	NR_074624.1
T6	*Desulfotomaculum sp.*	81	Firmicutes	NR_114758.1
T7	*Desulfotomaculum sp.*	83	Firmicutes	NR_114758.1
T8	*Tepidanaerobacter* spp.	83	Firmicutes	NR_074537.1
T9	*Ardenticatena sp.*	95	Chloroflexi	NR_113219.1
T10	*Tepidanaerobacter* spp.	89	Firmicutes	NR_074537.1
T11	*Garciella nitratireducens*	100	Firmicutes	NR_025688.1
T12	*Tepidanaerobacter acetatoxydans*	100	Firmicutes	NR_025688.1
T13	*Thermanaerovibrio sp.*	90	Firmicutes	NR_074537.1
T14	*Mesotoga sp.*	93	Thermotogae	NR_102952.1
T15	*Mycoplasma sp.*	81	Firmicutes	NR_108494.1
T16	*Mesotoga prima*	98	Thermotogae	NR_102952.1
T17	*Thermovirga sp.*	95	Synergistetes	NR_074606.1
T18	*Flavobacterium sp.*	90	Bacteroidetes	NR_109522.1
New Jersey				
N1	*Arcobacter nitrofigilis*	100	Proteobacteria	NR_102873.1
N2	*Tepidanaerobacter sp.*	92	Firmicutes	NR_074537.1
N3	*Thermanaerovibrio sp.*	92	Firmicutes	NR_074520.1
N4	*Thermanaerovibrio* spp.	88	Firmicutes	NR_074520.1

DGGE band	Closest match	Identity (%)	Phyla	Closest match Accession no.
N5	*Thermanaerovibrio* spp.	91	Firmicutes	NR_074520.1
N6	*Aminobacterium sp.*	77	Synergistetes	NR_074624.1
N7	*Tepidanaerobacter acetatoxydans*	100	Firmicutes	NR_074537.1
N8	*Tepidanaerobacter* spp.	96	Firmicutes	NR_074537.1
N9	*Tepidanaerobacter sp.*	96	Firmicutes	NR_074537.1
N10	*Tepidanaerobacter sp.*	88	Firmicutes	NR_074537.1
N11	*Tepidanaerobacter acetatoxydans*	100	Firmicutes	NR_074537.1
N12	*Soehngenia sp.*	91	Firmicutes	NR_025761.1
N13	*Mesotoga sp.*	87	Thermotogae	NR_102952.1
N14	*Cloacibacillus sp.*	91	Synergistetes	NR_115465.1
N15	*Garciella nitratireducens*	100	Firmicutes	NR_025688.1
N16	*Tepidanaerobacter* spp.	94	Firmicutes	NR_074537.1
N17	*Thermanaerovibrio* spp.	91	Firmicutes	NR_074520.1

T17, T18- Active control

N13, N14- Active control

N15, N16, N17- Background control

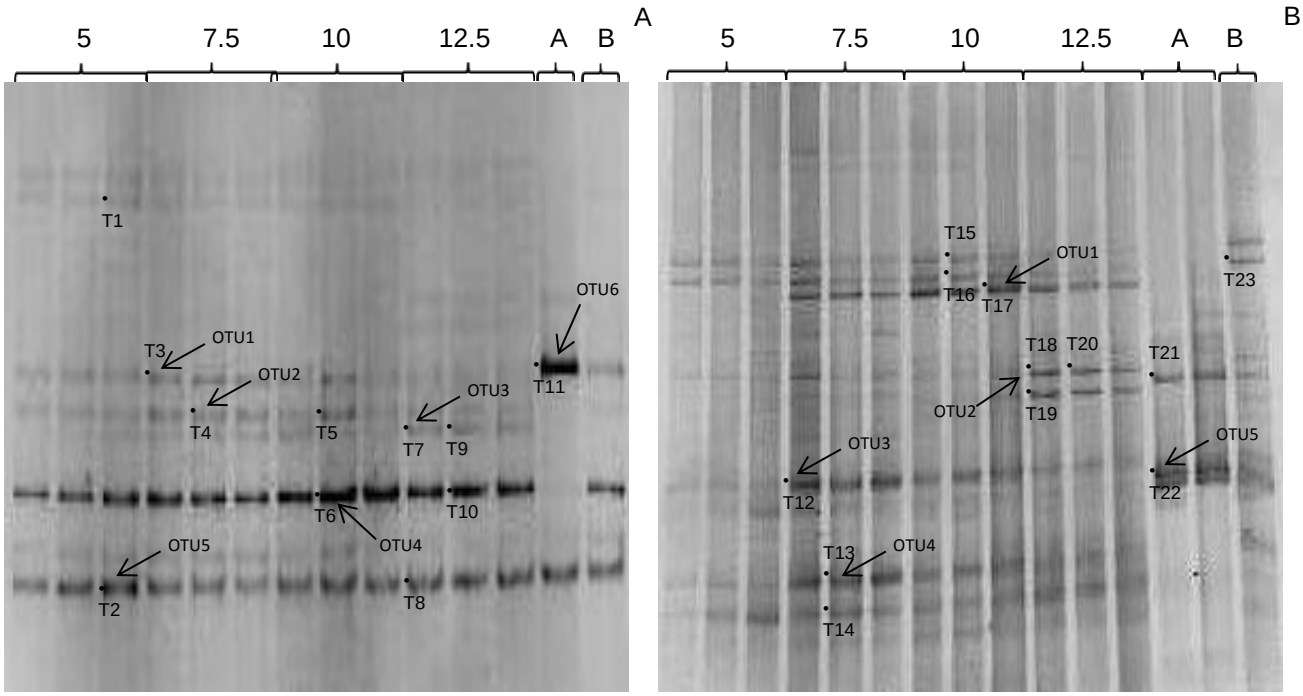

Fig. 3.7 Archaeal DGGE profiles of the 16S rRNA gene PCR products amplified from DNA extracted from reactors inoculated with Thailand leachate, Day 134 (A), and Day 218 (B). Lanes are labelled with target TAN concentrations (g TAN/L); lane A, B, and L indicate the DGGE profile of active control, background, and leachate from New Jersey, respectively. Dots and numbers indicate the bands sequenced.

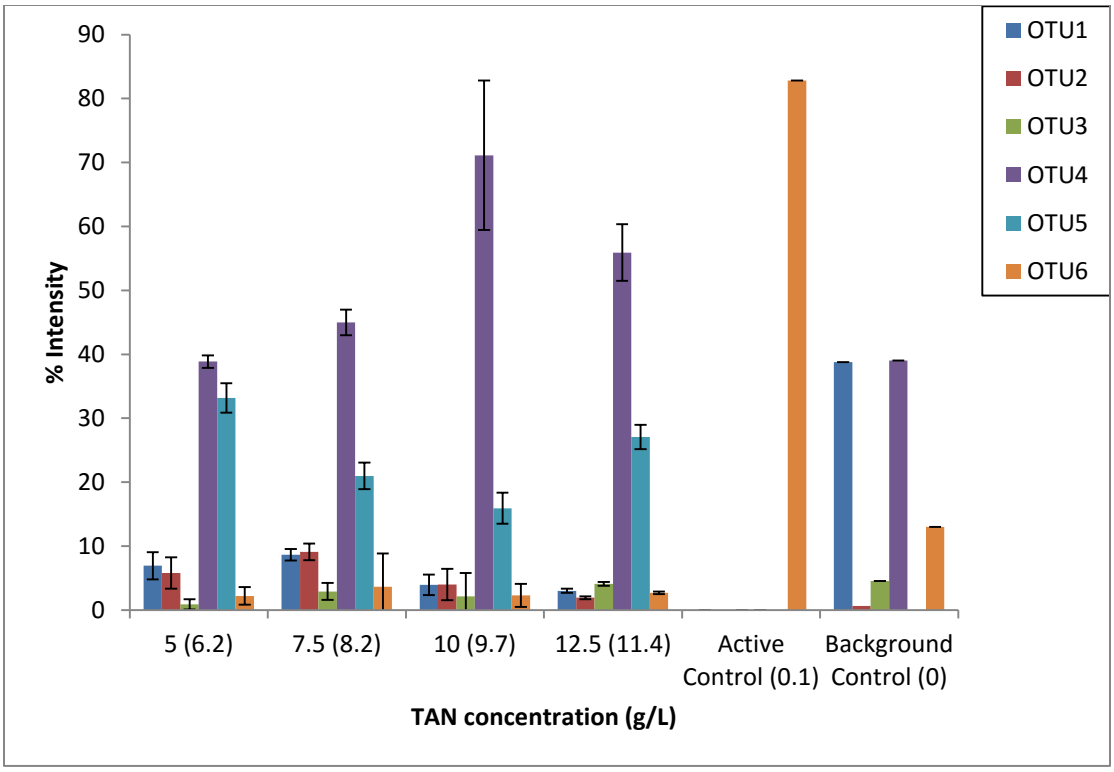

Fig. 3.8 The archaeal DGGE band intensity from reactors inoculated with Thailand leachate, Day 134, at target 5-12.5 g TAN/L. The numbers in parentheses represent actual TAN concentrations. Bars are averages and error bars are one standard deviation of the % of the total band intensity from triplicate DGGE lanes. The matches to specific phylotypes are: OTU1- *Methanosarcina* spp.; OTU2- *Methanosarcina* spp.; OTU3- *Methanocalculus* spp., *Methanomicrobium sp.;* OTU4- *Methanosarcina* spp.; OTU5- *Methanosarcina* spp.; and OTU6- *Methanosaeta concilii*

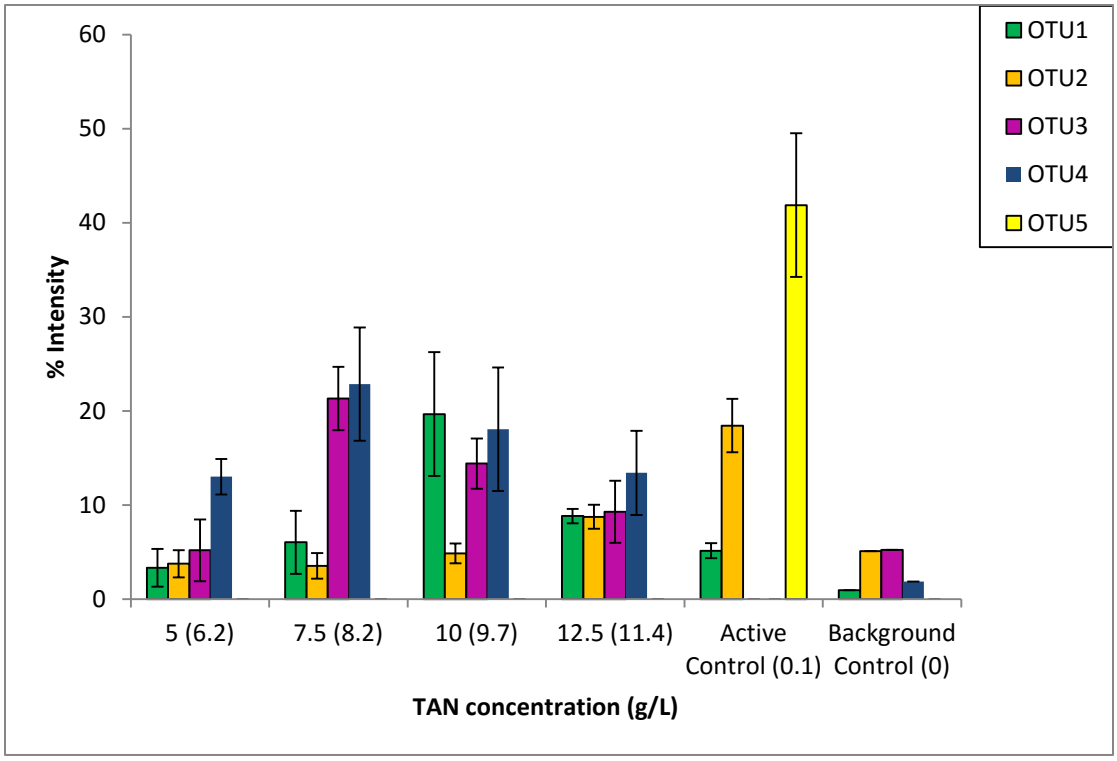

Fig. 3.9 The archaeal DGGE band intensity from reactors inoculated with Thailand leachate, Day 218, at target 5-12.5 g TAN/L. The numbers in parentheses represent actual TAN concentrations. Bars are averages and error bars are one standard deviation of the % of the total band intensity from triplicate DGGE lanes. The matches to specific phylotypes are: OTU1- *Methanosarcina* spp.; OTU2- *Methanoculleus bourgensis*; OTU3- *Methanosarcina* spp.; OTU4- *Methanosarcina* spp.; and OTU5- *Methanosaeta concilii*

Table 3.5 Archaeal DGGE 16S rRNA gene band identifications from Thailand leachate inoculated reactors

DGGE band	Closest match	Identity (%)	Phyla	Closest match Accession no.
Day 134				
T1	*Methanosarcina mazei*	100	Euryarchaeota	NR_074221.1
T2	*Methanosarcina* spp.	99	Euryarchaeota	NR_104757.1
T3	*Methanosarcina* spp.	99	Euryarchaeota	NR_104757.1
T4	*Methanosarcina* spp.	97	Euryarchaeota	NR_104757.1
T5	*Methanosarcina* spp.	98	Euryarchaeota	NR_104757.1
T6	*Methanosarcina* spp.	98	Euryarchaeota	NR_104757.1
T7	*Methanocalculus* spp.	91	Euryarchaeota	NR_028148.1
	Methanomicrobium sp.	91	Euryarchaeota	NR_044726.1
T8	*Methanosarcina* spp.	98	Euryarchaeota	NR_104757.1
T9	*Methanoculleus* spp.	95	Euryarchaeota	NR_042786.1
T10	*Methanosarcina* spp.	98	Euryarchaeota	NR_104757.1
T11	*Methanosaeta concilii*	99	Euryarchaeota	NR_102903.1
Day 218				
T12	*Methanosarcina* spp.	99	Euryarchaeota	NR_104757.1
T13	*Methanosarcina* spp.	97	Euryarchaeota	NR_104757.1
T14	*Methanoculleus bourgensis*	99	Euryarchaeota	NR_042786.1
T15	*Methanosarcina* spp.	99	Euryarchaeota	NR_104757.1
T16	*Methanosarcina* spp.	99	Euryarchaeota	NR_074221.1
T17	*Methanosarcina* spp.	92	Euryarchaeota	NR_104757.1
T18	*Methanoculleus bourgensis*	99	Euryarchaeota	NR_042786.1
T19	*Methanoculleus bourgensis*	98	Euryarchaeota	NR_042786.1
T20	*Methanoculleus bourgensis*	98	Euryarchaeota	NR_042786.1
T21	*Methanosaeta sp.*	94	Euryarchaeota	NR_102903.1

DGGE band	Closest match	Identity (%)	Phyla	Closest match Accession no.
T22	*Methanosaeta concilii*	98	Euryarchaeota	NR_102903.1
T23	*Methanosarcina* spp.	99	Euryarchaeota	NR_074221.1

T11, T21, T22- Active control

T23- Background control

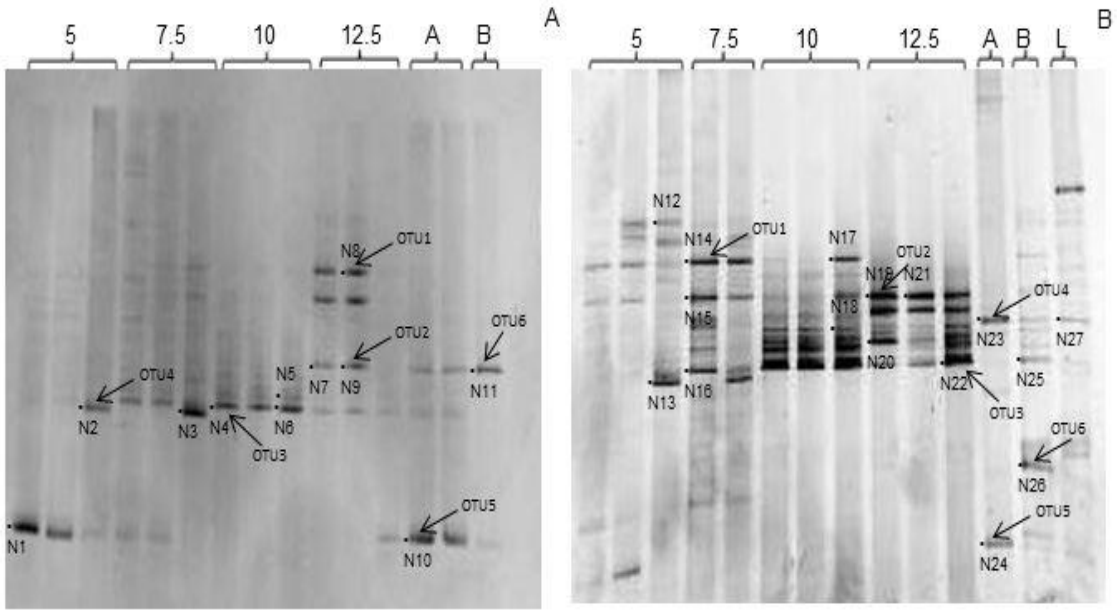

Fig. 3.10 Archaeal DGGE profiles of the 16S rRNA gene PCR products amplified from DNA extracted from reactors inoculated with New Jersey leachate, Day 154 (A), and Day 292 (B). Lanes are labelled with target TAN concentrations (g TAN/L); lane A, B, and L indicate the DGGE profile of active control, background, and leachate from New Jersey, respectively. Dots and numbers indicate the bands sequenced.

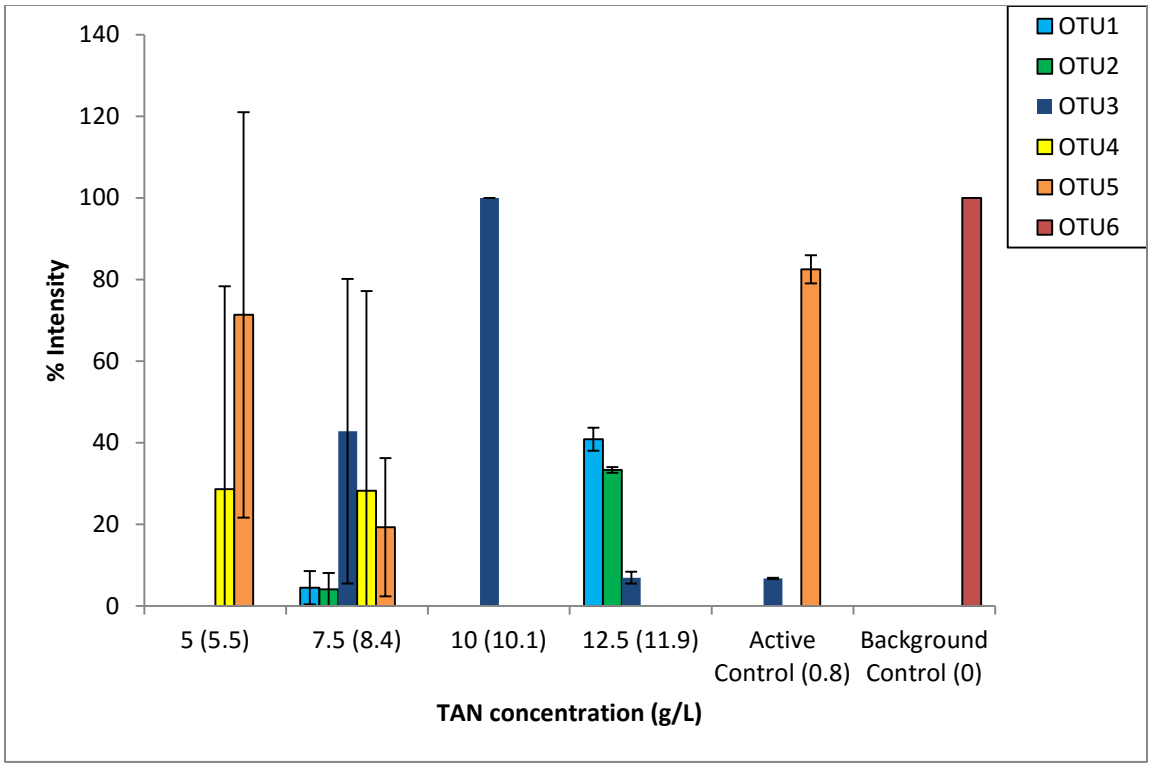

Fig. 3.11 The archaeal DGGE band intensity from reactors inoculated with New Jersey leachate, Day 154, at target 5-12.5 g TAN/L. The numbers in parentheses represent actual TAN concentrations. Bars are averages and error bars are one standard deviation of the % of the total band intensity from triplicate DGGE lanes. The matches to specific phylotypes are: OTU1- *Methanoculleus bourgensis*; OTU2-*Methanoculleus bourgensis*; OTU3- *Methanoculleus bourgensis*; OTU4- *Methanosaeta sp.*; OTU5- *Methanosarcina* spp.; and OTU6- *Methanosaeta sp.*

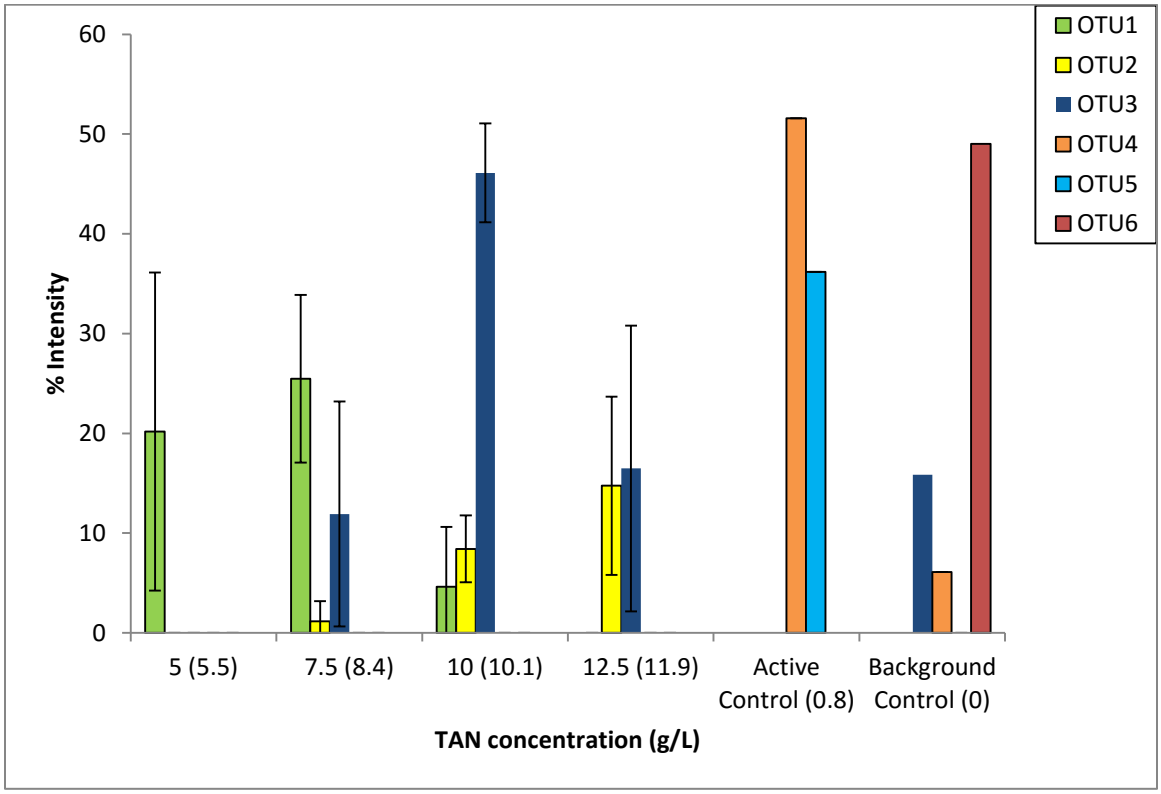

Fig. 3.12 The archaeal DGGE band intensity from reactors inoculated with New Jersey leachate, Day 292, at target 5-12.5 g TAN/L. The numbers in parentheses represent actual TAN concentrations. Bars are averages and error bars are one standard deviation of the % of the total band intensity from triplicate DGGE lanes. The matches to specific phylotypes are: OTU1- *Methanoculleus bourgensis*; OTU2-*Methanoculleus bourgensis*; OTU3- *Methanoculleus sp.*; OTU4- *Methanosaeta concilli*; OTU5- *Methanosarcina* spp.; and OTU6- *Methanosarcina* spp.

Table 3.6 Archaeal DGGE 16S rRNA gene band identifications from New Jersey leachate inoculated reactors

DGGE band	Closest match	Identity (%)	Phyla	Closest match Accession no.
Day 154				
N1	*Methanosarcina* spp.	99	Euryarchaeota	NR_074221.1
N2	*Methanosaeta sp.*	96	Euryarchaeota	NR_102896.1
N3	*Methanosaeta harundinacea*	98	Euryarchaeota	NR_102896.1
N4	*Methanoculleus bourgensis*	100	Euryarchaeota	NR_042786.1
N5	*Methanoculleus bourgensis*	100	Euryarchaeota	NR_042786.1
N6	*Methanoculleus bourgensis*	100	Euryarchaeota	NR_042786.1
N7	*Methanoculleus bourgensis*	98	Euryarchaeota	NR_042786.1
N8	*Methanoculleus bourgensis*	99	Euryarchaeota	NR_042786.1
N9	*Methanoculleus bourgensis*	99	Euryarchaeota	NR_042786.1
N10	*Methanosarcina* spp.	99	Euryarchaeota	NR_074221.1
N11	*Methanosaeta sp.*	93	Euryarchaeota	NR_102903.1
Day 292				
N12	*Methanoculleus* spp.	99	Euryarchaeota	NR_042786.1
N13	*Methanosaeta sp.*	86	Euryarchaeota	NR_102896.1
N14	*Methanoculleus bourgensis*	98	Euryarchaeota	NR_042786.1
N15	*Methanoculleus* spp.	99	Euryarchaeota	NR_043961.1
N16	*Methanoculleus bourgensis*	100	Euryarchaeota	NR_042786.1
N17	*Methanoculleus bourgensis*	99	Euryarchaeota	NR_042786.1
N18	*Methanoculleus bourgensis*	100	Euryarchaeota	NR_042786.1
N19	*Methanoculleus bourgensis*	98	Euryarchaeota	NR_042786.1
N20	*Methanoculleus bourgensis*	97	Euryarchaeota	NR_042786.1

DGGE band	Closest match	Identity (%)	Phyla	Closest match Accession no.
N21	*Methanoculleus sp.*	88	Euryarchaeota	NR_043961.1
N22	*Methanoculleus bourgensis*	100	Euryarchaeota	NR_042786.1
N23	*Methanosaeta concilii*	97	Euryarchaeota	NR_102903.1
N24	*Methanosarcina* spp.	82	Euryarchaeota	NR_074221.1
N25	*Methanoculleus bourgensis*	100	Euryarchaeota	NR_042786.1
N26	*Methanosarcina* spp.	99	Euryarchaeota	NR_104757.1
N27	*Methanosaeta concilii*	99	Euryarchaeota	NR_102903.1

N10, N23, N24- Active control

N11, N25, N26- Background control

N27- Leachate inoculum

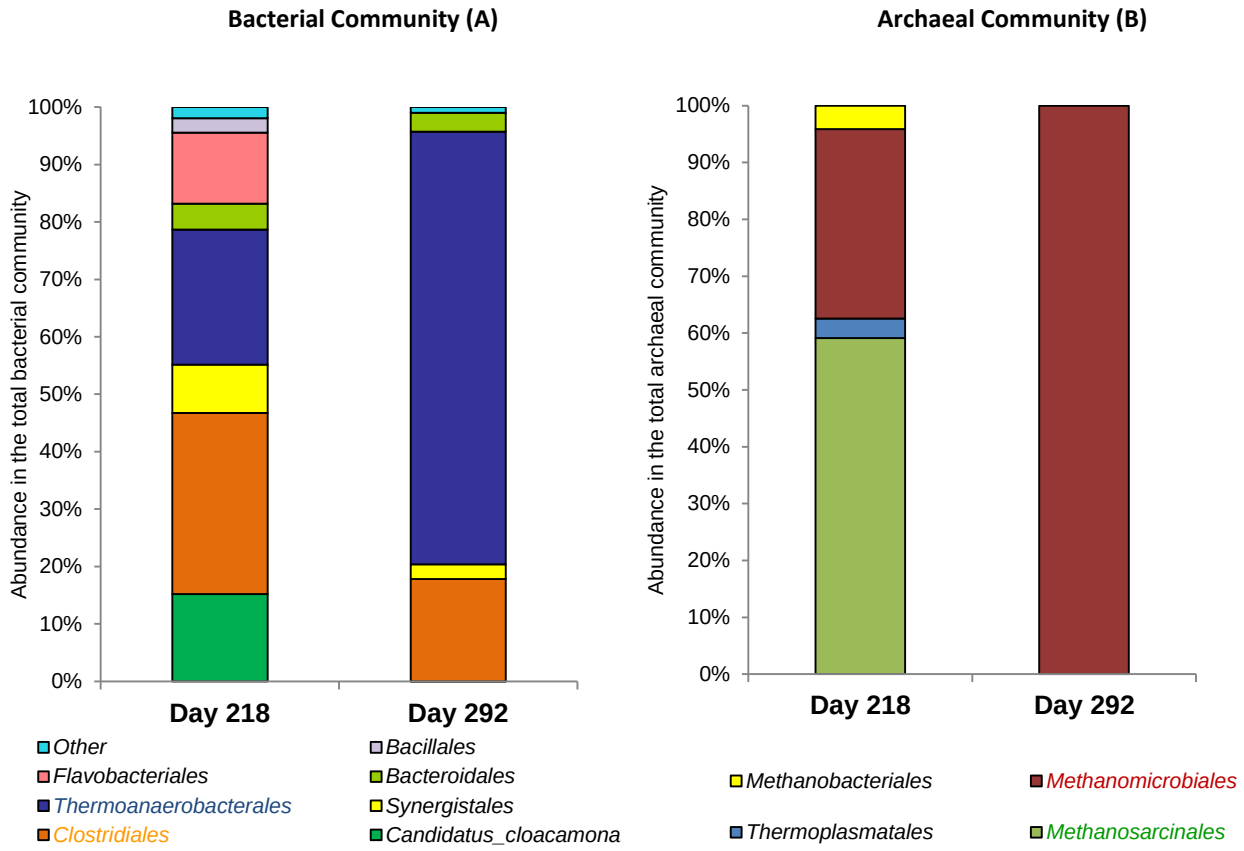

Fig. 3.13 The distribution of the major orders of the bacterial community (A) and the archaeal community (B) from the highest target TAN reactor, 12.5 g TAN/L (actual 11 g TAN/L). LT218 represents reactor inoculated with Thailand leachate Day 218 and L292 represents reactor inoculated with New Jersey leachate Day 292.

Chapter 4 Ammonia Tolerant Microorganisms from Swine Waste Digestate and Wastewater Sludge Digestate Inocula

4.1 Abstract

Ammonia tolerance of microorganisms enriched from swine waste digestate and wastewater sludge digestate was investigated in mesophilic anaerobic reactors under target total ammonia nitrogen (TAN) concentrations up to 12.5 g TAN/L. Results indicated that swine waste digestate reactors revealed that the microorganisms acclimation occurred over time in the second treatment (5 g TAN/L) set up 185 days later using inoculum from the first experiment, whereas reactors with 7.5, 10, and 12.5 g TAN/L exhibited low methane production and volatile fatty acid (VFA) accumulation, especially propionate. However, using swine waste digestate as inoculum suggested better reactor performances than using wastewater sludge digestate. Microbial community analysis revealed different dominance of bacteria and archaea from both reactors. Phylotypes related to *Tepidanaerobacter acetatoxydans*, *Methanosarcina* spp., and *Methanoculleus* spp. dominated in swine waste digestate reactors. In contrast, phylotypes related to *Thermanaerovibrio* spp. and *Methanoculleus* spp. are dominant bacteria and archaea in reactors inoculated with wastewater sludge digestate.

4.2 Introduction

Operating systems for the anaerobic digestion (AD) of high-N residues and agricultural wastes has proven to be challenging. This is especially true for swine manure due to the high content of ammonia and sulfur derived from the protein-rich diet of the

animals (Hansen et al. 1999). Ammonia at an optimum level is a necessary nutrient for bacteria involved in the AD process (Koster and Koomen 1988). However, the instability of anaerobic treatment processes for high-N wastes such as swine manure may also be caused by high amounts of free ammonia released during the process. Ammonia is released from N-containing organic compounds such as proteins and urea. Since ammonia has no known degradation pathways when oxygen or nitrite is absent (Berge et al. 2006), it tends to accumulate in these anaerobic systems. Operation of AD reactors at high ammonia concentrations has been known to cause reactor failure from ammonia inhibition. Several studies have demonstrated the inhibitory effect of ammonia. Free ammonia (NH_3) was shown to inhibit reactors in the range of 0.08-1.1 g NH_3-N/L (Gallert et al. 1998, Hansen et al. 1998, McCarty and McKinney 1961). Other studies reported ammonia inhibition by the ammonium ion (NH_4^+-N) between 1.2-2.4 g NH_4^+-N/L (Koster and Lettinga 1984, Velsen 1979), and further total ammonia nitrogen (TAN) of >4 g TAN/L (Angelidaki and Ahring 1993, Sung and Liu 2003) was also reported to be inhibitory. For swine manure, Hansen et al. (1998) reported that the free ammonia inhibition threshold of continuously stirred tank reactors (CSTRs) digesting swine manure at pH 8.0 was 1.1 g NH_3-N/L. Degradation of swine manure at higher ammonia concentrations (6 g TAN/L) was still possible, but with lower methane yield. Based on these and many other studies, a prevailing paradigm in the field of AD is that it is vital to control ammonia concentration to maintain reactor stability.

Focus on ammonia removal to improve reactor operation has been applied to AD treatment of swine waste through precipitation as struvite (Turker and Celen 2007); ion-exchange and electrochemical regeneration (Lahav et al. 2013); and ultrasonication (Cho

et al. 2014). However, operation of swine waste digestion systems without removing excess ammonia is also feasible. For example, operation of ammonia-rich swine waste AD at different temperatures has been reported. Psychrophilic (24.5°C) anaerobic sequencing batch reactors (SBR) treating swine manure at 8.2 g TAN/L revealed that low accumulation of total VFAs (<100 mg/L) (an indicator of stable operation) could be obtained within 4 weeks when microbial communities were capable of adaptation to high ammonia concentration (Massé et al. 2014). Mesophilic AD treating swine manure was well acclimated to ammonium concentrations of 3 g NH_4^+-N/L over a period of 80 days (Velsen 1979). In addition, SBR reactors treating swine waste subjected to 5.2 g TAN/L in the mesophilic temperature (35-38 °C) could overcome ammonia toxicity as evidenced by increasing the methane yield over a 100 day period (Garcia and Angenent 2009). Moreover, thermophilic AD of swine manure containing 6 g TAN/L improved by increasing the hydraulic retention times (HRT), adding activated carbon, glauconite or methanogenic granules, and sedimenting the biomass/particles in an effort to overcome ammonia inhibition (Hansen et al. 1999).

Characterization of bacterial strains from swine manure digesters has been reported. Iannotti et al. (1982) classified bacterial strains in swine waste digesters into the following genera: *Peptostreptococcus*, *Eubacterium*, *Bacteroides*, *Lactobacillus*, *Peptococcus*, *Clostridium*, and *Streptococcus* plus two unidentified groups. There are only a few studies that specifically focused on identifying microbial communities in high ammonia systems. Chung et al. (2013) reported the predominance of the Phyla Firmicutes, Proteobacteria, and Euryarchaeaota in mesophilic (35°C) anaerobic plug-flow swine waste reactors operated at free ammonia of 0.7 g NH_3-N/L. The microbial

community dynamics in anaerobic mesophilic digesters treating piggery wastewater at 3.2 g TAN/L showed the dominance of the phylum Firmicutes and phylotypes representing uncultured bacteria, and an overall higher bacterial diversity than the archaea, which included *Methanosarcina* and *Methanoculleus sp.* (Patil et al. 2010). In addition, the microbial community in mesophilic continuous stirred tank reactors (CSTR) fed chicken and swine manure at an ammonium concentration of 3.3-3.7 g NH_4^+-N/L was dominated by members of unclassified *Clostridiales*, and the genus *Methanosarcina* (Ziganshina et al. 2014). That study indicated that strictly hydrogenotrophic methanogens, in particular *Methanoculleus sp.*, was only a minor portion of the community.

Moreover, a dynamic shift in populations in AD responding to increasing ammonia concentrations was observed. The pathway shift from acetotrophic methanogenesis to syntrophic acetate oxidation (SAO) followed by hydrogenotrophic methanogenesis has been reported (Hattori 2008, Schnurer et al. 1994, Schnurer and Nordberg 2008, Ziganshina et al. 2014). *Tepidanaerobacter acetatoxydans*, an anaerobic, syntrophic acetate-oxidizing bacterium (SAOB) (Schnurer and Nordberg 2008), hydrogenotrophic methanogens *Methanoculleus sp.* (Westerholm et al. 2011c) and acetotrophic methanogens Methanosarcina *sp.* (Westerholm et al. 2011a) were observed to dominate in the presence of high ammonia during AD in those studies. However, these studies were subjected to ammonium concentration of only 3-7 g NH_4^+-N/L.

There is a potential benefit to operating digesters at high ammonia concentrations where ammonia recovery could be optimized. Therefore, it is of interest to investigate

microbial communities at higher ammonia concentrations that tend to accumulate in reactors, and to identify ammonia tolerant bacteria/archaea.

A potential use for ammonia liberated during AD is recovery and use as a bioenergy source. Babson et al. (2013) performed an energy balance of a theoretical AD system that incorporates ammonia separation and recovery of biologically-released ammonia with subsequent catalytic reforming to produce hydrogen. The study showed that at a C: N ratio of 17 or lower (corresponding to 2 g NH_4^+-N/L and greater) the energy output from the Anaerobic Digestion-Bioammonia to Hydrogen (ADBH) system was greater than AD generating methane alone. Therefore, it is likely that operating AD with high ammonia concentration is beneficial for resource recovery. Understanding of what microbes are ammonia tolerant, and how widely they are distributed could aid in this effort.

The overall goal of this study was to enrich and identify microorganisms tolerating high ammonia concentrations. We hypothesize that microbial communities that have developed over long periods of time in high ammonia anaerobic environments are ammonia tolerant. Thus, different engineered systems may have different intrinsic communities—some with tolerance and some without tolerance for ammonia. Swine waste digestate and wastewater sludge digestate were used as two different inocula (each coming from different prevailing conditions of ammonia concentration) to enrich and identify microbial communities *(bacteria, archaea)* in enrichments fed glutamate as a model high-N waste. Ammonia tolerant organisms may be beneficial for enhancing the efficiency of waste treatment by allowing stable operation at overall higher ammonia

concentrations in AD, which could untimately aid in more efficient recovery of ammonia/ammonium as a resource.

4.3 Materials and methods

4.3.1 Digestate inocula

Swine waste digestate was obtained from Pinehurst Acres Farm, Pennsylvania, USA. Pinehurst Acres operates a 4,400 unit grow/finish hog production facility. The facility operates a mesophilic anaerobic digester with a capacity of 143,000 gallons. The digester is designed to operate with an HRT of 28 days at 6% solids. Wastewater sludge digestate was obtained from the Joint Meeting of Essex and Union Counties (JMEUC) Edward P. Decher Secondary Wastewater Treatment Facility, Elizabeth, New Jersey, USA. The JMEUC is rated to treat 85 million gallons municipal wastewater per day and utilizes mesophilic anaerobic digestion as part of its biosolids production process.

Swine waste digestate samples (1 L) were placed in sterile Nalgene containers and shipped on ice at 4°C to Rutgers University. The samples from JMEUC were transported by car to Rutgers within one hour after collection. The samples were stored at 4°C from arrival for one day prior to use in establishing reactors. The characteristics of the swine waste digestate and wastewater sludge digestate are shown in Tables 4.1 and 4.2.

4.3.2 Reactor set-up and operations

The 160-mL serum bottles (VWR, Radnor, PA, USA) were sterilized by autoclaving, made anoxic by purging with sterile 99.998% nitrogen gas, which flowed through a sterile 0.45 μm filter, and 10 mL swine waste digestate or wastewater sludge digestate was added via a sterile glass pipette. The total liquid volume of each bottle was adjusted to 100 mL with sterile anaerobic minimal medium (Fennell and Gossett 1997). After setup, bottles were operated with a hydraulic retention time (HRT) of 70 days or 140 days by a fill and draw exchange of 10 % of the enrichment volume (10 mL) every week for the reactors with 0.5-5 g TAN/L or every two weeks for the reactors with 5-12.5 g TAN/L, to achieve semi-continuous operation. Glutamate (1 mmol) was added via a sterile syringe initially and thereafter every week or two weeks as the sole carbon and energy source from a sterile 500 mM sodium glutamate stock solution. The reactors inoculated with swine waste digestate were set up into two sets (low and high ammonia). For the first set of treatments, swine waste inoculated reactors were established in triplicate with a target TAN of 0.5, 1, 2.5, and 5 g TAN/L by adding appropriate volumes of sterile, anoxic 5 M NH_4Cl stock solution initially, and after each fill and draw to maintain a constant imposed concentration. For the second set of treatments, second generation reactors were set up at higher TAN concentrations (5, 7.5, 10, and 12.5 g TAN/L) using inoculum from the 5 g TAN/L reactors which had been operated for 185 days.

The reactors inoculated with wastewater sludge digestate were set up only once with a target TAN of 5, 7.5, 10, and 12.5 g TAN/L.

Actual TAN concentrations in the reactors as measured analytically were slightly different than these norminal values and are shown in Table 4.3. Active controls were fed

glutamate as a sole carbon and energy source and background controls received no carbon source. Active and background controls had no NH_4Cl added other than that in the original minimal medium and N was analytically determined to be 0.1 and 0.5 g TAN/L in the first and second control set reactors inoculated with swine waste digestate and 0.5 g TAN/L in the wastewater sludge digestate inoculated control reactor. Bottles were incubated at 35°C in the dark and manually shaken every few days.

4.3.3 Analytical methods

Biogas volume produced from each reactor was measured by water displacement. Methane content was determined from a 250 µL headspace sample using a Pressure-Lok® Series A-2 syringe (VICI® Precision Sampling, Baton Rouge, CA, USA) with a flame sterilized sideport needle. The sample was injected into an Agilent 6890 N gas chromatograph (Agilent Technologies, Santa Clara, CA, USA) equipped with a GS-GasPro capillary column (30 m x 0.32 mm I.D.; J&W Scientific, Folsom, CA, USA) and a flame ionization detector. Helium was the carrier gas at a constant pressure of 131 kPa. The oven temperature was 150°C. The resulting chromatographic peak area was compared to a five point calibration curve prepared using mixtures of 0 to 99% methane created by mixing volumes of methane (99% purity; Matheson Tri- Gas, Inc., Montgomeryville, PA, USA) and air. Methane production volume was calculated from the methane content and biogas volume at 998 mbar and 23°C. The moles of methane produced were then corrected to STP (1 atm, 0°C).

The volatile fatty acids acetate, propionate, and butyrate were measured by high performance liquid chromatography (HPLC). Reactor effluent samples (0.75 mL) were centrifuged at 9390 *g* (Eppendorf Model No. 5424) for 3 minutes and the supernatant was filtered using Spin-X Centrifuge Tube Filters, Corning Nylon Membrane, pore size 0.45 µm (VWR). Filtered samples were analyzed on a Beckman Coulter® System GoldTM HPLC (Beckman-Coulter, Inc., Fullerton, CA, USA) using a Bio-Rad® Aminex HPX-87H organic acid analysis column (Bio-Rad Laboratories, Hercules, CA). The column was held at 60°C. The mobile phase was 0.008 N H_2SO_4 at a flow rate of 0.6 mL/minute. UV detection was at a wavelength of 210 nm. Chromatographic peak areas were quantified by comparison to standard curves of acetic, propionic, and butyric acids (99-99.7% purity, Sigma-Aldrich Co., St. Louis, MO, USA) over a concentration range from 250 to 1,000 mg/L. The detection limit for the system was approximately 8.4 mg acetate/L.

Total ammonia nitrogen (TAN) was measured by ion chromatography (IC). To convert free ammonia to ammonium ion, the pH of aqueous samples was adjusted to < 2 using 10 N H_2SO_4 immediately after recovery. Next, samples were centrifuged at 9390 *g* for 3 minutes (Eppendorf Model No. 5424), and the supernatant was filtered using Spin-X Centrifuge Tube Filters, Corning Nylon Membrane, pore size 0.45 µm (VWR). The filtrate was diluted 800 times with MilliQ water, and analyzed for TAN using a Dionex ICS-1000 ion chromatograph equipped with an IonPac™ CS12A RFTC™ 4x250 mm cation column, and a CSRS™ 300 4 mm cation suppressor (Dionex Corporation, Salt Lake City, UT, USA). The mobile phase was 20 mN methanosulfonic acid. TAN was

calculated from a standard curve prepared over a range from 0.125 to 2 mM and corrected for dilution.

The pH was routinely measured using an Accumet® Basic AB15 (Fisher Scientific, Pittsburgh, PA, USA) pH meter with symphony Ag/AgCl pH electrode (VWR). Free ammonia was then calculated from the equilibrium equation (Eqn. 1) (Angelidaki and Ahring 1993):

$$[NH_3 - N] = \frac{[TAN]}{\left[1 + \frac{[H^+]}{K_a}\right]} \qquad \text{Eqn. 1}$$

where K_a (the dissociation constant) = 1.12×10^{-9} at 35°C

Methane, VFAs, and TAN data are reported as an average of triplicate reactors ± one standard deviation.

4.3.4 Microbial community analysis

Bacterial and archaeal communities were analyzed using polymerase chain reaction (PCR) coupled to denaturing gradient gel electrophoresis (DGGE). DNA extraction from 1-3 mL enrichment samples was performed using the PowerSoil™ DNA Isolation Kit (MoBio Laboratories, Carlsbad, CA, USA) according to the manufacturer's instructions. The PCR amplification of partial bacterial 16S rRNA genes was performed with forward (338-GC F) and reverse (519R) primers (Nakatsu 2000). The PCR protocol was as follows: initial denaturation at 94°C for 5 minutes, 33 cycles of denaturation at 94°C for 30 seconds, annealing at 55°C for 30 seconds, and elongation at 72°C for 30 seconds; followed by a final extension step of 7 minutes at 72°C (Chen 2010). The PCR

amplification of partial archaeal 16S rRNA genes was performed with ARC787f-GC and ARC1059r (Hwang et al. 2008, Merlino et al. 2013). To amplify the target DNA, a touchdown PCR amplification of archaeal 16S rRNA genes was used with the following conditions: initial denaturation at 94°C for 10 minutes, 20 cycles of denaturation at 94°C for 1 minute, annealing for 1 minute at a temperature that decreased by 0.5°C every cycle from 65°C to the 'touchdown' at 55°C, and elongation at 72°C for 1 minute; and finally, 20 cycles of denaturation at 94°C for 1 minute, annealing at 55°C for 1 minute, and extension at 72°C for 1 minute. Thus, the PCR was performed in a total of 40 cycles. A final extension step was performed at 72°C for 3 minutes. The PCR products were detected by electrophoresis on a 1.5% agarose gel and staining in 0.1% ethidium bromide (EtBr) solution for 30 minutes, then visualized using UV on a Molecular Imager Gel Doc XR system (Bio-Rad Laboratories).

For DGGE, the quantified DNA in PCR products was loaded onto 8% polyacrylamide gels containing a gradient of 30-60% and 40-60% denaturant (100% denaturant contained 7M urea and 40% formamide) for bacteria and archaea, respectively. Electrophoresis was run at 60°C in 1xTAE buffer with operating conditions for bacteria: 4 h at 150V; and for archaea, 17 h at 90V. Gels were stained with SYBR® Gold nucleic acid (Invitrogen, Grand Island, NY, USA) for 30 minutes and documented with a Molecular Imager Gel Doc XR system (Bio-Rad Laboratories). DGGE gel profiles were analyzed using a Molecular Imager Gel Doc XR system (Bio-Rad Laboratories). Dominant bands were excised and DNA was eluted to the same depth in the gel. The DNA fragment was then re-amplified using the DGGE primer set without GC clamp, and re-run on 1.5% agarose gel. The PCR products were purified with USB® ExoSAP-IT®,

and sequenced (Genewiz, South Plainfield, NJ, USA). The sequences were compared with sequences deposited in the National Center for Biotechnology Information (NCBI) database using the BLAST program. All sequencing results were additionally confirmed by the RDP Native Bayesian rRNA Classifier Version 2.6, Sep 2013 (http://rdp.cme.msu.edu/classifier/hierarchy.jsp). A resulting gel image was analyzed for relative band intensities in each lane and calculated as percentage of band intensities using the ImageJ 1.48v quantification software (National Institutes of Health, USA), according to the manufacturer's protocol (http://imagej.nih.gov/ij). For each phylotype detected, the band intensities are reported as an average of triplicates ± one standard deviation.

The 454 pyrosequencing was performed on DNA recovered from swine waste digestate inoculated reactors with TAN of 7.5 and 12.5 g N/L at day 189 and day 328 (one replicate only was sequenced for each condition based on the observation from DGGE that the replicates appeared to contain similar communities). The V2, V3, and V4 regions of the bacterial and archaeal 16S rRNA gene were targeted using the primers 515F and 909R (Wang and Qian 2009). Barcoded amplicon sequencing processes were performed by MR DNA (Shallowater, TX, USA) under the trademark (bTEFAP®). The bTEFAP® process was modified to utilize 16S rRNA gene bacterial primers (515F and 909R) (Wang and Qian 2009). A single-step 30 cycle PCR using HotStarTaq Plus Master Mix Kit (Qiagen, Valencia, CA, USA) was used under the following conditions: 94°C for 3 minutes, followed by 28 cycles of 94°C for 30 seconds; 53°C for 40 seconds and 72°C for 1 minute; after which a final elongation step at 72°C for 5 minutes was performed. Following PCR, all amplicon products from different samples were mixed in equal

concentrations and purified using Agencourt Ampure beads (Agencourt Bioscience Corporation, Beverly, MA, USA). Samples were sequenced utilizing Roche 454 FLX titanium instruments and reagents following the manufacturer's guidelines.

The nucleotide sequences reported in this chapter were deposited in the NCBI nucleotide sequence databases under accession number SRS892986.

4.3.4 Data analysis

Data are presented as average values of triplicates and error bars are one standard deviation. When the term "steady state" is used it refers to a pseudo- steady state condition defined as a period of operation where select average weekly output parameters (concentrations) were within ± 20%.

4.4 Results

The effects of high ammonia concentrations on the performances of anaerobic reactors and microbial communities were investigated. Anaerobic reactors were operated for more than 300 days under target TAN concentrations up to 12.5 g TAN/L using glutamate as the sole carbon and energy source.

4.4.1 Anaerobic reactor inoculated with swine waste digestate

4.4.1.1 Methane Production

Methane production from reactors inoculated with swine waste digestate at target 0.5-5 g TAN/L is shown in Fig. 4.1A. The results revealed that there was a longer start-

up phase and lower methane production at higher TAN concentrations. It took about 50 days for reactors with 5 g TAN/L to reach rapid rates of methane production, compared to 30 days for reactors with 0.5 g TAN/L. At steady state methane production in the reactors with 0.5, 1, and 2.5 g TAN/L were similar to the control, ranging from 40-50 mL/week (1.6-2.0 mmol/week) compared to the theoretical methane production predicted from glutamate to be 2.0 mmol/week (see Section 2.6). In contrast, the 5 g TAN/L reactors had the lowest methane production with less than 30 mL/week (1.0 – 1.7 mmol/week). Methane production from the second generation reactors with target 5- 12.5 g TAN/L is shown in Fig. 4.1B. These reactors were fed every other week. Reactors maintained at 5 g TAN/L in these second set of treatments (inoculated from the original 5 g TAN/L treatments) exhibited a shorter start-up phase than the reactor originally used as inoculum, with a slightly longer lag phase than the control. After day 160, methane production in reactors with 5 g TAN/L and the control were nearly the same. The treatment with 7.5 g TAN/L showed a different methane production trend. After a long start-up phase, methane production increased dramatically to 45 mL/two weeks then dropped to about half that value after 70 days. However, 90 days later (day 303), methane production recovered to the level originally produced. Less than 20 mL/two weeks of methane was produced in reactors with 10 and 12.5 g TAN/L, or 0.1-0.6 mmol/two weeks throughout the experimental period. A summary of pH, target TAN, calculated free ammonia (NH_3-N) and methane production in all reactors is shown in Table 4.3.

4.4.1.2 Volatile Fatty Acids

The results indicated that more acetate and propionate accumulated at high TAN concentration, than at lower concentration, or in the active control. At 0.5 g TAN/L,

acetate concentration reached a peak of 2,800 ± 78 mg/L within 20 days whereas acetate concentration reached 4,200 ± 15 mg/L within 33 days for the 5 g TAN/L reactors (Fig. 4.2A). Acetate accumulated or was utilized dynamically and reached pseudo-steady state values at different time points. Acetate concentration reached pseudo-steady state at day 98 and remained at approximately 22 ± 12 mg/L in most reactors except the treatment with 5 g TAN/L, which required a longer time (105 days) period to reach pseudo-steady state at 261 ± 0.6 mg/L. After day 127, acetate concentration in the 5 g TAN/L reactors dramatically increased and accumulated to 2,400 ± 570 mg/L at day 178. At the same time that acetate increased, propionate decreased (Fig. 4.2B). Changes in propionate concentrations in the reactors with 5 g TAN/L was different from other, lower concentrations. There was constantly an increase in propionate concentration up to 2,160 ± 950 mg/L within 100 days. After that, propionate decreased and remained at a stable concentration of 480 ± 240 mg/L, whereas only a small amount of propionate (17 ± 8 mg/L) was detected at the lower TAN concentrations. Butyrate concentrations remained less than 10 ± 4 mg/L in all reactors (data not shown).

4.4.1.3 Changes in methane and VFA concentrations

Changes in methane and VFA concentrations in the 5 g TAN/L reactors can be classified into four periods based on fluctuation of methane production and VFA accumulation (Fig. 4.3). Period 1 (day 0-50): Acetate increased dramatically and reached 64 mmol/L within 33 days, before decreasing to 45 mmol/L while propionate and methane remained at stable concentrations of 2 and 0.2 mmol/week, respectively. Period 2 (day 50-90): Acetate decreased dramatically at the same time methane was produced

and spiked to 2.5 mmol/week then dropped to 1.3 mmol/week compared to the theoretical methane production at 2 mmol/week. Propionate continuously increased and reached 17 mmol/L at the end of this period. Period 3 (day 90-180): Acetate remained stable at the beginning before increasing dramatically to 40 mmol/L whereas propionate gradually decreased, and methane fluctuated in the range of 1-1.3 mmol/week. Period 4 (day 180-200): Propionate slightly increased while acetate decreased and methane fluctuated and dropped to only 0.4 mmol/week at the end of the experiment.

Fig. 4.4 shows the relationships between methane production and VFAs concentration in reactors with target 5 - 12.5 g TAN/L. Ammonia stress resulted in different methane production and VFAs accumulation patterns in these reactors. The accumulation of VFAs in the reactors with 5-12.5 g TAN/L caused a slight pH drop, but it still remained in the neutral ranges (Table 4.3) Acetate and propionate concentrations in the 5 g TAN/L reactors (Fig. 4.4A) decreased initially and after 250 days acetate slightly increased while propionate was maintained at a stable concentration. Methane production increased dramatically after a start-up phase of 50 days, and stabilized at 1.6 mmol/two weeks compared to the theoretical methane production of 2 mmol/ two weeks. Unlike the 5 g TAN/L reactors, the reactors with 7.5 g TAN/L had a longer start-up phase of 78 days. Once the reactors started producing methane, a decrease in acetate was detected. During this period, propionate continuously accumulated (Fig. 4.4B). Methane production reached a peak of 1.7 mmol/two weeks on day 150, and fluctuated by decreasing to 0.8 mmol/two weeks and increasing to the previous level on day 300. On the contrary, recovery of methane productionwas not observed in reactors with 10 and 12.5 g TAN/L (Fig. 4.4C and Fig. 4.4D). Acetate and propionate concentration obviously

fluctuated in these high TAN reactors with more propionate accumulation than acetate. However, both parameters seemed to decrease at the end of the experimental period.

4.4.1.4 Microbial Community

4.4.1.4.1 Denaturing Gradient Gel Electrophoresis (DGGE)

Changes in microbial communities occurred under different TAN concentrations (Fig. 4.5). Bacterial phylotypes from the 5 g TAN/L reactors at different time points (day 112, 164, 198, 245) are shown in Fig. 4.5A. The bands from day 112, 164, and 198 were similar (band B1-B4). At day 245, additional light bands were detected. The dominant bands were cut, sequenced, and compared with sequences deposited in the NCBI database. Bacterial phylotypes were classified into phyla Firmicutes, Synergistetes, and Bacteroidetes. A phylotype from band B1-B3 (day 112, 164, and 198) matched *Tepidanaerobacter acetatoxydans* (95 - 99% similarity) and phylotypes matching *Anaerobaculum* spp. and *Acetomicrobium flavidum* (97% similarity) dominated in band B4 (day 198) (Table 4.6). Bacterial phylotypes from reactors with 5-12.5 g TAN/L are shown in Fig. 4.5B. Bacterial phylotypes from the phylum Firmicutes were the only ones detected. Phylotypes matching *Tepidanaerobacter* spp. (89 - 99% similarity) dominated in all TAN concentrations. The band intensity was monitored from the DGGE analysis for reactors operated with 5-12.5 g TAN/L (Fig. 4.6). The closest match to phylotypes matching *Tepidanaerobacter* spp. (97% similarity) are represented by OTU1 and OTU2. The band intensity of phylotypes matching *Tepidanaerobacter* spp. (97% similarity) (OTU2) and *Thermanaerovibrio* spp. (90%

similarity) (OTU3) increased in the reactors with 12.5 g TAN/L. Phylotypes matching *Thermanaerovibrio* spp. (92% similarity) (OTU4) dominated in the 5 g TAN/L reactors. A bacterial phylotype matching *Defluviitoga tunisiensis* (99% similarity) (OTU5) was only detected in a control and background reactor. A summary of bacterial DGGE 16S rRNA gene band identifications is shown in Table 4.6.

Archaeal DGGE profiles for reactors operated with target 0.5-5 g TAN/L and 5-12.5 g TAN/L are shown in Fig. 4.7A and 4.7B. Archaeal phylotypes indicated fewer bands than that observed for bacterial phylotypes. For the archaeal DGGE profile, only one dark band was detected at 0.5-5 g TAN/L (Fig. 4.7A) and two dark bands were detected at 5-12.5 g TAN/L (Fig. 4.7B) compared to several bands detected for bacterial profiles (Fig. 4.5). The dominant bands were cut, sequenced, and compared with sequences deposited in the NCBI database. Archaea were classified to the phylum Euryarchaeota with the closest match to *Methanosarcina* spp. (90 - 98% similarity) at 0.5 - 5 g TAN/L (Fig. 4.7A, Table 4.7). Change in the archaeal community was detected in reactors with 5-12.5 g TAN/L. The closest match to phylotypes *Methanoculleus* spp. are represented as OTU1, OTU2, OTU3, and OTU4. Phylotypes matching *Methanoculleus* spp. (95 and 99% similarity) (OTU1 and OTU2) dominated in reactors with 5-12.5 g TAN/L (40-44% band intensity) while phylotypes matching *Methanosarcina* spp. (OTU5) decreased in band intensity (Fig. 4.8). The control reactor revealed phylotypes matching *Methanosarcina* spp. (83% similarity) (OTU5) with band intensity of 83%. A summary of archaeal DGGE 16S rRNA gene band identifications is shown in Table 4.7.

4.4.1.4.2 Pyrosequencing

Bacterial and archaeal microbial composition at different taxonomic levels and the proportion of major phylotypes in swine waste digestate inoculated reactors are summarized in Table 4.4 (species level). One replicate reactor from each of the 7.5 and 12.5 g TAN/L treatments at day 147 and day 335 were investigated. Bacterial phylotypes were mainly distributed in the phyla Firmicutes and Synergistetes. *Tepidanaerobacter syntrophicus* was the most abundant, followed by phylotypes matching *Thermovirga* spp., and *Aminobacterium* spp. The results indicated that a shift of the bacterial community occurred over time. *Tepidanaerobacter syntrophicus* increased its abundance from 33% to 52% of the reads within 188 days of operation at target 7.5 g TAN/L. An increase in *Gelria* spp. abundance from 9% on day 147 to 17% of the reads on day 335 was detected in the reactors with target 7.5 g TAN/L.

Among archaea, pyrosequencing results indicated Euryarchaeota as the only dominant phylum with 100% abundance in the order Methanomicrobiales in all conditions (Table 4.4). This result is in agreement with the DGGE findings. A phylotype matching *Methanoculleus bourgensis* dominated throughout the experimental period (day 147 and day 335) in both target 7.5 and 12.5 g TAN/L reactors.

4.4.2 Anaerobic reactor inoculated with wastewater digestate

4.4.2.1 Methane Production

Methane production from reactors inoculated with wastewater sludge digestate at target 5-12.5 g TAN/L is shown in Fig. 4.9. All reactors exhibited lower methane production

compared to the control, which produced 45-50 mL methane /two weeks. The reactors inoculated with wastewater sludge digestate had a longer start-up phase than the reactor inoculated with swine waste digestate (Fig. 4.9). The start-up phase for the wastewater digestate inoculated reactors at target 5 g TAN/L was 82 days (Fig. 4.9) while a start-up phase of 50 days was observed for the swine waste digestate inoculated reactors (Fig. 4.1B). The methane production in the 5 g TAN/L wastewater sludge digestate inoculated reactors remained steady at about 20 mL/two weeks (0.6-0.8 mmol/two weeks) after 150 days. This amount of methane production was less than that produced from swine waste digestate inoculated reactors (1.6-1.8 mmol/two weeks). However, after 250 days methane production from wastewater sludge digestate inoculated reactors at 5 g TAN/L increased dramatically and was as much as that produced by the control (1.9 ± 0.2 mmol/two weeks) (Fig. 4.11A). In contrast, less than 0.5 mmol/two weeks of methane was produced in higher TAN reactors (Fig. 4.11B- 4.11D). The 12.5 g TAN/L reactors produced only trace amounts of methane throughout the experimental period (<0.1 mmol/two weeks). A summary of pH, target TAN, calculated free ammonia (NH_3-N) and methane production for the wastewater sludge digestate inoculated reactors is shown in Table 4.5.

4.4.2.2 Volatile Fatty Acids

The results indicated that more propionate accumulated in wastewater sludge digestate inoculated reactors than in the swine waste digestate inoculated reactors at target 5-12.5 g TAN/L. Propionate accumulated in a range of 3,000 - 24,000 mg/L (Fig. 4.10B). There was 2-5 times higher propionate concentrations in the wastewater sludge digestate inoculated reactors than in the swine waste digestate inoculated reactors. After

200 days of operation propionate concentration in the 10 g TAN/L reactors inoculated with wastewater digestate dramatically decreased whereas propionate concentration in the 12.5 g TAN/L reactors increased. At the end of the experimental period, propionate concentration in the 12.5 g TAN/L reactors was high (10,445 ± 5,500 mg/L). The active control wastewater sludge digestate inoculated reactors also required 165 days for propionate to be fully utilized (Fig. 4.10B) whereas only 40 days passed prior to propionate utilization in swine waste digestate inoculated reactors (Fig. 4.2B).

The acetate accumulation in reactors inoculated with wastewater digestate was higher than those inoculated with swine waste digestate. Acetate slightly decreased after reaching a peak of 3,700 mg/L in the wastewater sludge digestate inoculated reactors amended with 7.5 g TAN/L (Fig. 4.10A). In contrast, acetate concentration decreased from 2,720 ± 60 mg/L to 415 ± 100 mg/L in swine waste digestate reactors (data not shown). After 330 days most reactors inoculated with wastewater digestate, except the control, had acetate accumulation in a range of 530-2,700 mg/L. Butyrate did not accumulate; only 70 mg/L or less was detected (data not shown).

4.4.2.3 Changes in methane and VFAs concentration

The relationships between methane production and VFA concentration in wastewater sludge digestate inoculated reactors at target 5 - 12.5 g TAN/L loadings are shown in Fig. 4.11. The different TAN concentrations affected methane production and VFA accumulation patterns differently. The pH slightly dropped with increasing TAN concentrations. In wastewater sludge digestate inoculated reactors with 5 g TAN/L, propionate concentration accumulated to 128 ± 15 mmol/L within 137 days then

decreased and remained at 25 ± 20 mmol/L while acetate remained at less than 9.0 ± 4.1 mmol/L (Fig. 4.11A). In contrast, propionate and acetate in swine digestate inoculated reactors with 5 g TAN/L continuously decreased at the beginning and stabilized at 0.5 ± 0.02 mmol acetate/L and 6.8 ± 0.2 mmol propionate/L after 160 days (Fig. 4.4A). Methane production revealed different patterns for both sets of reactors. Start-up phases of 50 and 82 days were observed in swine digestate and wastewater sludge digestate inoculated reactors at 5 g TAN/L, respectively. Methane production from swine digestate inoculated reactors stabilized at 1.7 ± 0.1 mmol/two weeks for the entire experimental period (330 days) (Fig. 4.4A) whereas only 0.7 ± 0.1 mmol of methane /two weeks was produced in wastewater sludge digestate inoculated reactors, which then maintained at this level over 115 days before dramatically increasing to 1.9 ± 0.2 mmol/two weeks at the end of 330 days (Fig. 4.11A).

At high TAN concentrations, wastewater sludge digestate inoculated reactors accumulated propionate without acetate accumulation or methane production. In 10 g TAN/L reactors, propionate increased to 320 ± 43 mmol/L, then decreased to 50 ± 13 mmol/L at the end of operation (335 days), whereas acetate and methane were steady at 45 ± 1 mmol/L and 0.3 ± 0.04 mmol/two weeks (Fig. 4.11C). However, at 12.5 g TAN/L, propionate continued to accumulate to 143 ± 22 mmol/L (Fig. 4.11D).

4.4.2.4 Denaturing Gradient Gel Electrophoresis (DGGE)

Microbial communities as detected by DGGE of amplified 16S rRNA genes for the enrichments of reactors inoculated with wastewater sludge digestate at target 5-12.5 g

TAN/L are shown in Fig. 4.12. Similar bands were detected at the 5 and 7.5 g TAN/L reactors while those from the 10 g TAN/L reactors were similar to the 12.5 g TAN/L reactors. One replicate of the the 12.5 g TAN/L reactors had fewer bands than other two replicates. The control had different banding patterns than the TAN-stressed reactors. The high intensity bands were cut, sequenced, and compared to the NCBI database. Bacterial phylotypes were classified into phyla Firmicutes, Synergistetes, Thermodesulfobacteria, Chloroflexi, Proteobacteria and Thermotogae. Phylotypes matching *Thermanaerovibrio* spp. (89-92% similarity) was a dominant community member at all TAN concentrations. Phylotypes matching *Sedimentibacter* spp. (97% similarity) was a dominant member in the target 5 g TAN/L reactors while phylotypes matching *Aminobacterium* spp. and *Thermovirga* spp. (92% similarity) were dominant in the target 12.5 g TAN/L reactors. Phylotypes matching *Tepidanaerobacter* spp. (74% similarity) was detected in the 10 and 12.5 g TAN/L reactors.

The DGGE band intensity was determined to compare the relative abundances of different microbial community members in different treatments (Fig. 4.13). The band intensity analysis indicated that, interestingly, at target 10 and 12.5 g TAN/L, more bacterial phylotypes were detected than at lower TAN concentrations. The closest match to phylotypes *Aminobacterium* spp. (88% similarity) (OTU1) dominated in the 12.5 g TAN/L reactors. The closest match to phylotypes *Sedimentibacter* spp. (97% similarity) (OTU2) dominated in the 5 g TAN/L reactors. Phylotypes matching *Tepidanaerobacter* spp. (74% similarity) (OTU3) and *Thermotoga* spp. and *Geobacillus* spp. (90% similarity) (OTU4) were only detected in the 10 and 12.5 g TAN/L reactors. The band intensity of phylotypes matching *Thermanaerovibrio* spp. (89-90% similarity) (OTU 5)

decreased from 57% to 11% with increasing TAN while *Thermanaerovibrio* spp. (89% similarity) (OTU 6) increased from 2% to 24%. These phylotypes indicated 95% identity when blasting to each other according to the NCBI database. The microbial communities in wastewater sludge digestate inoculated reactors were different from those of swine waste digestate inoculated reactors. The dominant bacteria in wastewater sludge digestate inoculated reactors were phylotypes matching *Thermanaerovibrio* spp. whereas phylotypes matching *Tepidanaerobacter* spp. dominated in all TAN reactors inoculated with swine waste digestate. In addition, phylotypes matching *Sedimentibacter* spp. (97% similarity) (OTU2) members of order Clostridiales appeared only in wastewater digestate reactors. The microbial communities in the control and background reactors from both inocula were also different. In a control reactor inoculated with wastewater sludge digestate, bacterial phylotypes matching *Taylorella* spp., *Alicyclobacillus* spp., and *Thermogemmatispora* spp. (94% similarity) (OTU9) (Fig. 4.13) were detected, while a phylotype matching *Defluviitoga tunisiensis* (99% similarity) (OTU5) (Fig. 4.6) was detected in a control and background reactor inoculated with swine waste digestate. A summary of bacterial DGGE 16S rRNA gene band identifications from wastewater sludge digestate inoculated reactors is shown in Table 4.8.

Archaeal DGGE profiles for wastewater sludge digestate inoculated reactors with target 5-12.5 g TAN/L are shown in Fig. 4.14. The bands from the 5 and 7.5 g TAN/L reactors were different from those from the 10 and 12.5 g TAN/L reactors. More bands were detected in the 12.5 g TAN/L reactors compared to others. The dominant bands were cut, sequenced, and compared to the NCBI database. Archaea were classified to the phylum Euryarchaeota with the closest match to *Methanoculleus* spp. (97-99% similarity)

under all TAN concentrations. Phylotypes matching *Methanomicrobium* spp. (91% similarity) were detected in one replicate of the 5 and 7.5 g TAN/L reactors. A phylotype matching *Methanosaeta concilii* (95-98% similarity) was detected in control and background reactors. The band intensity analysis revealed that phylotypes matching *Methanomicrobium* spp. (91% similarity) (OTU1) was only detected in the 5 g TAN/L. Phylotypes matching *Methanoculleus* spp. (91% similarity) (OTU2) was detected in the 5 and 7.5 g TAN/L reactors. Phylotypes matching *Methanosaeta* spp. (95% similarity) (OTU3) were detected in the background control (21% band intensity) and *Methanosaeta* spp. (96% similarity) (OTU6) were detected both in the active (86% band intensity) and background controls (28% band intensity). Phylotype matching *Methanospirillum* spp. (95% similarity) (OTU4) were detected in the 7.5, 10, and 12.5 g TAN/L reactors with low band intensity of 5-12%. Phylotypes matching *Methanoculleus* spp. (99% similarity) (OTU5) were detected in the 10 and 12.5 g TAN/L with 12% band intensity. The closest match to phylotypes *Methanoculleus* spp. (97% similarity) (OTU7) were only detected in the 12.5 g TAN/L reactors with high band intensity of 41%. Phylotypes matching *Methanoculleus* spp. (97% similarity) (OTU8) were detected both in the 10 and 12.5 g TAN/L reactors with 17% and 31% band intensity, respectively. Phylotypes matching *Methanoculleus* spp. (99% similarity) (OTU9) dominated in the 5, 7.5, and 10 g TAN/L reactors with band intensity of 52% in the 5 and 7.5 g TAN/L reactors, and 24% in the 10 g TAN/L reactors, respectively (Fig. 4.15). These phylotypes had 97% identity to each other according to Blast analysis using the NCBI database. Similar archaeal communities with phylotypes matching *Methanoculleus* spp. were detected in swine waste digestate inoculated reactors with 5-12.5 g TAN/L. However, the control reactors revealed

different archaeal phylotypes. Phylotypes matching *Methanosarcina* spp. (82% similarity) (OTU5) (Fig. 4.8) were detected in swine waste digestate inoculated control reactors whereas a phylotype matching *Methanosaeta concilii* (96% similarity) (OTU6) (Fig. 4.15) was detected in wastewater sludge digestate inoculated control reactors. A summary of archaeal DGGE 16S rRNA gene band identifications is shown in Table 4.9.

4.5 Discussion

The swine waste digestate inoculated reactors that were established under different TAN concentrations (initial reactors at up to 5 g TAN/L; secondary enrichments at 5 – 12.5 g TAN/L, using the 5 g TAN/L reactor as inoculum) revealed ammonia inhibition with increasing TAN. The TAN inhibition was characterized by a long start-up phase, VFA accumulation, and low methane production. The initial reactors with target TAN of up to 5 g TAN/L revealed some degree of ammonia inhibition as less methane than theoretically predicted (2 mmol/week at standard temperature and pressure (STP)) was produced. In the secondary enrichments, the reactors with an actual TAN concentration of 11 g TAN/L (12.5 g TAN/L target) had methane production decreased by 94% compared to the control reactors (0.1 g TAN/L). It was reported that thermophilic AD treating cattle manure was 100% inhibited at ammonia concentration > 4 g TAN/L (Angelidaki and Ahring 1993). Sung and Liu (2003) stated that in thermophilic AD treating synthetic wastewater, 5.8 g TAN/L caused a drop in methane production by 64%, with respect to controls, and 100% inhibition occurred in the range of 8 – 13 g TAN/L. Thus, our study supports these previous findings that high ammonia concentration inhibited

methanogenesis (Gallert et al. 1998). Comparison between swine waste digestate and wastewater sludge digestate as inoculum at high TAN concentrations revealed that twice the amount of methane was produced from swine waste digestate inoculated reactors compared to wastewater sludge digestate inoculated reactors, therefore substantial community differences were evident

The accumulation of VFAs indicated that ammonia inhibition occurred in the systems. Previous studies have shown that VFAs concentration increased with increasing ammonia concentrations (Angelidaki and Ahring 1993, Hwang et al. 2008, Merlino et al. 2013, Nakakubo et al. 2008, Schnurer and Nordberg 2008). Our results revealed that swine waste digestate enrichment at target 5 g TAN/L accumulated more acetate and propionate compared to enrichments at lower TAN concentrations. However, the toxic effect of ammonia may be diminished by acclimation or adaptation of the populations (Gallert et al. 1998) as seen when reactors were subjected to ammonia concentrations for a long period. The result from the target 5 g TAN/L reactors in the second generation swine waste digestate inoculated reactors (Fig. 4.4A) showed that after microbial communities acclimated to high TAN, acetate and propionate were kept low while methane production was stable at near the theoretical methane production level (2 mmol/two weeks), unlike the result previously shown in the target 5 g TAN/L reactors in the first enrichment (Fig. 4.3). However, at higher TAN concentrations the ability of the microbial community to acclimate to ammonia was limited as indicated by a drop in methane production by 75% in the target 7.5 g TAN/L reactors and by 94% in the target 12.5 g TAN/L reactors compared to the theoretical methane production. In addition, the accumulation of VFAs was also evident at high TAN concentrations (Fig. 4.4B -4.4D).

Changes in VFA concentration and methane production at target 5 g TAN/L in the first reactor set are classified into four periods (Fig. 4.3) and indicated dynamic shifts in microbial communities. We hypothesized these changes as follow. Period 1 (day 1-50): Glutamate degrading bacteria play a role in fermenting glutamate fed as the sole carbon and energy source into propionate, which was further degraded to acetate by propionate oxidizing acetogens. As a result, the accumulation of acetate was observed. During this period, no methane was produced in the reactor. The reason might be that at the earlier stage, acclimation of acetate-utilizing methanogens had not sufficiently progressed. Nakakubo et al. (2008) reported that acetate-utilizing methanogens were sensitive to high ammonium, which resulted in loss of capability for conversion of VFAs to methane. Period 2 (day 50-90): Acetate drastically decreased while methane increased. The results indicated that acetate was utilized via acetotrophic methanogenesis to produce methane. Once acetate was used up, methane production then decreased. However, accumulation of propionate was detected during this period. This might indicate low activity or inhibition of propionate-oxidizing acetogens and/or hydrogen-consuming methanogens (Lier et al. 1993, Prochazka et al. 2012). Period 3 (day 90-180): Propionate-oxidizing acetogens started to be active, thus decrease of propionate was observed together with increases in acetate. Hydrogen concentrations were not measured during this study; however, it is known that when propionate is utilized, the H_2 concentration must be low. The partial pressure of H_2 must be kept below 10^{-6} to 10^{-4} atm (0.1 to 10.1 Pa) in order for propionate to degrade (see for example, Fukuzaki et al. (1990) and Fennell and Gossett (1997)). The pathway related to maintaining low H_2 concentration and stable methane production may involve hydrogenotrophic methanogenesis as reported by Schnurer and Nordberg (2008). They

stated that a shift from aceticlastic methanogenesis to syntrophic acetate oxidataion (coupled to hydrogenotrophic methanogenesis) thermodynamically provided more energy under high ammonium concentrations (Schnurer and Nordberg 2008). Even though acetate was maintained at low levels during the beginning of this period, at day 134 an increase in acetate was observed. This might have been a result of homoacetogens converting H_2 to acetate during this period. Period 4 (day 180-200): Propionate fluctuated, and a decrease of acetate was detected. One explanation for this observation might be that hydrogenotrophic methanogenesis was inhibited and H_2 was not utilized, causing propionate accumulation and decrease in methane production. In addition, decreasing concentrations of acetate may be related to the low activity of propionate oxidizing acetogens (acetate formation ceased). Overall, it was observed at 5 g TAN/L that the system is unstable and methane production fluctuatued greatly.

The type of inoculum originally used affected changes in VFA concentration and methane production. At target 5 g TAN/L, propionate and acetate in swine digestate inoculated reactors initially decreased (Fig. 4.4A) while propionate and acetate accumulated in reactors inoculated with wastewater sludge digestate (Fig. 4.11A). Propionate and acetate accumulated 2 to 5 times and 1 to 1.4 times more in wastewater sludge digestate compared to swine waste digestate inoculated reactors, respectively. The accumulation of propionate in high TAN concentration reactors may be explained by inhibition of propionate oxidizing acetogens, who utilize propionate and form acetate (Lier et al. 1993, Prochazka et al. 2012). The microbial community in reactors inoculated with wastewater sludge digestate was inhibited by high TAN concentrations more than those in swine digestate inoculated reactors as seen from a longer lag phase (Fig. 4.11).

Even though the microbial community in the target 5 g TAN/L reactors inoculated with wastewater sludge digestate was inhibited at the beginning, it was able to acclimate to ammonia stress over time as seen from increasing methane production (Fig. 4.11A) and a decreasing of propionate from 200 to 50 mmol/L (Fig. 4.11C) after 200 days. This finding indicated that propionate oxidizing acetogens were severely inhibited at 10 g TAN/L, but could acclimate to lower level ammonia stress over time. These results indicated that propionate oxidizing methanogens were more inhibited in wastewater sludge digestate inoculated reactors than reactors inoculated from swine waste digestate.

Microbial community analysis revealed that community shifts were related to TAN concentration, volatile fatty acids, and methane production. Dominant species and community shifts were also detected, as previously reported, at high ammonia concentrations (Calli et al. 2005, Westerholm et al. 2011b). The bacterial community shifted towards the phylum Firmicutes and Synergistetes in the target 5-12.5 g TAN/L reactors inoculated with swine digestate and wastewater sludge digestate. The most abundant class was Clostridia, which was also shown to be dominant in two-stage AD treating food waste leachate containing a high concentration of VFAs (Kim et al. 2014). Many members of the class Clostridia obtain energy by fermenting amino acids and are known as acid and hydrogen producers supplying hydrogen as a substrate to hydrogenotrophic methanogens (Madigan and Martinko 2006). Our results indicate that hydrogenotrophic methanogenesis becomes a dominant pathway in AD after long term exposure to high TAN in both inocula. At 12.5 g TAN/L, phylotypes matching *Tepidanaerobacter* spp. (97% similarity) could be enriched in the reactors inoculated

with swine digestate after 189 days of operation (Fig. 4.6) whereas phylotypes matching *Thermanaerovibrio* spp. (89-92% similarity) could be enriched in the reactors inoculated with wastewater sludge digestate (Fig. 4.13). *Tepidanaerobacter* spp. are an anaerobic, syntrophic acetate-oxidizing bacteria important in the syntrophic acetate oxidation pathway that has been detected in cultures with ammonium concentrations in the range of 3-7 g NH_4^+-N/L (Schnurer et al. 1994, Schnurer and Nordberg 2008, Westerholm et al. 2011b). *Thermanaerobacter* spp. are moderately thermophilic, syntrophic, glutamate-degrading bacteria that have been shown to grow in co-culture with the hydrogenotrophic methanogen *Methanobacterium thermoautotrophicum* Z245 (Baena et al. 1999, Plugge and Stams 2001). In contrast, a bacterial phylotype matching *Defluviitoga tunisiensis* (99% similarity) and reported to reduce elemental sulfur in anaerobic digesters (Hania et al. 2012) was the dominant bacterial community member detected in control and background reactors inocutated with swine digestate—this indicates a substantial shift over time as the system was enriched on glutamate (a model amino acid) and exposed to high TAN.

Pyrosequencing results generally confirmed the DGGE findings, indicating that a shift of bacterial community occurred over time. *Tepidanaerobacter syntrophicus* increased its abundance at higher TAN concentrations and over time. *T. syntrophicus* species abundance increased from 33% to 52% of the reads within 188 days of operation at target 7.5 g TAN/L (Table 4.4). *T. syntrophicus* is an anaerobic, moderately thermophilic, syntrophic-degrading bacterium that was isolated from digested sewage sludge and grew in co-culture with the hydrogenotropic methanogen *Methanothermobacter thermautotrophicus* (Sekiguchi et al. 2006). *Thermovirga* spp. and

Aminobacterium spp. were detected in both 7.5 and 12.5 g TAN/L with high abundance. Both *Thermovirga lienii* (Dahle and Birkeland 2006) and *Aminobacterium* spp. (Baena et al. 2000) are anaerobic, amino acid-degrading bacteria that likely oxidized glutamate in our systems. *Aminobacterium colombiense* oxidized glutamate in co-culture with hydrogenotrophic methanogen *Methanobacterium formicicum* (Baena et al. 1998). An increase in *Gelria* spp. abundance from 9% on day 147 to 17% on day 335 was detected in the reactor with target 7.5 g TAN/L. Plugge et al. (2002) identified *Gelria glutamica* as a moderately thermophilic, syntrophic, glutamate-degrading bacterium that in their study grew in co-culture with the hydrogenotrophic methanogen *Methanobacterium thermoautotrophicum* Z245. Therefore, detection of these bacteria at high TAN concentrations in our systems could suggest syntrophic relationships between syntrophic oxidizing bacteria and hydrogenotrophic methanogens which normally occurred at high ammonia stress conditions in AD (Schnurer et al. 1994, Schnurer and Nordberg 2008, Westerholm et al. 2011b). High abundance of *T. syntrophicus*, *Thermovirga* spp., and *Aminobacterium* spp. in the target 12.5 g TAN/L reactors suggested their ability to grow in the glutamate-fed systems and to acclimate to ammonia stress as observed from recovery of methane production and a decrease in acetate concentration.

Archaeal community analysis revealed Euryarchaeota as the only dominant phylum. Phylotypes matching *Methanosarcina* spp. (90 - 99% similarity) were dominant in target 0.5-5 g TAN/L swine waste digestate inoculated reactors while phylotypes matching *Methanoculleus* spp. (82-99% similarity) were dominant in both swine waste digestate and wastewater sludge digestate inoculated reactors with target 5-12.5 g TAN/L. This suggested the community shifted from *Methanosarcina* spp. to

Methanoculleus spp. at high TAN concentrations. Pyrosequencing results indicated the dominance of *Methanoculleus* spp. throughout the experimental period in both target 7.5 and 12.5 g TAN/L swine waste digestate inoculated reactors. Sprott and Patel (1986) reported that *Methanosarcina* spp., the acetoclastic methanogens, were found more sensitive than hydrogenotrophic methanogens to increasing ammonia concentrations. However, some studies indicated that *Methanosarcina sp*. was able to tolerate ammonium levels up to 7 g NH_4^+-N/L (Vrieze et al. 2012) and single coccus shaped *Methanosarcina* cells formed large multicellular structures at free ammonia of 750 mg NH_3-N/L (Calli et al. 2005). In addition, members belonging to the order Methanosarcinales may act as hydrogenotrophic methanogens during the SAO pathway (Westerholm et al. 2012). Even though *Methanosarcina* spp. can alter its metabolism to utilize hydrogen in response to the surrounding conditions (Hao et al. 2011), we did not find *Methanosarcina* spp. as a dominant member in the reactors with target 5-12.5 g TAN/L in both systems. Instead, *Methanoculleus* spp. dominated in target 5-12.5 g TAN/L reactors throughout the experimental period. *Methanoculleus bourgensis* is a hydrogenotrophic methanogen founded to be well adapted in biogas communities encountering high salt and ammonia (Maus et al. 2012). It was found that *M. bourgensis* formed methane through the hydrogenotrophic pathway (Barret et al. 2013), and played an important role as an SAOB partner under mesophilic conditions (Westerholm et al. 2012). Therefore, the existence of *Methanoculleus* spp. along with finding bacterial members of the SAO pathway, confirmed the shift to hydrogenotrophic methanogenesis in our TAN-stressed systems.

Enrichment of ammonia resistant microorganisms using the different inocula revealed that phylotypes matching *Tepidanaerobacter* spp. and *Methanoculleus* spp. were the dominant bacteria and archaea, respectively, in reactors inoculated with swine waste digestate up to target 12.5 g TAN/L. On the other hand, phylotypes matching *Thermanaerovibrio* spp. and *Methanoculleus* spp. were the dominant bacteria and archaea, respectively, in reactors inoculated with wastewater sludge digestate. The finding of a phylotype matching *Tepidanaerobacter* spp. revealed that ammonia tolerant bacterium could be enriched from swine waste digestate more readily than from wastewater sludge digestate. Archaeal community analysis indicated that a phylotype matching *Methanoculleus* spp. dominated in both swine and wastewater sludge digestate inocula at target 5-12.5 g TAN/L. In addition, a phylotype matching *Methanosarcina* spp. was detected in the swine waste digestate inoculated control reactors. This meant that a phylotype matching *Methanosarcina* spp. already existed in swine waste digestate and was more likely to acclimate to high TAN concentrations. In contrast, a phylotype matching *Methanosaeta concilii*, an ammonia- sensitive methanogen (Calli et al. 2003, Steinhaus et al. 2007), was detected in wastewater sludge digestate inoculated control reactors. This study revealed important information of phylotypes matching *Tepidanaerobacter* spp. and *Methanoculleus* spp., which dominated in high TAN digester systems and expected to be ammonia tolerant bacteria and archea in digester systems. Interestingly, the finding of phylotypes matching *Tepidanaerobacter* spp. was also detected Thailand landfill leachate observed previously. The discovery of these microbes tolerant to high TAN in digester systems could be advantages for stable AD operation. For example, to be used as biological indicators in AD treating high N wastes, to be

criteria for selecting proper co-substrates for co-digestion of waste on farm or wastewater treatment plants. Further, bioaugmentaiton of AD systems with these ammonia tolerant microbes might improve performance and strengthen microbial activity to better overcome ammonia toxicity.

Table 4.1 Characteristics of swine waste digestate inoculum[a]

Parameters	Values
Total Solids (%)	3.8 ± 0.5
pH	8.1 ± 0.1
Carbon (%)	1.6 ± 0.3
Total N (g N/L)	5.1 ± 0.2
TAN (g N/L)	3.9 ± 0.1
Calculated Free Ammonia (g N/L)	0.63[b]
Calculated Organic N (g N/L)	1.2 ± 0.2
Nitrate-N (mg/L)	0.26 ± 0.1
Sulfur (g/L)	0.36 ± 0.03

[a] Data from Meinen et al. (2014) as mean ± standard deviation

[b] Data calculated from this study

Table 4.2 Characteristics of wastewater sludge digestate inoculum[a]

Parameters	Values
Total Volatile Solids (%)	67.7 ± 1.1
Total Alkalinity (mg/L)	6,749 ± 82
Volatile Acid Alkalinity (mg/L)	312 ± 2
Volatile Acids (mg/L)	468 ± 3
Borate Alkalinity (mg/L)	6,466 ± 35
TAN (g N/L)	1.95 ± 0.01

[a] Data from the Joint Meeting of Essex and Union Counties wastewater treatment plant, Elizabeth, New Jersey as mean ± standard deviation

Table 4.3 Summary of pH, total ammonia nitrogen concentration (TAN), calculated free ammonia (NH_3-N) and methane (CH_4) production in low and high ammonium concentration in reactors inoculated with swine waste digestate.

Low Ammonia[a]					**High Ammonia**[b]				
Target TAN (g N/L)	pH	Actual TAN (g N/L)	Calculated NH_3-N (g N/L)	CH_4 Production (mL/week)	Target TAN (g N/L)	pH	Actual TAN (g N/L)	Calculated NH_3-N (g N/L)	CH_4 Production (mL/two weeks)
0.5	7.75 (0.04)	0.30 (0.02)	0.02 (0)	44.32 (2.15)	5	7.55 (0.07)	5.97 (0.12)	0.23 (0)	42.16 (0.99)
1	7.86 (0.20)	0.72 (0.38)	0.05 (0.03)	41.45 (0.76)	7.5	7.65 (0.09)	8.32 (0.20)	0.40 (0.01)	37.22 (3.28)
2.5	7.93 (0.09)	2.56 (0.08)	0.22 (0.01)	41.21 (1.87)	10	7.37 (0.06)	10.00 (0.74)	0.26 (0.02)	18.27 (9.91)
5	8.04 (0.07)	3.17 (0.09)	0.35 (0.01)	33.51 (6.41)	12.5	7.25 (0.11)	11.12 (0.14)	0.22 (0)	4.80 (1.01)
Active Control	7.74 (0.03)	0.08 (0.01)	0	47.25 (7.38)	Active Control	7.65 (0.17)	0.53 (0.12)	0.02 (0)	47.99 (1.26)
Background Control	7.72 (0.01)	0	0	0.06 (0)	Background Ctrl	7.71 (0)	0	0	0.56 (0)

[a]Data from day 127

[b]Data from day 331

The numbers in parentheses represent standard deviation

Table 4.4 Summary of the major bacterial and archaeal phylotypes of the microbial community detected by 454 pyrosequencing of 16S rRNA genes of one replicate reactor from each 7.5 and 12.5 g TAN/L treatment

Phylum	**Class**	**Order**	**Family**	**Genus**	**Species**	**% Species abundance of total community**			
Bacteria						7.5 g TAN/L		12.5 g TAN/L	
						D147	D335	D147	D335
Firmicutes	Clostridia	Thermoanaerobacterales	Thermoanaerobacteraceae	Tepidanaerobacter	*Tepidanaerobacter syntrophicus*	33.05	51.86	44.71	43.37
				Gelria	*Gelria spp.*	9.08	17.09	2.31	1.51
				Thermaceto genium	*Thermacetogenium spp.*	3.82	3.94	0.20	0.08
		Clostridiales	Syntrophomonadaceae	Thermovirga	*Thermovirga spp.*	29.66	9.38	31.76	35.14
Synergistetes	Synergistia	Synergistales	Synergistaceae	Aminobacterium	*Aminobacterium spp.*	18.82	8.96	16.80	15.45
				Anaerobaculum	*Anaerobaculum spp.*	2.43	3.02	0.32	0.15
					Other (Clostridium spp., Lutispora spp., etc.)	3.14	5.75	3.90	4.30
Archaea									
Euryarchaeota	Methano microbia	Methanomicrobiales	Methanomicrobiaceae	Methanoculleus	*Methanoculleus bourgensis*	100	99.17	100	100
	Thermo plasmata	Thermoplasmatales	Thermoplasmataceae	Thermoplasma	*Thermoplasma spp.*	0	0.83	0	0

Table 4.5 Summary of pH, total ammonia nitrogen concentration (TAN), calculated free ammonia (NH_3-N) and methane (CH_4) production in reactors inoculated with wastewater sludge digestate.

Target TAN (g N/L)	pH	Actual TAN[a] (g N/L)	Calculated NH_3-N[a] (g N/L)	CH_4 Production[b] (mL/two weeks)
5	7.47 (0.04)	5.93 (0.19)	0.19 (0)	46.69 (4.82)
7.5	7.29 (0.21)	8.50 (0.30)	0.18 (0)	21.02 (4.22)
10	7.20 (0.11)	10.04 (0.61)	0.17 (0.06)	7.67 (3.77)
12.5	7.23 (0.07)	11.48 (1.45)	0.21 (0.03)	2.22 (0.78)
Active Control	7.86 (0.01)	0.53 (0)	0.01 (0)	45.24 (3.81)
Background Control	7.51 (0)	0.53 (0)	0.01 (0)	0.30 (0)

[a]Data from day 335

[b]Data from day 333

The numbers in parentheses represent standard deviation

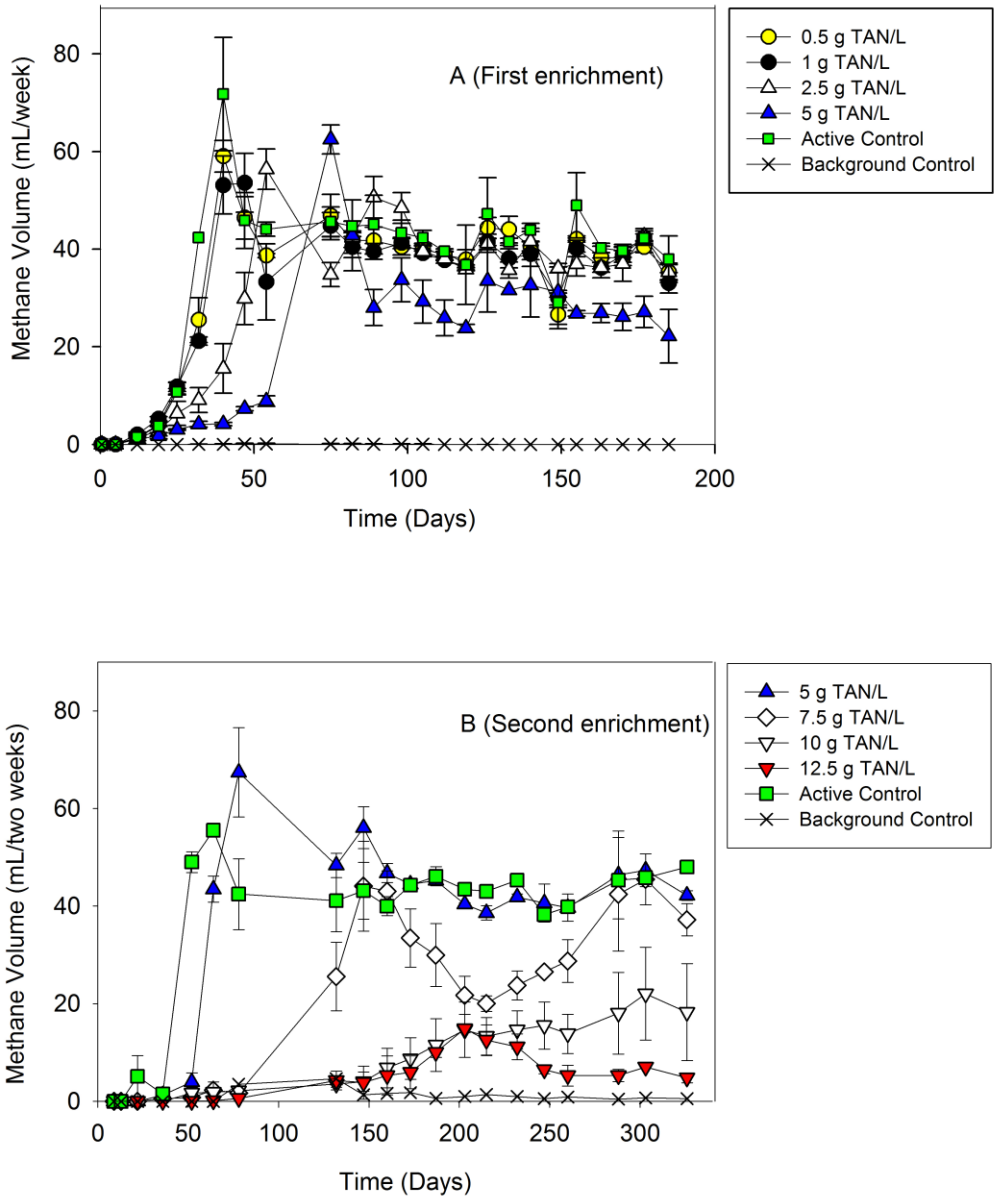

Fig. 4.1 Methane production from swine waste digestate inoculated reactors at low TAN concentrations (Target 0.5-5 g TAN/L) (A) and at high TAN concentrations (Target 5-12.5 g TAN/L) (B). Symbols are averages of triplicates and error bars are ± one standard deviation.

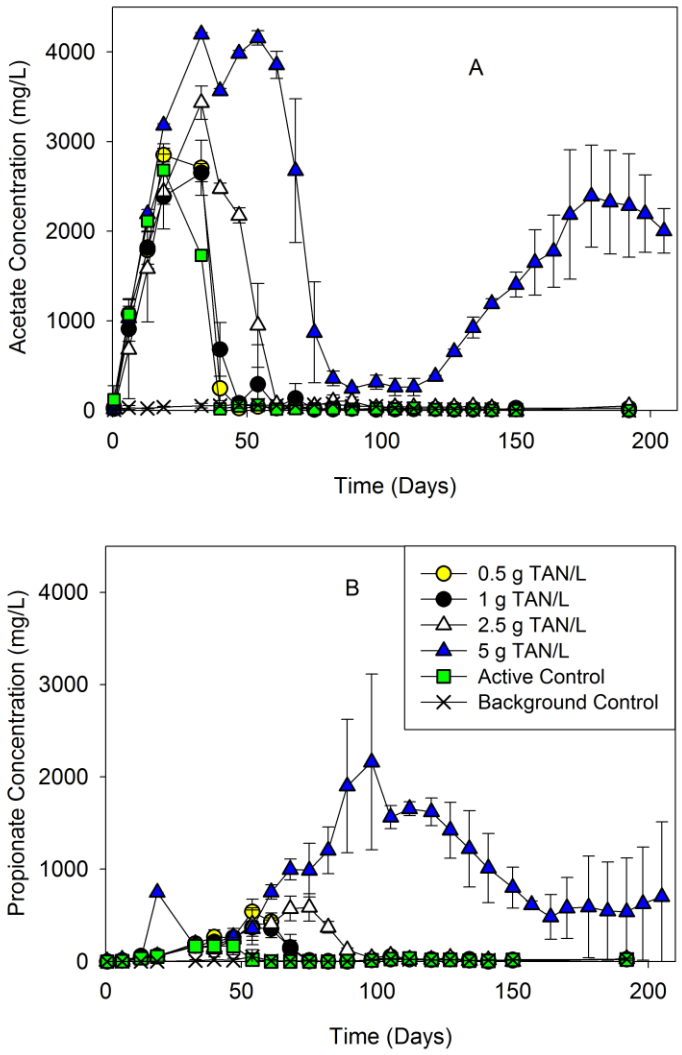

Fig. 4.2 Acetate (A) and propionate (B) concentration from swine waste digestate inoculated reactors with target 0.5- 5 g TAN/L. Symbols are averages of triplicates and error bars are ± one standard deviation.

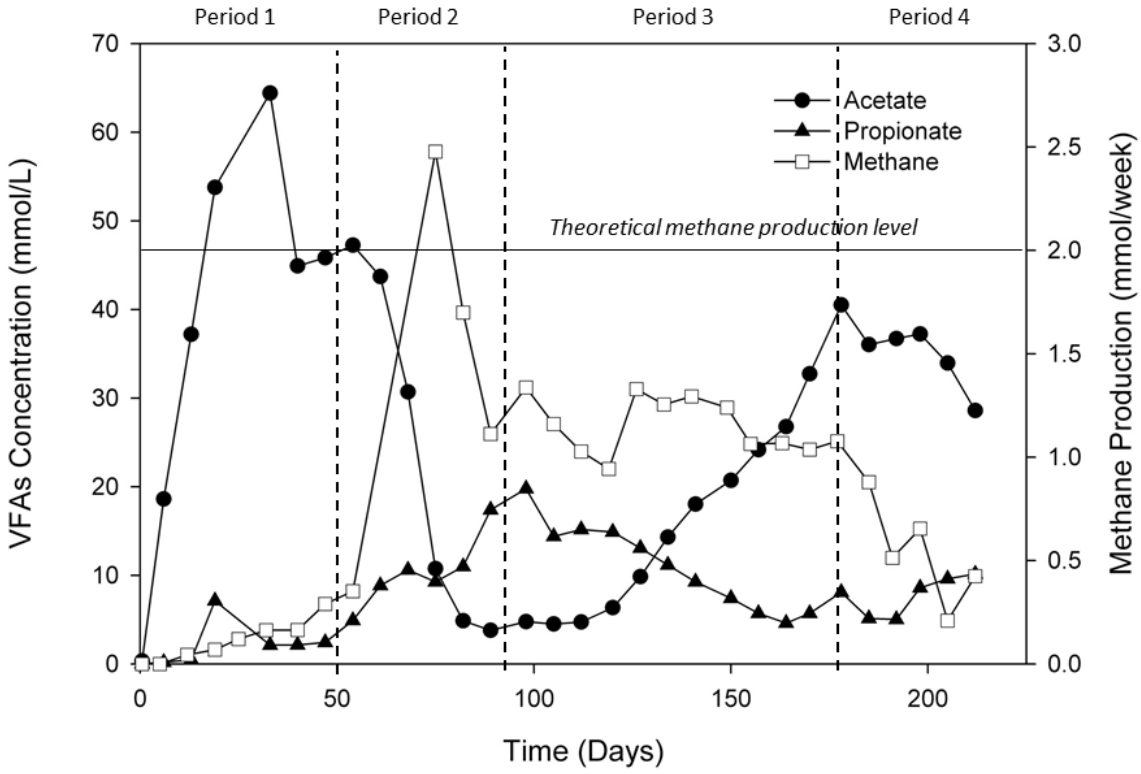

Fig. 4.3 The relationships of methane and VFAs in swine waste digestate inoculated reactor with target 5 g TAN/L. Symbols are average values of triplicates.

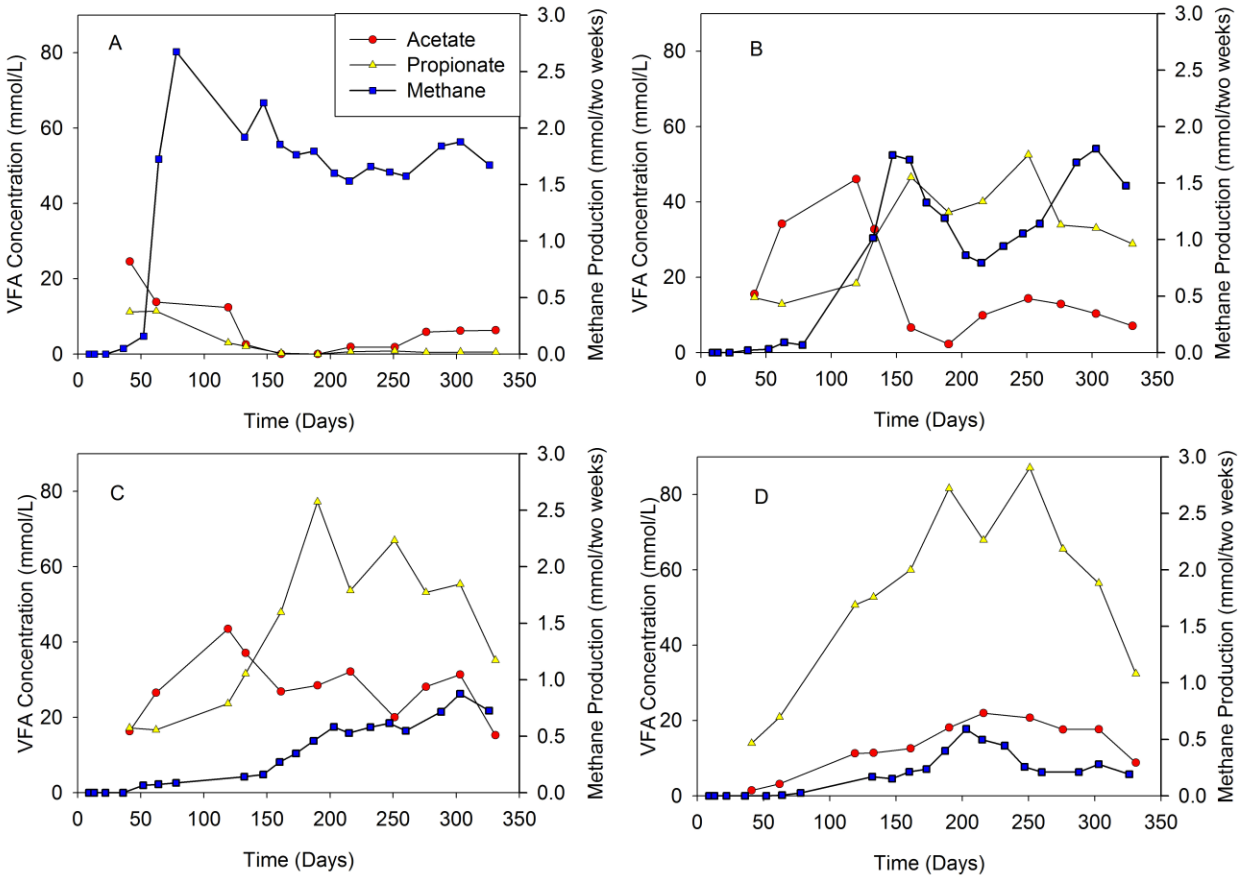

Fig. 4.4 The relationships of methane and VFAs in swine waste digestate inoculated reactors with target 5 g TAN/L (A), 7.5 g TAN/L (B), 10 g TAN/L (C), and 12.5 g TAN/L (D). Symbols are average values of triplicates.

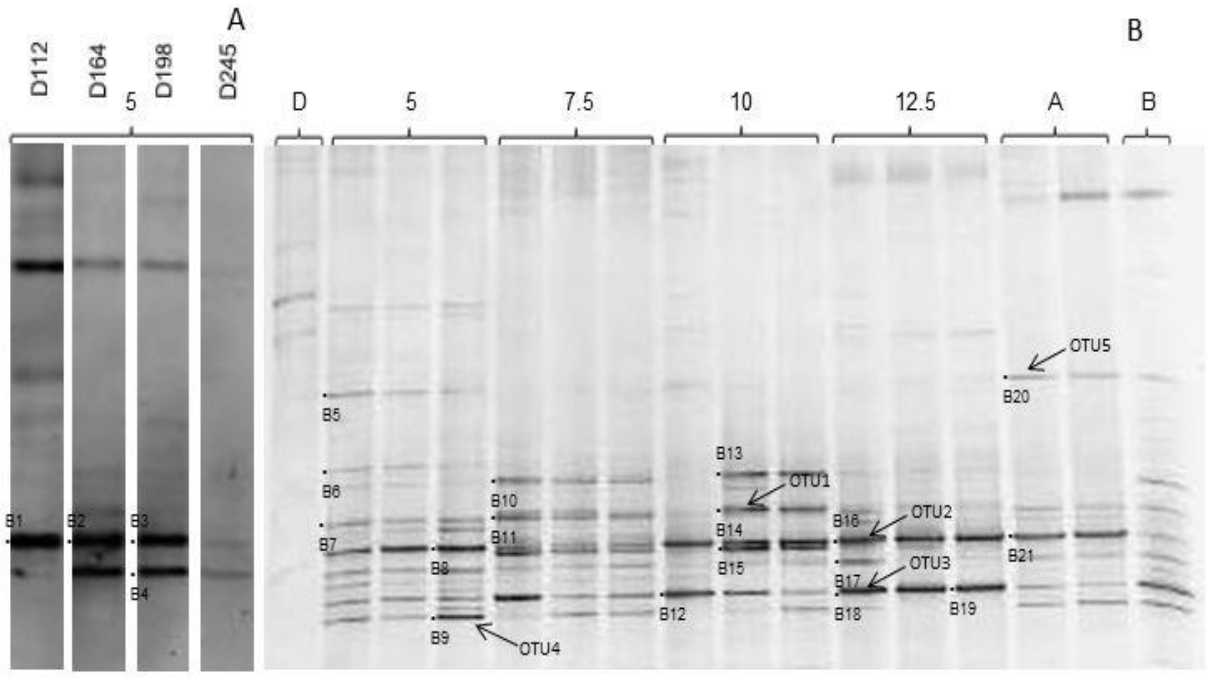

Fig. 4.5 Bacterial DGGE profiles of the 16S rRNA gene PCR products amplified from DNA extracted from swine waste digestate inoculated reactor with target 5 g TAN/L at day 112, 164, 198, and 245 (A) and from reactors with target 5-12.5 g TAN/L day 189 (B). Lanes are labelled with TAN concentrations (g TAN/L); lane A, B, and D indicate the DGGE profile of active control, background, and swine waste digestate, respectively. Dots and numbers indicate the bands sequenced.

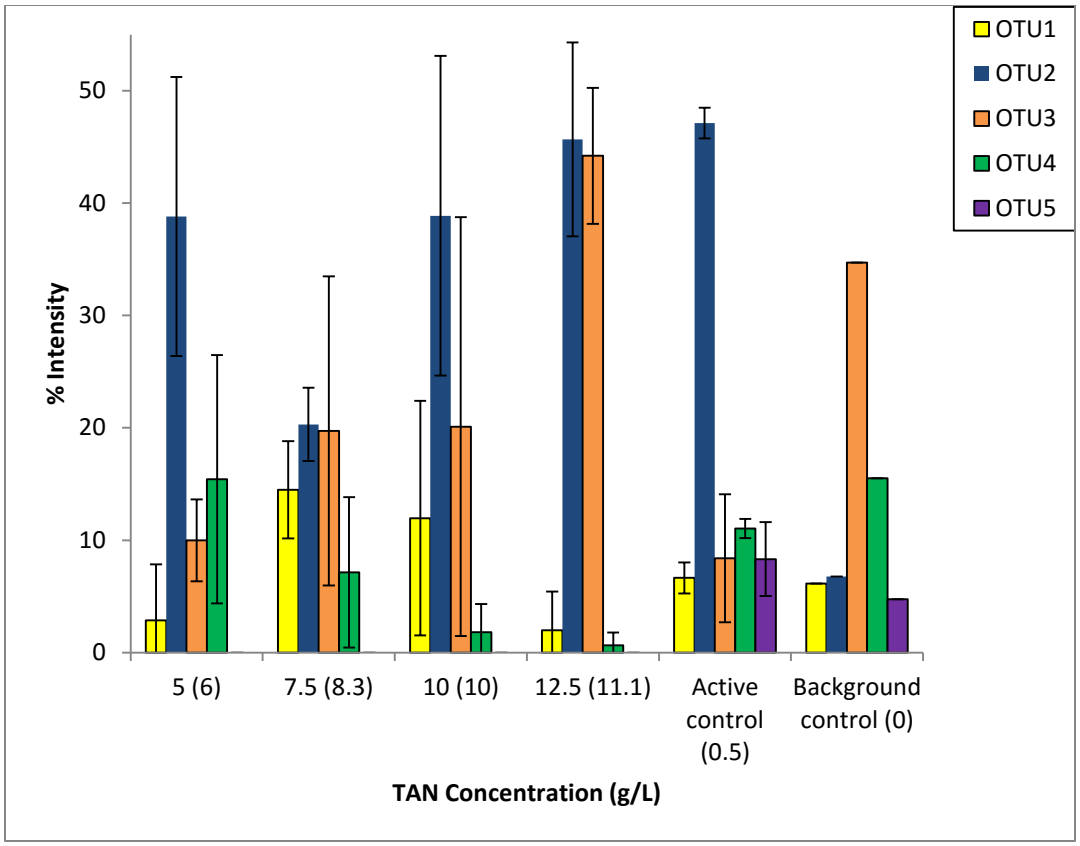

Fig. 4.6 The bacterial DGGE band intensity from swine waste digestate inoculated reactors with target 5-12.5 g TAN/L. The numbers in parentheses represent actual TAN concentrations. Bars are averages and error bars are one standard deviation of the % of the total band intensity from triplicate DGGE lanes. The matches to specific phylotypes are: OTU1- *Tepidanaerobacter acetatoxydans*, OTU2- *Tepidanaerobacter* spp., OTU3- *Thermanaerovibrio* spp., OTU4- *Thermanaerovibrio* spp., and OTU5- *Defluviitoga tunisiensis*.

Table 4.6 Bacterial DGGE 16S rRNA gene band identifications swine waste digestate inoculated reactors

DGGE band	Closest match	Identity (%)	Phyla	Closest match Accession no.
Low Ammonia				
B1	*Tepidanaerobacter acetatoxydans*	99	Firmicutes	NR_074537.1
B2	*Tepidanaerobacter* spp.	95	Firmicutes	NR_074537.1
B3	*Tepidanaerobacter acetatoxydans*	99	Firmicutes	NR_074537.1
B4	*Anaerobaculum* spp.	97	Synergistetes	NR_102954.1
	Acetomicrobium flavidum	97	Bacteroidetes	NR_104752.1
High Ammonia				
B5	*Acetobacterium* spp.	95	Firmicutes	NR_074548.1
B6	*Desulfotomaculum* spp.	93	Firmicutes	NR_117590.1
B7	*Desulfotomaculum sp.*	83	Firmicutes	NR_117747.1
	Thermanaerovibrio sp.	83	Firmicutes	NR_074520.1
B8	*Tepidanaerobacter* spp.	89	Firmicutes	NR_074537.1
B9	*Thermanaerovibrio* spp.	92	Firmicutes	NR_074520.1
B10	*Tepidanaerobacter* spp.	91	Firmicutes	NR_074537.1
B11	*Tepidanaerobacter* spp.	86	Firmicutes	NR_074537.1
B12	*Thermanaerovibrio* spp.	91	Firmicutes	NR_074520.1
B13	*Tepidanaerobacter acetatoxydans*	99	Firmicutes	NR_074537.1
B14	*Tepidanaerobacter acetatoxydans*	99	Firmicutes	NR_074537.1
B15	*Tepidanaerobacter* spp.	95	Firmicutes	NR_074537.1
B16	*Tepidanaerobacter* spp.	97	Firmicutes	NR_074537.1
B17	*Thermanaerovibrio* spp.	92	Firmicutes	NR_074520.1

DGGE band	Closest match	Identity (%)	Phyla	Closest match Accession no.
B18	*Thermanaerovibrio* spp.	90	Firmicutes	NR_074520.1
B19	*Thermanaerovibrio* spp.	90	Firmicutes	NR_074520.1
B20	*Defluviitoga tunisiensis*	99	Thermotogae	NR_122085.1
B21	*Tepidanaerobacter acetatoxydans*	100	Firmicutes	NR_074537.1

B20, B21- Active control

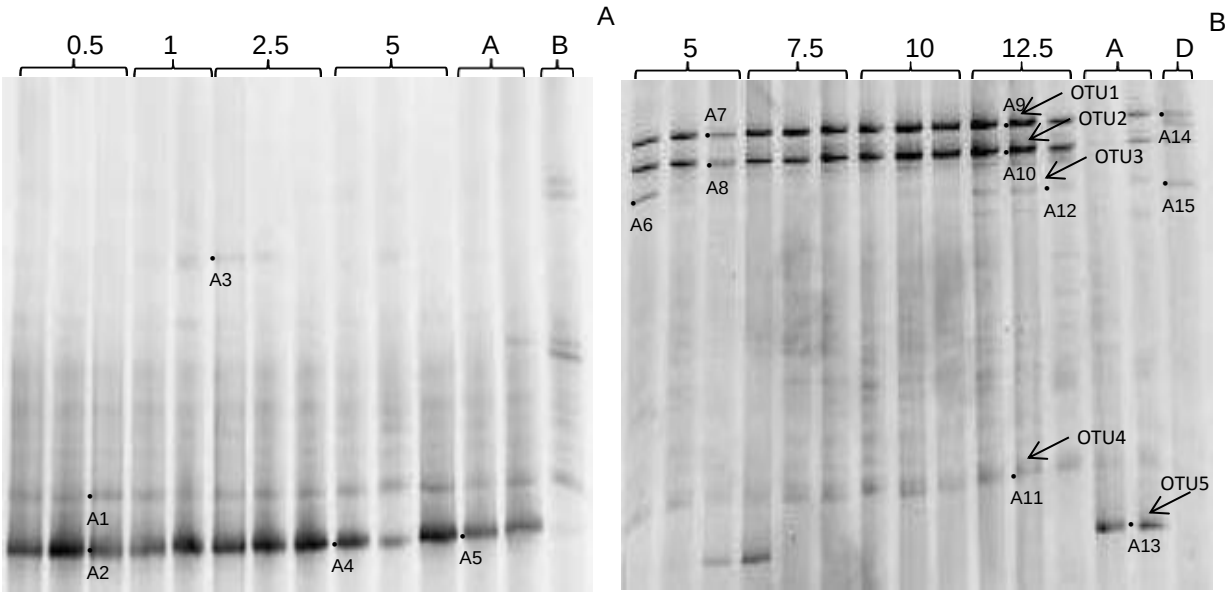

Fig. 4.7 Archaeal DGGE profiles of the 16S rRNA gene PCR products amplified from DNA extracted from swine waste digestate inoculated reactors with target 0.5-5 g TAN/L day 164 (A) and from reactors with target 5-12.5 g TAN/L day 189 (B). Lanes are labelled with TAN concentrations (g TAN/L); lane A, B, and D indicate the DGGE profile of active control, background, and swine waste digestate, respectively. Dots and numbers indicate the bands sequenced.

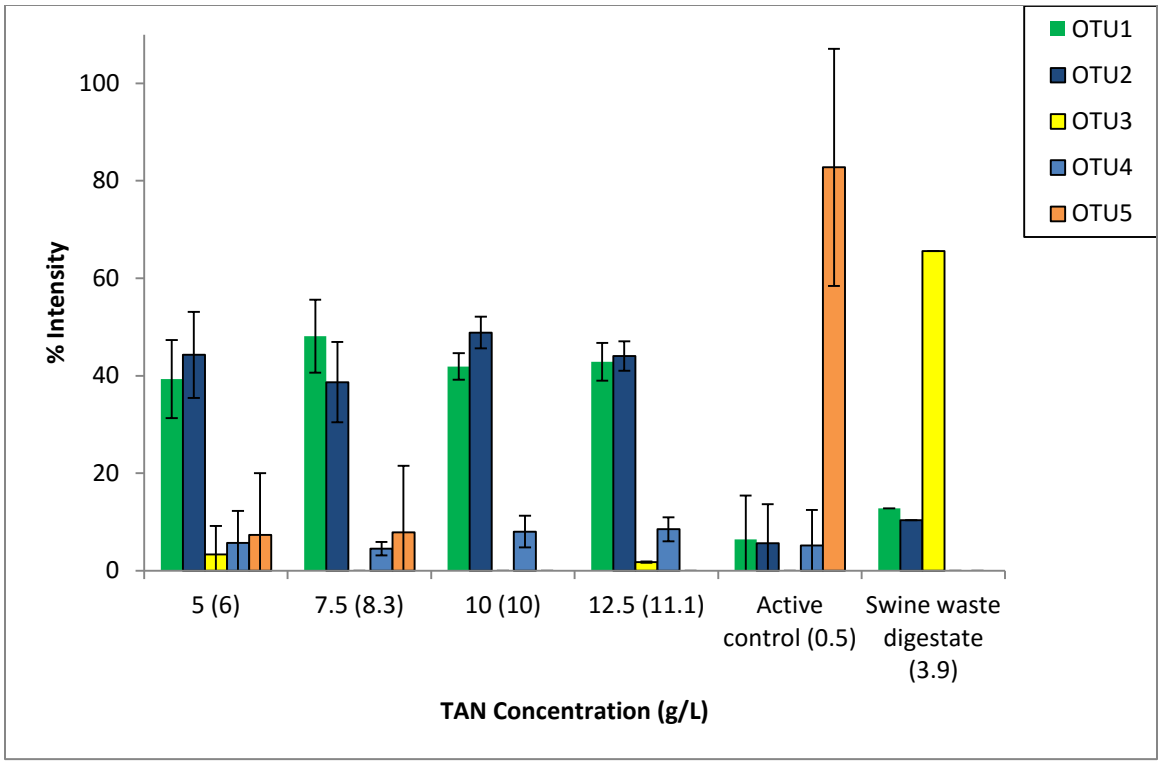

Fig. 4.8 The archaeal DGGE band intensity from swine waste digestate inoculated reactors with target 5-12.5 g TAN/L. The numbers in parentheses represent actual TAN concentrations. Bars are averages and error bars are one standard deviation of the % of the total band intensity from triplicate DGGE lanes. The matches to specific phylotypes are: OTU1- *Methanoculleus* spp., OTU2- *Methanoculleus* spp., OTU3- *Methanoculleus* spp., OTU4- *Methanoculleus* spp., and OTU5- *Methanosarcina* spp.

Table 4.7 Archaeal DGGE 16S rRNA gene band identifications from swine waste digestate

DGGE band	Closest match	Identity (%)	Phyla	Closest match Accession no.
Low Ammonia				
A1	*Methanosarcina* spp.	98	Euryarchaeota	NR_074221.1
A2	*Methanosarcina* spp.	97	Euryarchaeota	NR_074221.1
A3	*Methanosarcina* spp.	90	Euryarchaeota	NR_074221.1
A4	*Methanosarcina* spp.	96	Euryarchaeota	NR_074221.1
A5	*Methanosarcina* spp.	99	Euryarchaeota	NR_074221.1
High Ammonia				
A6	*Methanoculleus* spp.	89	Euryarchaeota	NR_042786.1
A7	*Methanoculleus* spp.	88	Euryarchaeota	NR_042786.1
A8	*Methanoculleus* spp.	97	Euryarchaeota	NR_043961.1
A9	*Methanoculleus* spp.	95	Euryarchaeota	NR_042786.1
A10	*Methanoculleus* spp.	99	Euryarchaeota	NR_043961.1
A11	*Methanoculleus* spp.	98	Euryarchaeota	NR_043961.1
A12	*Methanoculleus* spp.	91	Euryarchaeota	NR_042786.1
A13	*Methanosarcina* spp.	82	Euryarchaeota	NR_104757.1
A14	*Methanoculleus* spp.	98	Euryarchaeota	NR_042786.1
A15	*Methanoculleus* spp.	89	Euryarchaeota	NR_028156.1

A13- Active control
A14, A15- Digestate

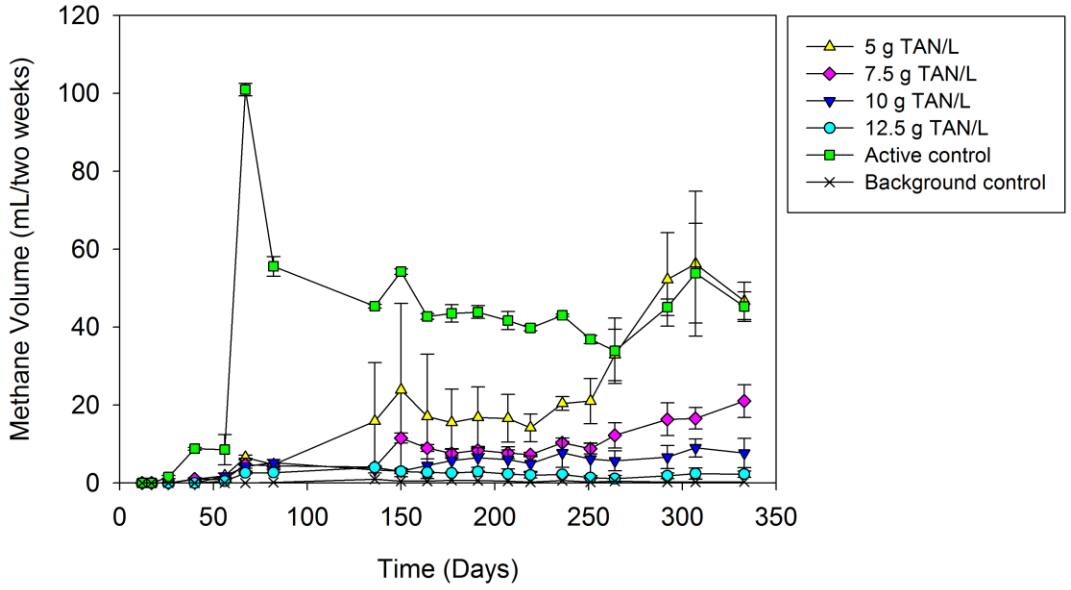

Fig. 4.9 Methane production from wastewater sludge digestate inoculated reactors at target 5-12.5 g TAN/L. Symbols are averages of triplicates and error bars are ± one standard deviation.

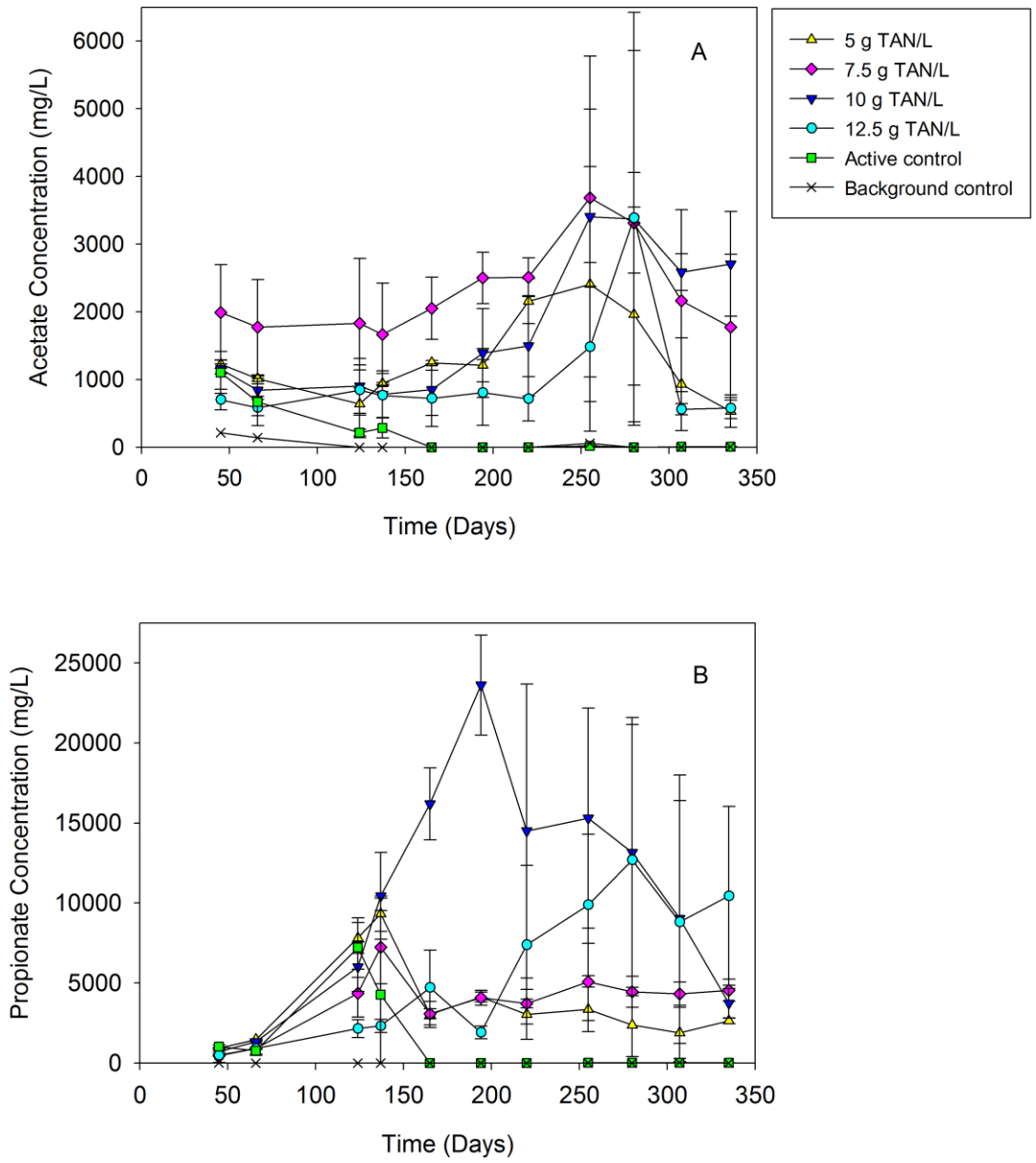

Fig. 4.10 Acetate (A) and propionate (B) concentration in wastewater sludge digestate inoculated reactors with target TAN of 5- 12.5 g TAN/L. Symbols are averages of triplicates and error bars are ± one standard deviation.

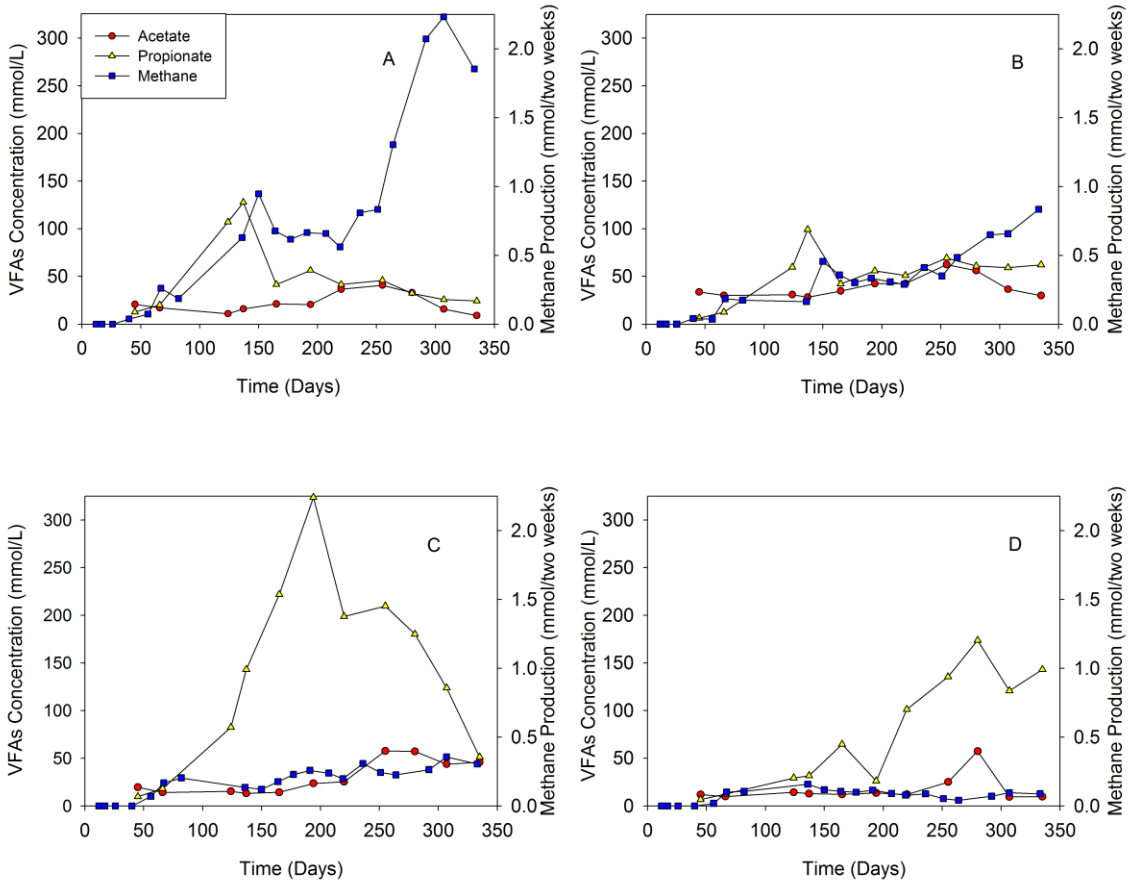

Fig. 4.11 The relationships of methane and VFAs in wastewater sludge digestate inoculated reactors with target 5 g TAN/L (A), 7.5 g TAN/L (B), 10 g TAN/L (C), and 12.5 g TAN/L (D). Symbols are average values of triplicates.

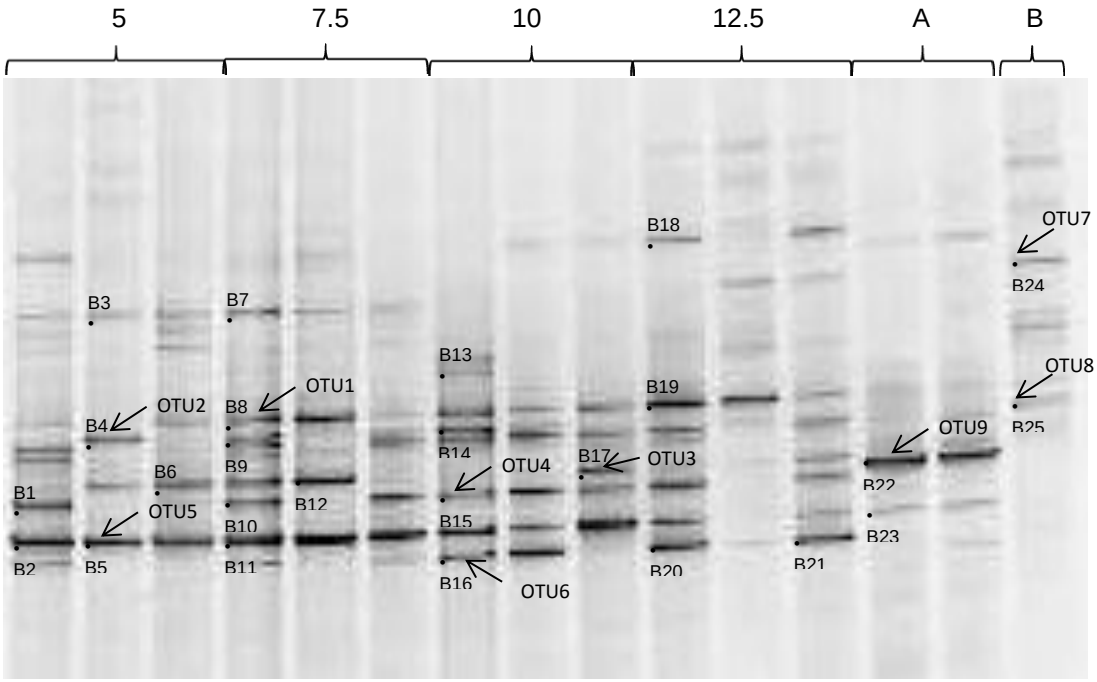

Fig. 4.12 Bacterial DGGE profiles of the 16S rRNA gene PCR products amplified from DNA extracted from wastewater sludge digestate inoculated reactors with target 5-12.5 g TAN/L day 335. Lanes are labelled with TAN concentrations (g TAN/L); lanes A and B indicate the DGGE profile of active control and background. Dots and numbers indicate the bands sequenced.

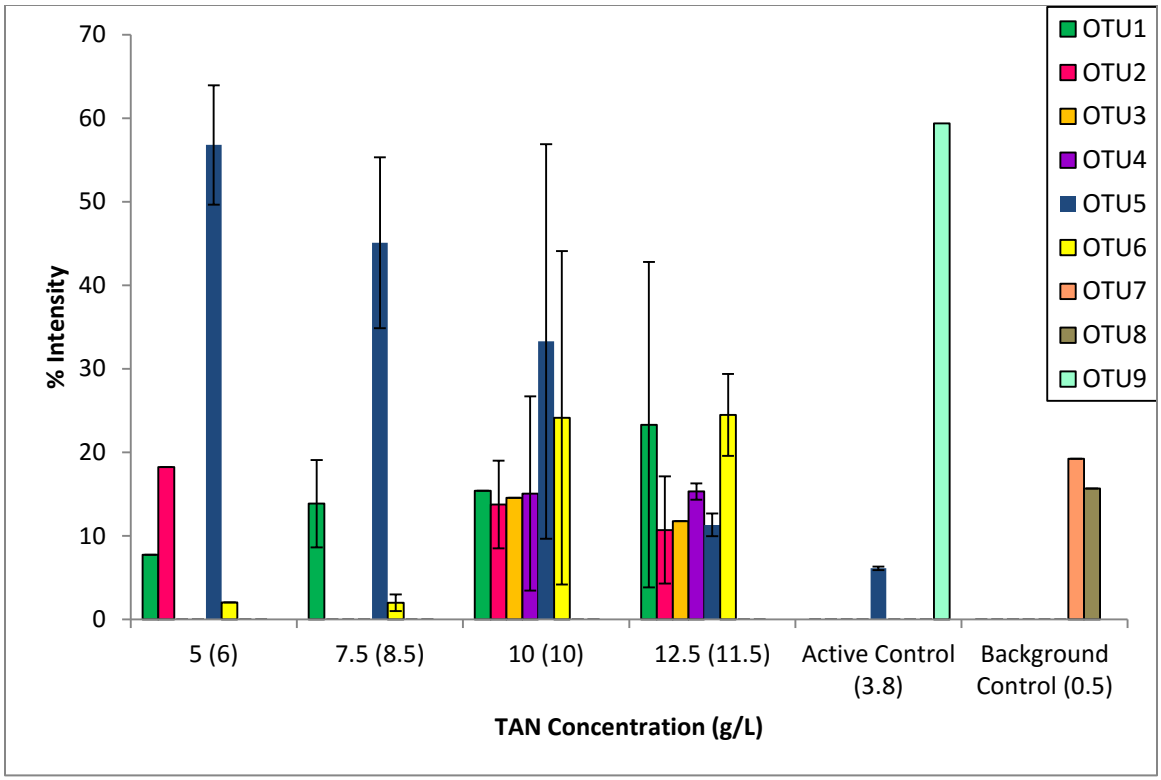

Fig. 4.13 The bacterial DGGE band intensity from wastewater sludge digestate inoculated reactors with target 5-12.5 g TAN/L. The numbers in parentheses represent actual TAN concentrations. Bars are averages and error bars are one standard deviation of the % of the total band intensity from triplicate DGGE lanes. The matches to specific phylotypes are: OTU1- *Aminobacterium sp.*, OTU2- *Sedimentibacter* spp., OTU3- *Tepidanaerobacter* spp., OTU4- *Thermotoga* spp./ *Geobacillus* spp., OTU5- *Thermanaerovibrio sp.*, OTU6- *Thermanaerovibrio* spp., OTU7- *Prolixibacter* spp., OTU8- *Acetobacterium* spp./*Eubacterium* spp., and OTU9- *Taylorella sp.*/ *Alicyclobacillus* spp./*Thermogemmatispora sp.*

Table 4.8 Bacterial DGGE 16S rRNA gene band identifications from wastewater sludge digestate inoculated reactors

DGGE band	Closest match	Identity (%)	Phyla	Closest match Accession no.
B1	*Thermanaerovibrio* spp.	91	Firmicutes	NR_074520.1
B2	*Thermanaerovibrio* spp.	90	Firmicutes	NR_074520.1
B3	*Thermanaerovibrio* spp.	89	Firmicutes	NR_074520.1
B4	*Sedimentibacter* spp.	97	Firmicutes	NR_029146.1
B5	*Cloacibacillus sp.*	89	Synergistetes	NR_115465.1
B6	*Calderihabitans sp.*	91	Firmicutes	NR_114349.1
	Geobacillus sp.	91	Firmicutes	NR_074931.1
B7	*Eubacterium sp.*	93	Firmicutes	NR_042074.1
	Thermodesulfobacterium spp.	93	Thermodesulfobacteria	NR_075031.1
B8	*Aminobacterium sp.*	88	Synergistetes	NR_074624.1
B9	*Desulfohalobium sp.*	88	Proteobacteria	NR_118816.1
B10	*Thermanaerovibrio* spp.	88	Firmicutes	NR_074520.1
B11	*Thermanaerovibrio* spp.	90	Firmicutes	NR_074520.1
B12	*Calderihabitans sp.*	84	Firmicutes	NR_114349.1
B13	*Sedimentibacter* spp.	90	Firmicutes	NR_029146.1
B14	*Sedimentibacter* spp.	82	Firmicutes	NR_029146.1
B15	*Thermotoga* spp.	90	Thermotogae	NR_117753.1
	Geobacillus spp.	90	Firmicutes	NR_075008.1
B16	*Thermanaerovibrio* spp.	89	Firmicutes	NR_074520.1
B17	*Tepidanaerobacter* spp.	74	Firmicutes	NR_074537.1
B18	*Aminobacterium* spp.	92	Synergistetes	NR_074624.1
	Thermovirga spp.	92	Firmicutes	NR_074606.1
B19	*Thermanaerovibrio* spp.	92	Firmicutes	NR_074520.1
B20	*Thermanaerovibrio spp.*	92	Firmicutes	NR_074520.1
B21	*Thermanaerovibrio* spp.	92	Firmicutes	NR_074520.1

DGGE band	Closest match	Identity (%)	Phyla	Closest match Accession no.
B22	*Taylorella sp.*	94	Proteobacteria	NR_074773.1
	Alicyclobacillus spp.	94	Firmicutes	NR_114205.1
	Thermogemmatispora sp.	94	Chloroflexi	NR_113127.1
B23	*Thermanaerovibrio* spp.	82	Firmicutes	NR_074520.1
B24	*Prolixibacter* spp.	77	Bacteroidetes	NR_113041.1
B25	*Acetobacterium* spp.	85	Firmicutes	NR_074548.1
	Eubacterium spp.	85	Firmicutes	NR_074533.1

B22, B23- Active control

B24, B25- Background control

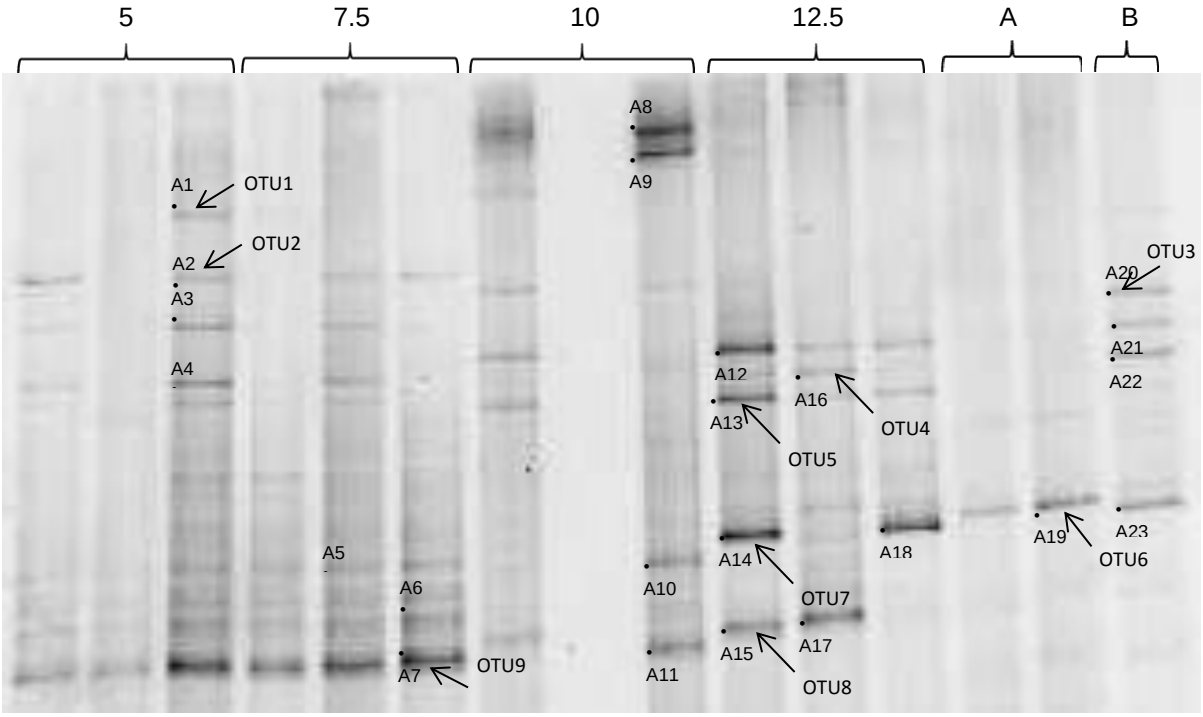

Fig. 4.14 Archaeal DGGE profiles of the 16S rRNA gene PCR products amplified from DNA extracted from wastewater sludge digestate inoculated reactors with target 5-12.5 g TAN/L day 335. Lanes are labelled with TAN concentrations (g TAN/L); lanes A and B indicate the DGGE profile of active control and background. Dots and numbers indicate the bands sequenced.

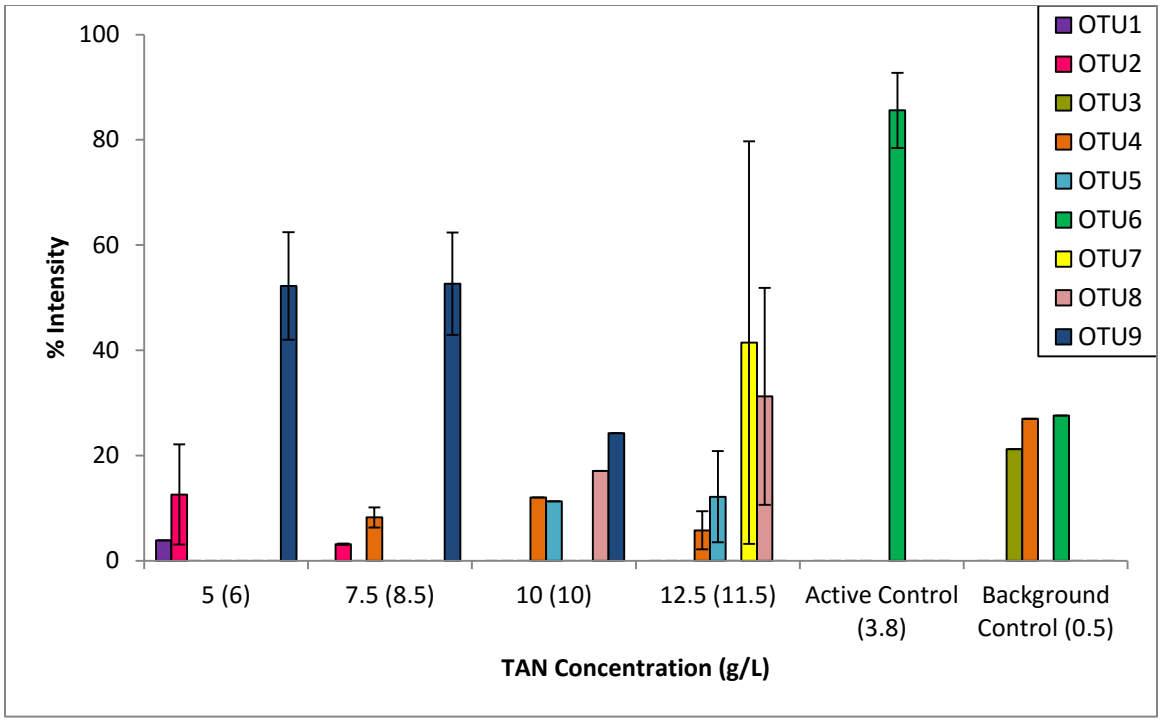

Fig. 4.15 The archaeal DGGE band intensity from wastewater sludge digestate inoculated reactors with target 5-12.5 g TAN/L. The numbers in parentheses represent actual TAN concentrations. Bars are averages and error bars are one standard deviation of the % of the total band intensity from triplicate DGGE lanes. The matches to specific phylotypes are: OTU1- *Methanomicrobium* spp., OTU2- *Methanoculleus* spp., OTU3- *Methanosaeta sp.*, OTU4- *Methanospirillum sp*., OTU5- *Methanoculleus* spp., OTU6- *Methanosaeta sp.*, OTU7- *Methanoculleus* spp., OTU8- *Methanoculleus* spp., and OTU9- *Methanoculleus* spp.

Table 4.9 Archaeal DGGE 16S rRNA gene band identifications from wastewater sludge digestate inoculated reactors

DGGE band	Closest match	Identity (%)	Phyla	Closest match Accession no.
A1	*Methanomicrobium* spp.	91	Euryarchaeota	NR_044726.1
A2	*Methanoculleus* spp.	91	Euryarchaeota	NR_043961.1
A3	*Methanoculleus* spp.	99	Euryarchaeota	NR_042786.1
A4	*Methanoculleus* spp.	99	Euryarchaeota	NR_043961.1
A5	*Methanoculleus* spp.	97	Euryarchaeota	NR_028156.1
A6	*Methanoculleus* spp.	99	Euryarchaeota	NR_042786.1
A7	*Methanoculleus* spp.	99	Euryarchaeota	NR_042786.1
A8	*Methanoculleus* spp.	99	Euryarchaeota	NR_112788.1
A9	*Methanoculleus* spp.	99	Euryarchaeota	NR_042786.1
A10	*Methanoculleus* spp.	99	Euryarchaeota	NR_112788.1
A11	*Methanoculleus* spp.	99	Euryarchaeota	NR_042786.1
A12	*Methanoculleus horonobensis*	99	Euryarchaeota	NR_112788.1
A13	*Methanoculleus* spp.	99	Euryarchaeota	NR_074174.1
A14	*Methanoculleus* spp.	97	Euryarchaeota	NR_112788.1
A15	*Methanoculleus* spp.	97	Euryarchaeota	NR_074174.1
A16	*Methanospirillum sp.*	95	Euryarchaeota	NR_118366.1
A17	*Methanoculleus* spp.	98	Euryarchaeota	NR_074174.1
A18	*Methanoculleus horonobensis*	99	Euryarchaeota	NR_112788.1
A19	*Methanosaeta sp.*	96	Euryarchaeota	NR_102903.1
A20	*Methanosaeta sp.*	95	Euryarchaeota	NR_102903.1
A21	*Methanospirillum sp.*	93	Euryarchaeota	NR_074177.1
A22	*Methanospirillum* spp.	96	Euryarchaeota	NR_074177.1
A23	*Methanosaeta concilii*	98	Euryarchaeota	NR_102903.1

A19 – Active control

A20, A21, A22, A23- Background control

Chapter 5 Divalent Cation Effects to Counteract Ammonia Toxicity

5.1 Abstract

Addition of divalent cations to anaerobic methanogenic reactors has previously been shown to counter ammonia toxicity (Sprott and Patel 1986). This study examined the effect of magnesium and calcium addition on counteracting ammonia toxicity in anaerobic reactors inoculated with swine waste digestate and fed glutamate as a sole carbon and energy source. Reactors were stressed with total ammonia nitrogen (TAN) concentrations poised at either 2.5 or 5 g TAN/L. In general, addition of these divalent cations increased methane production after 50 days of operation and decreased prevailing volatile fatty acids (VFAs), compare to reactors not receiving divalent cations indicating an overall positive outcome. Cation amended reactors accumulated more propionate than those without cation at the beginning; however, propionate was rapidly utilized within 60-70 days in both 2.5 and 5 g TAN/L reactors. Microbial community analysis revealed shifts in the bacterial community with increases in the prevalence of members of the phyla Firmicutes, Bacteroidetes, Synergistetes, and Proteobacteria (Fig. 5.4 – 5.7, Table 5.2). The phylum Euryarchaeota was the only dominant archaeal community enriched. Phylotypes related to *Thermanaerovibrio acidaminovorans*, a syntrophic, glutamate-degrading bacterium, dominated in most reactors. In addition, phylotypes related to *Tepidanaerobacter acetatoxydans*, an anaerobic, syntrophic acetate-oxidizing bacterium, dominated in the Ca^{2+}-amended reactors at both 2.5 and 5 g TAN/L. Cation addition also enhanced the dominance of phyloptypes matching *Methanosarcina sp.*, but the specific species present were different in Ca^{2+}- and Mg^{2+}-amended reactors.

5.2 Introduction

Deamination of protein during the AD process results in the formation of ammonium bicarbonate, which acts as a natural buffer for maintaining pH of the system from excessive volatile fatty acid intermediates (Ahn et al. 2006b, McCarty and McKinney 1961). However, a high amount of ammonium bicarbonate buffer and increased ammonia concentrations resulting from anaerobic digestion of high protein wastes have been reported to cause ammonia toxicity (Angelidaki and Ahring 1993, Foresti et al. 2006, Fotidis et al. 2012). Thus, there is a need to improve the efficiency of AD process during digestion of high-N wastes under conditions that produce high ammonia concentrations.

Studies on AD have been focused around the influences of ammonia inhibition. These include the effects of ammonia on mesophilic and thermophilic anaerobic degradation of biowaste protein (Gallert et al. 1998), on mesophilic AD of kitchen wastes (Liu et al. 2012), on the performances of anaerobic bioreactors treating synthetic wastewater at mesophilic (Calli et al. 2005) and thermophilic (Sung and Liu 2003) temperature, on the specific activity of pelletized methanogenic sludge (Koster and Lettinga 1984), and on the maximum growth rate of hydrogenotrophic methanogens at various pH-levels and temperatures (Koster and Koomen 1988). Ammonia inhibition thresholds have been demonstrated, and often reported, but the units of expression for the ammonia may be different. For example, a free ammonia (NH_3) threshold in the range of 0.08-1.1 g NH_3-N/L (Gallert et al. 1998, Hansen et al. 1998, McCarty and McKinney 1961); ammonium nitrogen (NH_4^+-N) in the range of 1.2-2.4 g NH_4^+-N/L (Koster and Lettinga 1984, Velsen 1979), and total ammonia nitrogen (TAN) of >4 g TAN/L

(Angelidaki and Ahring 1993, Sung and Liu 2003), were all shown to be inhibitory to AD to a certain extent. These values were reported differently and outcomes with respect to inhibition may also depend upon other factors such as substrates, pH, temperature, types of reactors, and other conditions or operating parameters.

Effects of high ammonia on microbial communities have also been studied. It was reported that anaerobic reactors acclimatized to an ammonium concentration of 7 g NH_4^+-N/L showed dominance of *Methanosarcinaceae* spp. (Fotidis et al. 2013). The microbial community makeup may shift upon acclimatization to ammonia over time. For example, a shift from aceticlastic acetate degradation to syntrophic acetate oxidation (SAO) in mesophilic anaerobic reactors with acetate as the only substrate (Schnurer et al. 1994), and with municipal waste (Westerholm et al. 2011b) was detected at 7 g NH_4^+-N/L. In a study of anaerobic sequencing batch reactors (SBR) operated at 3.6 g TAN/L, changes in the archaeal community from the genus *Methanosarcina* to hydrogenotrophic methanogens of the order Methanomicrobiales (Angenent et al. 2002) were observed. Therefore, microbial acclimatization and community shift are factors leading to sustainable AD in high ammonia reactors. Because the time needed for microbial community adaptation to ammonia stress may be prohibitively long, other options to immediately recover methane production in ammonia-stressed AD systems have been sought. An increased resistance to ammonia inhibition in anaerobic thermophilic reactors treating cattle manure was achieved by addition of zeolite (Borja et al. 1996). It was found that methane production in the zeolite-amended reactor operating at an ammonia concentration of 7 g TAN/L was greater than the methane production in the control. McCarty and McKinney (1961) observed that reactor failure from high ammonia

concentration can be alleviated by addition of cations such as magnesium (Mg^{2+}) and calcium (Ca^{2+}), which appeared to reverse ammonia toxicity. Addition of calcium or magnesium hydroxide can also neutralized volatile fatty acids that were at an inhibitory level (~10,000 mg/L) (McCarty and McKinney 1961).

Ammonia toxicity to pure cultures of methanogens has also been investigated. Sprott and Patel (1986) theorized that ammonia caused potassium (K^+) efflux to reduce ammonia toxicity in the cell through an ammonia/K^+ exchange reaction, and that this also caused inhibition of methane synthesis. When K^+ was added to the medium at the concentration found in the cytoplasm, the influx of ammonia into the cells was retarded (Sprott et al. 1984). Addition of Ca^{2+} was also indicated to counter the toxicity of ammonia to methane synthesis in cell suspensions of *Methanothrix concilii*, an ammonia sensitive aceticlastic methanogen, via activity at the outer face of the cytoplasmic membrane (Sprott and Patel 1986).

In addition to having a direct, mechanistic effect on ammonia toxicity, it is possible that calcium also alleviates symptoms of reactor upset caused by ammonia toxicity. Koster (1987) indicated that addition of calcium chloride can reverse lauric acid inhibition of methanogenesis because calcium salts of long-chain fatty acids (which may also be toxic to cells) are insoluble. In AD treating swine wastewater at mesophilic temperatures (35°C), an addition of calcium of 3 g/L (75 mM) resulted in a decrease in the lag phase, increase in biogas production, and decrease of volatile fatty acids (acetate, propionate, butyrate, and valerate). In that study, it was proposed that the positive effect of calcium was especially important for supporting propionate and *i*-valerate degraders to decrease propionate and *i*-valerate in AD treating the swine wastewater (Ahn et al.

2006b). Moreover, calcium enhanced the biomass accumulation and granulation process in an upflow anaerobic sludge blanket (UASB) treating synthetic wastewater (Yu et al. 2001), in a UASB treating distillery effluent (Sharma and Singh 2001), and in a expanded granular sludge bed bioreactor (EGSB) treating leachate (Liu et al. 2011). In those studies the effect of calcium was particularly thought to allow microbe aggregates to form and develope inter-species hydrogen and proton transfer. Further, addition of calcium was reported to precipitate long-chain fatty acids from upsetting AD.

Influence of calcium addition on a syntrophic co-culture of *Syntrophomonas wolfei*, an obligate hydrogen-producing bacterium, and *Methanospirillum hungatei*, an ammonia-sensitive methanogen, degrading long-chain fatty acids (LCFAs), was reported. LCFA degradation occurred in the presence of calcium in the medium with a fatty acid/calcium ratio of 2:1 (Roy et al. 1985).

Because calcium itself can be inhibitory to digesters if present in concentrations that are too high, it is important to limit calcium addition to alleviate ammonia toxicity to levels that are non-inhibitory. It is interesting in that regard to note that after acclimatization, methanogens in a UASB treating synthetic wastewater were able to adapt to high calcium concentration of 7 g/L (Jackson-Moss and Duncan 1989). In that study calcium was being investigated because calcium is known to be essential for the growth of some strains of methanogens. No community analysis was performed, but rather the acclimation was observed through an increase in methane production over time. The pH, VFAs, and percentage COD removed were maintained at a stable level.

The objective of this study was to examine the effects of calcium and magnesium addition to counteract ammonia inhibition in ammonia stressed anaerobic reactors by monitoring performance and the microbial community. Microbial enrichments from a swine waste digester, cultured on glutamate as a sole carbon and energy source, were operated under ammonia stress. Calcium and magnesium were added at different concentrations to determine whether methane production could be recovered to unstressed values. VFAs were also monitored. Finally bacterial and archaeal community analysis was performed to determine the link between divalent cations addition and ultimate performance of the process.

5.3 Materials and methods

5.3.1 Swine waste digestate inoculum

Swine waste digestate was obtained from Pinehurst Acres Farm, Danville, Pennsylvania, USA. Pinehurst Acres operates a 4,400 unit grow/finish hog production facility. The facility operates a mesophilic anaerobic digester with a capacity of 143,000 gallons. The digester is designed to operate with a HRT of 28 days at 6% solids. One L of swine waste effluent digestate samples were placed in sterile Nalgene containers and shipped on ice to Rutgers University at 4°C. The samples were stored at 4°C from arrival to one day prior to use in establishing reactors. The total time between collection of sample and use was about two days. The characteristics of the swine waste digestate are shown in Table 4.1.

5.3.2 Reactor set-up and operation

The 160-mL serum bottles (VWR, Radnor, PA, USA) were sterilized by autoclaving, made anoxic by purging with sterile 99.998% nitrogen gas, and then 10 mL swine waste digestate was added via a sterile glass pipette. The total liquid volume of each bottle was then adjusted to 100 mL by adding sterile anaerobic minimal medium (Fennell and Gossett 1997). After setup, bottles were operated with a hydraulic retention time (HRT) of 70 days by a fill and draw exchange of 10% of the enrichment volume (10 mL) with sterile anoxic medium every week to achieve semi-continuous operation. Glutamate (1 mmol) was added via a sterile syringe initially and thereafter every week as the sole carbon and energy source from a sterile, anoxic 500 mM sodium glutamate stock solution. Treatments were established in triplicate with a target TAN of 2.5 and 5 g N/L by adding appropriate volumes of sterile, anoxic 5 M NH_4Cl stock solution initially, and after each fill and draw to maintain a constant imposed TAN concentration. Designated "cation" addition reactor treatments established at each TAN concentration, were also amended with a sterile anoxic solution of 500 mM $MgCl_2 \bullet 6H_2O$ or 2 M $CaCl_2 \bullet 2H_2O$ to achieve and maintain concentrations of 5 mM or 10 mM $MgCl_2$ and 20 mM or 40 mM $CaCl_2$. Actual TAN concentrations in the reactors as measured analytically are shown in Table 5.1 and were slightly different than expected. A set of active controls deemed "No cation" reactors were fed only NH_4Cl and glutamate and had the TAN maintained at the designated concentration. Active unstressed controls were fed glutamate as a sole carbon and energy source and had no NH_4Cl added other than that in the original minimal medium recipe. In these reactors, N was analytically determined to be 0.1 g N/L. Background controls were operated to determine the methane produced by decay of the

inoculum and received no carbon source. All bottles were incubated at 35°C in the dark and manually shaken every two days.

5.3.3 Analytical methods

Biogas volume produced from each reactor was measured by water displacement. Methane content was determined from a 250 µL headspace sample using a Pressure-Lok® Series A-2 syringe (VICI® Precision Sampling, Baton Rouge, CA, USA) with a flame sterilized needle. The sample was injected into an Agilent 6890 N gas chromatograph (Agilent Technologies, Santa Clara, CA, USA) equipped with a GS-GasPro capillary column (30 m x 0.32 mm I.D.; J&W Scientific, Folsom, CA, USA) and a flame ionization detector. Helium was the carrier gas at a constant pressure of 131 kPa. The oven temperature was 150°C. The resulting chromatographic peak area was compared to a five point calibration curve prepared using mixtures of 0 to 99% methane created by mixing volumes of methane (99% purity; Matheson Tri- Gas, Inc., Montgomeryville, PA, USA) and air. Methane production volume was calculated from the methane content and biogas volume at 998 mbar and 23°C. The moles of methane produced were then corrected to STP (1 atm, 0°C).

The volatile fatty acids acetate, propionate, and butyrate were measured by high performance liquid chromatography (HPLC). Reactor effluent samples (0.75 mL) were centrifuged at 9390 *g* (Eppendorf Model No. 5424) for 3 minutes and the supernatant was filtered using Spin-X Centrifuge Tube Filters, Corning Nylon Membrane, pore size 0.45 µm (VWR). Filtered samples were analyzed on a Beckman Coulter® System Gold™ HPLC (Beckman-Coulter, Fullerton, CA, USA) using a Bio-Rad® Aminex HPX-87H

organic acid analysis column (Bio-Rad Laboratories, Hercules, CA, USA). The column was held at 60°C. The mobile phase was 0.008 N H_2SO_4 at a flow rate of 0.6 mL/minute. UV detection was at a wavelength of 210 nm. Chromatographic peak areas were quantified by comparison to standard curves of acetic, propionic, and butyric acids (99-99.7% purity, Sigma-Aldrich Co., St. Louis, MO, USA) over a concentration range from 250 to 1,000 mg/L. The detection limit for the system was approximately 8.4 mg acetate/L.

Total ammonia nitrogen (TAN) was measured by ion chromatography (IC). To convert free ammonia to ammonium ion, the pH of aqueous samples was adjusted to < 2 using 10 N H_2SO_4. Next, samples were centrifuged at 9390 *g* (Eppendorf Model No. 5424) for 3 minutes, and the supernatant was filtered using Spin-X Centrifuge Tube Filters, Corning Nylon Membrane, pore size 0.45 µm (VWR). The filtrate was diluted 800 times with MilliQ water, and analyzed for TAN using a Dionex ICS-1000 ion chromatograph equipped with an IonPac™ CS12A RFTC™ 4x250 mm cation column, and a CSRS™ 300 4 mm cation suppressor (Dionex Corporation, Salt Lake City, UT, USA). The mobile phase was 20 mN methanosulfonic acid. TAN was calculated from a standard curve prepared over a range of 0.125 to 2 mM and corrected for dilution.

The pH was routinely measured using an Accumet® Basic AB15 (Fisher Scientific, Pittsburgh, PA, USA) pH meter with symphony Ag/AgCl pH electrode (VWR). Free ammonia was then calculated from the equilibrium equation (Eqn. 1) (Angelidaki and Ahring 1993):

$$[NH_3 - N] = \frac{[TAN]}{\left[1 + \frac{[H^+]}{K_a}\right]} \quad \text{Eqn. 1}$$

where K_a (the dissociation constant) = 1.12 x 10^{-9} at 35°C

Methane, VFAs, and TAN data are reported as an average of triplicate reactors ± one standard deviation.

5.3.4 Microbial community analysis

Bacterial and archaeal communities were analyzed using polymerase chain reaction (PCR) coupled to denaturing gradient gel electrophoresis (DGGE). DNA extraction from 1-3 mL enrichment samples was performed using the PowerSoil™ DNA Isolation Kit (MoBio Laboratories, Carlsbad, CA, USA) according to the manufacturer's instructions. The PCR amplification of partial bacterial 16S rRNA genes was performed with forward (338-GC F) and reverse (519R) primers (Nakatsu 2000). The PCR protocol was as follows: initial denaturation at 94°C for 5 minutes; 33 cycles of denaturation at 94°C for 30 seconds, annealing at 55°C for 30 seconds, and elongation at 72°C for 30 seconds; followed by a final extension step of 7 minutes at 72°C (Chen 2010). The PCR amplification of partial archaeal 16S rRNA genes was performed with ARC787f-GC and ARC1059r (Hwang et al. 2008, Merlino et al. 2013). To amplify the target DNA, a touchdown PCR amplification of archaeal 16S rRNA genes was used with the following conditions: initial denaturation at 94°C for 10 minutes; 20 cycles of denaturation at 94°C for 1 minute, annealing for 1 minute at a temperature that decreased by 0.5°C every cycle from 65°C to the 'touchdown' at 55°C, and elongation at 72°C for 1 minute; and finally,

20 cycles of denaturation at 94°C for 1 minute, annealing at 55°C for 1 minute, and extension at 72°C for 1 minute. Thus, the PCR was performed in a total of 40 cycles. A final extension step was performed at 72°C for 3 minutes. The PCR products were analyzed by electrophoresis on a 1.5% agarose gel, stained in 0.1% ethidium bromide (EtBr) solution for 30 minutes and visualized using UV on a Molecular Imager Gel Doc XR system (Bio-Rad Laboratories).

For DGGE, the quantified DNA in PCR products was loaded onto 8% polyacrylamide gels containing a gradient of 30-60% and 40-60% denaturant (100% denaturant contained 7M urea and 40% formamide) for bacteria and archaea, respectively. Electrophoresis was run at 60°C in 1xTAE buffer; for bacteria: 4 h at 150V; for archaea, 17 h at 90V. Gels were stained with SYBR® Gold nucleic acid stain (Invitrogen, NY, USA) for 30 minutes and documented with a Molecular Imager Gel Doc XR system (Bio-Rad Laboratories). DGGE gel profiles were analyzed using a Molecular Imager Gel Doc XR system (Bio-Rad Laboratories). Dominant bands were excised and DNA was eluted. The DNA fragment was then re-amplified using the DGGE primer set without GC clamp, and re-run on 1.5% agarose gel. The PCR products were purified with USB® ExoSAP-IT®, and sequenced (Genewiz, South Plainfield, NJ, USA). The sequences were compared with sequences deposited in the National Center for Biotechnology Information (NCBI) database using the BLAST program. All sequencing results were additionally confirmed by the RDP Native Bayesian rRNA Classifier Version 2.6, Sep 2013 (http://rdp.cme.msu.edu/classifier/hierarchy.jsp).

A resulting gel image was analyzed for relative band intensities using the ImageJ 1.48v quantification software (National Institutes of Health, USA), according to the

manufacturer's protocol (http://imagej.nih.gov/ij). For each phylotype detected, the band intensities are reported as an average of triplicates ± one standard deviation.

5.3.5 Data analysis

Data are presented as average values of triplicates and error bars are one standard deviation. When the term "steady state" is used it refers to an approximate pseudo- steady state condition where select average weekly output parameters were within ± 20%. For statistical analysis, the methane production rate from each reactor condition was tested by ANOVA and the difference between means was tested using Duncan multiple range test at the 95% level of confidence ($p<0.05$). All statistical tests were analyzed by SPSS program version 19.

5.4 Results

5.4.1 Effects of calcium and magnesium addition on methane production

The results indicated that addition of divalent cations into a reactor with a specific TAN concentration affected methane production compared to the no cation addition controls (2.5 and 5 g TAN/L) and the active control without TAN addition. The cumulative methane production in treatments stressed with 2.5 and 5 g TAN/L are shown in Fig. 5.1A and Fig. 5.1B, respectively. During the start-up period and 86 days of operation (Fig. 5.1), the effects of cation to counteract ammonia inhibition were not readily evident. The active control without TAN addition produced the highest methane. At 2.5 g TAN/L, only the 5 mM $MgCl_2$ reactors produced as much methane as the active

control while other conditions produced less methane (Fig. 5.1A). However, long term exposure of cations did produce significant differences in the methane production rates for different treatments (Table 5.1). During 48 days of pseudo-steady state operation (day 136-184), the highest methane production rate at 1.93 ± 0.03 mmol/week was detected in the 5 mM $MgCl_2$ reactors with 2.5 g TAN/L. This value was not significantly different from that obtained from the 5 mM $MgCl_2$ reactors with 5 g TAN/L (1.75 ± 0.03 mmol/week), but was significantly different from the no cation controls at 2.5 g TAN/L (1.65 ± 0.03 mmol/week) and at 5 g TAN/L (1.64 ± 0.03 mmol/week) ($p<0.05$), and the active control without TAN addition (1.49 ± 0.02 mmol/week) ($p<0.05$). The 10mM $MgCl_2$ with 2.5 and 5 g TAN/L reactors, which had a lower methane production rate than the 5 mM $MgCl_2$ with 2.5 g TAN/L, were not significantly different from other conditions. The 20 and 40 mM $CaCl_2$ reactors with both TAN concentrations revealed similar results. All of these reactors had a lower methane production rate than the 5 mM $MgCl_2$ with 2.5 g TAN/L and were not significantly different from other conditions including the no cation controls and the active control without TAN addition. In addition, the methane production rate from the no cation controls at both 2.5 and 5 g TAN/L were not significantly different from the active control. Moreover, the 5 mM $MgCl_2$ reactors at 2.5 g TAN/L revealed methane production rate increased by 17% relative to the no cation addition controls and by 29% relative to the active control without TAN addition (Table 5.1).

5.4.2 Effect of calcium and magnesium addition on volatile fatty acids

Volatile fatty acids were monitored to indicate the performance of the AD reactors. Acetate and propionate concentrations in the reactors with 2.5 and 5 g TAN/L are shown in Fig. 5.2. In the first 60 days, there was acetate accumulation in both sets of reactors (Fig. 5.2A and 5.2C). After that, a decrease in acetate concentration was detected. All reactors with cation addition accumulated less acetate than the reactor without cations. $CaCl_2$ addition resulted in lower acetate concentrations than $MgCl_2$. The reactors amended with 40 mM $CaCl_2$ at 2.5 g TAN/L had a decrease in acetate to 42 ± 12 mg/L within 65 days compared to the 10 mM $MgCl_2$ reactors, which had a decrease in acetate to 70 ± 14 mg/L within 170 days (Fig. 5.2A). For the reactor at 5 g TAN/L, a similar trend in acetate reduction was observed (Fig. 5.2C). However, the acetate concentration in the 20 mM $CaCl_2$-amended reactors was higher than the no cation control reactors after 190 days. Propionate concentrations in the reactors at 2.5 and 5 g TAN/L are shown in Fig. 5.2B and 5.2D. Propionate gradually accumulated at the beginning then decreased over the period of operation. At 2.5 g TAN/L, reactors with cation addition had a higher propionate concentration than reactors without cations (Fig. 5.2B). However, at 5 g TAN/L, the $MgCl_2$-amended reactors accumulated as much propionate as that in the no cation control reactors whereas the $CaCl_2$-amended reactors accumulated more propionate than the no cation control reactors. Propionate in the $MgCl_2$-amended reactors with 5 g TAN/L was 915 ± 280 mg/L at day 72 compared to 945 ± 88 mg/L in the no cation control reactors (Fig. 5.2D). The $CaCl_2$-amended reactors with 2.5 and 5 g TAN/L accumulated propionate up to 1,870 ± 675 mg/L and 1,845 ± 77 mg/L, respectively. However, the propionate concentration in $CaCl_2$ reactors dramatically

decreased to less than 10 ± 5 mg/L within 60-70 days, similar to the $MgCl_2$-amended and the no cation control reactors. Butyrate concentrations remained less than 10 mg/L in all reactors during the operational period (data not shown).

5.4.3 Dynamic changes in methane prodution and VFA concentrations

To understand the relationships between methane production and VFA concentrations, changes in methane and VFA concentrations in the best case scenario (2.5 g TAN/L with 5 mM $MgCl_2$) (Fig. 5.3A) and the worst case scenario (5 g TAN/L with 40 mM $CaCl_2$) (Fig. 5.3C) during the pseudo-steady state operational period were compared with the no cation control reactors at 2.5 g TAN/L (Fig. 5.3B) and 5 g TAN/L (Fig. 5.3D) including the active control without TAN (Fig. 5.3E). These changes can be classified into three periods. During the first period (day 0-58), acetate in all reactors dramatically increased, then decreased at the end of this period. Acetate concentration in the 5 mM $MgCl_2$-amended reactors decreased to 5 ± 1.6 mmol/L (Fig. 5.3A) similar to that of the no cation control reactors (Fig. 5.3B). Acetate in the 40 mM $CaCl_2$-amended reactors decreased to non-detectable levels at day 58 (Fig. 5.3C) compared to 8 ± 0.5 mmol/L in the no cation control reactors (Fig. 5.3D). During this period, propionate and methane also increased. Propionate in both cation reactors was higher than that of the no cation control reactors. Propionate in the 5 mM $MgCl_2$-amended reactors accumulated to 4 ± 0.6 mmol/L (Fig. 5.3A) and 25 ± 0.3 mmol/L in the 40 mM $CaCl_2$-amended reactors (Fig. 5.3C), respectively. Methane production was substantial while acetate decreased during this period. During the second period (day 58-150), the $MgCl_2$ and $CaCl_2$ reactors

revealed opposite trends of acetate concentration changes. Acetate concentrations in the $MgCl_2$-amended reactors increased to 18 ± 6.2 mmol/L at day 100 (Fig. 5.3A), but were still less than that of the no cation control at 32 ± 4 mmol/L at day 150 (Fig. 5.3B). Acetate concentration in the $CaCl_2$-amended reactors remained at 0.3 to 0.7 mmol/L over this period (Fig. 5.3C), which was different from the no cation control reactors with acetate concentration up to 44 ± 5 mmol/L at day 135 (Fig. 5.3D). Propionate decreased in all reactors to non-detectable levels at the end of the experimental period. Methane production fluctuated from 1.3 to 1.6 mmol/week at the end of this period in all reactors. During period 3 (day 150-300), acetate and propionate were maintained at stable concentrations from the previous period in both $MgCl_2$-amended and $CaCl_2$-amended reactors. At 2.5 g TAN/L, acetate concentration both in the $MgCl_2$-amended reactors and the no cation control reactors remained at <3 mmol/L while propionate was at non-detectable levels (Fig. 5.3A - 5.3B). At 5 g TAN/L, both acetate and propionate in the $CaCl_2$-amended reactors remained at non-detectable levels (Fig. 5.3C) whereas acetate concentration in the no cation control reactor remained at 5 ± 3.2 mmol/L and propionate remained at non-detectable levels (Fig. 5.3D). Methane production in most reactors fluctuated from 1.3 to 1.6 mmol/week except methane production in the $CaCl_2$-amended reactors at the end of the period was 0.6 ± 0.04 mmol/week). Acetate and propionate concentration in the active control reactor without TAN (Fig. 5.3E) were generally lower than that of other conditions. Methane production fluctuated similar to other conditions.

5.4.4. Effect of calcium and magnesium addition on the microbial community

Microbial community analysis revealed the effects of cation addition at different TAN concentrations. More bacterial phylotypes than archaeal phylotypes were identified by DGGE for all treatments. The bacterial communities at 2.5 g TAN/L are shown in Fig. 5.4 and 5.5 and those at 5 g TAN/L are shown in Fig. 5.6 and 5.7, respectively. Similar bands were detected in both TAN conditions including the no cation control reactors and the active control reactors without TAN addition. The dark bands were cut, sequenced, and compared to the NCBI database. These were classified into the phyla Firmicutes, Bacteroidetes, Synergistetes, and Proteobacteria. The closest match to phylotypes *Pontibacter sp.* (84% similarity) (OTU1) and *Coenonia sp.* (89% identity) (OTU2) were only detected in the $MgCl_2$-amended reactors with 3 to 13% band intensity. The closest match to phylotypes *Clostridium purinilyticum* (98% similarity) (OTU3) were detected in the 40 mM $CaCl_2$-amended reactors. The closest match to phylotypes *Clostridiisalibacter paucivorans* and *Tepidibacter mesophilus* (97% similarity) (OTU4) were detected only in the background control. The closest match to phylotypes *Cloacibacillus sp.* and *Thermanaerovibrio sp.* (91% similarity) (OTU5) were detected with the highest band intensity (59%) in the active control reactors without TAN addition and in other reactors except the 2.5 g TAN/L with 5 mM $MgCl_2$ and the background control. Phylotypes matching *Tepidanaerobacter sp.* (96% similarity) (OTU6) were detected in the $CaCl_2$-amended reactors, the 10 mM $MgCl_2$ reactors, and the no cation control reactors. Phylotypes matching *Thermanaerovibrio sp.* (91% similarity) (OTU7) were detected in all reactors except the 2.5 g TAN/L with 5 mM $MgCl_2$ and the background control, with the highest band intensity (31%) in the 20 mM $CaCl_2$-amended reactors (Fig. 5.5). At 5 g

TAN/L, phylotypes matching *Desulfotomaculum sp.* and *Thermanaerovibrio sp.* (89% similarity) (OTU1) were only detected in the $MgCl_2$-amended reactors and the 20 mM $CaCl_2$-amended reactors. Phylotypes matching *Tepidanaerobacter sp.* (84-99% similarity) (OTU2) were detected in the $MgCl_2$-amended, 40 mM $CaCl_2$-amended, and the no cation control reactors. Phylotypes matching *Desulfonauticus sp.* (89% similarity) (OTU3) were only detected in the active and background control reactors. Phylotypes matching *Thermanaerovibrio sp.* (89-92% similarity) (OTU4) were detected in all reactors except the background control reactors with the highest band intensity of 48% in the 40 mM $CaCl_2$-amended reactors. Overall, the 2.5 g TAN/L reactors with 5 mM $MgCl_2$, which had the highest methane production rate during day 136-184, had a different bacterial community than the $CaCl_2$-amended reactors, the no cation controls, the active control, and background control reactors. Of further note is the detection of phylotypes matching *Pontibacter sp.* and *Coenonia sp.*, albeit at relatively low abundance as determined by band intensity. A summary of bacterial DGGE 16S rRNA gene band identifications from the swine waste digestate inoculated reactors with cations addition at 2.5 and 5 g TAN/L is shown in Table 5.2.

Archaeal community analysis detected phylotypes of the phylum Euryarchaeota with Methanosarcinales as the major order in the 2.5 g TAN/L reactors, and the order Methanosarcinales and Methanomicrobiales in the 5 g TAN/L reactors, according to blast analysis using the NCBI database. The communities at 2.5 g TAN/L are shown in Fig. 5.8. All reactors revealed similar bands with only one dark band and some light bands in each lane. These bands were cut, and sequenced. At 2.5 g TAN/L, phylotypes matching *Methanoculleus sp.* (89% similarity) (OTU1) and *Methanoculleus* spp. (79% similarity)

(OTU2) were detected only in the $MgCl_2$-amended reactors. Phylotypes matching *Methanosarcina* spp. (85% similarity) (OTU3) were detected in most reactors except the active control reactors without TAN addition and the background control. Phylotypes matching *Methanosarcina* spp. (73% similarity) (OTU4) dominated in all reactors with high band intensity of 12-72% (Fig. 5.9). The archaeal communities at 5 g TAN/L are shown in Fig. 5.10. The $MgCl_2$- and $CaCl_2$-amended reactors indicated different band patterns. More bands were detected in the $MgCl_2$-amended reactors. However, darker bands were detected in the $CaCl_2$-amended reactors. The no cation control reactors indicated similar bands to the $MgCl_2$-amended reactors while the active control reactors without TAN addition indicated similar bands to the $CaCl_2$-amended reactors. The band intensity analysis revealed the dominance of phylotypes matching *Methanosarcina* spp. and *Methanoculleus* spp. at 5 g TAN/L (Fig. 5.11). Phylotypes matching *Methanoculleus* spp. (90% similarity) (OTU1) and *Methanoculleus* spp. (98% similarity) (OTU2) were detected in most reactors except the active control reactors without TAN addition and the background control. Phylotypes matching *Methanosarcina sp.* (90% similarity) (OTU3) were detected in the $CaCl_2$-amended and the active control reactors. Phylotypes matching *Methanosarcina* spp. (90% similarity) (OTU4) were detected in the $MgCl_2$–amended and the no cation control reactors with the band intensity of 32-54%. Phylotypes matching *Methanosarcina* spp. (93-98% similarity) (OTU5) were detected in the $CaCl_2$–amended and the active control reactors with the band intensity of 81-96%. Overall, the archaeal communities at 2.5 g TAN/L indicated the dominance of phylotypes matching *Methanosarcina* spp. whereas those at 5 g TAN/L indicated the dominance of phylotypes

matching *Methanoculleus* spp. in the $MgCl_2$–amended and the no cation control reactors; and *Methanosarcina* spp. in the $CaCl_2$–amended and the active control reactors.

5.5 Discussion

The results of this study indicate effects of cation addition to anaerobic reactors fed glutamate as the sole carbon and energy source and operated at high TAN. Addition of cation, especially magnesium (5 mM) can counteract ammonia inhibition at 2.5 g TAN/L. The methane production rate during 48 days of pseudo-steady state of the 5 mM $MgCl_2$-amended reactors at 2.5 g TAN/L were the highest and significantly different from other reactors ($p<0.05$). In addition, lower VFA accumulation was observed in these reactors compared to the no cation control rectors at the same TAN concentration (2.5 g TAN/L). The bacterial and archaeal communities were also monitored to determine how cations addition affected specific populations and changes in these communities enriched from swine waste digestate were also observed.

The results suggested that specific cations promoted methane production only at certain TAN concentrations. During the start-up phase, the advantages of cations were not clearly shown (Fig. 5.1). However, during 48 days of pseudo-steady state (days 136 to 184), the rate of methane production at 2.5 g TAN/L in the 5 mM $MgCl_2$-amended reactors were 17% higher than that of the no cation control reactors and 29% higher than that of the active control reactors without TAN addition (Table 5.1). This finding was supported by the previous studies that divalent cation such as Mg^{2+} is important for flocculation and microbial aggregation (Mahoney et al. 1987, Schmidt and Ahring 1993, Yu et al. 2001). Separate results also revealed that struvite precipitation that may cause

operational problems at both TAN concentrations that were operated, did not occur in these reactors. Addition of calcium (20 and 40 mM) in the reactors at 2.5 and 5 g TAN/L did not counteract ammonia inhibition since the methane production rate during 48 days of pseudo-steady state was not significantly different from the no cation control and the active control reactors without TAN addtion. Calcium has been reported to promote the methanogenic activity of granular sludge in different systems: 75-150 mg/L in an upflow anaerobic sludge blanket (UASB) system treating sewage sludge (Chang and Lin 2006); 150-300 mg/L in an UASB reactor treating synthetic wastewater (Yu et al. 2001); 500 and 1000 mg/L in an expanded granular sludge bed (EGSB) reactor treating leachate (Dang et al. 2014, Liu et al. 2011); and 3000 mg/L in mesophilic AD treating swine wastewater (Ahn et al. 2006b). However, these studies did not report the effects of calcium at high TAN concentrations. The results from our study, thus, indicated that calcium addition did not counteract methane production inhibition in these particular AD reactors operating at 2.5 and 5 g TAN/L.

VFA accumulation is an indicator of AD instability due to ammonia inhibition. The results revealed that addition of 5 mM $MgCl_2$ with 2.5 g TAN/L and 40 mm $CaCl_2$ with 5 g TAN/L appeared to alleviate ammonia toxicity as indicated by a more rapid decrease in acetate concentration compared to the no cation control reactors (Fig. 5.3). Even though cation addition resulted in higher propionate accumulation than the no cation control reactors, propionate in cation-amended reactors (Fig. 5.3A and 5.3C) was utilized within 135 days, similar to the no cation control reactors (Fig. 5.3B and 5.3D). Changes in VFA concentrations and methane production in the cation-amended reactors

classified into three peroids in section 5.4.3 can be explained as follows. Period 1 (day 0-58), accumulation of acetate and propionate in the cation-amended reactors may have been a result of a positive effect of cation addition on fermentative bacteria and propionate-oxidizing bacteria. Then acetate was utilized by acetotrophic methanogens causing methane production to increase. Period 2 (day 58-150) acetate in the $MgCl_2$-amended reactors increased, but was still less than the concentration detected in the no cation control reactors. On the other hand, acetate in the $CaCl_2$-amended reactors continuously decreased while that of the no cation control reactors increased dramatically. This may relate to the effectiveness of Ca^{2+} and Mg^{2+} ions in restoring activity of acetotrophic methanogens under ammonia stress. Nakakubo et al. (2008) reported that acetate-utilizing methanogens were sensitive to high ammonium, which results in lack of further transformation of VFAs ultimately to methane. Thus, addition of cation could provide advantages for aceticlastic methanogens at high TAN concentrations, especially addition of $CaCl_2$. Propionate concentration in cation-amended reactors decreased during this period, especially propionate in the $CaCl_2$-amended reactors which dramatically decreased from (25 ± 0.3 mmol/L) to non-detectable levels. Ahn et al. (2006a) reported previously that calcium supported propionate and *i*-valerate degraders and stimulated the turnover of longer chain acids. During period 3 (day 150-300), cations may have promoted hydrogenotrophic methanogenesis by encouraging H_2 and CO_2 consumption to produce methane, thus helped maintain low VFAs throughout the experimental period. The partial pressure of H_2 must be kept below 10^{-6} to 10^{-4} atm (0.1 to 10.1 Pa) for the oxidation of propionate to be thermodynamically favorable (see for

example, Fukuzaki et al. (1990) and Fennell and Gossett (1997)). During this period, both VFAs were maintained at low concentrations, indicating that hydrogen was also being utilized.

Microbial community shifts related to TAN concentration, VFAs, and methane production have been reported previously (Calli et al. 2005, Westerholm et al. 2011b). Gallert et al. (1998) reported that the toxic effects of ammonia may be diminished by acclimation or adaptation of the populations. In our study, the bacterial community shifted toward the phyla Firmicutes, Bacteroidetes, Synergistetes, and Proteobacteria. Bacterial community analysis indicated the dominance of phylotypes matching *Thermanaerovibrio sp.* in both 2.5 and 5 g TAN/L reactors, including the no cation control reactors. *T. acidaminovorans* is a moderately thermophilic, syntrophic, glutamate-degrading bacterium (Baena et al. 1999, Plugge and Stams 2001) previously studied in co-culture with the hydrogenotrophic methanogen *Methanobacterium thermoautotrophicum* Z245. Similary, phylotypes matching *Tepidanaerobacter* spp. (98-99% similarity) also dominated in both 2.5 and 5 g TAN/L reactors, including the no cation control reactors. *Tepidanaerobacter acetatoxydans* is an anaerobic, syntrophic acetate-oxidizing bacterium previously reported to be involved in the syntrophic acetate oxidation pathway when ammonium concentrations were in the range of 3-7 g NH_4^+-N/L (Schnurer et al. 1994, Schnurer and Nordberg 2008, Westerholm et al. 2011c). The presence of phylotypes matching *Thermanaerovibrio sp.* and *Tepidanaerobacter* spp. in the $MgCl_2$- and $CaCl_2$-amended reactors with 2.5 and 5 g TAN/L, including the no cation control reactors could suggest that addition of these cations may not affect bacterial community at high TAN. However, a few studies have shown positive calcium effects in AD systems. Calcium allowed microbe aggregates to form and developed inter-species

hydrogen and proton transfer (Yu et al. 2001). In addition, addition of calcium was reported to enhance sewage sludge microbiota granulation in an UASB system, thus elevating hydrogen production efficiency (Chang and Lin 2006). These studies were related to inter-species hydrogen transfer and hydrogen production in calcium-amended reactors but did not focus on high TAN concentrations. The results from our study, therefore, revealed new findings of cation effects in AD operated with high TAN concentrations.

A phylotype matching *Clostridium purinilyticum* (98% similarity) (OTU3) dominated in the 40 mM $CaCl_2$ reactors with 2.5 g TAN/L. Dang et al. (2014) indicated the dominance of class Clostridia in the expanded granular sludge bed (EGSB) reactor treating leachate at high calcium concentration of 2,000-7,000 mg/L. Additionally, Clostridia dominated in two-stage AD treating food waste leachate containing a high concentration of VFAs (4,900 mg/L in methanogenic reactor and 3,100 mg/L in stabilizing reactor) (Kim et al. 2014). The result from our study indicated that high propionate concentration (1,850 ± 77 mg/L or 25 ± 0.3 mmol/L) was detected in a reactor with a phylotype matching *Clostridium purinilyticum*. Furthermore, members of the class Clostridia obtain energy by fermenting amino acids and have been known as hydrogen producers supplying hydrogen as a substrate to hydrogenotrophic methanogens (Kim et al. 2014, Madigan and Martinko 2006). These findings suggested that reactors with calcium addition (40 mM) may proceed through hydrogenotrophic methanogenesis.

Archaeal community analysis revealed Euryarchaeota as the only dominant phylum. Acclimatization to high ammonia concentrations was previously reported to

result in lower Archaea diversity (Fotidis et al. 2013). Westerholm et al. (2012) reported that phylotypes matching *Methanosarcina* spp., most often known as aceticlastic methanogens, may also act as hydrogenotrophic methanogens during the SAO pathway at high TAN concentration. Indeed it is known that most *Methanosarcina* spp. can use acetate as well as hydrogen as direct substrates for methanogenesis (Hao et al. 2011). Our finding that phylotypes from the order Methanosarcinales dominated in 2.5 and 5 g TAN/L reactors, thus suggests that the pathway could have switched to hydrogen-based methane production under ammonia stress. In addition, at 5 g TAN/L phyloptypes matching *Methanosarcina* spp. (93-98% similarity) (OTU5) had the highest band intensity in the $CaCl_2$-amended reactors similar to what was detected in the active control reactors without TAN addition, whereas phylotypes matching *Methanosarcina* spp. (90% similarity) (OTU4) showed the highest band intensity in the $MgCl_2$-amended reactors, suggesting a different selective effect for the two cations (Fig. 5.11 and Table 5.3). The presence of phlotypes matching *Methanosarcina* spp. (OTU5) in both the $CaCl_2$-amended reactors and the active control reactors with a decrease of acetate concentration in the $CaCl_2$-amended reactors compared to others suggest that addition of $CaCl_2$ resulted in the presence of *Methanosarcina* spp. that consume acetate at high TAN concentrations. In addition, phylotypes matching *Methanoculleus* spp. (90-98% similarity) was only detected in the 5 g TAN/L reactors with higher band intensity in the $MgCl_2$-amended reactors than the $CaCl_2$-amended reactors (Fig. 5.11). Maus et al. (2012) reported that Mg^{2+} led to enrichment of phylotypes matching *Methanoculleus* spp.—hydrogenotrophic methanogens found to be well adapted in biogas communities encountering high salt and

ammonia. This was also indicated in our results since no phylotypes matching *Methanoculleus* spp. were detected in the active control without TAN addition.

Overall, the dominance of phylotypes matching *Methanosarcina* spp. in our study with addition of Mg^{2+} and Ca^{2+} revealed the importance of these methanogens to counteract ammonia toxicity. Ahring et al. (1991) suggested that 30 mM of Mg^{2+} should be present for the growth of the thermophilic *Methanosarcina thermophile* TM-1. Schmidt and Ahring (1993) concluded that Mg^{2+} concentrations of 0.5-10 mM resulted in a better performance of the Methanosarcinae-dominated granules in thermophilic UASB reactors fed acetate. However, these studies did not specify TAN concentration in the reactors. In our study, after exposure up to 5 g TAN/L for 200 days, a shift from aceticlastic methanogenesis (period 1) to syntrophic acetate oxidation (coupled to hydrogenotrophic methanogenesis) (period 3) may have occurred as has been reported previously (Schnurer and Nordberg 2008).

Table 5.1 Target and actual total ammonia nitrogen concentration (TAN), methane production rate, and % increase of methane production rate from active and no cation control

	Target TAN (g N/L)	**Actual TAN[A] (g N/L)**	**Methane Production Rate [B] (mmol/week)**	**% Increase of Methane Production Rate from Active Control**	**% Increase of Methane Production Rate from No Cation Control**
5 mM $MgCl_2$	2.5	2.95 ± 0.05	1.93 ± 0.03^{d}	29.11	16.9
	5	4.30 ± 0.03	1.75 ± 0.03^{cd}	17.41	6.8
10 mM $MgCl_2$	2.5	2.89 ± 0.18	1.70 ± 0.02^{bc}	13.64	2.9
	5	4.22 ± 0.02	1.64 ± 0.03^{abc}	9.63	-0.3
20 mM $CaCl_2$	2.5	3.04 ± 0.03	1.59 ± 0.02^{abc}	6.56	-3.5
	5	3.35 ± 0.62	1.50 ± 0.02^{ab}	0.11	-9.0
40 mM $CaCl_2$	2.5	3.06 ± 0.08	1.51 ± 0.01^{ab}	0.93	-8.6
	5	4.06 ± 0.004	1.47 ± 0.02^{a}	-1.93	-10.8
No cation	2.5	2.85 ± 2.04	1.65 ± 0.03^{abc}	10.48	0
	5	4.30 ± 0.02	1.64 ± 0.03^{abc}	9.98	0
Active control	-	1.35 ± 0.006	1.49 ± 0.02^{ab}	0	-9.1

[A]Data from day 298

[B]Data from day 136-184 (48 days during pseudo-steady state)

$^{a, b, c, d}$ represent statistically significant difference at the 95% level of confidence ($p<0.05$)

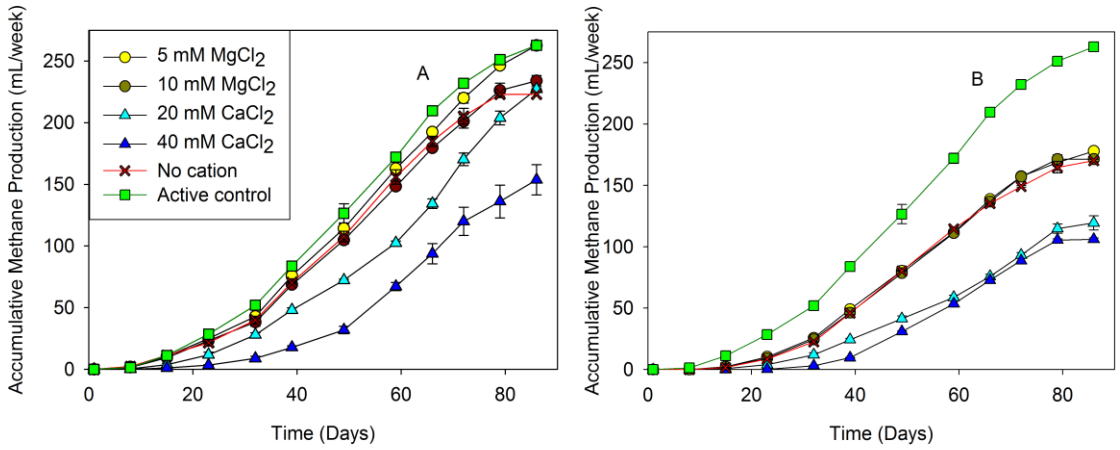

Fig. 5.1 Accumulated methane production from swine waste digestate inoculated reactors with cation addition at target 2.5 g TAN/L (A) and 5 g TAN/L (B). Symbols are averages of triplicates and error bars are ± one standard deviation.

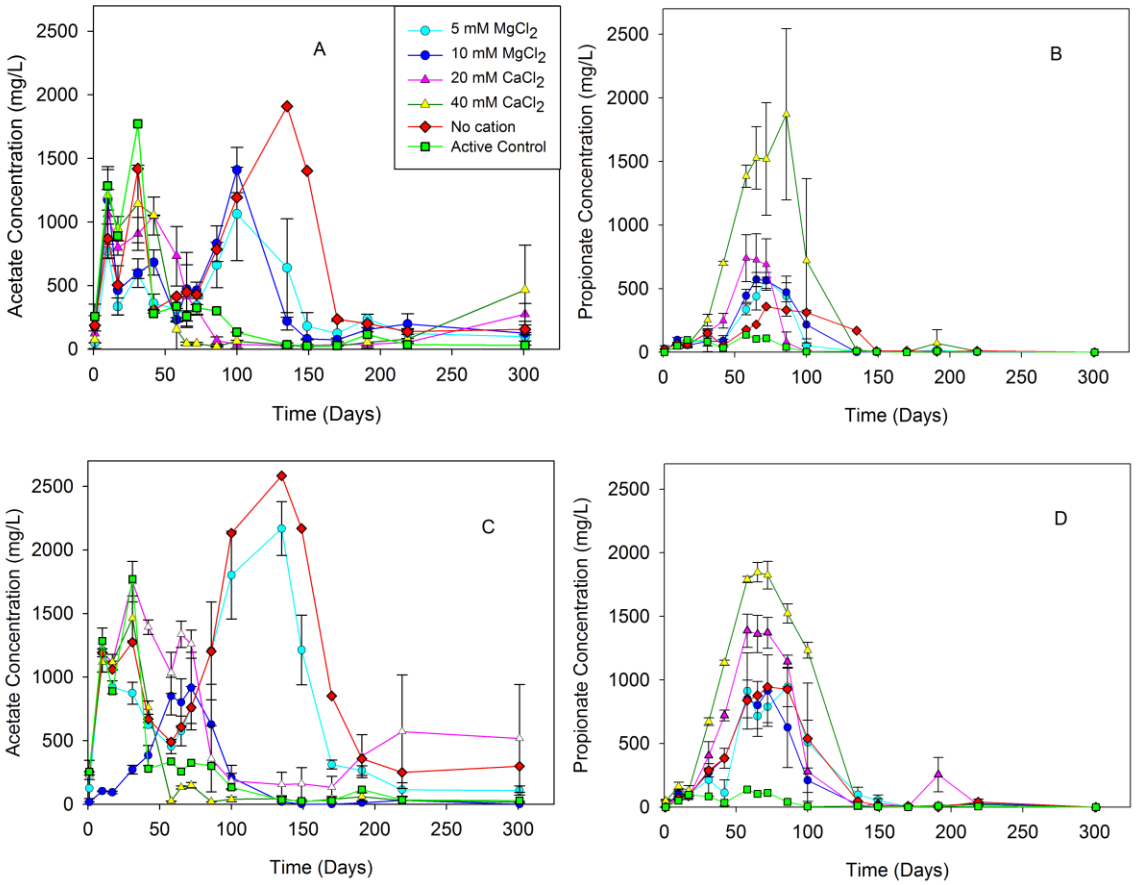

Fig. 5.2 Acetate (A) and propionate (B) concentration from swine waste digestate inoculated reactors with cation addition at target 2.5 g TAN/L; and acetate (C) and propionate (D) concentration from reactors at target 5 g TAN/L. Symbols are averages of triplicates and error bars are ± one standard deviation.

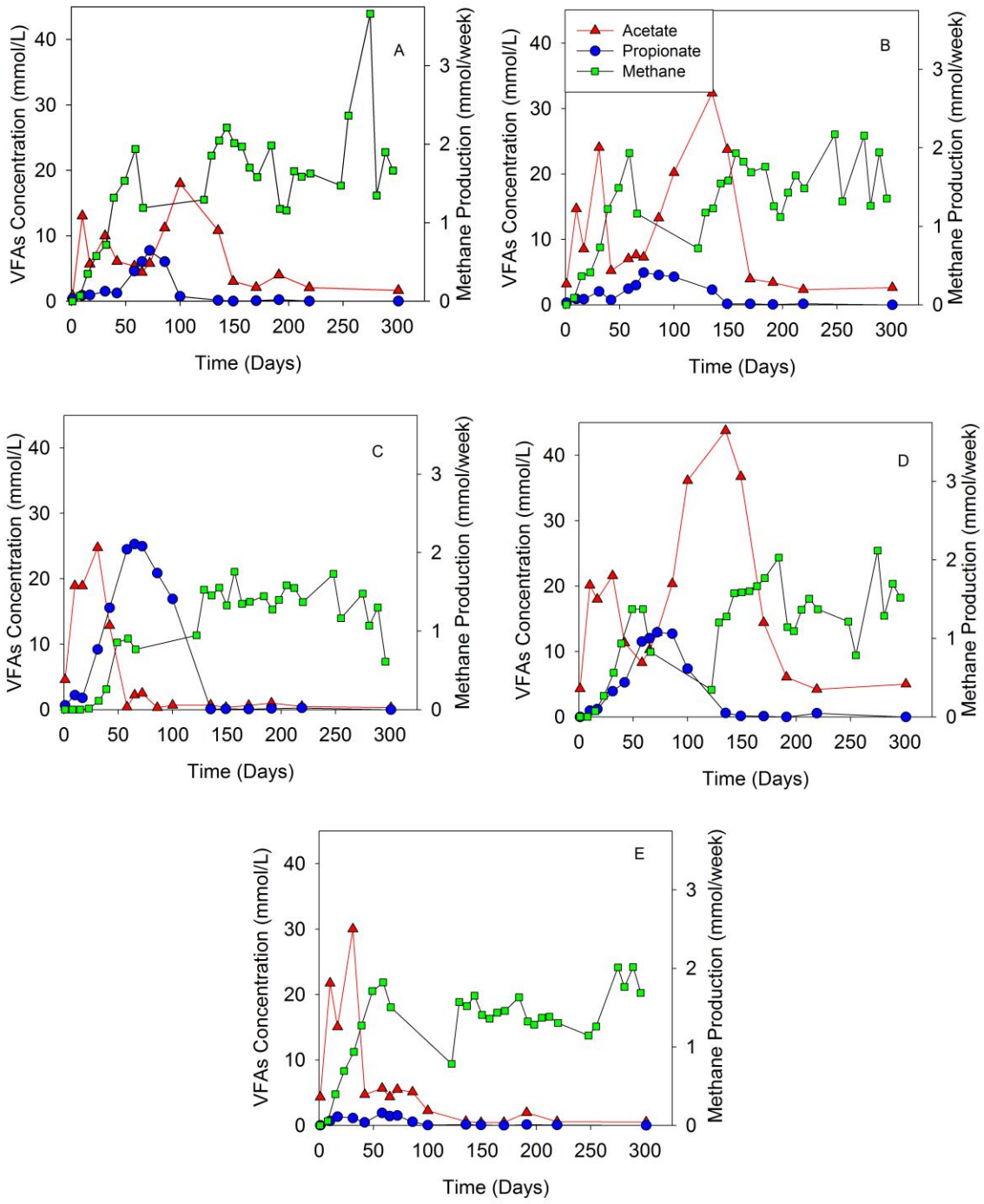

Fig. 5.3 The relationships between methane and VFAs in swine waste digestate inoculated reactors at target 2.5 g TAN/L with 5 mM $MgCl_2$ (A); no cation control (B); at target 5 g TAN/L with 40 mM $CaCl_2$ (C); no cation control (D); and active control without TAN addition (E). Symbols are average values of triplicates.

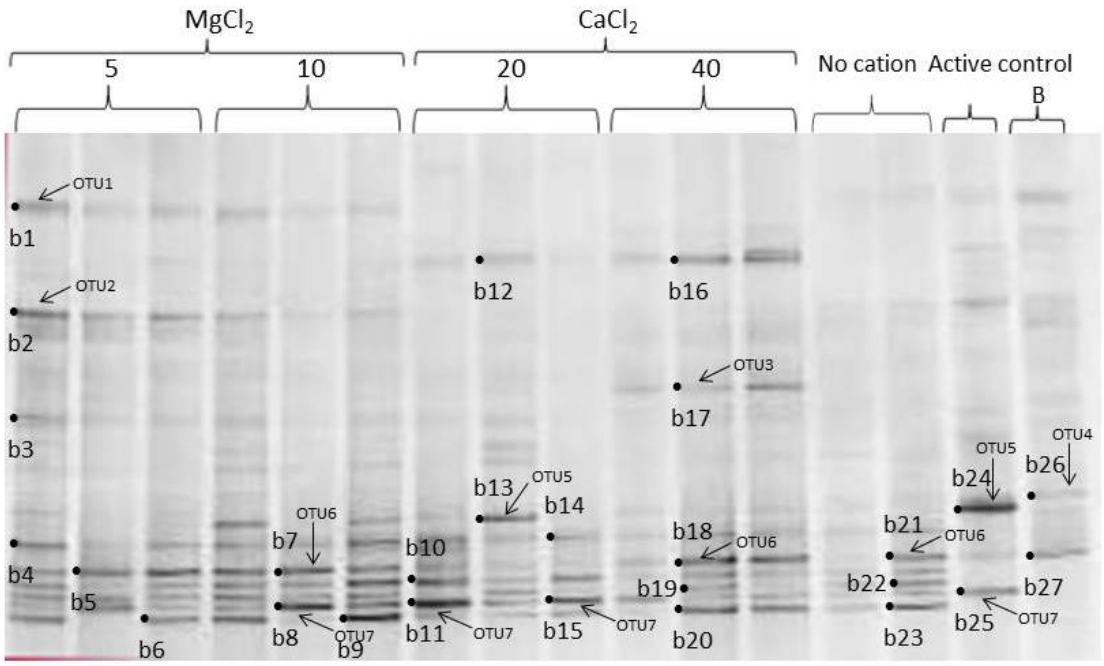

Fig. 5.4 Bacterial DGGE profiles of the 16S rRNA gene PCR products amplified from DNA extracted from swine waste digestate inoculated reactors with cation addition at target 2.5 g TAN/L day 191. Lanes are labelled with TAN concentrations (g TAN/L); lane B indicates the DGGE profile of background reactor (inoculum and medium). Dots and numbers indicate the bands sequenced.

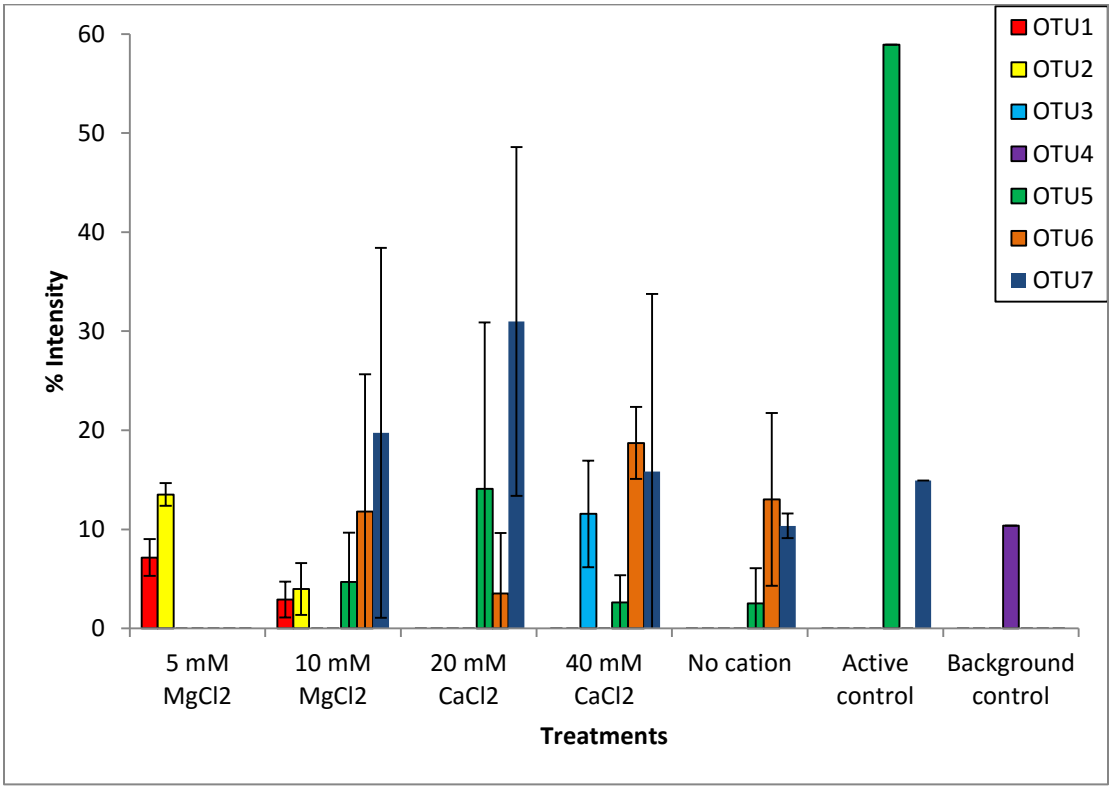

Fig. 5.5 The bacterial DGGE band intensity for selected bands from swine waste digestate inoculated reactors with cation addition at target 2.5 g TAN/L. Bars are averages and error bars are one standard deviation of the % of the total band intensity from triplicate DGGE lanes. The matches to specific phylotypes are: OTU1-*Pontibacter sp.*; OTU2- *Coenonia sp.*; OTU3- *Clostridium purinilyticum*; OTU4- *Clostridiisalibacter paucivorans, Tepidibacter mesophilus*; OTU5- *Cloacibacillus sp., Thermanaerovibrio sp.*; OTU6- *Tepidanaerobacter* spp.; and OTU7- *Thermanaerovibrio sp.*

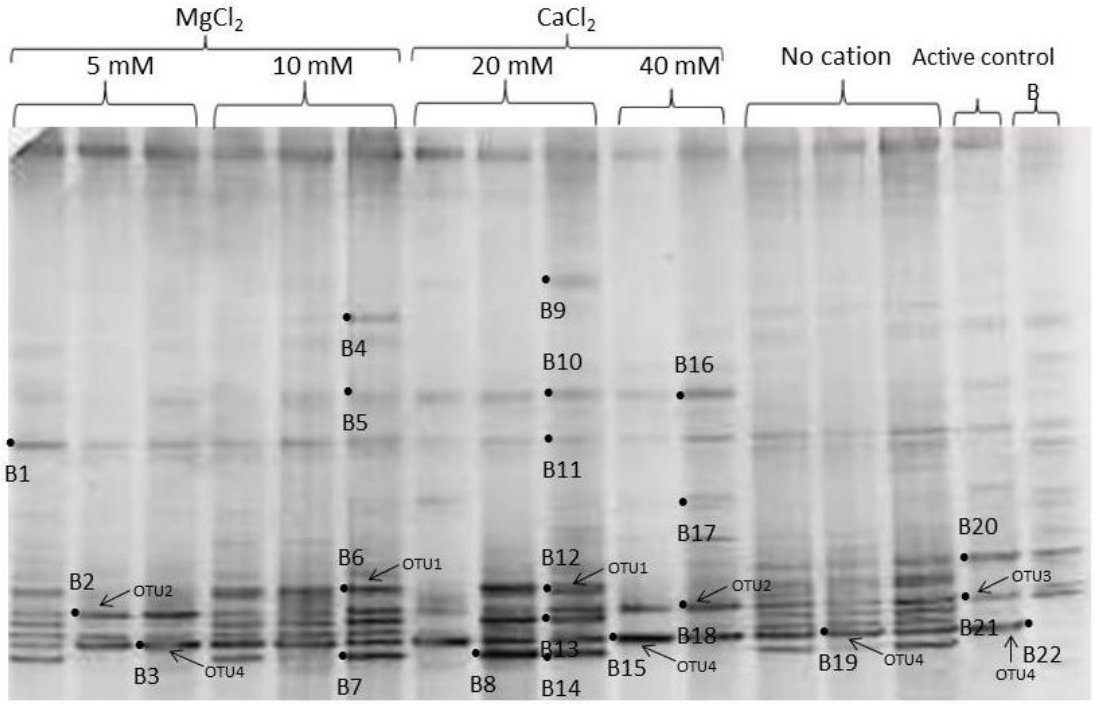

Fig. 5.6 Bacterial DGGE profiles of the 16S rRNA gene PCR products amplified from DNA extracted from swine waste digestate inoculated reactors with cation addition at target 5 g TAN/L day 191. Lanes are labelled with TAN concentrations (g TAN/L); lane B indicates the DGGE profile of background reactor (inoculum and medium). Dots and numbers indicate the bands sequenced.

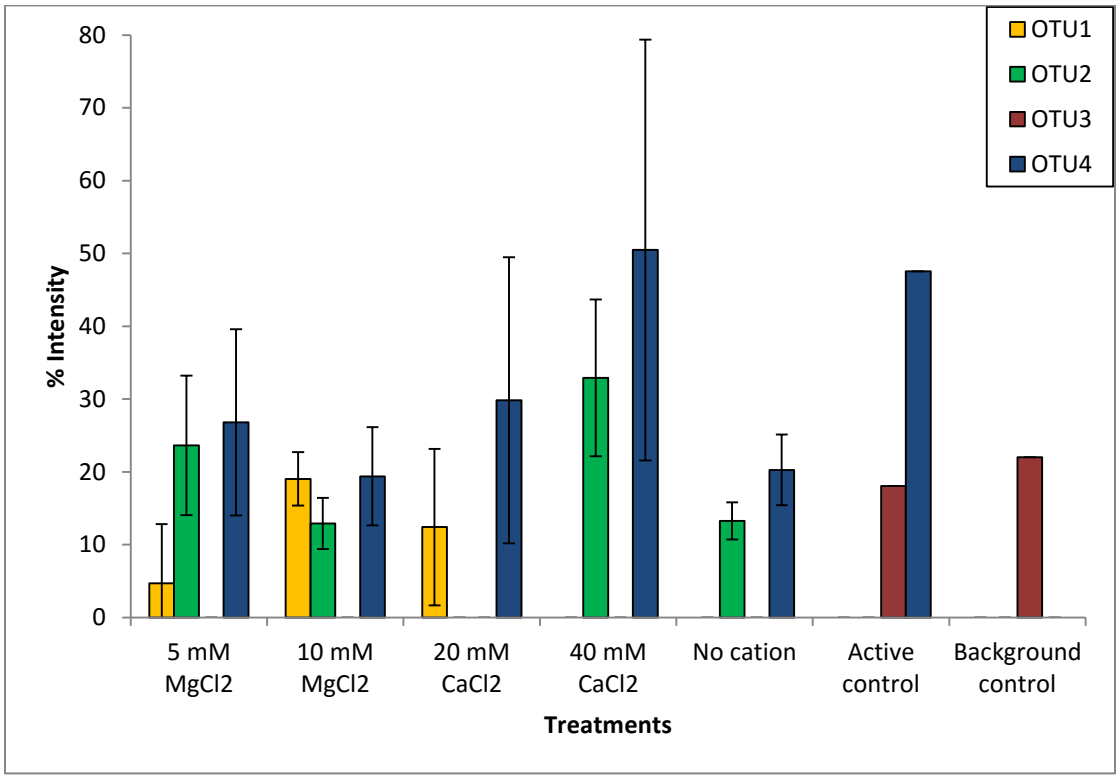

Fig. 5.7 The bacterial DGGE band intensity for selected bands from swine waste digestate inoculated reactors with cation addition at target 5 g TAN/L. Bars are averages and error bars are one standard deviation of the % of the total band intensity from triplicate DGGE lanes. The matches to specific phylotypes are: OTU1- *Desulfotomaculum sp.*, *Thermanaerovibrio sp.*; OTU2- *Tepidanaerobacter acetatoxydans*; OTU3- *Desulfonauticus sp.*; and OTU4- *Thermanaerovibrio sp.*

Table 5.2 Bacterial DGGE 16S rRNA gene band identifications from swine waste digestate inoculated reactors with cation addition at target 2.5 and 5 g TAN/L

DGGE band	Closest match	Identity (%)	Phyla	Closest match Accession no.
Target TAN 2.5 g N/L				
b1	*Pontibacter sp.*	84	Bacteroidetes	NR_109634.1
b2	*Coenonia sp.*	89	Bacteroidetes	NR_029353.1
b3	*Thermogemmatispora* spp.	88	Chloroflexi	NR_113127.1
b4	*Aminomonas sp.*	82	Firmicutes	NR_114458.1
b5	*Bacillus sp.*	95	Firmicutes	NR_074988.1
b6	*Thermanaerovibrio sp.*	91	Firmicutes	NR_074520.1
b7	*Tepidanaerobacter acetatoxydans*	100	Firmicutes	NR_074537.1
b8	*Thermanaerovibrio sp.*	91	Firmicutes	NR_074520.1
b9	*Thermanaerovibrio sp.*	92	Firmicutes	NR_074520.1
b10	*Thermanaerovibrio sp.*	90	Firmicutes	NR_074520.1
b11	*Thermanaerovibrio sp.*	91	Firmicutes	NR_074520.1
b12	*Bacteroides* spp.	92	Bacteroidetes	NR_112945.1
b13	*Cloacibacillus sp.*	90	Synergistetes	NR_115465.1
b14	*Thermanaerovibrio sp.*	91	Firmicutes	NR_074520.1
b15	*Thermanaerovibrio sp.*	91	Firmicutes	NR_074520.1
b16	*Bacteroides* spp.	91	Bacteroidetes	NR_112945.1
b17	*Clostridium purinilyticum*	98	Firmicutes	NR_117121.1
b18	*Tepidanaerobacter sp.*	96	Firmicutes	NR_074537.1
b19	*Thermanaerovibrio sp.*	89	Firmicutes	NR_104765.1
b20	*Thermanaerovibrio sp.*	92	Firmicutes	NR_074520.1

DGGE band	Closest match	Identity (%)	Phyla	Closest match Accession no.
b21	*Tepidanaerobacter* spp.	98	Firmicutes	NR_074537.1
b22	*Anaerobaculum sp.*	95	Synergistetes	NR_102954.1
	Acetomicrobium sp.	95	Bacteroidetes	NR_104752.1
b23	*Thermanaerovibrio* spp.	89	Firmicutes	NR_074520.1
b24	*Cloacibacillus sp.*	91	Synergistetes	NR_115465.1
	Thermanaerovibrio sp.	91	Firmicutes	NR_104765.1
b25	*Thermanaerovibrio sp.*	91	Firmicutes	NR_074520.1
b26	*Clostridiisalibacter paucivorans*	97	Firmicutes	NR_044043.1
	Alkaliphilus spp.	97	Firmicutes	NR_074435.1
	Brassicibacter mesophilus	97	Firmicutes	NR_108841.1
	[Clostridium] litorale	97	Firmicutes	NR_029270.1
	Tepidibacter mesophilus	97	Firmicutes	NR_108539.1
b27	*Clostridium* spp.	100	Firmicutes	NR_044841.2
Target TAN 5 g N/L				
B1	*Capnocytophaga sp.*	81	Bacteroidetes	NR_074409.1
B2	*Tepidanaerobacter sp.*	84	Firmicutes	NR_074537.1
B3	*Thermanaerovibrio sp.*	87	Firmicutes	NR_074520.1
B4	*Desulfotomaculum sp.*	84	Firmicutes	NR_026348.1
B5	*Thermanaerovibrio sp.*	91	Firmicutes	NR_074520.1
B6	*Desulfotomaculum sp.*	89	Firmicutes	NR_117747.1
	Thermanaerovibrio sp.	89	Firmicutes	NR_074520.1
B7	*Thermanaerovibrio sp.*	92	Firmicutes	NR_074520.1
B8	*Thermanaerovibrio sp.*	92	Firmicutes	NR_074520.1

DGGE band	Closest match	Identity (%)	Phyla	Closest match Accession no.
B9	*Acidobacterium sp.*	78	Acidobacteria	NR_074106.1
	Microvirga sp.	78	Proteobacteria	NR_114298.1
B10	*Thermus sp.*	83	Deinococcus-Thermus	NR_102473.1
	Oceanithermus sp.	83	Deinococcus-Thermus	NR_074604.1
	Marinithermus sp.	83	Deinococcus-Thermus	NR_074587.1
B11	*Mucilaginibacter sp.*	74	Bacteroidetes	NR_118395.1
	Pedobacter sp.	74	Bacteroidetes	NR_118090.1
B12	*Thermanaerovibrio sp.*	92	Firmicutes	NR_074520.1
B13	*Thermanaerovibrio sp.*	86	Firmicutes	NR_074520.1
B14	*Thermanaerovibrio* spp.	92	Firmicutes	NR_074520.1
B15	*Thermanaerovibrio sp.*	92	Firmicutes	NR_074520.1
B16	*Bradyrhizobium sp.*	85	Proteobacteria	NR_119191.1
	Rhizobium sp.	85	Proteobacteria	NR_044869.2
B17	*Desulfovibrio* spp.	98	Proteobacteria	NR_121705.1
B18	*Tepidanaerobacter acetatoxydans*	99	Firmicutes	NR_074537.1
B19	*Thermanaerovibrio sp.*	92	Firmicutes	NR_074520.1
B20	*Synergistes sp.*	88	Synergistetes	NR_044616.1
B21	*Desulfonauticus sp.*	89	Proteobacteria	NR_044591.1
B22	*Thermanaerovibrio sp.*	92	Firmicutes	NR_074520.1

b24, b25, B20, B21, B22 - Active control

b26, b27 - Background control

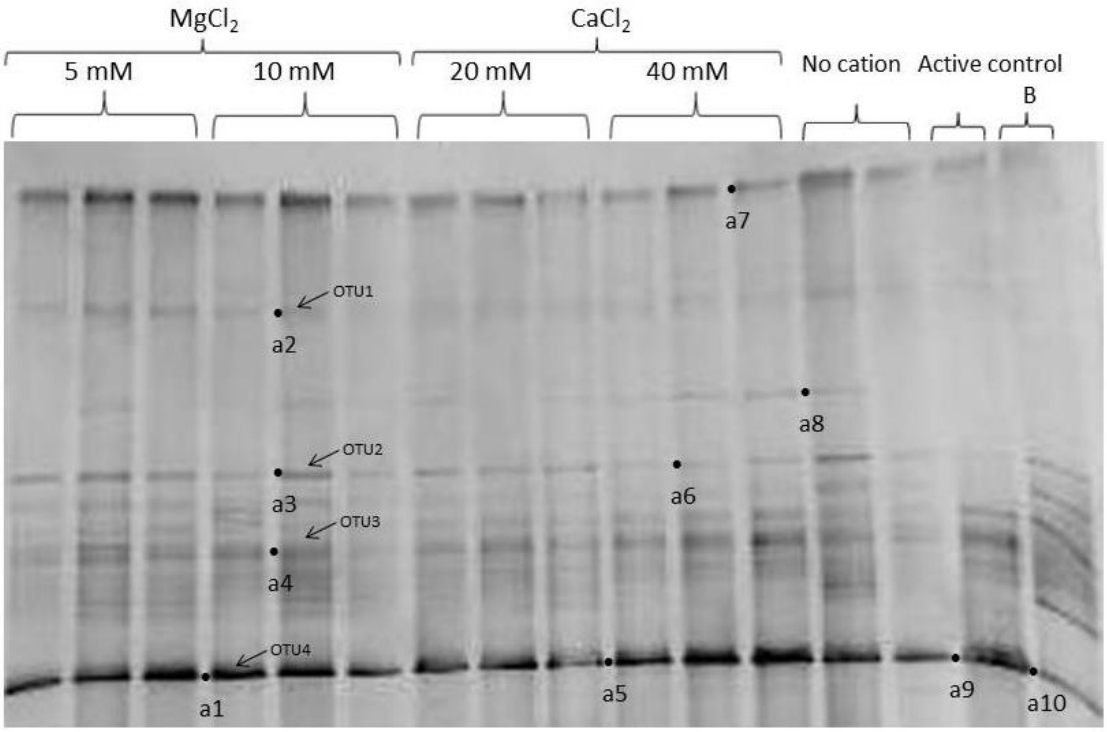

Fig. 5.8 Archaeal DGGE profiles of the 16S rRNA gene PCR products amplified from DNA extracted from swine waste digestate inoculated reactors with cation addition at target 2.5 g TAN/L day 191. Lanes are labelled with TAN concentrations (g TAN/L); lane B indicates the DGGE profile of background reactor (inoculum and medium). Dots and numbers indicate the bands sequenced.

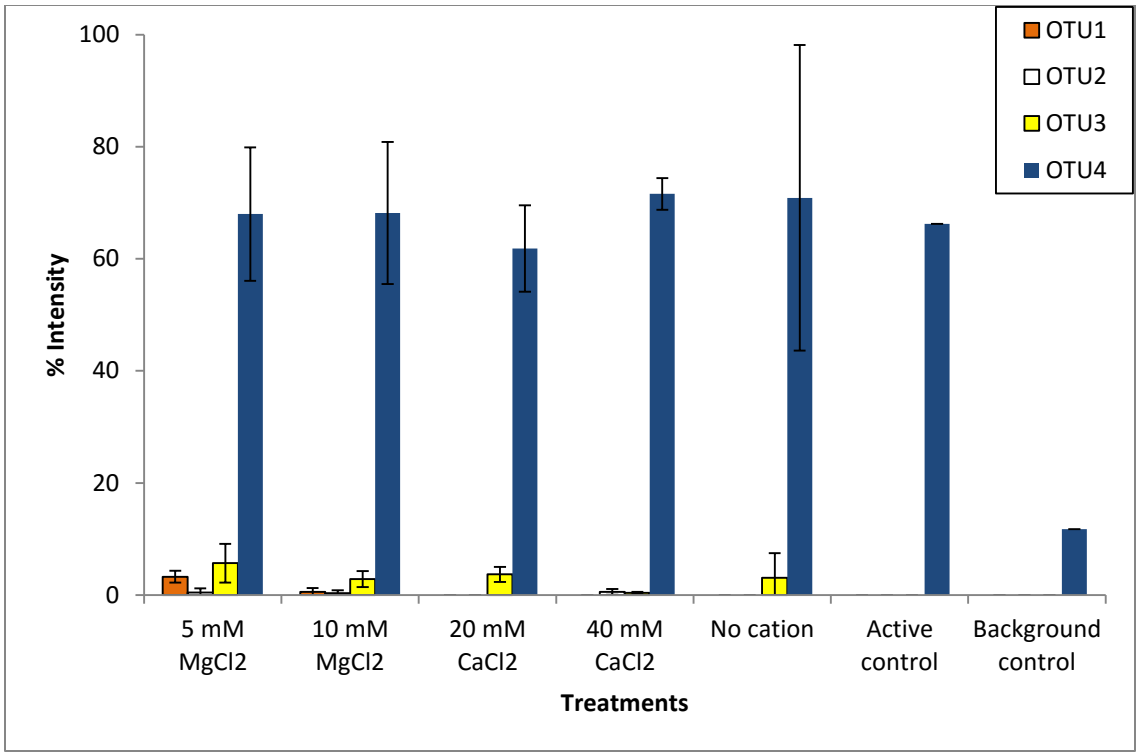

Fig. 5.9 The archaeal DGGE band intensity from swine waste digestate inoculated reactors with cation addition at target 2.5 g TAN/L. Bars are averages and error bars are one standard deviation of the % of the total band intensity from triplicate DGGE lanes. The matches to specific phylotypes are: OTU1- *Methanoculleus sp.*; OTU2- *Methanoculleus* spp.; OTU3- *Methanosarcina* spp.; and OTU4- *Methanosarcina* spp.

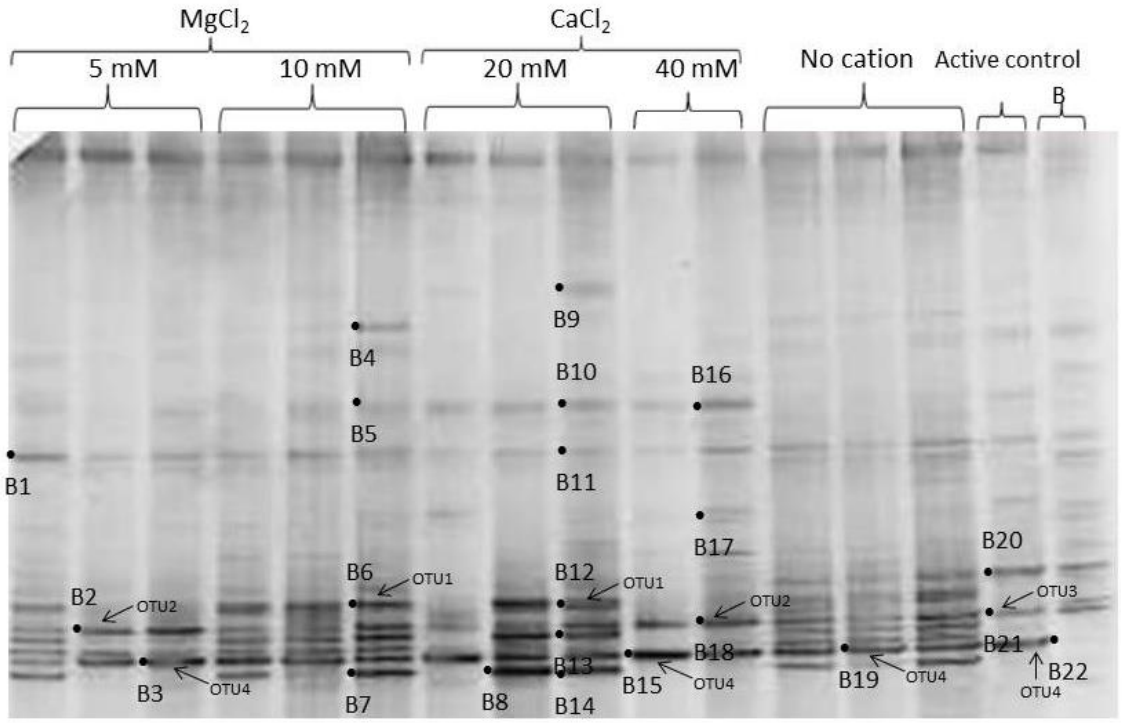

Fig. 5.10 Archaeal DGGE profiles of the 16S rRNA gene PCR products amplified from DNA extracted from swine waste digestate inoculated reactors with cation addition at target 5 g TAN/L day 191. Lanes are labelled with TAN concentrations (g TAN/L); lane B indicates the DGGE profile of background reactor (inoculum and medium). Dots and numbers indicate the bands sequenced.

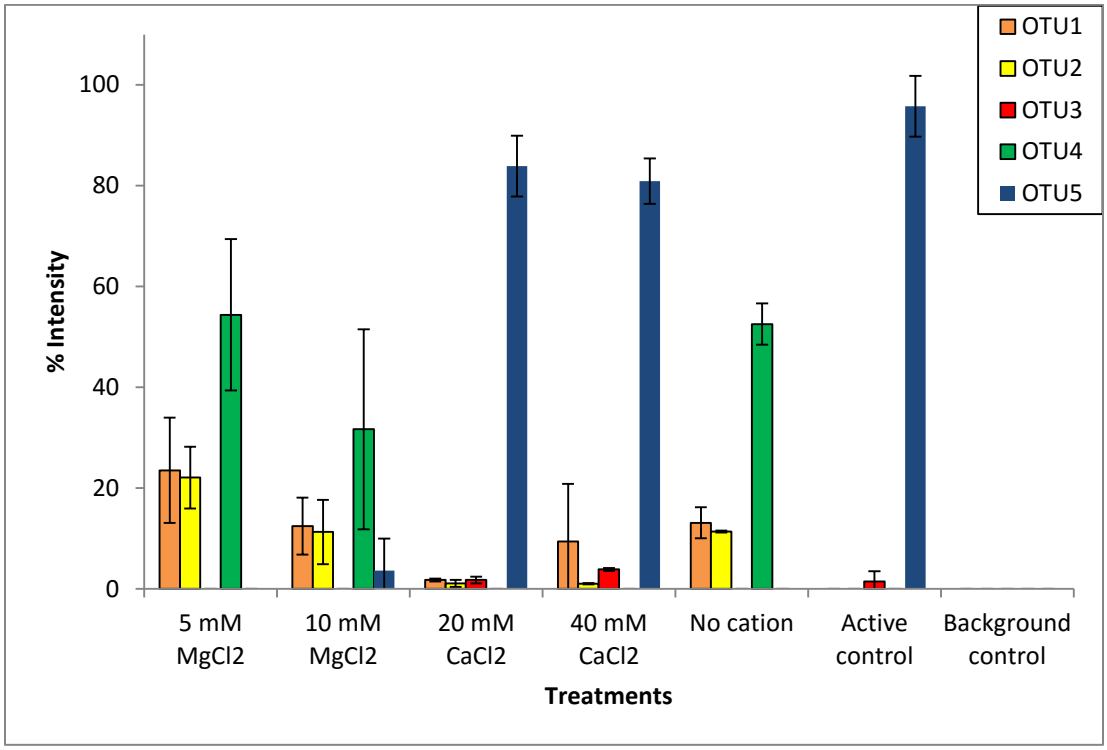

Fig. 5.11 The archaeal DGGE band intensity from swine waste digestate inoculated reactors with cation addition at target 5 g TAN/L. Bars are averages and error bars are one standard deviation of the % of the total band intensity from triplicate DGGE lanes. OTUs represent each of these phylotypes: OTU1- *Methanoculleus* spp.; OTU2- *Methanoculleus* spp.; OTU3- *Methanosarcina sp.*; OTU4- *Methanosarcina* spp.; and OTU5- *Methanosarcina* spp.

Table 5.3 Archaeal DGGE 16S rRNA gene band identifications from swine waste digestate inoculated reactors with cation addition at target 2.5 and 5 g TAN/L

DGGE band	Closest match	Identity (%)	Phyla	Closest match Accession no.
Target TAN 2.5 g N/L				
a1	*Methanosarcina* spp.	73	Euryarchaeota	NR_074221.1
a2	*Methanoculleus sp.*	89	Euryarchaeota	NR_028156.1
a3	*Methanoculleus* spp.	79	Euryarchaeota	NR_042786.1
a4	*Methanosarcina* spp.	85	Euryarchaeota	NR_074221.1
a5	*Methanosarcina* spp.	92	Euryarchaeota	NR_074221.1
a6	*Methanosarcina* spp.	95	Euryarchaeota	NR_074221.1
a7	*Methanoculleus* spp.	93	Euryarchaeota	NR_043961.1
a8	*Methanoculleus* spp.	87	Euryarchaeota	NR_042786.1
a9	*Methanosarcina* spp.	99	Euryarchaeota	NR_074221.1
a10	*Methanoculleus* spp.	90	Euryarchaeota	NR_042786.1
Target TAN 5 g N/L				
A1	*Methanoculleus* spp.	90	Euryarchaeota	NR_042786.1
A2	*Methanoculleus* spp.	98	Euryarchaeota	NR_043961.1
A3	*Methanosarcina* spp.	98	Euryarchaeota	NR_104757.1
A4	*Methanosarcina* spp.	94	Euryarchaeota	NR_074221.1
A5	*Methanoculleus sp.*	96	Euryarchaeota	NR_042786.1
A6	*Methanosarcina sp.*	96	Euryarchaeota	NR_074221.1
A7	*Methanoculleus* spp.	90	Euryarchaeota	NR_042786.1
A8	*Methanosarcina* spp.	95	Euryarchaeota	NR_104757.1
A9	*Methanosarcina* spp.	92	Euryarchaeota	NR_104757.1
A10	*Methanosarcina* spp.	85	Euryarchaeota	NR_104757.1
A11	*Methanosarcina* spp.	98	Euryarchaeota	NR_074221.1
A12	*Methanoculleus sp.*	88	Euryarchaeota	NR_042786.1
A13	*Methanosarcina* spp.	93	Euryarchaeota	NR_074221.1

DGGE band	Closest match	Identity (%)	Phyla	Closest match Accession no.
A14	*Methanosarcina* spp.	90	Euryarchaeota	NR_074221.1
A15	*Methanosarcina* spp.	90	Euryarchaeota	NR_104757.1
A16	*Methanosarcina* spp.	95	Euryarchaeota	NR_074221.1

a9, A16 – Active control

a10 – Background control

Chapter 6 Conclusions and Environmental Implications

6.1 Conclusions

Bioprocessing strategies for wastes, including anaerobic digestion (AD) have long been established, however there is an ever-increasing trend to improve this technology to reduce dependency on fossil fuels and decrease environmental pollution. These bioprocesses can provide bioenergy or valuable chemicals through strategies such as biological methane production from industrial and agricultural wastes, biological hydrogen production, biological electricity production, and biological chemical production (Angenent et al. 2004).

Biogas produced from the AD process represents a substantial potential source of renewable energy, which could fill the gap as fossil fuel use diminishes. AD research has been focused on how to optimize the process in order to achieve efficient and reliable waste-to-energy schemes. Waste composition has been known to limit the capacity and performance of AD. Anaerobic microorganisms have relatively slow growth rates (Rittmann and McCarty 2001) and long periods of time may be needed for acclimation to changing environments, operational parameters, or substrate variability. For stable operation, AD therefore requires a continuous feedstock supply that is maintained at a relatively constant makeup. Challenge for anaerobic treatment of high nitrogen wastes is of particular concern because the ammonia released during organic matter degradation may become an environmental pollutant or an inhibitor of the microbial process. To prevent ammonia toxicity, operators of AD often blend high N wastes with low N wastes to prevent accumulation of high ammonia/ammonium concentrations in the reactors

(Drennan and DiStefano 2014, Parameswaran and Rittmann 2012). To achieve the most efficient and optimal use of feedstocks for AD, it may be unrealistic to import high C:N feedstocks to blend with local low C:N feedstocks to facilitate more stable low ammonia concentration AD. Further, production of digestate with higher ammonia/ammonium concentrations could allow more effective use of this valuable resource. A recent theoretical study showed that at AD feedstock C:N ratio of 17 (corresponding to >2 g TAN/L in the digester), the energy output from a combined Anaerobic Digestion-Bioammonia to Hydrogen (ADBH) system where ammonia was captured and converted to hydrogen gas was greater than AD generating methane alone (Babson et al. 2013). These issues raise the idea of how to optimize an AD reactor treating high-N wastes. Stable AD operation at high ammonia concentrations scould be applied for capturing biologically-produced ammonia to use directly as an energy or fertilizer source; or, to crack to produce hydrogen, as an alternative renewable energy. To operate AD using high nitrogen feedstocks, more information is needed about microbial communities that can tolerant the resulting high soluble TAN in the digester environment.

The research activities described in this dissertation aimed to enrich and identify microbial communities (bacteria and archaea) from a variety of anaerobic systems that are tolerant to high ammonia concentrations. Sources of inoculum were digestate from anaerobic digesters containing relatively different TAN concentrations. Landfill leachate from two sites—New Jersey and Thailand—were investigated for presence of ammonia-tolerant microbes as summarized in Chapter 3. In Chapter 4 an investigation of swine waste digestate as inoculum for ammonia tolerant microbial communities was presented.

In all cases, the microbial community was challenged by poising the prevailing TAN concentrations at up to 12.5 g TAN/L. Chapter 5 focused on the effects of the addition of divalent cations, Mg^{2+} and Ca^{2+}, previously shown to alleviate ammonia stress, on swine waste digestate inoculated reactors operated under TAN concentrations at up to 12.5 g TAN/L. These studies have shown interesting findings related to reactor performance and microbial community shifts that occurred under ammonia stressed conditions.

Reactor stability and response to high TAN concentrations for each anaerobic inoculum source is summarized in sections 6.1.1-6.1.6.

6.1.1 Free ammonia (NH_3-N)

It has been known that toxicity of ammonia leads to reactor failure through inhibition of one or more microbial groups important in AD. Free ammonia plays an important role in inhibition of anaerobic reactors. Our study indicated that reactors enriched at high TAN concentrations and maintained for over 300 days did not show significant ($P<0.05$) increases in NH_3-N concentration with increasing TAN at neutral pH. At a target TAN of up to 12.5 g TAN/L (actual concentrations 11.1 to 11.9 g TAN/L), free ammonia was calculated to be 0.2 g NH_3-N/L in most reactors using Equation 2.12 (see Table 3.2, 4.3, 4.5). However, the reactors with 7.5 g TAN/L inoculated with New Jersey leachate and swine waste digestate from the second set of treatments significantly increased NH_3-N concentration with increasing TAN ($P<0.05$). It was reported in previous studies that free ammonia at 0.2 g NH_3-N/L is a threshold value for ammonia inhibition (Angelidaki and Ahring 1993, Gallert and Winter 1997, Koster and Lettinga 1984, McCarty and McKinney 1961). This finding suggested that our systems were indeed operated under free ammonia stress conditions, but that increasing

TAN was not necessarily uniformly increasing the free ammonia concentration in our reactors because of variability in prevailing reactor pH. In addition, Nakakubo et al. (2008) indicated that TAN was a more important factor than free ammonia in affecting the methanogenic activity of a well-acclimatized bacterial system. Our findings also supported this fact as evidenced from low reactor stability at high TAN concentrations, despite the relatively constant level of corresponding free ammonia in some instances.

6.1.2 Methane production

High TAN concentrations (> 5 g TAN/L) resulted in inhibition of methanogenesis, and a longer start-up phase was detected in all inocula. The source of the inocula greatly affected the ultimate methane production from the primary substrate (the model amino acid, glutamate). Thailand leachate inoculum resulted in enrichments with near-stoichiometric methane production similar to controls, even at a target 12.5 TAN/L (actual 11.4 g TAN/L), which produced 80% of methane of the active control. In contrast, the New Jersey leachate enrichments that were operated at target 5 g TAN/L, were the only ones to produce as much methane as the active control. Higher TAN concentrations exerted severe inhibition of methanogenesis relative to the control. Swine waste digestate inoculated reactors were set up in two sets- the first reactor set with target 0.5 to 5 g TAN/L and the second reactor set with target 5 to 12.5 g TAN/L using inoculum from the first set of 5 g TAN/L. Besides a longer start-up phase detected at higher TAN concentration, the 5 g TAN/L enrichments in the first reactor set exhibited slightly less methane production than other, lower TAN enrichments. However, after an acclimation period, methane production from the 5 g TAN/L enrichments in the second reactor set produced methane at 88% of that of the control. On the contrary, methane

production in the highest TAN swine waste digestate second generation enrichments (actual 11.1 g TAN/L) was inhibited by 90%. The wastewater treatment plant (WWTP) sludge digestate- inoculated reactors produced the least methane of all. Methanogenesis was inhibited in all target 5 to 12.5 g TAN/L wastewater sludge digestate inoculated reactors. Even with a long acclimation period (250 days), only the 5 g TAN/L enrichment eventually recovered methane production that was near that of the controls. A summary of methane production as % of the corresponding active control for each enrichment is shown in Table 6.1

Table 6.1 Summary of methane production as a % of the active control for the highest TAN for each set of enrichments from different inoculum sources

Enrichments	**Actual TAN Concentration (g TAN/L)**	**Methane Production % of Active Control**
Thailand landfill leachate	11.4	80
New Jersey landfill leachate	11.8	21
Swine waste digestate	11.1	10
Wastewater sludge digestate	11.5	5
Swine waste digestate with cation addition		
- $MgCl_2$	4.0	113
- $CaCl_2$	4.0	111

6.1.3 Volatile fatty acids (VFAs)

The results indicated that the reactor (either prevailing or intermittent) VFA concentrations (acetate and propionate) increased with increasing TAN concentrations. Thailand leachate microbes utilized both acetate and propionate relatively rapidly and without lag, and only low accumulation (0.1 mmol acetate and propionate/L) was detected in the 5 g TAN/L reactors after 218 days. Only the reactors at target 12.5 g TAN/L showed acetate and propionate accumulation at the beginning of the operation

period, which then declined to near 4.4 mmol acetate/L and 4.5 mmol propionate/L by the end of the experiment (day 218). New Jersey leachate enrichments accumulated VFAs in the target 10 and 12.5 g TAN/L reactors to as high as 71 mmol acetate/L and 47 mmol propionate/L and never decreased. Swine waste digestate inoculated reactors at target 5 g TAN/L responded differently from lower TAN concentrations. After acetate was utilized, these reactors again began to accumulate acetate at the same time propionate decreased - presumably produced through propionate oxidation. At TAN of 7.5 to 12.5 g TAN/L, propionate fluctuated from 87 to 32 mmol /L over a course of 300 days while acetate and methane slightly accumulated at 8 mmol acetate/L and 0.2 mmol methane/two weeks, respectively. Reactors inoculated with wastewater sludge digestate mostly accumulated propionate. Propionate accumulated to 127 mmol/L in the 5 g TAN/L reactors while 323 mmol/L accumulated in the 10 g TAN/L reactors. However, propionate concentration in the 10 g TAN/L reactors decreased to 50 mmol/L at the end of the experimental period (335 days) whereas it still accumulated up to 140 mmol/L in the 12.5 g TAN/L reactors. Overall, the Thailand landfill leachate inoculated reactors accumulated the least VFAs, whereas wastewater sludge digestate inoculated reactors accumulated the most VFAs. Different inocula thus resulted in reactor stability to high TAN.

6.1.4 Relationships between methane production and volatile fatty acids (VFAs) accumulation

Changes in VFA concentrations and methane production in reactors inoculated with swine waste digestate at target 5 g TAN/L (first experiment) and Thailand landfill

leachate at target 12.5 g TAN/L, revealed similar trends, in general. These conditions from the two reactors were chosen to explain the relationship between methane and VFAs because they represented active reactor responses even at high TAN concentrations with interesting and relevant microbial community dynamics. The methane production and VFA concentrations in swine waste digestate inoculated reactors with target 5 g TAN/L and Thailand leachate inoculated reactors with target 12.5 g TAN/L, are shown in Fig. 6.1 and 6.2, respectively.

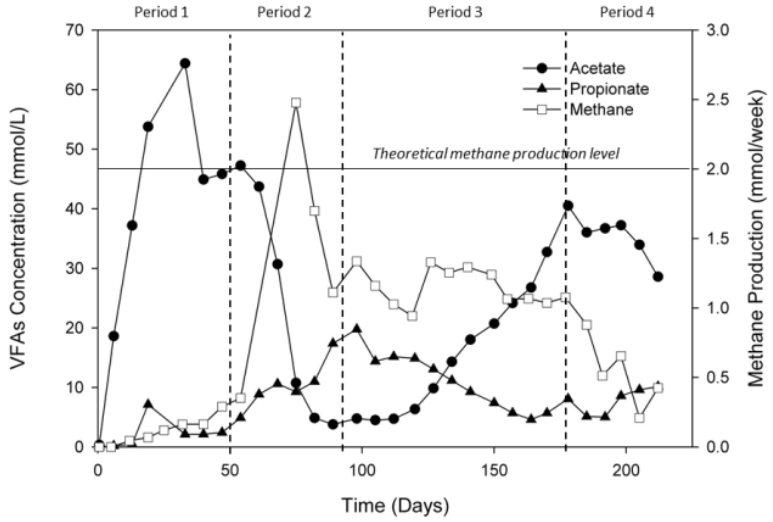

Fig. 6.1 Methane production and VFA concentrations in swine waste digestate inoculated reactors with target 5 g TAN/L. Symbols are average values of triplicates.

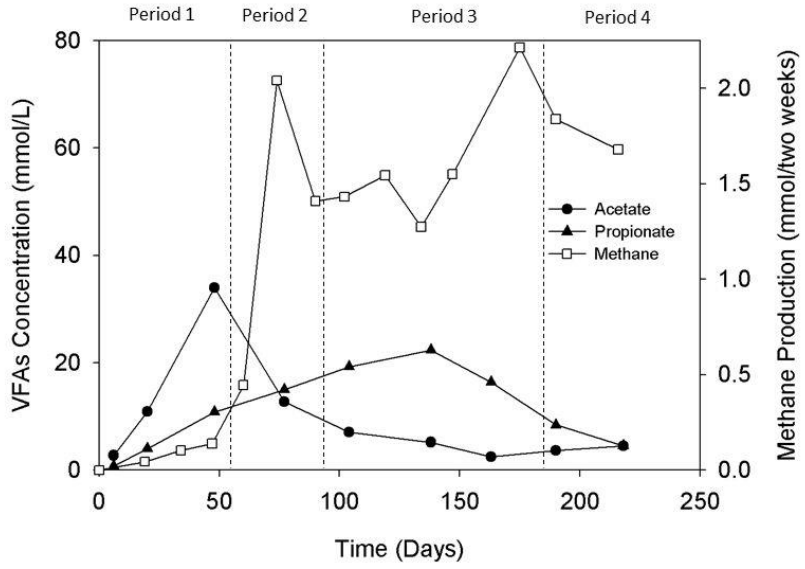

Fig. 6.2 Methane production and VFA concentrations in Thailand leachate inoculated reactor with target 12.5 g TAN/L. Symbols are average values of triplicates.

The relationships between methane and VFAs in reactors inoculated with swine waste digestate and Thailand leachate can be classified into four periods.

1) Period 1 (day 1-50) glutamate degrading bacteria play a role in fermenting glutamate, fed as the sole carbon and energy source, into propionate, which was further degraded to acetate and hydrogen by propionate oxidizing acetogens via syntrophic propionate oxidation (Boone and Bryant 1980, Stams et al. 1993). As a result, accumulation of acetate was observed. During this period, little methane was produced in the reactor. The reason might be that at the early stage acetate-utilizing methanogens were not acclimated to the ammonia.

2) Period 2 (day 50-90) acetate drastically decreased while methane increased. The results indicated that acetate was utilized via acetotrophic methanogenesis

to produce methane. Once acetate was used up, methane production then decreased. However, accumulation of propionate was detected during this period. This might indicate low activity or inhibition of propionate-oxidizing acetogens and/or on the hydrogen-consuming methanogens which are essential to produce thermodynamically favorable conditions for propionate oxidation (Lier et al. 1993, Prochazka et al. 2012).

3) Period 3 (day 90-180) propionate-oxidizing acetogens started to be active, thus decreases of propionate with increases of acetate were detected. When propionate decreased, it was expected that H_2 concentration was kept low. We did not measure hydrogen gas content in this study; however, Fukuzaki et al. (1990) stated that the partial pressure of H_2 must be kept below 10^{-6} to 10^{-4} atm (0.1 to 10.1 Pa) in order for propionate to degrade. Similarly, Fennell and Gossett (1997) reported that propionic acid can only be fermented when H_2 partial pressure is lower than $10^{-4.4}$ atm during reductive declorination of tetrachloroethene. The pathway related to maintaining low H_2 concentrations and stable methane production may involve hydrogenotrophic methanogenesis as reported by Schnurer and Nordberg (2008). They stated that a shift from aceticlastic methanogenesis to syntrophic acetate oxidataion (coupled to hydrogenotrophic methanogenesis) thermodynamically provided more energy under high ammonium concentration (Schnurer and Nordberg 2008). However, later during period 3 the swine waste digestate and Thailand leachate enrichments responded differently in terms of acetate and methane production. An increase in acetate concentration was detected in swine waste digestate enrichments after day 134 while Thailand leachate inoculated reactors maintained stable acetate concentrations. In addition, methane production in swine waste digestate inoculated reactors declined, whereas it increased in Thailand leachate

inoculated reactors. This suggested that methanogenesis in swine waste digestate inoculated reactors was inhibited but not in the Thailand leachate inoculated reactors. Moreover, DGGE and pyrosequencing also detected a phylotype matching *Acetobacterium sp.*, a homoacetogen, in swine waste digestate inoculated reactors. These homoacetogens may play a role in converting H_2 to acetate according to Kotsyurbenko et al. (2001) who reported that *Acetobacterium bakii* has strong competitiveness for hydrogen at high hydrogen concentrations. Thus, acetate accumulation was detected during this period.

4) Period 4 (day 180-200) hydrogenotrophic methanogenesis was likely inhibited as seen from decreasing methane production from both reactors. In the case of the swine waste digestate inoculated reactor, propionate accumulation may be a result of the fact that H_2 was not utilized. In addition, the decrease of acetate concentration may relate to low activity of propionate oxidizing acetogens. However, in Thailand leachate inoculated reactors, propionate oxidizing acetogens were still active.

6.1.5 Microbial community analysis

Microbial communities were examined using DNA sequencing following PCR-DGGE, DGGE band intensity analysis, and in some cases pyrosequencing of 16S rRNA genes. All these methods were used to assess the dominant microbial makeup in the reactors. It should be noted that the band intensity analysis of DGGE using ImageJ 1.48v quantification software has some limitations. This software can provide a density histogram which was then modified and reported as relative percent band intensities in each lane. In the case of an overlapped density histogram or an unstable baseline, the

analysis of the histogram may be incorrect. For each phylotype detected, the band intensities are reported as an average of triplicates ± one standard deviation to provide information about the variability of the results.

Microbial community analysis of reactors inoculated with microbes from different sources generally produced similar bacterial and archaeal communities after long incubations times that were more resistant to high TAN concentrations. The results revealed the presence of a variety of putative glutamate-degrading bacteria. At high TAN concentrations, phylotypes related to glutamate-degrading bacteria such as *Clostridium* spp., *Thermovirga* spp., *Aminobacterium* spp., and *Gelria* spp. were detected. In addition, a phylotype matching *Thermanaerovibrio* spp., a moderately thermophilic, syntrophic, glutamate-degrading bacteria, was detected at low TAN concentrations, mainly in reactors inoculated with wastewater sludge digestate.

In Thailand leachate inoculated reactors, phylotypes related to syntrophic propionate-oxidizing bacteria such as *Smithella sp.* and *Desulfovibrio* spp. were detected. *Smithella* spp. is one of four phylogenic groups of syntrophic propionate-oxidizing bacteria (Ariesyady et al. 2007). *Desulfovibrio* spp. (in the absence of sulfate) and *Syntrophobacter wolinii* both oxidize propionate in co-culture with methanogens (Boone and Bryant 1980).

The main pathways of AD at high TAN concentrations may proceed through syntrophic acetate oxidation coupled to hydrogenotrophic methanogenesis. Our study has shown that syntrophic acetate-oxidizing bacteria with a phylotype matching *Tepidanaerobacter* spp. in the Firmicutes phylum dominated in reactors inoculated with

landfill leachate (both Thailand and New Jersey) and swine waste digestate (including when $CaCl_2$ was added to the reactor). These results confirmed previous findings that *Tepidanaerobacter acetatoxydans,* an anaerobic syntrophic acetate-oxidizing bacterium, can be enriched at high TAN concentrations. We detected phylotypes related to *T. acetatoxydans* up to target 12.5 g TAN/L, a concentration higher than the levels reported in previous studies of 3 to 7 g NH_4^+-N/L (Schnurer et al. 1994, Schnurer and Nordberg 2008, Westerholm et al. 2011c).

Archaeal community analysis revealed that *Methanosarcina* spp. in the phylum Euryarchaeota was dominant in reactors inoculated with Thailand leachate, swine waste digestate (target 0.5 to 5 g TAN/L) and swine waste digestate with cation addition. The results suggested that the presence of *Methanosarcina* spp. may have contributed to reactor resistance to inhibition by high TAN concentrations when compared to New Jersey leachate, swine waste digestate (target 5 to 12.5 g TAN/L), and wastewater sludge digestate enrichments, which had *Methanoculleus sp.* dominance. Our results support earlier findings that members belonging to the order Methanosarcinales may act as hydrogenotrophic methanogens during the SAO pathway (Westerholm et al. 2012). A build-up of ammonium was previously shown to inhibit *Methanosaetaceae* and resulted in shifts from acetate to hydrogen utilization (Williams et al. 2013). Methanogenic archaeal community composition in biowaste and sewage sludge co-digestion reactors under meso- and thermophilic conditions with high concentrations of acetate and propionate had a predominance of *Methanosarcina* spp. (Yu et al. 2014a).

Our findings indicated overall that reactors containing phylotypes matching *Tepidanaerobacter* spp. and *Methanosarcina* spp. produced relatively high amounts of

methane compared to non-stressed controls, with correspondingly low acetate and propionate accumulation at high TAN concentrations— i.e., they exhibited the most stable and TAN-resistant operation. Among all inocula tested, the Thailand leachate inoculated reactor represented the most active TAN-resistant response. Therefore, the ammonia resistant bacteria and archaea from our study are phylotypes matching *Tepidanaerobacter* spp. and *Methanosarcina* spp., respectively. Based on all evidence from this study a proposed model of AD using glutamate as substrate and the microbial community in low and high TAN concentrations is shown in Fig. 6.3

6.1.6 Sources of ammonia tolerant microorganisms

This study revealed that sources of ammonia tolerant microorganisms may occur in existing waste treatment systems. A summary of TAN, NH_3-N, and BOD values from different inocula is shown in Table 6.2. These values describe to some extent the environment that the microbial sources were exposed to prior to use as inocula in these experiments.

During enrichment on glutamate as a model amino acid serving as a sole carbon and energy source, among different inocula, the Thailand landfill leachate was superior for treating high nitrogen wastes. Thailand landfill leachate was sampled from a 30-year old municipal conventional landfill. In contrast, the New Jersey landfill leachate was sampled from a more than 25-year old bioreactor landfill. The TAN concentrations indicated that Thailand landfill leachate contained higher TAN concentration (1.32 g TAN/L) than New Jersey landfill leachate (0.82 g TAN/L) (Table 6.2). The conventional

landfill in Thailand, with higher temperature operation, has no leachate recirculation system as in the New Jersey bioreactor landfill. In addition, leachate from the landfill in New Jersey was obtained from a mixed waste reservoir where the leachate is routinely mixed with wastewater from an associated composting facility and with sanitary wastewater generated within the waste handling complex prior to off site disposal. This may mean that the true landfill microbial community was somewhat diluted compared to the Thailand leachate. The BOD values of the two leachates were also different, with lower BOD (600 mg/L) in the New Jersey landfill leachate than Thailand landfill leachate (28,000 mg/L) (Table 6.2). These could be among the in situ environmental factors resulting in greater enrichment of ammonia tolerant microorganisms in the Thailand landfill leachate.

The results suggested that swine waste digestate could also be used as a source of ammonia tolerant inoculum because the digestate contained a typically high TAN concentration of 3.9 g TAN/L. However, the results indicated that the swine waste digestate enrichments had limited presence of a phylotype matching *Methanosarcina* spp. up to target 5 g TAN/L, even though the dominant SAO bacteria were the same as for Thailand leachate (phylotypes related to *Tepidanaerobacter* spp.).

The use of wastewater sludge digestate inoculum was unsuccessful in enriching phylotypes matching *Tepidanaerobacter* spp. and *Methanosarcina* spp. despite the relatively high TAN reported (1.95 g TAN/L) for this source.

In all control (not ammonia stressed) reactors except the swine waste digestate enrichment, a phylotype matching *Methanosaeta sp.* was detected. *Methanosaeta concilii*

is known as an ammonia-sensitive methanogen abundant in AD with low acetate levels (Calli et al. 2003, Hattori 2008, Zhu et al. 2012).

Table 6.2 Summary of TAN, NH_3-N, and BOD values from different inocula

Sources of Inoculum	**TAN (g TAN/L)**	**NH_3-N (g N/L)**	**BOD (mg/L)**
Thailand landfill leachate	1.32	0.10	28,000
New Jersey landfill leachate	0.82	0.06	600
Swine waste digestate	3.90	0.63	22,000
Wastewater sludge digestate	1.95	0.14	ND

ND – no data

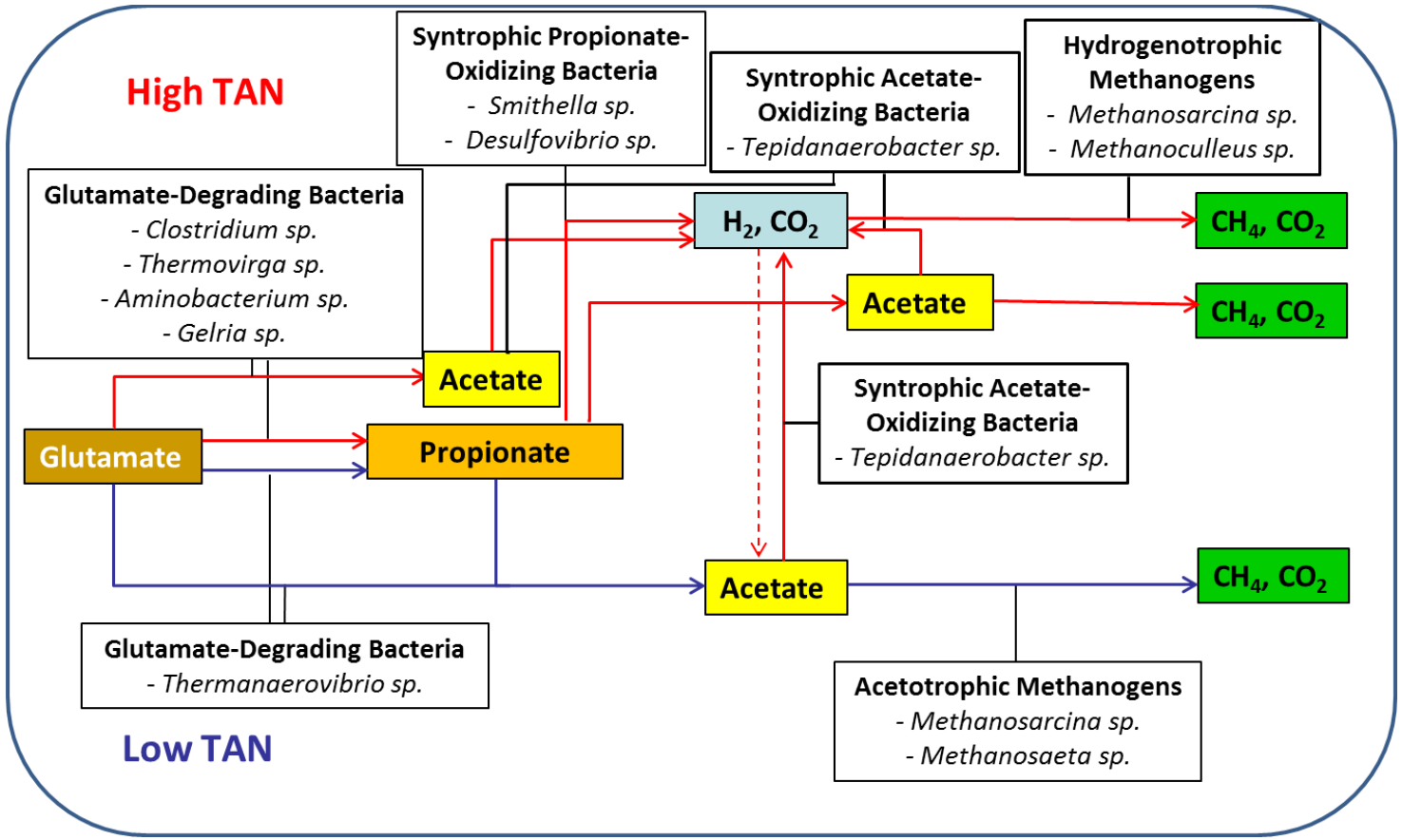

Fig. 6.3 Proposed model of AD using glutamate as substrate and microbial community in low and high TAN concentrations

6.2 Environmental Implications

This study highlighted the effects of AD treating high N wastes on metabolic intermediates (the VFAs acetate and propionate) along with methane production and microbial community shifts. The results have shown that routinely monitoring these chemical parameters and microbial populations could provide better understanding of reactor performance and stability.

The identification of ammonia tolerant microorganisms can lead to optimization of AD with high TAN concentrations to avoid reactor failure. It would be desirable to anaerobically digest high N wastes without the need to blend low N substrates to maintain low digester ammonia concentrations (Angelidaki and Ahring 1993, Schnurer et al. 1999, Velsen 1979). Further, ammonia stripping optimized for AD with high TAN concentrations could capture ammonia as an alternative energy source more economically (Babson et al. 2013).

The observation of microbial communities in enrichments with resistance to high TAN suggests the possibility of operating AD with high N wastes. Indeed, further ability to culture highly tolerant strains and gaining new knowledge of why particular strains are resistant could lead to development of bioaugmentation for these systems. Bioaugmentation could be a technique for optimizing AD at high TAN concentrations. Development of bioaugmentation was recently found successful in landfill leachate reactors enriched with ammonia and humic acid resistant bacteria, *Bacillus cereus* and *Enterococcus casseliflavus* (Yu et al. 2014a). Fotidis et al. (2013) stated that maximizing methanogen growth rates is a factor leading to bioaugmentation success. That study

reported success in bioaugmentation of *Methanoculleus bourgensis* MS2^{T}, a fast-growing hydrogenotrophic methanogen, in an ammonia tolerant SAO co-culture containing *Clostridium ultunense* spp. nov. living in association with *Methanoculleus* spp. strain MAB1, a slow-growing methanogen. The bioaugmentation was performed in fed-batch reactors up to ammonium concentration of 5 g NH_4^+-N/L. Therefore, bioaugmentation of ammonia tolerant microorganisms found in this study such as *T. acetatoxydans*, and *Methanosarcina sp.* should be investigated at high HRT (i.e., low dilution rate), which may accelerate build up of slow growing-methanogens (Kim et al. 2014, Shigematsu et al. 2003). Bioaugmentaton or process control to establish ammonia resistant communities could improve process performance in AD processing high N wastes such as municipal solid waste or swine manure. These alterations could avoid the need for dilution and allow higher concentration TAN leachates to be produced. In turn this could allow ammonia to be economically harvested to produce hydrogen or to be used directly as an alternative energy source.

Our results have shown sources of ammonia tolerant microorganisms that can be enriched in AD treating wastes containing high TAN concentrations. In practice, development of ammonia tolerant microorganisms in the digester may be limited by factors such as organic loading rate (OLR), reactor design, and operating parameters including temperature, VFAs, alkalinity, and waste composition. Previous studies have demonstrated that anaerobic co-digestion of multiple substrates resulted in enhancement of biogas production and improved reactor performance (Drennan and DiStefano 2014, Parameswaran and Rittmann 2012). Semi-continuous reactors performing co-digestion of swine waste and paper sludge at a 2:1 ratio showed 1.5 times higher methane production

than baseline swine waste-only reactors (Parameswaran and Rittmann 2012). Results from our study revealed that swine waste digestate is a good source of inoculum for reactors with high TAN. However, undesired substances such as antibiotics and pathogens in swine waste digestate can be problematic. Currently, food wastes have drawn attention as clean substrate for AD. Drennan and DiStefano (2014) have reported success of a high solid co-digestion of food and landscape waste at low loading of 2 g COD/L-day. However, ammonia inhibition was reported at a high loading of 15 g COD/L-day because of the low C:N ratio of the food waste plus low biodegradability of landscape waste. Co-digestion of food waste with a substrate high in bioavailable carbon is recommended to increase the C:N ratio (Drennan and DiStefano 2014). The results from this study suggest that food waste digesters may also be good candidates for examination of ammonia tolerant microorganisms. Further, bioaugmentation of ammonia tolerant microbes to food digesters could be beneficial, especially when there is limitation of balancing substrates.

It has been known that single-stage continuous mesophilic AD reactors are the most attractive for small-scale AD with high process stability. However, a study on single-stage AD of high-strength food wastewater revealed shifts of bacterial communities with the dominance of phyla Bacteroidetes, Firmicutes, Synergistetes, and Actinobacteria. In addition, the archaeal communities indicated that methanogenic communities shifted from aceticlastic to hydrogenotrophic methanogens with a large increase in the proportion of syntrophic bacterial communities (Jang et al. 2014). Thus, when high protein wastes with potential of ammonia toxicity are treated, two phase

digestion may be an option to maintain methanogenesis separately from fermentation and acidification.

The results from this dissertation research also revealed that wastewater sludge digestate from a municipal digester (the Joint Meeting of Essex and Union Counties wastewater treatment plant, Elizabeth, New Jersey) exhibited a microbial community sensitive to high TAN concentration, with no intrinsic phylotypes matching *Tepidanaerobacter* spp. or *Methanosarcina* spp. being detected. Thus, future consideration of selecting the blend of substrates that could be amended to municipal digesters must carefully consider co-substrate composition. In particular, use of food waste containing high nitrogen content in this system could cause reactor instability, if ammonia tolerant microbes are not native to the digester, or are not established in advance of the amendment. Thus, optimization methods for substrate blends could be applied to achieve AD stable operation with careful consideration of the ammonia-sensitive nature of the prevailing microbial community in this particular AD system.

Overall, this study provides important information about ammonia tolerant microorganisms from different waste treatment systems. Knowledge of inoculum source for enrichment could be applied for bioaugmentation of these ammonia tolerant microorganisms in AD treating high N wastes. Thus, better AD performance and process stability can be achieved when TAN is high.

References

Ahn, J.-H., Do, T.H., Kim, S.D. and Hwang, S. (2006a) The effect of calcium on the anaerobic digestion treating swine wastewater. Biochemical Engineering Journal 30, 33-38.

Ahn, J.H., Do, T.H., Kim, S.D. and Hwang, S. (2006b) The effect of calcium on the anaerobic digestion treating swine wastewater. Biochemical Engineering Journal 30, 33-38.

Ahring, B.K., Alatriste-Mondragon, F., Westerman, P. and Mah, R.A. (1991) Effects of cation on Methanosarcina thermophila TM-1 growing on moderate concentrations of acetate: production of single cells. Applied Microbiology and Biotechnology 35, 686-689.

Ahring, B.K., Sanberg, M. and Angelidaki, I. (1995) Volatile fatty acids as indicators of process imbalance in anaerobic digestors. Applied Microbiology and Biotechnology 43, 559-565.

Alvarez, R. and Liden, G. (2008) Semi-continuous co-digestion of solid slaughterhouse waste, manure, and fruit and vegetable waste. Renewable Energy 33(4), 726-734.

Angelidaki, I. and Ahring, B.K. (1993) Thermophilic anaerobic digestion of livestock waste: the effect of ammonia. Applied Microbiology and Biotechnology 38, 560-564.

Angelidaki, I. and B.K.Ahring (1994) Anaerobic Thermophilic Digestion of Manure at Different Ammonia Loads: Effect of Temperature. Water Research 28(3), 727-731.

Angenent, L.T., Karim, K., Al-Dahhan, M.H., Wrenn, B.A. and Domiguez-Espinosa, R. (2004) Production of bioenergy and biochemicals from industrial and agricultural wastewater. TRENDS in Biotechnology 22(9), 477-485.

Angenent, L.T., Sungb, S. and Raskin, L. (2002) Methanogenic population dynamics during startup of a full-scale anaerobic sequencing batch reactor treating swine waste. Water Research 36, 4648–4654.

Ariesyady, H.D., Ito, T., Yoshiguchi, K. and Okabe, S. (2007) Phylogenetic and functional diversity of propionate-oxidizing bacteria in an anaerobic digester sludge. Applied Microbiology and Biotechnology 75, 673-683.

Babson, D.M., Bellman, K., Prakash, S. and Fennell, D.E. (2013) Anaerobic digestion for methane generation and ammonia reforming for hydrogen production: A thermodynamic energy balance of a model system to demonstrate net energy feasibility. Biomass and Bioenergy 56, 493-505.

Baena, S., Fardeau, M.-L., Labat, M. and al., e. (1998) *Aminobacterium colombiense* gen. nov. sp. nov., an amino acid-degrading anaerobe isolated from anaerobic sludge. Anaerobe 4, 241-250.

Baena, S., Fardeau, M.-L., Labat, M. and al., e. (2000) Aminobacterium mobile sp. nov., a new anaerobic amino-acid-degrading bacterium. International Journal of Systematic and Evolutionary Microbiology 50, 259-264.

Baena, S., Fardeau, M.-L., Woo, T.H.S., Ollivier, B., Labat, M. and Patel, B.K.C. (1999) Phylogenetic relationships of three amino-acid -utilizing anaerobes, *Selenomonas acidaminovorans*, '*Selenomonas acidaminophila*' and *Eubacterium*

acidaminophilum, as inferred from partial 16S rDNA nucleotide sequences and proposal of *Thermanaerovibrio acidaminovorans* gen. nov., comb. nov. and *Anaeromusa acidaminophila* gen. nov., comb nov. International Journal of Systematic Bacteriology 49, 969-974.

Barredo, M.S. and Evison, L.M. (1991) Effect of propionic toxicity on methanogenic sludge, *Methanobrevibacter smithii*, and *Methanospirillum hungatii* at different pH values. Applied and Environmental Microbiology 57(6), 1764-1769.

Barret, M., Gagnon, N., Kalmokoff, M.L. and al., e. (2013) Identification of *Methanoculleus* spp. as active methanogens during anoxic incubations of swine manure storage tank samples Applied and Environmental Microbiology 79 (2), 424-433

Berge, N.D., Reinhart, D.R., Dietz, J. and Townsend, T. (2006) In situ ammonia removal in bioreactor landfill leachate. Waste Management 26, 334-343.

Berge, N.D., Reinhart, D.R. and Townsend, T.G. (2005) The fate of nitrogen in bioreactor landfills. Critical Reviews in Environmental Science and Technology 35, 365-399.

Bok, F.A.M.d., Plugge, C.M. and Stams, A.J.M. (2004) Interspecies electron transfer in methanogenic propionate degrading consortia. Water Research 38, 1368-1375.

Boone, D.R. and Bryant, M.P. (1980) Propionate-degrading bacterium, Syntrophobacter wolinii sp. nov. gen. nov. , from methanogenic ecosystems. Applied and Environmental Microbiology 40(3), 626-632.

Borja, R., Sanchez, E. and Duran, M.M. (1996) Effect of the clay mineral zeolite on ammonia inhibition of anaerobic thermophilic reactors treating cattle manure. Journal of Enrironmental Science and Health A31(2), 479-500.

Bufflere, P., Loisel, D., Bernet, N. and Delgenes, J.P. (2006) Towards new indicators for the prediction of solid waste anaerobic digestion properties. Water Science and Technology 53(8), 233-241.

Calli, B., Mertoglu, B., Inanc, B. and Yenigun, O. (2005) Methanogenic diversity in anaerobic bioreactors under extremely high ammonia levels. Enzyme and Microbial Technology 37, 448-455.

Calli, B., Tas, N., Mertoglu, B., Inanc, B. and Ozturk, I. (2003) Molecular analysis of microbial communities in nitrification and denitrification reactors treating high ammonia leachate. Journal of Enrironmental Science and Health A38(10), 1997-2007.

Chang, F.Y. and Lin, C.Y. (2006) Calcium effect on fermentative hydrogen production in an anaerobic up-flow sludge blanket system. Water Science and Technology 54(9), 105-112.

Chen, L. (2010) Inhibition of aaerobic dgradation of treated paperssample under simulated landfill conditions, Rutgers, The State University of New Jersey, New Brunswick, NJ.

Cho, S.-K., Lee, M.-K., Kim, D.-H. and al., e. (2014) Enhanced anaerobic digestion of livestock waste by ultrasonication: A tool for ammonia removal and solubilization. Korean Journal of Chemical Engineering 31(4), 619-623.

Chung, Y.C., Chang, Y.C., Chen, Y.P., Lin, W.C., Lin, H.H. and Tseng, C.P. (2013) Analysis of microbial diversity and optimal conditions for enhanced biogas

production from swine waste anaerobic digestion. Journal of renewable and sustainable energy 5, 053143-053141 - 053143-053112.

Dahle, H. and Birkeland, N.-K.r. (2006) Thermovirga lienii gen. nov., sp. nov., a novel moderately thermophilic, anaerobic, amino-acid-degrading bacterium isolated from a North Sea oil well. International Journal of Systematic and Evolutionary Microbiology 56, 1539-1545.

Dang, Y., Zhang, R., Wu, S., Liu, Z., Qiu, B., Fang, Y. and Sun, D. (2014) Calcium effect on anaerobic biological treatment of fresh leachate with extreme high calcium concentration. International Biodeterioration & Biodegradation 95, 76-83.

Demirel, B. and Scherer, P. (2008) The roles of acetotrophic and hydrogenotrophic methanogens during anaerobic conversion of biomass to methane: a review. Reviews in Environmental Science and Biotechnology 7, 173-190.

Deppenmeier, U., A., J., T., H. and al., e. (2002) The genome of *Methanosarcina mazei*: Evidence for lateral gene between bacterial and archael. Journal of Molecular Microbiology and Biotechnology 4(4), 453-461.

Drennan, M.F. and DiStefano, T.D. (2014) High solids co-digestion of food and landscape waste and the potential for ammonia toxicity. Waste Management 34, 1289-1298.

Fennell, D.E. and Gossett, J.M. (1997) Comparison of butyric acid, ethanol, lactic acid, and propionic acid as hydrogen donors for the reductive dechlorination of tetrachloroethene. Environmental Science and Technology 31, 918-926.

Foresti, E., Zaiat, M. and Vallero, M. (2006) Anaerobic processes as the core technology for sustainable domestic wastewater treatment: Consolidated applications, new trends, perspective, and challenges. Reviews in Environmental Science and Bio/Technology 5, 3-19.

Fotidis, I.A., Karakashev, D. and Angelidaki, I. (2013) Bioaugmentation with an acetate-oxidizing consortium as a tool to tackle ammonia inhibition of anaerobic digestion. Bioresource Technology 146, 57-62.

Fotidis, I.A., Karakashev, D., Kotsopoulos, T.A., Martzopoulos, G.G. and Angelidaliki, I. (2012) Effect of ammonium and acetate on methanogenic pathway and methanogenic community composition. FEMS Microbiology Ecology 83, 38-48.

Fukusaki, S., Nishio, N., Shobayashi, M. and Nagai, S. (1990) Inhibition of the fermentation of propionate to methane by hydrogen, acetate, and propionate. Applied and Environmental Microbiology 56(3), 719-723.

Fukuzaki, S., Nishio, N., Shobayashi, M. and Nagai, S. (1990) Inhibition of the fermentation of propionate to methane by hydrogen, acetate, and propionate. Applied and Environmental Microbiology 56(3), 719.

Gallert, C., Bauer, S. and Winter, J. (1998) Effect of ammonia on the anaerobic degradation of protein by a mesophilic and thermophilic biowaste population. Applied Microbiology and Biotechnology 50, 495-501.

Gallert, C. and Winter, J. (1997) Mesophilic and thermophilic anaerobic digestion of source-sorted organic wastes: effect of ammonia on glucose degradation and methane production. Applied Microbiology and Biotechnology 48, 405-410.

Garcia, M.L. and Angenent, L.T. (2009) Interaction between temperature and ammonia in mesophilic digesters for animal waste treatment. Water Research 43, 2373-2382.

Hania, W.B., Godbane, R. and Postec, A. (2012) Defluviitoga tunisiensis gen. nov., sp. nov., a thermophilic bacterium isolated from a mesothermic and anaerobic whey digester. International Journal of Systematic and Evolutionary Microbiology 62, 1377-1382.

Hansen, K.H., Angelidaki, I. and Ahring, B.K. (1998) Anaerobic digestion of swine manure. Water Research 32(1), 5-12.

Hansen, K.H., Angelidaki, I. and Ahring, B.K. (1999) Improving thermophilic anaerobic digestion of swine manure. Water Research 33(8), 1805-1810.

Hao, L.P., Lu, F., He, P.J., Li, L. and Shao, L.M. (2011) Predominat contribution of syntrophic acetate oxidation to thermophilic methane formation at high acetate concentrations. Environmental Science and Technology 45, 508-513.

Hattori, S. (2008) Syntrophic acetate-oxidizing microbes in methanogenic environments. Microbes and Environments 23(2), 118-127.

Herrero, M. and Stuckey, D.C. (2015) Bioaugmentation and its application in wastewater treatment: A review. Chemosphere 140, 119-128.

Hwang, K., Shin, S.G., Kim, J. and Hwang, S. (2008) Methanogenic profiles by denaturing gradient gel electrophoresis using order-specific primers in anaerobic sludge digestion. Applied Microbiology and Biotechnology 80, 269-276.

Iannotti, E.L., Fischer, J.R. and Sievers, D.M. (1982) Characterization of Bacteria from a Swine Manure Digestert. Applied and Environmental Microbiology 43(1), 136-143.

IEA (2013) World Energy Outlook 2013 Factsheet, France.

Jackson-Moss, C.A. and Duncan, J.R. (1989) The effect of calcium on anerobic digestion. Biotechnology Letters 11(3), 219-224.

Jang, H.M., Kim, J.H., Ha, J.H. and Park, J.M. (2014) Bacterial and methanogenic archaeal communities during the single-stage anaerobic digestion of high-strength food wastewater. Bioresource Technology 165, 174-182.

Kadam, P.C. and Boone, D.R. (1996) Influence of pH on ammonia accumulation and toxicity in halophilic, methylotrophic methanogens. Applied and Environmental Microbiology 62(12), 4486-4492.

Kidby, D.W. and Nedwell, D.B. (1991) An investigation into the suitability of biogas hydrogen concentration as a performance monitor for anaerobic sewage sludge digesters. Water Research 25(8), 1007-1012.

Kim, S., Bae, J., Choi, O., Ju, D., Lee, J., Sung, H., Park, S., Sang, B.-I. and Um, Y. (2014) A pilot scale two-stage anaerobic digester treating food waste leachate (FWL): Performance and microbial structure analysis using pyrosequencing. Process Biochemistry 49, 301-308.

Klass, D.L. (1984) Methane from anaerobic fermentation. Science 223(4640), 1021-1028.

Koster, I.W. (1987) Abatement of long-chain fatty acid inhibition of methanogenesis by calcium addition. Biological Wastes 22, 295-301.

Koster, I.W. and Koomen, E. (1988) Ammonia inhibition of the maximum growth rate of hydrogenotrophic methanogens at various pH-levels and temperatures. Applied Microbiology and Biotechnology 28, 500-505.

Koster, I.W. and Lettinga, G. (1984) The Influence of ammonia-Nitrogen on the specific activity of pelletized methanogenic sludge. Agricultural Wastes 9, 205-216.

Kotsyurbenko, O.R., Glagolev, M.V., Nozhevnikova, A.N. and Conrad, R. (2001) Competition between homoacetogenic bacteria and methanogenic archaea for hydrogen at low temperature. FEMS Microbiology Ecology 38, 153-159.

Lahav, O., Schwartz, Y., Nativ, P. and Gendel, Y. (2013) Sustainable removal of ammonia from anaerobic-lagoon swine waste effluents using an electrochemically-regenerated ion exchange process. Chemical Engineering Journal 218, 214-222.

Leeson, A., Stroo, H.F. and Johnson, P.C. (2013) Groundwater remediation today and challenges and opportunities for the future. Groundwater 51(2), 175-179.

Lesteur, M., V.Bellon-Maurel, C.Gonzalez, E.Latrille, J.M.Roger, G.Junqua and J.P.Steyer (2010) Alternative methods for determining anaerobic biodegradability: A review. Process Biochemistry 431, 431-440.

Lier, J.B.v., Grolle, K.C.F., Frijters, C.T.M.J., Stams, A.J.M. and Lettinga, G. (1993) Effects of acetate, propionate, and butyrate on the thermophilic anaerobic degradation of propionate by methanogenic sludge and defined cultures. Applied and Environmental Microbiology 59(4), 1003-1011.

Liu, J., Hu, J., Zhong, J., Luo, J., Zhao, A., Liu, F., Hong, R., Qian, G. and Xu, Z.P. (2011) The effect of calcium on the treatment of fresh leachate in an expanded granular sludge bed bioreactor. Bioresource Technology 102, 5466-5472.

Liu, J., Zhao, S. and Zhang, L. (2012) Study on anaerobic digestion performance of kitchen wastes: Inhibition of ammonia nitrogen and volatile acid on the anaerobic methanogenesis. Trans Tech Publications 347-353, 2497-2501.

Madigan, M.T. and Martinko, J.M. (2006) Brock Biology of Microorganisms, Pearson Education, Inc., Upper Saddle River, NJ.

Mahoney, E.M., Varangu, L.K., Cairns, W.L., Kosaric, N. and Murray, R.G.E. (1987) The effect of calcium on microbial aggregation during UASB reactor start-up. Water Science and Technology 19, 249-260.

Massé, D.I., Rajagopal, R. and Singh, G. (2014) Technical and operational feasibility of psychrophilic anaerobic digestion biotechnology for processing ammonia-rich waste. Applied Energy 120, 49-55.

Maus, I., Wibberg, D., Stantscheff, R. and et., a. (2012) Complete genome sequence of the hydrogenotrophic, methanogenic archaeon *Methanoculleus bourgensis* Strain MS2(T), Isolated from a sewage sludge digester JOURNAL OF BACTERIOLOGY 194 (19), 5487-5488

McCarty, P.L. (1964) Anaerobic waste treatment fundamentals. Public Works 95(9-12), 107-112.

McCarty, P.L. and McKinney, R.E. (1961) Salt toxicity in anaerobic digestion. Water Pollution Control Federation 33, 399-415.

McInerney, M. and Bryant, M. (1981) Basic principles of anaerobic degradation and methane production, Plenum Publications, Inc.

Meinen, R.J., Kephart, K.B. and Graves, R.E. (2014) Economic feasibility and evaluation of a novel manure collection and anaerobic digestion system at a commercial swine finisher enterprise Biomass and Bioenergy 63, 10-21.

Merlino, G., Rizzi, A., Schievano, A., Tenca, A., Scaglia, B., Oberti, R., Adani, F. and Daffonchio, D. (2013) Microbial community structure and dynamics in two-stage vs single-stage thermophilic anaerobic digestion of mixed swine slurry and market biowaste. Water Research 47, 1983-1995.

Miranda-Tello, E., Fardeau, M.-L., Sepulveda, J., Fernandez, L., Cayol, J.-L., Thomas, P. and Ollivier, B. (2003) *Garciella nitratireducens* gen. nov., sp. nov., an anaerobic, thermpphilic, nitrate- and thiosulfate-reducing bacterium isolated from an oilfield separator in teh Gulf of Mexico. International Journal of Systematic and Evolutionary Microbiology 53, 1509-1514.

Nakakubo, R., Moller, H.B., Nielsen, A.M. and Matsuda, J. (2008) Ammonia Inhibition of Methanogenesis and Identificaiton of Process Indicators during Anaerobic Digestion. Environmental Engineeing Science 25(10), 1487-1496.

Nakatsu, C.H., Torsvik, V. and Ovreas, L. (2000) Soil community analysis using DGGE of 16S rDNA polymerase chain reaction products. Soil Science Society of America Journal 64, 1382-1388.

Nielsen, H.B. and Angelidaki, I. (2008) Strategies for optimizing recovery of the biogas process following ammonia inhibition. Bioresource Technology 99, 7995-8001.

Nielson, H.B. and Angelidaki, I. (2008) Strategies for optimizing recovery of the biogas process following ammonia inhibition. Bioresource Technology 99, 7995-8001.

Ortner, M., Leitzinger, K., Skupien, S., Bochmann, G. and Fuchs, W. (2014) Efficient anaerobic mono-digestion of N-rich slaughterhouse waste: Influence of ammonia, temperature and trace elements. Bioresource Technology 174, 222-232.

Owen, W.F., Stuckey, D.C., J.B.Healy, J., Young, L.Y. and McCarty, P.L. (1979) Bioassay for montioring biochemical methane potential and anaerobic toxicity. Water Research 13, 485-492.

Parameswaran, P. and Rittmann, B.E. (2012) Feasibility of anaerobic co-digestion of pig waste and paper sludge. Bioresource Technology 124, 163-168.

Patil, S.S., Kumar, M.S. and Ball, A.S. (2010) Microbial community dynamics in anaerobic bioreactors and algal tanks treating piggery wastewater. Applied Microbiology and Biotechnology 87, 353-363.

Plugge, C.M., Balk, M., Zoetendal, E.G. and Stams, A.J.M. (2002) *Gelria glutamica* gen. nov., sp. nov., a thermophilic, obligately syntrophic, glutamate-degrading anaerobe. International Journal of Sytematic and Evolutionary Microbiology 52, 401-407.

Plugge, C.M. and Stams, A.J.M. (2001) Arginine catabolism by *Thermanaerovibrio acidaminovorans*. FEMS Microbiology Letters 195, 259-262.

Plugge, C.M., Zoetendal, E.G. and Stams, A.J.M. (2000) Caloramator coolhaasii sp. nov., a glutamate-degrading, moderately thermophilic anaerobe. International Journal of Sytematic and Evolutionary Microbiology 50, 1155-1162.

Prochazka, J., Dolejs, P., Maca, J. and Dohanyos, M. (2012) Stability and inhibition of anaerobic processes caused by insufficiency or excess of ammonia nitrogen. Applied Microbiology and Biotechnology 93, 439-447.

Ragsdale, S.W. and Pierce, E. (2008) Acetogenesis and the Wood-Ljungdahl pathway of CO_2 fixation. Biochimica et Biophysica Acta 1784, 1873-1898.

Razaviarani, V. and Buchanan, I.D. (2015) Anaerobic co-digestion of biodiesel waste glycerine with municipal wastewater sludge: Microbial community structure dynamics and reactor performance. Bioresource Technology 182, 8-17.

Rittmann, B.E. and McCarty, P.L. (2001) Environmental Biotechnology: Principles and Applications, The McGraw-Hill Companies, Inc., New York, NY.

Roy, F., Albagnac, G. and Samain, E. (1985) Influence of calcium addition on growth of highly purified syntrophic cultures degrading long-chain fatty acids. Applied and Environmental Microbiology 49(3), 702-705.

Russell, J.B., Strobel, H.J. and Chen, G.J. (1988) Enrichment and isolation of a ruminal bacterium with a very high specific activity of ammonia production. Applied and Environmental Microbiology 54(4), 872-877.

Santos, C.A., Panchoni, L.C., Bini, D., Kuwano, B.H., Carmo, K.B., Silva, S.M.C.P., Marines, A.M., Andrade, G., Andrade, D.S., Cardoso, E.J.B.N., Zangaro, W. and Nogueira, M.A. (2013) Land application of municipal landfill leachate: Faat of ions and ammonia volatization. Journal of Environmental Quality 42, 523-531.

Santosh, Y., Sreekrishnan, T.R., Kohli, S. and Rana, V. (2004) Enhancement of biogas production from solid substrates using different techniques- a review. Bioresource Technology 95, 1-10.

Schmidt, J.E. and Ahring, B.K. (1993) Effects of magnesium on thermophilic acetate-degrading granules in upflo anaerobic sludge blanket (UASB) reactors. Enzyme and Microbial Technology 15, 304-310.

Schnurer, A., Houwen, F.P. and Svensson, B.H. (1994) Mesophilic syntrophic acetate oxidation during methane formation by a triculture at high ammonium concentration. Archives of Microbiology 162, 70-74.

Schnurer, A. and Nordberg, A. (2008) Ammonia, a selective agent for methane production by syntrophic acetate oxidation at mesophilic temperature. Water Science and Technology 57(5), 735-740.

Schnurer, A., Zellner, G. and Svensson, B.H. (1999) Mesophilic syntrophic acetate oxidation during methane formation in biogas reactors. FEMS Microbiology Ecology 29, 249-261.

Sekiguchi, Y., Imachi, H., Susilorukmi, A., Muramatsu, M., Ohashi, A., Harada, H., Hanada, S. and Kamagata, Y. (2006) *Tepidanaerobacter syntrophicus* gen. nov., sp. nov., an anaerobic, moderately thermophilic, syntrophic alcohol- and lactate-degrading bacterium isolated from thermophilic digested sludges. International Journal of Sytematic and Evolutionary Microbiology 56, 1621-1629.

Sharma, J. and Singh, R. (2001) Effect of nutrients supplementation on anaerobic sludge developement and activity for treating distillery effluent. Bioresource Technology 79, 203-206.

Sheng, K., Chen, X., Pan, J., Kloss, R. and Wei, Y. (2013) Effect of ammonia and nitrate on biogas production from food waste via anaerobic digestion. Biosystem Engineeering 116, 205-212.

Shigematsu, T., Tang, Y., Kawaguchi, H., Ninomiya, K., Kijima, J., Kobayashi, T., Morimura, S. and Kida, K. (2003) Effect of dilution rate on structure of a

mesophilic acetate-degrading methanogenic community during continuous cultivation. Journal of Bioscience and Bioengineering 96(6), 547-558.

Sossa, K., Alarcon, M., Aspe, E. and Urrutia, H. (2004) Effect of ammonia on the methanogenic activity of methylaminotrophic methane producing archaea enriched biofilm. Anaerobe 10, 13-18.

Sowers, K.R., Baron, S.F. and Ferry, J.G. (1984) *Methanosarcina acetivorans* sp. nov., an acetotrophic methane-producing bacterium isolated from marine sediments. Applied and Environmental Microbiology 47(5), 971-978.

Sprott, G.D. and Patel, G.B. (1986) Ammonia toxicity in oure cultures of methanogenic bacteria. Systematic and Applied Microbiology 7, 358-363.

Sprott, G.D., Shaw, K.M. and Jarrell, K.F. (1984) Ammonia/potassium exchange in methanogenic bacteria. The Journal of Biological Chemistry 259(20), 12602-12608.

Stams, A.J.M. (1994) Metabolic interactions between anaerobic bacteria in methanogenic environment. Antonie van Leeuwenhoek 66(1-3), 271-294.

Stams, A.J.M., Dijk, J.B.V., Dijkema, C. and Plugge, C.M. (1993) Growth of syntrophic propionate-oxidizing bacteria with fumarate in the absence of methanogenic bacteria. Applied Microbiology and Biotechnology 59(4), 1114-1119.

Steinhaus, B., Garcia, M.L., Shen, A.Q. and Angenent, L.T. (2007) A portable anaerobic microbioreactor reveals optimum growth conditions for the methanogen Methanosaeta concilii. Applied and Environmental Microbiology 73 (5), 1653-1658

Stephenson, D. and Stephenson, T. (1992) Bioaugmentation for enhancing biological wastewater treatment. Biotechnology Advances 10, 549-559.

Stroo, H.F., Leeson, A., Marqusee, J.A. and Johnson, P.C. (2012) Chlorinated ethene source remediation: lessons learned. Environmental Science and Technology 46, 6438-6447.

Sung, S. and Liu, T. (2003) Ammonia inhibition on thermophilic anaerobic digesiton. Chemosphere 53, 43-52.

Tchobanoglous, G., Burton, F.L. and Stensel, H.D. (2003) Wastewater Engineering: Treatment and Reuse, McGraw-Hill Companies, Inc., New York, NY.

Turker, M. and Celen, I. (2007) Removal of ammonia as struvite from anaerobic digester effluents and recycling of magnesium and phosphate. Bioresource Technology 98, 1529-1534.

USDOE (2013) Biogas and Fuel Cells Workshop Summary Report Colorado, USA.

USEIA (2014) Annual Energy Outlook Administration, U.S.E.I. (ed).

USEPA (2014) Overview of Greenhouse Gases.

Vaccari, D.A., Strom, P.F. and Alleman, J.E. (2006) Environmental Biology for Engineers and Scientists, John Wiley & Sons, Inc. , New York

Velsen, A.F.M.v. (1979) Adaptation of methanogenic sludge to high ammoni-nitrogen concentrations. Water Research 13, 995-999.

Vrieze, J.D., Hennebel, T., Boon, N. and Verstraete, W. (2012) Methanosarcina: The rediscovered methanogen for heavy duty biomethanation. Bioresource Technology 112, 1-9.

Wang, Y. and Qian, P.-Y. (2009) Conservative fragments in bacterial 16S rRNA genes and primer design for 16S Ribosomal DNA amplicons in metagenomics studies. PLoS ONE 4(10), e7401.

Wang, Y., Zhang, Y., Wang, J. and Meng, L. (2009) Effects of volatile fatty acid concentrations on methane yield and methanogenic bacteria. Biomass and Bioenergy 33, 848-853.

Weber, W.J. and Digiano, F.A. (1996) Process dynamics in environmental systems, John Wiley & Son, Inc., New York, NY.

Weiland, P. (2010) Biogas production:current state and perspective. Applied Microbiology and Biotechnology 85, 849-860.

Weng, C.-N. and Jerist, J.S. (1976) Biochemical mechanisms in the methane fermentation of glutamic and oleic acids. Water Research 10, 9-18.

Werner, J.J., Garcia, M.L., Perkins, S.D., Yarasheski, K.E., Smith, S.R., Muegge, B.D., Stadermann, F.J., DeRito, C.m., Floss, C., Madsen, E.L., Gordon, J.I. and Angenent, L.T. (2014) Microbial community dynamics and stability during an ammonia-induced shift to syntrophic acetate oxidation. Applied and Environmental Microbiology 80(11), 3375-3383.

Westerholm, M., Dolfing, J., Sherry, A. and al., e. (2011a) Quantification of syntrophic acetate-oxidizing microbial communities in biogas processes. Environmental Microbiology Reports 3 (4), 500-505.

Westerholm, M., Leven, L. and Schnurer, A. (2012) Bioaugmentation of syntrophic acetate-oxidizing culture in biogas reactors exposed to increasing levels of ammonia. Applied and Environmental Microbiology 78(21), 7619-7625.

Westerholm, M., Muller, B., Arthurson, V. and Schnurer, A. (2011b) Changes in the acetogenic population in a mesophilic anaerobic digester in response to increasing ammonia concentraton. Microbes and Environments 26(4), 347-353.

Westerholm, M., Roos, S. and Schnurer, A. (2011c) *Tepidanaerobacter acetatoxydans* sp. nov., an anaerobic, syntrophic acetate-oxidizing bacterium isolated from two ammonium-enriched mesophilic methanogenic processes. Systematic and Applied Microbiology 34, 260-266.

Williams, J., Williams, H., Dinsdale, R., Guwy, A. and Esteves, S. (2013) Monitoring methanogenic population dynamics in a full-scale anaerobic digester to facilitate operational management. Bioresource Technology 140, 234-242.

Worm, P., Muller, N., Plugge, C.M., Stams, A.J.M. and Schink, B. (2010) Syntrophy in methanogenic degradation, Springer, Heidelberg.

Yu, D., Kurola, J.M., Lahde, K., Kymalainen, M., Sinkkonen, A. and Romantschuk, M. (2014a) Biogas production and methanogenic archaeal community in mesophilic and thermopilic anaerobic co-digestion processes. Journal of Environmental Management 143, 54-60.

Yu, D., Yang, J., Teng, F. and Feng, L. (2014b) Bioaugmentation treatment of mature landfill leachate by new isolated ammonia nitrogen and humic acid resistant microorganism. Journal of Microbiology and Biotechnology 24(7), 987-997.

Yu, H.Q., Tay, J.H. and Fang, H.H.P. (2001) The roles of calcium in sludge granulation during UASB reactor start-up. Water Research 35(4), 1052-1060.

Zhu, J., Zheng, H., Ai, G., Zhang, G., Liu, D., Liu, X. and Dong, X. (2012) The genome characteristics and predicted function of methyl-group oxidation pathway in the obligate aceticlastic methanogens, *methanosaeta* spp. PLoS ONE 7(5), e36756.

Ziganshina, E.E., Belostotskiy, D.E. and Shushlyaev, R.V. (2014) Microbial community diversity in anaerobic reactors digesting turkey, chicken, and swine wastes. Journal of Microbiology and Biotechnology 24(11), 1464-1472.